Phycoremediation of acid mine drainage

Abinandan Sudharsanam

BTech (Biotechnology); MTech (Energy & Environmental Engineering)

A thesis submitted in fulfilment of the requirements for the degree of Doctor of Philosophy in Environmental Remediation

Global Centre for Environmental Remediation,

Faculty of Science

September 2019

This research was supported by an Australian Government Research Training Program (RTP) Scholarship

TABLE OF CONTENTS

LIST OF FIGURES

LIST OF TABLES

DECLARATION

STATEMENT OF ORIGINALITY

I hereby certify that the work embodied in the thesis is my own work, conducted under normal supervision. The thesis contains no material which has been accepted, or is being examined for the award of any other degree or diploma in any university or other tertiary institution and to the best of my knowledge and belief, contains no material previously published or written by another person, except where due reference has been made. I give consent to the final version of my thesis being made available worldwide when deposited in the University's Digital Repository, subject to the provisions of the Copyright Act 1969 and any approved embargo.

Signature:

Your name: Abinandan Sudharsanam

ACKNOWLEDGEMENT OF AUTHORSHIP

I hereby certify that the work embodied in this thesis contains published paper/s/scholarly work of which I am a joint author. I have included as part of thesis a written declaration endorsed in writing by my supervisor, attesting contribution to the joint publication/s/scholarly work. By signing below, I confirm that Abinandan Sudharsanam contributed more than 50% of the work to the paper/publication entitles as follows

1. **Abinandan S**, Subashchandrabose SR, Venkateswarlu K, Megharaj M (2018a): Microalgae–bacteria biofilms: a sustainable synergistic approach in remediation of acid mine drainage. Applied Microbiology and Biotechnology 102, 1131–1144 *(Chapter 2)*
2. **Abinandan S**, Subashchandrabose SR, Venkateswarlu K, Megharaj M (2018b): Nutrient removal and biomass production: advances in microalgal biotechnology for wastewater treatment. Critical reviews in biotechnology, 38, 1224–1260 *(Chapter 2)*
3. **Abinandan S**, Subashchandrabose SR, Cole N, Dharmarajan R, Venkateswarlu K, Megharaj M (2019a): Sustainable production of biomass and biodiesel by acclimation of non-acidophilic microalgae to acidic conditions. Bioresource Technology 271, 316–324 *(Chapter 3)*
4. **Abinandan S**, Subashchandrabose SR, Pannerselvan L, Venkateswarlu K, Megharaj M (2019b): Potential of acid-tolerant microalgae, *Desmodesmus* sp. MAS1 and *Heterochlorella* sp. MAS3, in heavy metal removal and biodiesel production at acidic pH. Bioresource Technology 278, 9–16 *(Chapter 4a)*
5. **Abinandan S**, Subashchandrabose SR, Venkateswarlu K, Perera IA, Megharaj M (2019c): Acid-tolerant microalgae can withstand higher concentrations of invasive cadmium and produce sustainable biomass and biodiesel at pH 3.5. Bioresource Technology 281, 469–473. *(Chapter 4c)*
6. **Abinandan S,** Subashchandrabose SR, Venkateswarlu K, Megharaj M (2020a): Sustainable Iron Recovery and Biodiesel Yield by Acid-Adapted Microalgae, *Desmodesmus* sp. MAS1 and *Heterochlorella* sp. MAS3, Grown in Synthetic Acid Mine Drainage. ACS omega, 5(12), pp.6888–6894. *(Chapter 5)*
7. **Abinandan S,** Perera IA, Subashchandrabose SR, Venkateswarlu K, Cole N, Megharaj M (2020b): Acid-adapted microalgae exhibit phenotypic changes for their survival in acid mine drainage samples. FEMS Microbiology Ecology. fiaa113, https://doi.org/10.1093/femsec/fiaa113. *(Chapter 6)*

Signature of supervisor:

Name of supervisor: Megharaj Ma

ACKNOWLEDGEMENT

It takes an immense pleasure to work under the competent guidance of my supervisor Professor. Megharaj Mallavarapu. My sincere thanks for his dexterous, meticulous, patience and persistent guidance from the beginning of my PhD programme. I thank him for keeping the trust on me and his availability at any time for discussions especially during coffee and tea break. I also like to owe a great deal of gratitude and indebtedness respect to him who proved a source of great inspiration throughout the course of investigation.

I am extremely grateful to my co-supervisor Dr. Suresh Subashchandrabose for his guidance, motivation and many brain stroming session during my research tenure that gave me enough confidence to carry out my works with ease.

I would like to owe my thanks and respect to my Professor. Venkateswaralu Kadiyala for moulding me with his immense experencie and advice on research data analysis, interpretation and suggestions all through my out research.

I appreciate Dr. Logeshwaran for his deep understanding, valuable and skillful guidance to carry out my research and moral support at in need situations.

I thank my lab mates Isiri, Kartik for their support in the lab during this research period and Shankar, Shruthi, Aravind for their valuable support through discussion, analysis mostly in personal that drove me to successfully complete my research during the entire course of time.

I express my gradittude for Prof Ravi Naidu for providing a world class research environment GCER and CRC Care for their valuable support and help.

I express my deep sense of thanks to Raji akka, Anita akka and their family whose care, affection and support motivated me to work towards the cherished goal.

Words are inadequate to express my immense pleasure in acknowledging the moral support, source of encouragement and peace of mind showered upon me by my beloved dad.

ABSTRACT

Mining plays a crucial role in the economy of many countries and is one of the primary sources of mineral commodities that are essential in everyday life. The natural process of oxidation (induced by microbial activity or weathering of waste rocks and tailings), lead to the dissolution of pyrite that tends to produce acid mine drainages (AMD). The critical characteristics of AMD are the low pH (2-4) and bioavailability of metals and metalloids including iron, arsenic, cadmium, zinc, cobalt, copper, etc. which at significant levels pose a serious threat to the environment. Conventional treatment involves both active and passive approaches which include the mechanisms such as complexation, sedimentation, and adsorption to immobilize metals and neutralize pH of AMD. However, several limitations, such as excessive chemicals, capital investment, treatment efficiency, and disposal to the environment necessitate the practice of alternative treatment techniques. Microalgae are ubiquitous organisms and some of which can thrive in extreme environments including acid mine drainages are commonly known as acidophiles.,. Besides acquiring innate tolerance to survive in AMDs, the potential of acidophilic microalgae in remediation is very limited. Therefore, this study was aimed to develop green approaches using acid-tolerant microalgae (phycoremediaiton) for cost-effective AMD treatment.

Non-acidophilic microalgae species *Desmodesmus* sp. MAS1 and *Heterochlorella* sp. MAS3 were found to grow in acid pH with a minimal cell density of 5×10^5 cells mL^{-1} compared to other reference strains of microalgae. Growth analysis indicated that both the microalgal strains possessed a passive uptake of CO_2 at pH 3.0. Flow cytometry analysis for reactive oxygen species, membrane permeability, and neutral lipids revealed the capabilities of both the strains to adapt to the stress imposed by acidic pH. Lipid production doubled in both the strains when grown at pH 3.0. *In-situ* transesterification of biomass resulted in 13-15% FAME yield in the selected microalgae, indicating their great potential in biofuel production.

Desmodesmus sp. MAS1 and *Heterochlorella* sp. MAS3, isolated from neutral pH environments were investigated for their ability to simultaneously remove heavy metals such as copper (Cu), cadmium (Cd), iron (Fe), manganese (Mn), and zinc (Zn) and produce biodiesel when grown at pH 3.5. Excepting Cu, the selected metals at concentrations of 10−20 mg L^{-1} supported good growth of both the strains. MAS1 was tolerant even to 20 mg L^{-1} of Cd while strain MAS3 could withstand only up to 5 mg $L^{-1.}$ Cellular analysis for metal removal revealed the predominance of intracellular mechanism in both the strains resulting in 40−80 and

40−60% removal of Fe and Mn, respectively. FTIR analysis revealed that the symmetric vibrational stretch observed in Amide-I region (1650-1670 cm^{-1}) increased with increasing concentrations of metals in MAS1, but not in MAS3. However, the symmetric and asymmetric vibrational stretches characteristic of carboxylic esters (1735-1750 cm^{-1}) and methylene groups (2925 and 2960 cm^{-1}) of lipids were significant in strain MAS3 than in strain MAS1. FTIR analysis of metal-laden biomass indicated the production of substantial amounts of biodiesel rich in fatty acid esters.

Sustainable resource recovery is the key to manage the overburden of various waste entities of mining practices. The present study demonstrates for the first time a novel approach for iron recovery and biodiesel yield from two acid-adapted microalgae, *Desmodesmus* sp. MAS1 and *Heterochlorella* sp. MAS3, grown in synthetic acid mine drainage (SAMD). Virtually, there was no difference in growth of the strain MAS3 both in Bold's basal medium (control) and SAMD. Using IC50 level (200 mg L^{-1}) and a lower concentration (50 mg L^{-1}) of iron in SAMD, the cell granularity, exopolysaccharide (EPS) secretion, iron recovery, and biodiesel were assessed in both the strains. Both cell granularity and accumulation of EPS were significantly altered under metal stress in SAMD, resulting in an increase in total accumulation of iron. Growth of the microalgal strains in SAMD yielded 12–20% biodiesel, with no traces of heavy metals, from the biomass. The entire amount of iron, accumulated intracellularly, was recovered in the residual biomass. Our results on the ability of the acid-adapted microalgal strains in iron recovery and yield of biodiesel when grown in SAMD indicate that they could be the potential candidates for use in bioremediation of extreme habitats like AMD.

Phenotypic plasticity or genetic adaptation in an organism provides phenotypic changes when exposed to the extreme environmental conditions. The resultant physiological and metabolic changes greatly enhance the organism's potential for its survival in such harsh environments. In the present novel approach, we tested the hypothesis whether acid-adapted microalgae, initially isolated from non-acidophilic environments, can survive and grow in acid-mine-drainage (AMD) samples. Two acid-adapted microalgal strains, *Desmodesmus* sp. MAS1 and *Heterochlorella* sp. MAS3, were tested individually or in combination (co-culture) for phenotypic changes during their growth in samples collected from AMD. The acid-adapted microalgae in AMD exhibited a two-fold increase in growth when compared with those grown at pH 3.5 in BBM up to 48h and then declined. Furthermore, oxidative stress triggered several alterations such as increased cell size, granularity, and enhanced lipid accumulation in AMD-grown microalgae. Especially, the apparent limitation of phosphate in AMD inhibited the

uptake of copper and iron in the cultures. Interestingly, growth of the acid-adapted microalgae in AMD downregulated amino acid metabolic pathways as a survival mechanism. This study demonstrates for the first time that acid-adapted microalgae can survive under extreme environmental conditions as exist in AMD by effecting significant phenotypic changes.

Acid mine drainage (AMD) resulting from mining activities is a serious threat to the environment affecting terrestrial and aquatic life. In this study, acid-adapted microalgae, *Desmodesmus* sp. MAS1 and *Heterochlorella* sp. MAS3, were assessed for their ability in iron (Fe) removal from acid mine drainage samples using varying cell densities in non-immobilized and immobilized systems. Use of free-cells and immobilized cells exhibited 46-48% and 65-79% Fe removal, respectively, after 48 h of incubation. Flow cytometry analysis revealed significant changes in morphology (FSC) and granularity (SSC) in non-immobilized cells than in cells immobilized in alginate beads exposed to AMD samples. Second derivative spectra from Fourier transform infrared (FTIR) spectroscopy revealed vibration stretching for polysaccharides (1094 cm^{-1}) of free-cells, and protein (1500-1700 cm^{-1}), hydroxyl (3000-3500 cm^{-1}) of immobilized cells as a protective mechanism against Fe present in AMD samples. Group clustering of variables of free-cells and immobilized cells of microalgal strains was very evident as revealed by principal component analysis. Artificial neural network modelling validated the experimental data obtained in column studies with $R2 > 0.95$. Fixed bed column was conducted using two different bed depths of 1 cm and 2 cm with immobilized microalgal strains of MAS1 and MAS3 achieved a greater breakthrough time for 2 cm bed height, indicating the requirement for an extended contact time of the adsorbate to the adsorbent. The present study demonstrates the application of microalgal cells entrapped in alginate beads in batch and column in a greener and economical approach to treat AMD for sustainable mining.

All these experiments comprehend the effectiveness of acid-tolerant microalgae MAS1, and MAS3 as promising candidates for AMD remediation. Further, the studies also revealed possible recovery of metal (Fe) from the residual biomass after biodiesel extraction.

List of publications

1. **Abinandan S**, Subashchandrabose SR, Venkateswarlu K, Megharaj M (2018a): Microalgae–bacteria biofilms: a sustainable synergistic approach in remediation of acid mine drainage. Applied Microbiology and Biotechnology 102, 1131–1144 *(Chapter 2)*
2. **Abinandan S**, Subashchandrabose SR, Venkateswarlu K, Megharaj M (2018b): Nutrient removal and biomass production: advances in microalgal biotechnology for wastewater treatment. Critical reviews in biotechnology, 38, 1224–1260 *(Chapter 2)*
3. **Abinandan S**, Subashchandrabose SR, Cole N, Dharmarajan R, Venkateswarlu K, Megharaj M (2019a): Sustainable production of biomass and biodiesel by acclimation of non-acidophilic microalgae to acidic conditions. Bioresource Technology 271, 316–324 *(Chapter 3)*
4. **Abinandan S**, Subashchandrabose SR, Pannerselvan L, Venkateswarlu K, Megharaj M (2019b): Potential of acid-tolerant microalgae, *Desmodesmus* sp. MAS1 and *Heterochlorella* sp. MAS3, in heavy metal removal and biodiesel production at acidic pH. Bioresource Technology 278, 9–16 *(Chapter 4a)*
5. **Abinandan S**, Subashchandrabose SR, Venkateswarlu K, Perera IA, Megharaj M (2019c): Acid-tolerant microalgae can withstand higher concentrations of invasive cadmium and produce sustainable biomass and biodiesel at pH 3.5. Bioresource Technology 281, 469–473. *(Chapter 4c)*
6. **Abinandan S,** Subashchandrabose SR, Venkateswarlu K, Megharaj M (2020a): Sustainable Iron Recovery and Biodiesel Yield by Acid-Adapted Microalgae, *Desmodesmus* sp. MAS1 and *Heterochlorella* sp. MAS3, Grown in Synthetic Acid Mine Drainage. ACS omega, 5(12), pp.6888–6894. *(Chapter 5)*
7. **Abinandan S,** Perera IA, Subashchandrabose SR, Venkateswarlu K, Cole N, Megharaj M (2020b): Acid-adapted microalgae exhibit phenotypic changes for their survival in acid mine drainage samples. FEMS Microbiology Ecology. fiaa113, https://doi.org/10.1093/femsec/fiaa113. *(Chapter 6)*
8. Perera IA, **Abinandan S**, Subashchandrabose SR, Venkateswarlu K, Naidu R, Megharaj M (2019): Advances in the technologies for studying consortia of bacteria and cyanobacteria/microalgae in wastewaters. Critical Reviews in Biotechnology 39, 709–731. *(Others)*
9. **Abinandan S**, Subashchandrabose SR, Venkateswarlu K, Megharaj M (2019). Soil microalgae and cyanobacteria: the biotechnological potential in the maintenance of soil fertility and health. Critical reviews in biotechnology 39, 981–998. *(Others)*

Chapter 1 Introduction and Scope of Study

1.1. Mining industry

Due to an overwhelming rate of population increase, the role of water has become critical, which necessitates sustainable approaches to be adopted in industries to reuse and efficiently manage the resources. The mining sector is the primary source of income in many countries, which plays an essential role in gross domestic product (GDP). Notably, open-cut mining operations lead to higher loads of water pollution compared to underground mining that is practiced mostly in coal mine operations (Weng et al., 2012). According to world mining data (2016), the total mineral production over the world is about 17 billion metric tons until 2014, among them China, USA, Russia, Australia, and India are the top five nations contributing to the production rate. However, the mining process involves water-intensive operations sourced from all the available water resources (Thiruvenkatachari et al., 2016). For instance, the mining industries in Australia consume 652 GL in 2013-2014, which is a 29% increase compared to 2008-2009 (ABS, 2016). More specifically, the water consumption in mining industries is region-specific depending on the mining operations. The Hunter Valley has the most significant mining operations in the New South Wales region in Australia, predominantly the mining of coal and metal ore utilizes 97% of the water allocated for activities.

These processes also cause environmental impacts on air, water, and soil pollution unless managed thoughtfully with policies and frameworks (Akcil and Koldas, 2006; Azapagic, 2004). For instance, the sediments exposed to AMD constitute metal and metalloids viz., As, Pb, Zn, Cu with a concentration of >1000 mg kg-1 (Valente et al., 2015). Further, the impoundments showed potential AMD formation consisting of 2.5 -3.7 wt% equivalent of pyrite before oxidation process (Sima et al., 2011). In the waste pile, pyrite fraction was found increasing with the depth showing the signs of reduced oxidation process (Jodeiri Shokri et al., 2016). China alone generates 242.2 MT tailings in metal ore mining and processing (Li, 2006). Similarly, the Chilean copper mine has produced 100 tons of tailings per ton of copper in 2007. Hence, it is very clear and evident from the above geochemistry the potential of AMD formation and its negative implications for the environment. The initial identification of environmental impact due to the discharge of acid mine drainage and its percolating ability is undeniable. A few reports have also studied the remediation options (chemical, bacterial),

stream impacts and climate change (Anawar, 2013; Gazea et al., 1996; Johnson and Hallberg, 2005; Matlock et al., 2002; Papirio et al., 2013; Sheoran et al., 2010; Simate and Ndlovu, 2014).

1.2. Acid mine drainage

The acidic effluent produced from the rock interaction is most hazardous and usually stockpiled in tailing dams. Earlier, the term acid rock drainage (ARD) was used for the water polluted with sulfate oxidation during mining activity. Since these polluted streams predominately originate during mining operations, ARD is renamed as acid mine drainage (Dold, 2010; Simate and Ndlovu, 2014). The acid rock drainage also generates neutral/base (higher pH values due to lower permeability of rock, bicarbonate exchange and abundant feldspars) and saline mine drainage (seawater intrusion in mining) (Nordstrom et al., 2015). Besides, the neutral mine drainage (NMD) and saline mine drainage (SMD) would be natural to control or reduce the pollutant loads using membrane technology, and evaporation ponds. Nevertheless, the possibility of having elevated metal and metalloids concentration is higher than the sulfate content for neutral mine drainage and high salinity in saline mine drainage (GARD, 2009). However, acid mine drainage continue to be an immediate hazardous threat. For example, Nordstrom et al. (2000) identified the lowest pH range for acid mine drainage as -3.6-1.51 based on Pitzer ion-interaction and also contains TDS with a density of 1.4 g cm-3, respectively. Furthermore, the acid mine drainage (AMD) is produced especially, by pyrite oxidation (iron sulfide minerals) that is abundant in coal and metallic ore beds (Qureshi et al., 2016).

The source of AMD from the mining sites include waste rock dumps, ore stockpiles, tailings deposits, mine pits, heap leach pads and slags (Blowes et al., 2014; Johnson and Hallberg, 2005; Nordstrom et al., 2015). Usually, the pH of the acid mine drainage varies from 1-3, where the potential for oxidation is low (Stumm and Morgan, 1970). Previous reports have suggested the mechanism of AMD formation based on oxidation (Evangelou and Zhang, 1995; Lowson, 1982). Nevertheless, at the pH >4, the influence of biological or chemical mediated oxidation is very intense (Akcil and Koldas, 2006). Taylor et al. (1984) found that oxidation of sulfides in the anaerobic and aerobic zone was primarily due to chemical and biological intervention. Iron-oxidizing bacteria such as Thiobacillus ferroxidans and Leptospirillum ferroxidans were mostly responsible for initiating these mechanisms in the aerobic zone (Johnson and McGinness, 1991; Leduc et al., 2002). Conversely, the count of neutrophilic heterotrophs was found to be higher than iron-oxidizing bacteria over the distance from the drain (McGinness

and Barrie Johnson, 1993). Lefebvre et al. (2001a) reported that oxidation of permeable rock would exhibit temperature-driven air convection, whereas low permeable rock follows gaseous diffusion and convection. The pyrite oxidation rates due to the action of microbes are 106 times faster than the abiotic process (Butler, 2007).

The participation of secondary minerals such as gypsum and jarosite significantly contribute to AMD by establishing foliation planes in the rock thereby intensify the access of oxidants (O^2 and Fe^{3+}) (Sracek et al., 2004). Also, the rare earth elements (REE) present can be precipitated during the oxidation of Fe(III) to hydrous oxide forms of Fe(III) (da Silveira et al., 2009). These species can be used as a tracer for AMD to identify the progression of percolation in the surface waters (da Silveira et al., 2009; Ferreira da Silva et al., 2009; Verplanck et al., 2004). This precipitation usually occurs at a higher temperature and pH resulting in the formation of lepidocrocite (at neutral pH–), a mixture of schwertmannite, goethite, ferrihydrite (at acidic pH) (Jönsson et al., 2006). Other minerals such as quartz, kaolinite, calcite, dolomite, and pyrite were also found in coal mining areas which can able to predict the extent of acidity of AMD (Pinetown et al., 2007). However, the weathering process did not seem to affect the concentration of dissolved organic carbon (DOC) compared to dissolved inorganic carbon (DIC). As a result of the exchange between protons and electrons (HCO_3 in DIC) the hydrolysis of Fe2+ to Fe (OH)3 takes place (Fonyuy and Atekwana, 2008; Søndergaard et al., 2008). This hydrolysis reaction tends to exhibit more acidity and aggravates the buffering nature of AMD with pH ranging 2.5-3.5 (Fe-Fe (OH) redox equilibrium) thus enhancing the mobility and toxicity of the heavy metals. (Sánchez España et al., 2005; Tutu et al., 2008). For example, the heterogeneous oxidation of arsenite is very crucial during the weathering process of pyrite oxidation (Cheng et al., 2009). Further, there are studies on geologic variation presenting two mechanisms of pyrite oxidation with sulfide and ferric iron as separate primary oxidants with water as the main source for oxygen to initiate the process (Hubbard et al., 2009). However, there is the possibility of slow rates of oxidation by an alteration in gouge minerals such as Mg/Fe-carbonates (Lei and Watkins, 2005).

1.3. Environmental Impact of AMD

The geochemistry provides sufficient information on the generation of AMD as well as it helps to understand the leaching behavior of AMD. For example, nearly 19000 km of streams and 72,000 ha of lakes and reservoirs are affected throughout the world (Johnson and Hallberg, 2005). The reason behind thispollution load is the formation of hydrous iron oxides, which

precipitates and form colloids with the help of bicarbonates in the water (Kimball et al., 1995). However, the concentration of heavy metals (Zn, Cu) varies during wetter months and leads to higher toxicity in nearby river streams (Gray, 1998). These river streams have the potential to transport the heavy metal loads into the ocean. Olías et al. (2006) found that Odiel and Tinto rivers located in Spain exhibit massive quantity of heavy metal loads, especially global gross flux of around 60% (1700 t a^{-1}) and 17% (3500 t a^{-1}) of Cu and Zn into the ocean. Later, these amounts peak during the rainy season resulting in higher floods and enhancing the reactivity of heavy metals with bicarbonates (Nieto et al., 2013). Hence, a tremendous decrease in the phytoplankton community occurred as a result of the bioavailability of Zn, As, Cd and Fe (Bortnikova et al., 2001). For example, mussel growth was adversely affected by the over-accumulation of Cu in the contaminated creek following the reduction of other phytoplankton (Grout and Levings, 2001). Similarly, experiments by Gerhardt et al. (2004) on *Gambusia holbrooki* (mosquito), and *Atyaephyra desmaresti* (shrimp) revealed shrimp was more sensitive, and toxicity was pH-dependent which led to a decrease in the activity of locomotion.

In another study, it was found that macroinvertebrates were significantly tolerant of heavy metal load rather than pH (Solà et al., 2004). Nevertheless, the sites contaminated with vast quantities of mine drainage showed less population of macroinvertebrate density due to the high specific conductance caused by the concentration of heavy metals (MacCausland and McTammany, 2007). Also, the soil in the vicinity of AMD storage showed contamination levels up to 15 m from the ponds and 2-6 m depth from the surface leading to contamination of groundwater (Mapanda et al., 2007). Further, these streams contaminated with AMD will cause the hydrolysis of carbonates and bicarbonates, leading to carbon release from the water associated with DIC loss (Fonyuy and Atekwana, 2008). Unenviably, the heavy metals from AMD also affect other characteristics such as ionic strength and contaminate the bed sediments intermittently affecting the ecology (Butler, 2009). Boukhalfa and Chaguer (2012) observed the dominance of jarosite and schwertmannite as precipitates in the Essouk river near the vicinity of the mine. Similarly, it was noted that the downstream of the river tributary, sediments are enriched with copper ions, which originated from the evolution of AMD (Sracek et al., 2012). Significant distribution of heavy metals at elevated levels near the mine site and watersheds located in the vicinity also affected the soil quality (Zhao et al., 2012a). Besides, the sediments in the streambed possess minerals in the order of schwertmannite, goethite, quartz and transforms to bidentate, monodentate complexes along the downstream due to natural attenuation process. (Zhao et al., 2012b).

Also, these sediments tend to adsorb heavy metals by two-fold magnitude and can re-diffuse to the water under affluent aerobic circumstances (Torres et al., 2013). This trend was consistent with a study that highlighted the toxicity, which was higher when the bacteria population was directly exposed to the sediments (Han et al., 2015). Besides, these effects tend to disrupt the genetic diversity of the natural community in the aquatic region and increase the mortality rate despite tolerance (Belfiore and Anderson, 2001). Martins et al. (2009) found that there was a significant genetic differentiation among the tolerant species of *Daphnia longispina.* Similarly, the acute lethal toxicity observed in indigenous species *Moina macrocopa* due to the partial neutralization of AMD treated plants suggested the importance of toxic potential when mixing with river bodies. (Seo et al., 2012). Further, it was recommended that the possibilities of the genotoxicity to the invertebrate might significantly change seasonally by inducing a higher degree of toxicity, especially during monsoon season due to the excess bioavailability of the toxic compounds (Talukdar et al., 2016). Nonetheless, these metal interferences disrupt physiological functions of plant cell, especially at molecular and cellular levels (He et al., 2005). For instance, the toxicity was higher in *Allium cepa* L. (bioindicator) when exposed to AMD, resulting in DNA damage compared to the exposure to treated AMD. Thus, these facts demonstrate that AMD is a severe threat to the environment, which necessitates the need for its remediation.

1.4. Conventional treatment technologies for AMD

The use of chemicals such as limestone is one of the predominantly used technology to treat acid mine drainage, but this technology has a limitation due to its lower solubility and dissolution rate. However, the structure of a passive technology system with limestone is accessible due to low-cost and easy maintenance. Application of limestone in channel drains well are the standard options in the passive system (Cravotta Iii and Trahan, 1999). Despite, limestone tends to possess hydroxide coatings that reduced the efficiency of treatment systems and can show improvement only by modifying the technology. Hammarstrom et al. (2003) showed that the use of the pulsed limestone bed systems had reduced the formation of coatings. The use of pulp solution along with biomass has shown recovery of metals and also improved filtration and sedimentation rates (Santos et al., 2004). Still, reconfiguration or redesigning of the flow path to the limestone treatment bed could increase the surface area along with a cross-sectional area in perpendicular and can prevent the system from clogging thereby reduce the heavy metal loads (Cravotta Iii, 2008). However, the clogging was also observed during the treatment of the dispersed alkaline substrate with a

chemical gradient and a coarse inert matrix (Rötting et al., 2008). The formation of gypsum when the flow gets in contact with the limestone is one of the hindrances in the process, which could be prevented by pre-neutralization step. For instance, the use of olivine (magnesium-rich silicate) for pre-treatment can prevent gypsum formation only at the pH>3 (Kleiv and Thornhill, 2008). The re-dissolution of heavy metals from the sludge that formed while treating the AMD with flocculants is a setback to the chemical dosing of AMD. However, identifying effective flocculants is a strategy to resist the re-dissolving nature of heavy metals from the sludge. Demers et al. (2009) used activated silica sol as flocculant, which formed metal silica bonds with sludge resisting the dissolution. Diao et al. (2013) used tetraethylorthosilicate (TEOS) and N-propyltrimethoxysilane (NPS) coatings to control the generation of AMD in the source, i.e., pyrite rock that showed effectiveness in suppressing pyrite oxidation.

The use of industrial by-products or waste materials to mitigate AMD streams has also been receiving overwhelming interest. AMD treatment with fly ash and dolomite resulted in the reduction of heavy metals as well as cost savings due to reduced cost of chemicals (esp. lime) involved in the treatment systems (Potgieter-Vermaak et al., 2006). Calcium-rich additives from coal combustion by-products such as lime kiln dust were tested as grout to suppress the action of AMD (Bulusu et al., 2007). The use of $CaCO_3$ recovered from waste gypsum in AMD has significantly helped in the neutralization process when compared with commercial $CaCO_3$ (Zvimba et al., 2012). Besides, coal fly ash also reduced the radioactive materials that are dissolved in AMD upon treatment (Madzivire et al., 2014). Since, the AMD is rich in metals such as iron and aluminum depending upon the sources of mine which necessitate the recovery of minerals from the process. Herrera et al. (2007) used two-step neutralization process using magnesium oxide and sodium hydroxide to recover ferrite from the AMD. Masindi et al. (2015) showed that post neutralization, heavy metals are available in mineral forms for Fe: hydroxides, goethite, jarosite; Al: basaluminite, boehmite, jurbanite, gibbsite, diaspore; Mn: rhodochrosite, manganite; Ca, SO_4: gypsum; Mg: brucite and dolomite. Other treatment methods include electrochemical treatment and filtration, which seems very expensive to treat on a field scale. The use of plant biomass is one of the practical solutions to absorb heavy metals from the acid mine drainage due to its metal binding capacities. Similarly, chemical treatment with Fenton process resulted in a higher reduction of Fe^{2+}, Cu^{2+} along with easy sludge dewaterability (Mahiroglu et al., 2009). But, the use of H_2O_2/Fe(II) showed higher removal rates and are economically cheaper, ranging from 17-32% when compared to chemical coagulation (Dong et al., 2011). The life cycle assessment of active treatment systems

(chemical dosing) and passive treatment systems (sulfidogenic reactors) have shown that passive treatment is an environmentally friendly approach, but doesn't meet the sustainable AMD treatment (Hengen et al., 2014). Nonetheless, the combination of both the active and passive treatments can reduce the costs and environmental impacts associated with each despite using waste resources in the treatment. The combination of chemical and biological treatment or other measures has produced much better results, and the toxicity to aquatic life has reduced (Pagnanelli et al., 2008). The combination of the natural iron-oxidizing lagoon along with limestone-DAS had reduced heavy metals (>90%) such as Fe, Al, Cu, Pb and As, respectively (Ayora et al., 2013). Besides, the potential of microbial life that thrives in the AMD environments may serve as a viable alternative strategy in finding new treatment technology for remediating AMD streams.

1.5. Microalgae

Microalgae are ubiquitous and versatile photoautotrophic microorganisms that possess the ability to adapt effortlessly to diverse conditions (Lau et al., 1995). Oswald (1957) initiated the microalgal technology, referred to as phycoremediation in the 1950s. The microalgal biomass is known for biofuels, biofertilizers, and biochemical metabolites for pharmaceutical and nutraceutical applications (Oswald and Gotaas, 1957). Commercial cultivation of algae also provides the opportunity for large scale value-added product generation (Lam and Lee, 2012; Ugwu et al., 2008). The widely adopted methods for algal cultivation with wastewater systems include open pond cultivation systems viz., raceway pond, high rate algal ponds and bioreactors with light energy, often called photobioreactors (PBRs) that are available in commercial-scale as well. However, these systems possess both merits and demerits under certain conditions. Both fresh and marine waters have been utilized to generate microalgal biomass and further to develop value-added products. Since the cost involved in the production of growth media to culture microalgal biomass is enormous, the use of wastewaters as a source for algal cultivation simultaneously provides both opportunities for bioremediation and biomass production (Kumar et al., 2015; Liu et al., 2016a; Liu et al., 2016b; Subramaniyam et al., 2016).

1.6. Research Gaps

This review reveals that the impact of acid mine drainage on the environment is very detrimental. Although, chemical methods and biological remediation using specific bacteria have shown some positive trend, yet, other aspects of the situation, life cycle assessment and

more importantly sustainability at the field scale application is still not established. Certain studies have pointed out the existence of microbial life in the AMD and its characteristics. Interestingly, metagenomics analysis shows the presence of algae in many AMD sites. The role of algae in the community and its part in remediation is still unknown at this stage. Algae have shown to sequester heavy metals via accumulation in their cell walls. Besides, few studies have been carried out using algae to treat AMD which are based on the combined approach with alkaline material (Choi and Lee, 2015), post-treatment as polishing step (Oberholster et al., 2016), hybrid technologies (Park et al., 2013). Recently Orandi and Lewis (2013) used green microalgae native to copper mine (Iran) in biofilm development to treat artificial mine drainage with metal removal. Microalgae in neutrophilic habitats are shown capable of remediating metal based on the functional groups, polysaccharide, and other intrinsic mechanisms and the application towards AMD remediation is not explored. We hypothesized that acclimated non-acidophilic microalgae together with their acidophilic counterparts, can enhance the performance of biofilms in continuous treatment of AMDs (Abinandan et al., 2018). Hence, the research focused on identifying acid-tolerant microalgae from various environments and evaluating their potential for AMD remediation. The conceptual framework of the Ph. D. study is outlined in Fig. 1

1.7 The primary objectives of this research are:

- Isolation and characterization of acid-tolerant microalgae from non-acidophilic environments.
- Investigation of growth and biochemical responses of acid-tolerant microalgae to various metal concentrations.
- Unraveling the tolerance potential of microalgae to synthetic AMD.
- Mechanistic exploration of microalgae responses in real AMD.
- Development of novel bio-filter based on acid-tolerant microalgae for AMD remediation.

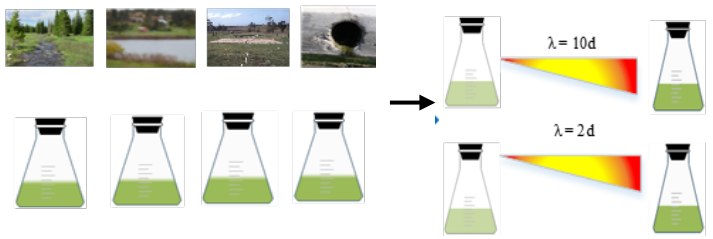

Section 1- Screening of microalgae

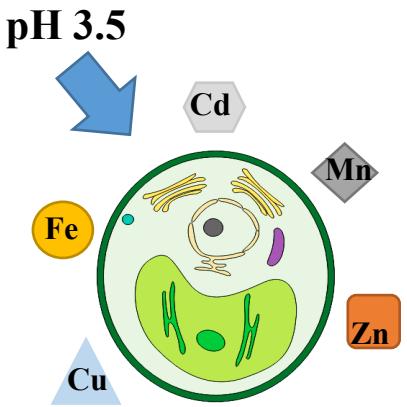

Section 2-Responses of microalgae to HMs at acid pH

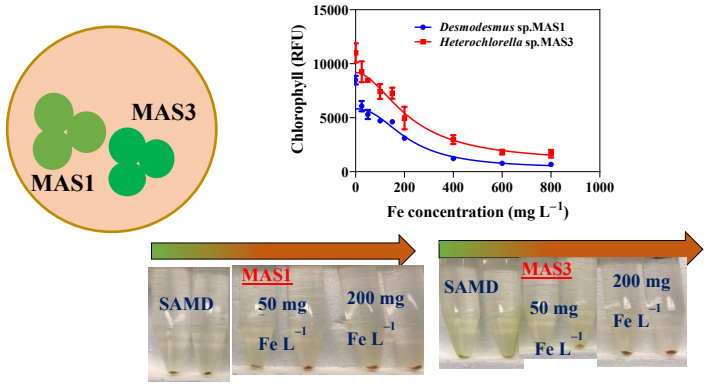

Section 3- Tolerance potential of microalgae to synthetic AMD

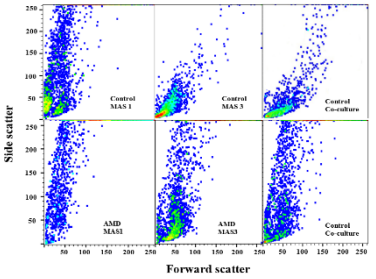

Cell properties

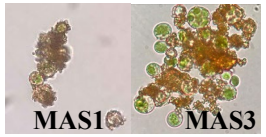

Microscopic image

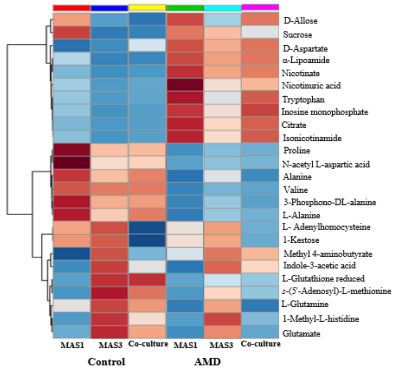

Metabolomic

Section 4- Microalgae response in real AMD

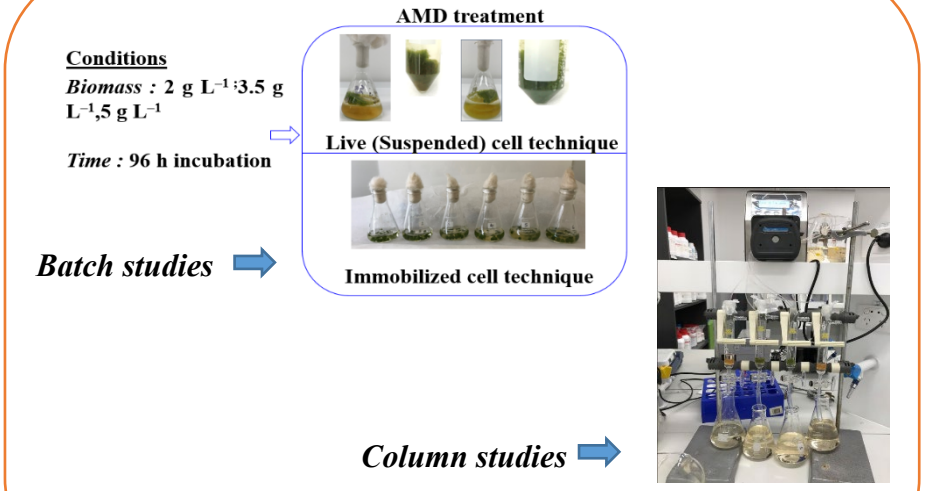

Section 5- Novel bio-filter development for AMD remediation

Fig. 1.1. Conceptual framework

1.8. Significance of the work

The use of chemicals is the most extensive treatment option along with wetland in treating AMD, which leads to serious environmental disaster. In some cases, formation of chemical precipitates such as hydroxide coatings in the treatment systems decreases the remediation potential. The microbes present in the streams inherently develop tolerance to the acidic pH and metals ,their potential to remediate AMD has been low. This research focuses on fostering the acid-tolerant strains from non-acidophilic environments, which can provide a leap towards its role in remediating AMD. Further, this will decrease the input of chemicals involved in treatment, making the process very cheap and sustainable. Further, the resulting biomass from AMD treatment can be used for value-added product generation such as biofuels and resource recovery. The AMD treatment proposed in this study is unique and sustainable which integrates three key technologies such as remediation, energy production and resource recovery. This method is also less energy-intensive when compared to the existing conventional approaches.

1.9. References

Abinandan, S., Subashchandrabose, S.R., Venkateswarlu, K., Megharaj, M., 2018. Microalgae–bacteria biofilms: a sustainable synergistic approach in remediation of acid mine drainage. Applied Microbiology and Biotechnology 102(3), 1131–1144.

ABS, 2016. 4655.0-Australian Environmental- Economic Accounts, 14.04.2016 ed. Australian Bureau of Statistics.

Akcil, A., Koldas, S., 2006. Acid Mine Drainage (AMD): causes, treatment and case studies. Journal of Cleaner Production 14(12–13), 1139–1145.

Anawar, H.M., 2013. Impact of climate change on acid mine drainage generation and contaminant transport in water ecosystems of semi-arid and arid mining areas. Physics and Chemistry of the Earth, Parts A/B/C 58–60, 13–21.

Azapagic, A., 2004. Developing a framework for sustainable development indicators for the mining and minerals industry. Journal of Cleaner Production 12(6), 639–662.

Belfiore, N.M., Anderson, S.L., 2001. Effects of contaminants on genetic patterns in aquatic organisms: a review. Mutation Research/Reviews in Mutation Research 489(2–3), 97–122.

Blowes, D.W., Ptacek, C.J., Jambor, J.L., Weisener, C.G., Paktunc, D., Gould, W.D., Johnson, D.B., 2014. 11.5 - The Geochemistry of Acid Mine Drainage A2 - Holland, Heinrich D, in:

Turekian, K.K. (Ed.) Treatise on Geochemistry (Second Edition). Elsevier, Oxford, pp. 131–190.

Bortnikova, S.B., Smolyakov, B.S., Sidenko, N.V., Kolonin, G.R., Bessonova, E.P., Androsova, N.V., 2001. Geochemical consequences of acid mine drainage into a natural reservoir: inorganic precipitation and effects on plankton activity. Journal of Geochemical Exploration 74(1–3), 127–139.

Boukhalfa, C., Chaguer, M., 2012. Characterisation of sediments polluted by acid mine drainage in the northeast of Algeria. International Journal of Sediment Research 27(3), 402–407.

Bulusu, S., Aydilek, A.H., Rustagi, N., 2007. CCB-based encapsulation of pyrite for remediation of acid mine drainage. Journal of Hazardous Materials 143(3), 609–619.

Butler, B.A., 2009. Effect of pH, ionic strength, dissolved organic carbon, time, and particle size on metals release from mine drainage impacted streambed sediments. Water Research 43(5), 1392–1402.

Butler, T.W., 2007. Isotope geochemistry of drainage from an acid mine impaired watershed, Oakland, California. Applied Geochemistry 22(7), 1416–1426.

Cheng, H., Hu, Y., Luo, J., Xu, B., Zhao, J., 2009. Geochemical processes controlling fate and transport of arsenic in acid mine drainage (AMD) and natural systems. Journal of Hazardous Materials 165(1–3), 13–26.

Choi, H.-J., Lee, S.-M., 2015. Heavy metal removal from acid mine drainage by calcined eggshell and microalgae hybrid system. Environmental Science and Pollution Research 22(17), 13404–13411.

Cravotta Iii, C.A., 2008. Laboratory and field evaluation of a flushable oxic limestone drain for treatment of net-acidic drainage from a flooded anthracite mine, Pennsylvania, USA. Applied Geochemistry 23(12), 3404–3422.

Cravotta Iii, C.A., Trahan, M.K., 1999. Limestone drains to increase pH and remove dissolved metals from acidic mine drainage. Applied Geochemistry 14(5), 581–606.

da Silveira, A.N., Silva, R., Rubio, J., 2009. Treatment of Acid Mine Drainage (AMD) in South Brazil: Comparative active processes and water reuse. International Journal of Mineral Processing 93(2), 103–109.

Demers, I., Finch, J., El-Ammouri, E., 2009. Use of activated silica sol as a flocculant in the treatment of acid mine drainage to promote sludge stability. Minerals Engineering 22(5), 506–512.

Diao, Z., Shi, T., Wang, S., Huang, X., Zhang, T., Tang, Y., Zhang, X., Qiu, R., 2013. Silane-based coatings on the pyrite for remediation of acid mine drainage. Water Research 47(13), 4391–4402.

Dold, B., 2010. Basic concepts in environmental geochemistry of sulfidic mine-waste management. INTECH Open Access Publisher.

Dong, H., Guan, X., Wang, D., Li, C., Yang, X., Dou, X., 2011. A novel application of H2O2–Fe(II) process for arsenate removal from synthetic acid mine drainage (AMD) water. Chemosphere 85(7), 1115–1121.

Evangelou, V.P., Zhang, Y.L., 1995. A review: Pyrite oxidation mechanisms and acid mine drainage prevention. Critical Reviews in Environmental Science and Technology 25(2), 141–199.

Ferreira da Silva, E., Bobos, I., Xavier Matos, J., Patinha, C., Reis, A.P., Cardoso Fonseca, E., 2009. Mineralogy and geochemistry of trace metals and REE in volcanic massive sulfide host rocks, stream sediments, stream waters and acid mine drainage from the Lousal mine area (Iberian Pyrite Belt, Portugal). Applied Geochemistry 24(3), 383–401.

Fonyuy, E.W., Atekwana, E.A., 2008. Effects of acid mine drainage on dissolved inorganic carbon and stable carbon isotopes in receiving streams. Applied Geochemistry 23(4), 743–764.

GARD, 2009. Global Acid Rock Drainage Guide (GARD Guide). INAP: The International Network for Acid Prevention.

Gazea, B., Adam, K., Kontopoulos, A., 1996. A review of passive systems for the treatment of acid mine drainage. Minerals Engineering 9(1), 23–42.

Gerhardt, A., Janssens de Bisthoven, L., Soares, A.M.V.M., 2004. Macroinvertebrate response to acid mine drainage: community metrics and on-line behavioural toxicity bioassay. Environmental Pollution 130(2), 263–274.

Gray, N.F., 1998. Acid mine drainage composition and the implications for its impact on lotic systems. Water Research 32(7), 2122–2134.

Grout, J.A., Levings, C.D., 2001. Effects of acid mine drainage from an abandoned copper mine, Britannia Mines, Howe Sound, British Columbia, Canada, on transplanted blue mussels (Mytilus edulis). Marine Environmental Research 51(3), 265–288.

Hammarstrom, J.M., Sibrell, P.L., Belkin, H.E., 2003. Characterization of limestone reacted with acid-mine drainage in a pulsed limestone bed treatment system at the Friendship Hill National Historical Site, Pennsylvania, USA. Applied Geochemistry 18(11), 1705–1721.

Han, Y.-S., Youm, S.-J., Oh, C., Cho, Y.-C., Ahn, J.S., 2015. Geochemical and eco-toxicological characteristics of stream water and its sediments affected by acid mine drainage. CATENA.

He, Z.L., Yang, X.E., Stoffella, P.J., 2005. Trace elements in agroecosystems and impacts on the environment. Journal of trace elements in medicine and biology: organ of the Society for Minerals and Trace Elements (GMS) 19(2-3), 125–140.

Hengen, T.J., Squillace, M.K., O'Sullivan, A.D., Stone, J.J., 2014. Life cycle assessment analysis of active and passive acid mine drainage treatment technologies. Resources, Conservation and Recycling 86, 160–167.

Herrera, P., Uchiyama, H., Igarashi, T., Asakura, K., Ochi, Y., Iyatomi, N., Nagae, S., 2007. Treatment of acid mine drainage through a ferrite formation process in central Hokkaido, Japan: Evaluation of dissolved silica and aluminium interference in ferrite formation. Minerals Engineering 20(13), 1255–1260.

Hubbard, C.G., Black, S., Coleman, M.L., 2009. Aqueous geochemistry and oxygen isotope compositions of acid mine drainage from the Río Tinto, SW Spain, highlight inconsistencies in current models. Chemical Geology 265(3–4), 321–334.

Jodeiri Shokri, B., Doulati Ardejani, F., Ramazi, H., 2016. Environmental Geochemistry and Acid Mine Drainage Evaluation of an Abandoned Coal Waste Pile at the Alborz-Sharghi Coal Washing Plant, NE Iran. Natural Resources Research 25(3), 347–363.

Johnson, D.B., Hallberg, K.B., 2005. Acid mine drainage remediation options: a review. Science of The Total Environment 338(1–2), 3–14.

Johnson, D.B., McGinness, S., 1991. A highly effecient and universal solid medium for growing mesophilic and moderately thermophilic, iron-oxidizing, acidophilic bacteria. Journal of Microbiological Methods 13(2), 113–122.

Jönsson, J., Jönsson, J., Lövgren, L., 2006. Precipitation of secondary Fe(III) minerals from acid mine drainage. Applied Geochemistry 21(3), 437–445.

Kimball, B.A., Callender, E., Axtmann, E.V., 1995. Effects of colloids on metal transport in a river receiving acid mine drainage, upper Arkansas River, Colorado, U.S.A. Applied Geochemistry 10(3), 285–306.

Kleiv, R.A., Thornhill, M., 2008. Predicting the neutralisation of acid mine drainage in anoxic olivine drains. Minerals Engineering 21(4), 279–287.

Kumar, K., Mishra, S.K., Shrivastav, A., Park, M.S., Yang, J.-W., 2015. Recent trends in the mass cultivation of algae in raceway ponds. Renewable and Sustainable Energy Reviews 51, 875–885.

Lam, M.K., Lee, K.T., 2012. Microalgae biofuels: a critical review of issues, problems and the way forward. Biotechnology advances 30(3), 673–690.

Lau, P., Tam, N., Wong, Y., 1995. Effect of algal density on nutrient removal from primary settled wastewater. Environmental Pollution 89(1), 59–66.

Leduc, D., Leduc, L.G., Ferroni, G.D., 2002. Quantification of Bacterial Populations Indigenous to Acidic Drainage Streams. Water, Air, and Soil Pollution 135(1), 1–21.

Lei, L., Watkins, R., 2005. Acid drainage reassessment of mining tailings, Black Swan Nickel Mine, Kalgoorlie, Western Australia. Applied Geochemistry 20(3), 661–667.

Li, M.S., 2006. Ecological restoration of mineland with particular reference to the metalliferous mine wasteland in China: A review of research and practice. Science of The Total Environment 357(1–3), 38–53.

Liu, C., Subashchandrabose, S., Ming, H., Xiao, B., Naidu, R., Megharaj, M., 2016a. Phycoremediation of dairy and winery wastewater using Diplosphaera sp. MM1. Journal of Applied Phycology, 1–11.

Liu, C., Subashchandrabose, S.R., Megharaj, M., Hu, Z., Xiao, B., 2016b. Diplosphaera sp. MM1 – A microalga with phycoremediation and biomethane potential. Bioresource Technology 218, 1170–1177.

Lowson, R.T., 1982. Aqueous oxidation of pyrite by molecular oxygen. Chemical Reviews 82(5), 461–497.

MacCausland, A., McTammany, M.E., 2007. The impact of episodic coal mine drainage pollution on benthic macroinvertebrates in streams in the Anthracite region of Pennsylvania. Environmental Pollution 149(2), 216–226.

Madzivire, G., Maleka, P.P., Vadapalli, V.R.K., Gitari, W.M., Lindsay, R., Petrik, L.F., 2014. Fate of the naturally occurring radioactive materials during treatment of acid mine drainage with coal fly ash and aluminium hydroxide. Journal of Environmental Management 133, 12–17.

Mahiroglu, A., Tarlan-Yel, E., Sevimli, M.F., 2009. Treatment of combined acid mine drainage (AMD)—Flotation circuit effluents from copper mine via Fenton's process. Journal of Hazardous Materials 166(2–3), 782–787.

Mapanda, F., Nyamadzawo, G., Nyamangara, J., Wuta, M., 2007. Effects of discharging acid-mine drainage into evaporation ponds lined with clay on chemical quality of the surrounding soil and water. Physics and Chemistry of the Earth, Parts A/B/C 32(15–18), 1366–1375.

Martins, M., Faleiro, M.L., Barros, R.J., Veríssimo, A.R., Barreiros, M.A., Costa, M.C., 2009. Characterization and activity studies of highly heavy metal resistant sulphate-reducing bacteria to be used in acid mine drainage decontamination. Journal of Hazardous Materials 166(2–3), 706–713.

Masindi, V., Gitari, M.W., Tutu, H., De Beer, M., 2016. Fate of inorganic contaminants post treatment of acid mine drainage by cryptocrystalline magnesite: Complimenting experimental results with a geochemical model. Journal of Environmental Chemical Engineering.4 (4), 4846–56.

Matlock, M.M., Howerton, B.S., Atwood, D.A., 2002. Chemical precipitation of heavy metals from acid mine drainage. Water Research 36(19), 4757–4764.

McGinness, S., Barrie Johnson, D., 1993. Seasonal variations in the microbiology and chemistry if an acid mine drainage stream. Science of The Total Environment 132(1), 27–41.

Nieto, J.M., Sarmiento, A.M., Canovas, C.R., Olias, M., Ayora, C., 2013. Acid mine drainage in the Iberian Pyrite Belt: 1. Hydrochemical characteristics and pollutant load of the Tinto and Odiel rivers. Environmental Science and Pollution Research 20(11), 7509–7519.

Nordstrom, D.K., Alpers, C.N., Ptacek, C.J., Blowes, D.W., 2000. Negative pH and Extremely Acidic Mine Waters from Iron Mountain, California. Environmental Science & Technology 34(2), 254–258.

Nordstrom, D.K., Blowes, D.W., Ptacek, C.J., 2015. Hydrogeochemistry and microbiology of mine drainage: An update. Applied Geochemistry 57, 3–16.

Oberholster, P.J., De Klerk, A.R., De Klerk, L., Chamier, J., Botha, A.-M., 2016. Algal assemblage responses to acid mine drainage and steel plant wastewater effluent up and downstream of pre and post wetland rehabilitation. Ecological Indicators 62, 106–116.

Olías, M., Cánovas, C.R., Nieto, J.M., Sarmiento, A.M., 2006. Evaluation of the dissolved contaminant load transported by the Tinto and Odiel rivers (South West Spain). Applied Geochemistry 21(10), 1733–1749.

Orandi, S., Lewis, D.M., 2013. Biosorption of heavy metals in a photo-rotating biological contactor--a batch process study. Appl Microbiol Biotechnol 97(11), 5113–5123.

Oswald, W.J., Gotaas, H.B., 1957. Photosynthesis in sewage treatment. Transactions of the American Society of Civil Engineers 122(1), 73–97.

Pagnanelli, F., De Michelis, I., Di Muzio, S., Ferella, F., Vegliò, F., 2008. Bioassessment of a combined chemical–biological treatment for synthetic acid mine drainage. Journal of Hazardous Materials 159(2–3), 567–573.

Papirio, S., Villa-Gomez, D.K., Esposito, G., Pirozzi, F., Lens, P.N.L., 2013. Acid Mine Drainage Treatment in Fluidized-Bed Bioreactors by Sulfate-Reducing Bacteria: A Critical Review. Critical Reviews in Environmental Science and Technology 43(23), 2545–2580.

Park, Y.-T., Lee, H., Yun, H.-S., Song, K.-G., Yeom, S.-H., Choi, J., 2013. Removal of metal from acid mine drainage using a hybrid system including a pipes inserted microalgae reactor. Bioresource Technology 150, 242–248.

Pinetown, K.L., Ward, C.R., van der Westhuizen, W.A., 2007. Quantitative evaluation of minerals in coal deposits in the Witbank and Highveld Coalfields, and the potential impact on acid mine drainage. International Journal of Coal Geology 70(1–3), 166–183.

Potgieter-Vermaak, S.S., Potgieter, J.H., Monama, P., Van Grieken, R., 2006. Comparison of limestone, dolomite and fly ash as pre-treatment agents for acid mine drainage. Minerals Engineering 19(5), 454–462.

Qureshi, A., Maurice, C., Öhlander, B., 2016. Potential of coal mine waste rock for generating acid mine drainage. Journal of Geochemical Exploration 160, 44–54.

Rötting, T.S., Caraballo, M.A., Serrano, J.A., Ayora, C., Carrera, J., 2008. Field application of calcite Dispersed Alkaline Substrate (calcite-DAS) for passive treatment of acid mine drainage with high Al and metal concentrations. Applied Geochemistry 23(6), 1660–1674.

Sánchez España, J., López Pamo, E., Santofimia, E., Aduvire, O., Reyes, J., Barettino, D., 2005. Acid mine drainage in the Iberian Pyrite Belt (Odiel river watershed, Huelva, SW Spain): Geochemistry, mineralogy and environmental implications. Applied Geochemistry 20(7), 1320–1356.

Santos, S., Machado, R., Joana Neiva Correia, M., Carvalho, J.R., 2004. Treatment of acid mining waters. Minerals Engineering 17(2), 225–232.

Seo, J., Kang, S.-W., Ji, W., Jo, H.-J., Jung, J., 2012. Potential Risks of Effluent from Acid Mine Drainage Treatment Plants at Abandoned Coal Mines. Bulletin of Environmental Contamination and Toxicology 88(6), 990–996.

Sheoran, A.S., Sheoran, V., Choudhary, R.P., 2010. Bioremediation of acid-rock drainage by sulphate-reducing prokaryotes: A review. Minerals Engineering 23(14), 1073–1100.

Sima, M., Dold, B., Frei, L., Senila, M., Balteanu, D., Zobrist, J., 2011. Sulfide oxidation and acid mine drainage formation within two active tailings impoundments in the Golden Quadrangle of the Apuseni Mountains, Romania. Journal of Hazardous Materials 189(3), 624–639.

Simate, G.S., Ndlovu, S., 2014. Acid mine drainage: Challenges and opportunities. Journal of Environmental Chemical Engineering 2(3), 1785–1803.

Solà, C., Burgos, M.a., Plazuelo, Á., Toja, J., Plans, M., Prat, N.s., 2004. Heavy metal bioaccumulation and macroinvertebrate community changes in a Mediterranean stream affected by acid mine drainage and an accidental spill (Guadiamar River, SW Spain). Science of The Total Environment 333(1–3), 109–126.

Søndergaard, J., Elberling, B., Asmund, G., 2008. Metal speciation and bioavailability in acid mine drainage from a high Arctic coal mine waste rock pile: Temporal variations assessed through high-resolution water sampling, geochemical modelling and DGT. Cold Regions Science and Technology 54(2), 89–96.

Sracek, O., Choquette, M., Gélinas, P., Lefebvre, R., Nicholson, R.V., 2004. Geochemical characterization of acid mine drainage from a waste rock pile, Mine Doyon, Québec, Canada. Journal of Contaminant Hydrology 69(1–2), 45–71.

Sracek, O., Kříbek, B., Mihaljevič, M., Majer, V., Veselovský, F., Vencelides, Z., Nyambe, I., 2012. Mining-related contamination of surface water and sediments of the Kafue River drainage system in the Copperbelt district, Zambia: An example of a high neutralization capacity system. Journal of Geochemical Exploration 112, 174–188.

Stumm, W., Morgan, J.J., 1970. Aquatic chemistry; an introduction emphasizing chemical equilibria in natural waters.

Subramaniyam, V., Subashchandrabose, S.R., Ganeshkumar, V., Thavamani, P., Chen, Z., Naidu, R., Megharaj, M., 2016. Cultivation of Chlorella on brewery wastewater and nano-particle biosynthesis by its biomass. Bioresource Technology 211, 698–703.

Talukdar, B., Kalita, H.K., Baishya, R.A., Basumatary, S., Sarma, D., 2016. Evaluation of genetic toxicity caused by acid mine drainage of coal mines on fish fauna of Simsang River, Garohills, Meghalaya, India. Ecotoxicology and Environmental Safety 131, 65–71.

Taylor, B.E., Wheeler, M.C., Nordstrom, D.K., 1984. Stable isotope geochemistry of acid mine drainage: Experimental oxidation of pyrite. Geochimica et Cosmochimica Acta 48(12), 2669–2678.

Thiruvenkatachari, R., Francis, M., Cunnington, M., Su, S., 2016. Application of integrated forward and reverse osmosis for coal mine wastewater desalination. Separation and Purification Technology 163, 181–188.

Torres, E., Ayora, C., Canovas, C.R., García-Robledo, E., Galván, L., Sarmiento, A.M., 2013. Metal cycling during sediment early diagenesis in a water reservoir affected by acid mine drainage. Science of The Total Environment 461–462, 416–429.

Tutu, H., McCarthy, T.S., Cukrowska, E., 2008. The chemical characteristics of acid mine drainage with particular reference to sources, distribution and remediation: The Witwatersrand Basin, South Africa as a case study. Applied Geochemistry 23(12), 3666–3684.

Ugwu, C., Aoyagi, H., Uchiyama, H., 2008. Photobioreactors for mass cultivation of algae. Bioresource technology 99(10), 4021–4028.

Valente, T., Grande, J.A., de la Torre, M.L., Gomes, P., Santisteban, M., Borrego, J., Sequeira Braga, M.A., 2015. Mineralogy and geochemistry of a clogged mining reservoir affected by historical acid mine drainage in an abandoned mining area. Journal of Geochemical Exploration 157, 66–76.

Verplanck, P.L., Nordstrom, D.K., Taylor, H.E., Kimball, B.A., 2004. Rare earth element partitioning between hydrous ferric oxides and acid mine water during iron oxidation. Applied Geochemistry 19(8), 1339–1354.

Weng, Z., Mudd, G.M., Martin, T., Boyle, C.A., 2012. Pollutant loads from coal mining in Australia: Discerning trends from the National Pollutant Inventory (NPI). Environmental Science & Policy 19–20, 78–89.

Zhao, H., Xia, B., Fan, C., Zhao, P., Shen, S., 2012a. Human health risk from soil heavy metal contamination under different land uses near Dabaoshan Mine, Southern China. Science of The Total Environment 417–418, 45–54.

Zhao, H., Xia, B., Qin, J., Zhang, J., 2012b. Hydrogeochemical and mineralogical characteristics related to heavy metal attenuation in a stream polluted by acid mine drainage: A case study in Dabaoshan Mine, China. Journal of Environmental Sciences 24(6), 979–989.

Zvimba, J.N., Mulopo, J., Bologo, L.T., Mathye, M., 2012. An evaluation of waste gypsum-based precipitated calcium carbonate for acid mine drainage neutralization. Water Science and Technology 65(9), 1577–1582.

Chapter 2 Literature review

2.1 Introduction

The mining sector is the primary source of income in many countries and plays an important role in gross domestic product. According to world mining data, the total mineral production over the world is about 17 billion MT until 2014 (Thiruvenkatachari et al. 2016). The top five nations contributing to this production rate include China, USA, Russia, Australia and India. For instance, the mining industries in Australia consumed 652 GL of water during 2013–2014 which is 29% increase as compared to 2008–2009 seasons (ABS 2016). The Hunter valley is the largest mining operation in New South Wales region in Australia, and the mining of coal and metal ore predominantly utilizes 97% of water allocated for operations. China alone generates 242.2 MT tailings in metal ore mining and processing (Li 2006). As per the UNEP estimates in 2001, the metal mining activities around the world left behind about one million derelict mines (Venkateswarlu et al. 2016).

The acidic effluent produced from the rock interactions is the most hazardous, and usually stockpiled in tailing dams. The term, acid rock drainage (ARD), was applicable earlier to identify the water polluted with chemicals of sulfate oxidation during mining activity. Since these polluted streams predominately originate during mining operations, ARD was renamed as acid mine drainage (AMD) (Simate and Ndlovu 2014). Especially, AMD is produced by pyrite oxidation (iron-sulfide minerals) that is abundant in coal and metallic ore beds (Qureshi et al. 2016). The source of AMD from the mining sites includes waste rock dumps, ore stockpiles, tailings deposits, mine pits, heap leach pads and slags (Johnson and Hallberg 2005). The mine water also generates neutral/base mine drainage (higher pH values due to lower permeability of rock, bicarbonate exchange and abundant feldspars) and saline mine drainage (seawater intrusion in mining). Nordstrom et al. (2000) observed a pH range of 1.51–3.6 in AMD based on pitzer ion-interaction that contains total dissolved salts with a density of 1.4 g cm^{-3}. Taylor et al. (1984) found that oxidation of sulfides in anaerobic zone was primarily mediated by chemicals and was biologically-mediated in aerobic zone. Iron-oxidizing bacteria (IOB) such as *Thiobacillus ferrooxidans* and *Leptospirillum ferrooxidans* are primarily responsible to initiate these mechanisms (Leduc et al. 2002). Yet, the pyrite oxidation rates due to the action of microbes are 10^6–fold faster than the abiotic process (Butler 2007).

The participation of secondary minerals such as gypsum and jarosite significantly contributed to AMD by establishing foliation planes in the rock thereby intensifying the access

of oxidants (O_2 and Fe^{3+}) (Sracek et al. 2004). Also, the rare earth elements present can be precipitated during oxidation of Fe(III) to hydrous oxide forms of iron (da Silveira et al. 2009). These species can be used as tracers of AMD to identify the progression of percolation in surface waters (Verplanck et al. 2004). This precipitation usually occurs at a higher temperature and pH resulting in forming lepidocrocite (at neutral pH 7), and a mixture of schwertmannite, goethite and ferrihydrite (at lower pH 5.5) (Jönsson et al. 2006). Other minerals such as quartz, kaolinite, calcite, dolomite and pyrite abundantly found in coal mining areas can help in predicting the extent of acidity of AMD (Pinetown et al. 2007).

As a result of the exchange between protons and electrons, the hydrolysis of Fe^{2+} to $Fe(OH)_3$ takes place (Søndergaard et al. 2008). This hydrolysis reaction tends to exhibit more acidity and aggravates the buffering nature of AMD with a pH ranging from 2.5 to 3.5 resulting in an increase in the mobility and toxicity of heavy metals (Sánchez et al. 2005). For example, the heterogeneous oxidation of arsenite is very crucial during the weathering process of pyrite oxidation (Cheng et al. 2009). Based on geological variation, Hubbard et al. (2009) presented two mechanisms of pyrite oxidation with sulfide and ferric iron wherein water is used as the main source of oxygen to initiate the process. The sediments exposed to AMD constituted metals and metalloids such as As, Pb, Zn, Cu with a concentration of >1000 mg kg^{-1} (Valente et al. 2015). The impoundments showed potential AMD formation consisting of 2.5–3.7% (weight basis) equivalent of pyrite before oxidation process (Sima et al. 2011). In the waste pile, pyrite fraction increased with the depth showing the signs of reduced oxidation process (Jodeiri et al. 2016). Thus, the potential of AMD formation and its negative implications for the environment are very clear and evident from the established geochemistry.

Several studies reported the remediation options (chemical and bacterial), stream impacts and climate changes (Johnson and Hallberg 2005; Simate and Ndlovu 2014). Although biological approach for any treatment offers a promising solution to environmental clean-up and sustainable production, the implication of microalgae and bacteria that occur in biofilms of AMDs has not been properly understood. In the present review, microbial diversity inhabiting these environments has been presented to show proof of principle to validate the viability of microalgae and bacteria in biofilms of the extreme environment of AMD. Critical emphasis has also been laid on the possible role of acidophilic and non-acidophilic microalgae in synergistic approach with bacteria, all contained in biofilms, in bioremediation of AMD. Finally, microbial biotechnology has been suggested as a futuristic approach for effecting AMD bioremediation.

2.2 Microbial diversity in AMD: Survival of the fittest

It is very important to identify the microbial diversity in any area of contamination that makes to understand the process of toxicity, remediation and help to determine survival of the fittest in the environment. For example, the bioavailability of mercury drastically changed the microbial diversity even under lower guideline value (Mahbub et al. 2017). As the AMD environment consists of higher acidic concentrations, sulfate, toxic metals, and are not ideal for most of the microbes that grow under neutral conditions (Johnson 1995). It was found that sulfate-reducing bacteria (SRB) were 1.27×10^3 MPN g^{-1} and IOB were 9.56×10^5 MPN g^{-1} in the tailings (Benner et al. 2000). Conversely, the count of neutrophilic heterotrophs was found to be higher than IOB over the distance from the drain (McGinness and Barrie Johnson 1993). The ratio of microbes such as SRB and IOB changes seasonally especially during summer when the generation of sulfuric acid will be high limiting them due to inadequate metabolically active reactions (Leduc et al. 2002; Baker and Banfield 2003). Interestingly, Hallberg and Johnson (2003) identified the presence of moderate acidophilic microbes that outnumbered the dominant IOB in AMD. The presence of other microbial communities such as fungi and protists has also been characterized using rRNA-specific oligonucleotide probes and fluorescent in situ hybridization (FISH) (Baker et al. 2004). The FISH characterization of *Acidobacillus ferrooxidans* varied among the bacteria isolated due to inaccessibility of some target regions to the probe (Mahmoud et al. 2005). However, these bacteria were detected by sequence analysis of 16S rDNA and through RFLP due to lower interference of organic substrates and a higher population of bacteria (Okabayashi et al. 2005). Other techniques such as SYBR Green II direct counting, Taqman real time quantitative-PCR, catalyzed reporter deposition-FISH were used to quantify microbial abundance in the tailings (Kock and Schippers 2006). Lipid biomarkers were also used to identify microbial communities such as archaea, fungi, bacteria and eukarya in the AMD system (Fang et al. 2007). In AMD of Xiang Mountain sulfide mine in China, Hao et al. (2007) identified moderately thermophilic acidophiles belonging to the phyla *Actinobacteria, Thermomicrobia, Acidobacteria, Proteobacteria* and *Planctomycetes* using 16S rRNA gene clone library, and these observations were consistent with results from denaturing gradient gel electrophoresis (DGGE). On the contrary, PCA and cluster analysis revealed that the microbial diversity and functional gene distribution in AMDs and bioleaching systems remained consistent with similar environmental variables (Yin et al. 2007). A comparative metagenomics study of lead/zinc mine tailings revealed that the microbial reactions induce denitrification and sulfur oxidation leading to

acidification of the tailings (Chen et al. 2013). Using combination of cultivation-based molecular approaches, lower counts of IOB and sulfur-oxidising bacteria (SOB) with dominating archaeal sequences and acidophilic heterotrophs were observed in the mine tailings (Tan et al. 2008). This trend was similar in tests associated with molecular markers such as *gyrB* gene and 16S rRNA suggesting that pH and iron concentrations play a major role in the microbial community in AMD environment (Yin et al. 2008). In a controlled environment, biofilm community was observed to change with AMD impacted water, associated higher pH changes and increased sulfate concentration (Cole et al. 2011). Furthermore, during the initiation of biofilm, microbes undergo severe abiotic stress followed by external stress at the mature period leading to competition due to decreased resources (Mueller et al. 2011).

The main reason for the presence of heterotrophs is due to the activity of IOB that convert CO_2 to organic matter. Based on molecular diversity of 16S rRNA and 18S rRNA genes, there was a dominance of mixotrophic acidophiles over autotrophic acidophiles in bacterial clone library derived from AMD (Hao et al. 2010). The supporting carbon may be from formation of simple organic substances such as acetate due to the action of acid hydrolysis (Kamjunke et al. 2005). Also, dissolved organic carbon from the adjacent soil and other grass community can also support the mixotrophic metabolism (Hallberg 2010). Nevertheless, a lower concentration of sulfidic and organic compounds in AMD gave 89% of total clones, based on amino acid sequences derived from *cbbL* genes (Kamimura et al. 2010). Certain photosynthetic microorganisms (such as cyanobacteria and microalgae) cannot grow in subsurface of AMD (Baker and Banfield 2003). Interestingly, molecular approach (16S rRNA genes) showed the dominance of cyanobacterial diversity in AMD with a pH of 2.8 (Hao et al. 2012). The use of OMICS tools has always been an added advantage to get an insight into the mechanism of microbial acclimation or adaptation to the environments. For instance, both metagenomics and metatranscriptomics approach revealed that the microbial diversity exhibited higher gene expression for *in situ* functional activities such as stress resistance, nutrient limitation and distinct strategies for survival in AMD environments (Chen et al. 2013). It is evident from Table 2.1 that microalgae can thrive in AMD environments despite the abundance of other bacteria and archaea. However, studies using OMICS approach that could explore the microbial role especially in AMD with diverse organisms are scarce.

Table 2.1 Microalgal diversity in AMD environments

Algae Class	Genera/species	Location	Extent of pH	Extent of heavy metal conc.	Reference
Euglenophyceae	*Euglena mutabilis*	Tinto River, in South-western Spain	2.2	Fe 2.3 g/L, Zn 0.22 g/L, Cu 0.11 g/L	López-Archilla et al. (2001)
Chlorophyceae	*Chlamydomonas acidophila*				
Ulvophyceae	*Chlorella sp.*				
Rhodophyceae	*Klebsormidium sp*				
Conjugatophyta	*Galdieria sulphurarin*				
	Zygnema sp				
Cyanidiaceae	*Cyanidium sp.*	Nymph Creek, Yellowstone National Park (YNP), WY, USA	2-3	N.A	Amaral-Zettler (2012)
Chlorophyceae	*Chlorella sp.*				
Euglenophyceae	*Euglena mutabilis*	Davis Mine, Rowe, MA, USA			
Chlorophyceae	*Zygnematales sp.*	Copper mine of Touro, Spain	2.3	Total Fe - 39.6 % Total Cu- 102 mg/kg	Lucheta et al. (2013)
Chlorophyceae	*Chlorella protothecoides var. acidicola*	Copper mine Cantareras, Spain	2.5-2.6	N.A	Johnson (2012)
Euglenophyceae	*Euglena mutabilis*	Mynydd Parys, Wales	2.4		

Chlorophyceae	*Klebsormidium rivulare*	Five near sites near south eastern Ohio impacted by AMD	<4.0-5.6	N.A	Stevens et al. (2001)
Euglenophyceae	*Chlamydomonas*				
Chlorophyceae	*Euglena mutabilis*				
	Microspora sp				
Chlorophyceae	*Chlamydomonas sp.,*	Nuestra Señora del Carmen, Spain	2.4	SO_4 6.6 g/L ; Fe(II) 0.9 mg/L , Fe(III)596 mg/L Cu 27.4 mg/L , Co 0.65 mg/L ; Zn 8.20 mg/L Mn 77.8 mg/L , Ni 0.78 mg/L	Gonzalez-Toril et al. (2014)
	Klebsormidium sp.,				
	Zygnemopsis sp.,				
Chlorophyta	*Chlamydomonas sp.,*	Lusatia (Germany)	2.3-2.9	1000–5000 µS/cm	Lessmann et al. (2000)
Chrysophyceae	*Nanochlorum sp.,*				
Cryptophyta	*Scourfieldia cordiformis*				
Euglenophyta	*Ochromonas, Chromulina*				
	Cyathomonas,Lepocinclis,				
	Euglena mutabilis				
Chlorophyceae	*Klebsormidium acidophilum*	West coast of the South Island. New Zealand	pH <3.0	Ec 2500 µS/cm	Novis (2006)
Chlorophyceae	*Chlamydomonas acidophila*	Langau & Lake ML 111 in the Lusatian mining area	2.3 to 3.0.	Fe- 110–430 mg/L SO_4^{2-}-1100–1600 mg/L	Moser and Weisse (2011)
	Negoro; Ochromonas spp.				
	Vysotskii sp.,				

2.3 Acidophilic/non-acidophilic microalgae and heavy metal tolerance

AMD environments predominately limit the survival and physiology of natural microbes allowing the evolution of acidophiles based on genetic variation. The lower pH in these environments is the important factor that makes the metal bioavailability in rich amounts compared to other settings, and this pH itself is a hardship to manage by the cell. Although certain species of cyanobacteria are reported to survive in AMD environments, they are more prone to cell death compared to green algae. The chlorophyll inside the chloroplasts of microalgae is surrounded by cytoplasm that maintains neutral pH, while the external acidic pH makes the photosynthetic apparatus in cyanobacteria susceptible for damage (Brock 1973). Perseverance of cytoplasmic neutral pH in acidophilic/acidotolerant microalgae is solely dependent on the permeability coefficient which is lesser than algae that grow in circumneutral pH (Gross 2000). Microalgae usually tend to possess steady proton influx and efflux for meeting proper energy requirement whereas under acidic conditions proton leakage causes the release of weak acids like carbonic acids and contribute to greater proton influx. Such a mechanism in acidophiles/acidotolerants suggests that enhanced proton efflux than influx leads to acidification of the environment (Gross 2000).

In acidophilic or acidotolerant microalgae, CO_2 demand in carbon-concentrating mechanism (CCM) is more since the external carbonic anhydrase (CA) is in excess under normal conditions (Diaz and Maberly 2009). However, CA enzyme has higher affinity to CO_2 empowering the CCM in acidic conditions (Gimmler 2001). Balkos and Colman (2007) suggested that extrenal CA maintains CO_2 equlibrium concentration at surface of the cell. Intrestingly, the intracellular pH was found to be near neutral at both acidic and neutral pH supporting the conversion of carbonic acid to assimalable bicarbonate ion in CCM (Cid et al. 2010). *Chlamydomonas acidophila* Negoro, isolated from an acidic habitat (pH 2.65) of the mine-impacted stream, lacked external CA whereas the enzyme was observed at pH 1.0 due to stress response (Spijkerman 2005). However, some acidophilic species are unable to take up CO_2 under lower pH indicating the built-up of oxygen in carboxysome that kills algae (Diaz and Maberly 2009). Certain algae lack the transport or accumulative organelles inside the cell to adapt to the heavy metals for storage. For example, *Euglena gracilis* lacks vacuole inside the cell which is a significant storage area of heavy metals for many algae (Mendoza-Cozatl et al. 2002). However, this alga exhibited the accumulation of cadmium in chloroplasts up to 60% from the simulated growth medium (Mendoza-Cózatl and Moreno-Sánchez 2005).

In situ proteo-metabolomics revealed that algae in biofilms tend to enhance secretion of endo metabolites (amino acids, sugars with no fatty acids) and get vitamins from bacteria exhibiting mutualism (Halter et al. 2012a). Acidophilic algae assimilate fatty acids ~30% dry weight under lower pH without metal stress (Hirooka et al. 2014). Especially in acidic environments, algae are known to produce stress proteins which help to tolerate the other toxic compounds such as metals and metalloids. Highly positive membrane potential and surface charge are some other resistance mechanisms to cut the influx of protons which also participate in preventing toxicity from contaminants. Halter et al. (2012b) reported that *Euglena mutabilis* resisted arsenic toxicity through hydrophobicity and cell surface properties than *Euglena gracilis*. Algae inhabiting copper-contaminated soil exhibited higher levels of GSH and phytochleatin as a defense mechanism rather than accumulating copper intracellularly (Kalinowska and Pawlik-Skowrońska 2010).

The utilization of iron (Fe-III) and copper that are abundant in AMD depends upon the source which is a prerequisite to regulation of photosynthesis in algal cells. When these elements are bioavailable, higher concentrations can also affect the growth by inducing toxicity or affecting metabolic pathways (Subramaniyam et al. 2016). Spijkerman et al. (2007) suggested that algae survive by increasing tolerance to heavy metals successfully in an acidic environment by producing heat shock proteins. Under metal exposure, *Chlamydomonas acidophila* accumulated metals inside the polyphosphate bodies enriched near vacuoles with a change in ultrastructure (Nishikawa et al. 2003).

Even in presence of abnormal metal concentrations, green algae showed metal resistance due to sufficient phosphate concentration (Chia et al. 2017). Likewise, aresnate toxicity in microalgae was also observed to be higher due to phosphate limitation (Bahar et al. 2013, 2016). Nevertheless, acidiophilic algae tend to produce luetin compounds in presence of high iron concentrations as a means to alleviate the stress (Garbayo et al. 2012). However, there was a significant reduction in photosynthetic proteins under metal stress and lower pH exhibitied by acidiophilic algae (Cid et al. 2010). Acidophiles respond counter-intuitively by synthesizing higher amounts of transcripts that are involved in combating metal stress (Puente-Sánchez et al. 2016). Most studies suggest that indigenous algae can survive in acidic environments along with other microbes which may be useful for indirect remediation measures. Thus, it is evident from the literature that there exist many unknown mechanisms for withstanding metal toxicity, but resolving the adaptation process could pave the way to harness the biotechnological potential of microalgae in remediating AMDs. Also, microalgae that are already acclimated to

low pH should be exploited by providing proper nutrient conditions for making them successful in AMD bioremediation.

2.4 Microalgae–bacteria biofilms: An unopened paradox in AMD remediation

The role of microalgae in biofilms is crucial to understand the overall activities and relationships with other microbes within a biofilm. The eukaryotic microalgae are mostly abundant in biofilms in extreme acid environment together with other microbes that are responsible for algae to survive (Aguilera et al. 2006). However, the acidic condition makes bioavailability of ions to ensure only the presence of acidophiles. Generally, algae & bacteria interactions are categorized into signal transduction, nutrient exchange and gene transfer (Kozuma and Watanabe 2015). The predominant occurrence of bacteria in AMD indicates that their metabolism is nutrient exchange viz., dependent on sugar and lipid derivatives from other microbes which secrete and form biofilms (Nancucheo and Johnson 2010). CO_2 released by heterotrophic archaea and bacteria is utilized by microalgae which in turn provide the organic substrates via biochemicals excreted (Aguilera et al. 2006). In certain cases, other microbes such as hyphomycetous fungi and SRB utilized even the biomass of algae (López-Archilla et al. 2001). Nevertheless, SRBs also thrive under different modes of growth such as obligate autotrophy, heterotrophy and facultative autotrophy which make them utilize organic carbon and CO_2 for their metabolic activity using other electron donors like ferrous iron and reduced forms of sulfur (Dopson and Johnson 2012). Furthermore, SRBs generate metal sulfides as insoluble forms with neutralization capacity even in AMD (Hard et al. 1997). The capabilities of other bacteria that thrive under anaerobic conditions utilizing a limited quantity of sulfate ions as the electron acceptors while using organic compounds for growth and releasing the rest of sulfur as H_2S (Pfennig et al. 1981) should also be explored for AMD remediation. Several studies used SRB for AMD remediation with the help of electron donors for sulfate reduction (Table 2.2).

Table 2.2 Treatment of AMD using SRB

Source of SRB	Reactor	Electron donor	pH Influent	pH Effluent	Days of operation	Sulphate removal (%)	Reference
Brukunga pyrite mine, South Australia	Column bioreactor	Sodium lactate	3.25	5.82	42	38.3	Elliott et al. (1998)
Chessy copper mines, Rhône-Alpes, France	Stirred tank reactor	H_2/CO_2	2.55				Foucher et al. (2001)
Lignite mine water	Continuous bioreactor	Methanol	2.9	6.5	>25	42.3	Glombitza (2001)
Domingos mine, Southeast of Portugal.	Column Reactor	Solid sewage, sludge and acidic soil	2.4	6-8	90	35%	Costa et al. (2008)
***Tab-Simco site*, Illinois, USA**	Flow-through bioreactors	Mixed substrate	2.5	>3	460	35%	Lefticariu et al. (2015)
Copper mine area near Elazığ, Turkey	Fluidized bed reactor	Ethanol	3.0	N.A	100	70%	Sahinkaya et al. (2011)
Leviathan Mine, Alpine County, CA	Pilot scale bioreactor	Methanol	3.6	6.5	N.A	30.6	Tsukamoto and Miller (1999)

N.A Not available

From the evolutionary viewpoint, the existence of bacteria and microalgae together supports their growth and survival at extreme or oligotrophic conditions. The cyanobacteria observed in oligotrophic acid mine lake (which may not be a favourable environment for growth) was fairly dominant along with heterotrophic acidophiles indicating their undelved synergy with other microbes (Hao et al. 2012). At the surface of AMD, the presence of microalgae and other heterotrophs is supported by dissolved organic carbon (DOC), lysate and other metabolites (Rowe et al. 2007). The biofilm formed in AMD can stimulate the reduction of sulfate by the oxidation process induced by photosynthesis from microalgae. Orandi et al. (2007) explored various species of microalgae, fungi, and bacteria that are associated with AMD stream with high concentration of heavy metals. Similarly, Becerra et al. (2009) observed microcosms near the algal mats as the exudates supply was enough to support SRB. These exudates also contain amino acids, polyamine compounds and urea in environments where the ecological niches are often limited by nitrogen sources (Halter et al. 2012a).

Ivan and Johnson (2012) found that glycolic acid was the major constituent in DOC excreted by *Euglena* sp. and *Chlorella* sp. upon synthesis by the action of RuBisCo from phosphopglyceric acid and phosphor glycolate. Glycolic acid can be utilized by limited microbes belonging to SRB such as *Sulfobacillus* sp. (Nancucheo and Johnson 2010). Notably, heterotrophic acidophiles feed on monosaccharides such as glucose, fructose and mannitol that are produced by acidophilic algae in AMD environments (Johnson and Hallberg 2003; Ivan and Johnson 2012). The structure of algal biofilms formed in AMD surface can also provide micro-niche environments that could inhabit SRB or IOB (Souza-Egipsy et al. 2008). Nevertheless, organic carbon from the algal biomass can also create anaerobic environments that would be detrimental as iron precipitates in AMD (Senko et al. 2011). Signal transduction helps in inducing or inhibiting the gene expression in response to the environment. In microalgae, most molecules involved in quorum sensing(QS) are found out to be phosphor lipids, flavonoids, IAA etc (Zhou et al. 2016). Especially in biofilms the algae tend to produce ecological niches to support other microbial activities (Chen 2013). For example, the formation of anoxic microzones is due to the biological respiration and intermediate chemical formation as O_2 consumption rates regulate molecular diffusion where the mats inhabit microaerophilic and anaerobic taxa (Paerl et al. 2000). Algae produce QS inhibitors especially in biofilms that helps in balancing the microbial population (Dworjanyn et al. 1999). These inhibitor block the signal transduction pathway in bacteria most commonly acyl homoserine lactones (AHL) by halogenated furanones (Teplitski, M. and Rajamani 2001). In AMD, the acidophilic bacterium

contains *Afe* genes (T, R) that is responsible for Lux protein and contributing for AHL production. Hence, algae can tend to produce molecules that blocks the AHL receptors to control over population of bacteria in biofilms (Montgomery et al., 2013).In biofilms, the presence of polyphosphate bodies in bacteria and algae is likely to be higher in extreme environment like AMD (Seufferheld et al. 2008). Werner et al. (2007) shows that algae tend to produce intracellular and extracellular phosphate bodies due to distinct mechanism under stress environments. Horizontal gene transfer is one of the common phenomenon in AMD and studies has supported this trait in microalgae. Acidophilic red alga in AMD has found to possess protein coding genes from bacteria through HGT for its survival mechanism (Schönknecht et al. 2013). Furthermore, the green acidophilic algae has also found to encode phytochleatin synthase (PCS gene commonly found in bacteria) may acquire through horizontal gene transfer to alleviate heavy metal toxicity (Olsson et al. 2017). In addition, the acidophilic algae *Chlamydomonas sp* has highly expressed arsenate reductase and transporter genes through HGT with acidophilic bacteria of the same environment (Hirooka et al. 2017).Overall, the mutualism between acidophilic microalgae and bacteria would contribute for reduction of metal load as depicted in Fig. 2.1. For instance, microalgal biofilms isolated from mine tailings water (pH 6.1) showed a reduction of metal with >20% and high metabolite secretion (Palma et al. 2017). Orandi et al. (2012) showed that the microalgal–bacterial biofilm in RBC could remove heavy metals (20–50%) in synthetic AMD solution. In addition, the influence of pH on algal–bacterial biofilm immobilized in photo-RBC showed a significant difference in heavy metal uptake (Orandi and Lewis 2013).

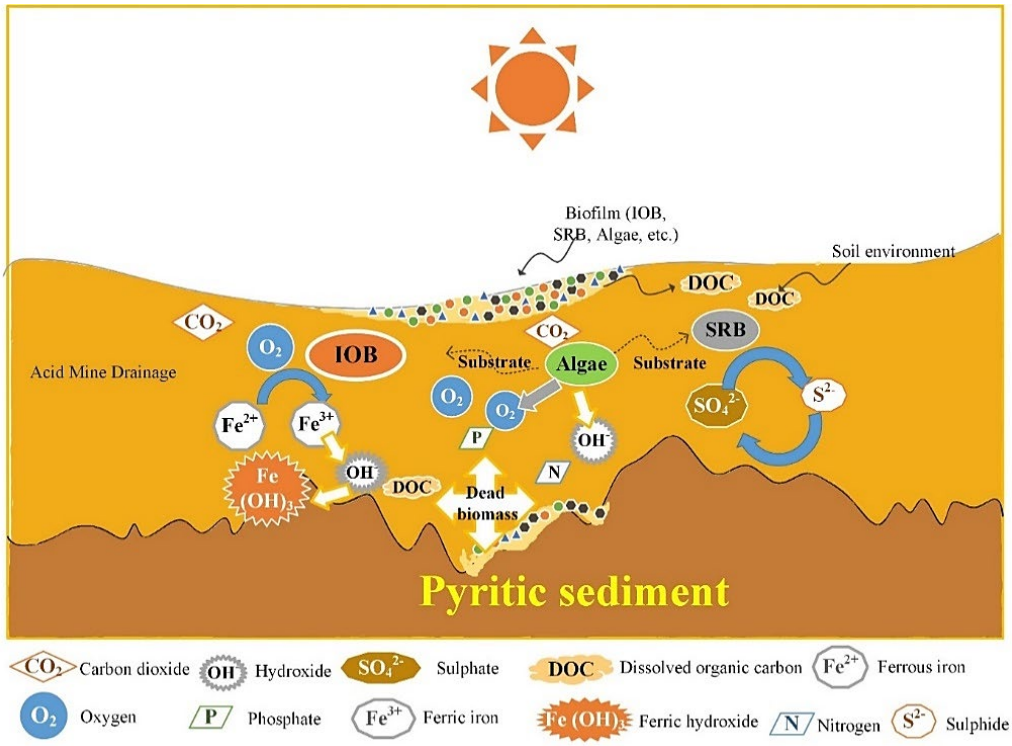

Fig 2.1. Microalgal–bacterial synergism in biofilms of AMD

As discussed above, the remediation potential of algal biofilms is likely to be stumpy amid the synergism evolved. Non-acidophilic microalgal species that occur in many habitats can also play a crucial role in AMD remediation. Several reports suggest that non-acidophilic microalgae tend to grow in neutral or cirumneutral pH and sometimes in alkaline range resisting the risk of acidic pH (Kosourov et al. 2003). Very recently, Kassim and Meng (2017) reported that algae can thrive well under higher CO_2 levels even at pH 4. In another study, non-acidophilic algae were shown to resist acidic pH levels upon acclimation (Jiang et al. 2012). It has been shown recently that a wide array of microalgae is efficient in metal removal at pH ≥5 (Zeraatkar et al. 2016). This clearly indicates that non-acidophilic microalgae upon their adaptation to lower acidic conditions and subsequent co-cultivation with acidophilic counterparts can mediate promising and rapid AMD remediation. But, the major concern is whether such coexistence would cause competition among both the categories of microalgae. In fact, certain algae can exhibit allelopathy by releasing chemicals such as chlorellin for inhibiting growth of other algae (Fergola et al. 2007). However, synthesis of these allelochemicals during coexistence depends upon biotic factors including pH (Gonçalves et al. 2017). It is therefore expected that microalgae can exhibit mutualism even in extreme environments as exist in AMD by involving growth promoting exudates and improving acidification by acclimated non-acidophiles. Thus, inclusion of acclimated non-acidophilic

microalgae together with acidophilic microalgae and heterotrophic bacteria in biofilms could be a sustainable and promising technology for AMD remediation. The metal-laden microalgal biomass can subsequently be harvested for production of biofuel.

2.5 Microbial fuel cells − Spotlight for futuristic approach in AMD remediation

Microbial biotechnology is always the easiest approach to examine the consequence and behaviour towards foreign materials especially in the field of remediation. Microbial solar cell is one such technology wherein photosynthesis- and electrochemical-based organisms generate energy using substrates in wastewaters (Subashchandrabose et al. 2011; Logan and Rabaey 2012). In context with AMD, Cheng et al. (2007) developed microbial fuel cell (MFC) which produces power denisty of 290 mW m^{-2} during the process and recover insoluble Fe(III) at the anode. Notably, the important factor in operating the fuel cell to treat AMD is pH, and is a favourable parameter for oxidation process (Cheng et al. 2007). The development of biofilm consisting of microalgae and bacteria in AMD environment is an added advantage for application in microbial fuel cell since microalgae supply organic matter and heterotrophic bacteria supply CO_2 during synergism. Figure 2.2 is a schematic representation that depicts the role of biofilm in microbial fuel cell for remediation of AMD environment. However, the anode compartment is usually an anaerobic environment which may not be ideal for algal growth. The IOB in biofilm can help to transfer electrons directly to the anode during the process of Fe(II) oxidation resulting in generation of larger currents (Nevin and Lovley 2000). cidic environments, the transfer of protons to cathode is inevitably high resulting in an increase in pH of the solution at the cathode (Lefebvre et al. 2011).

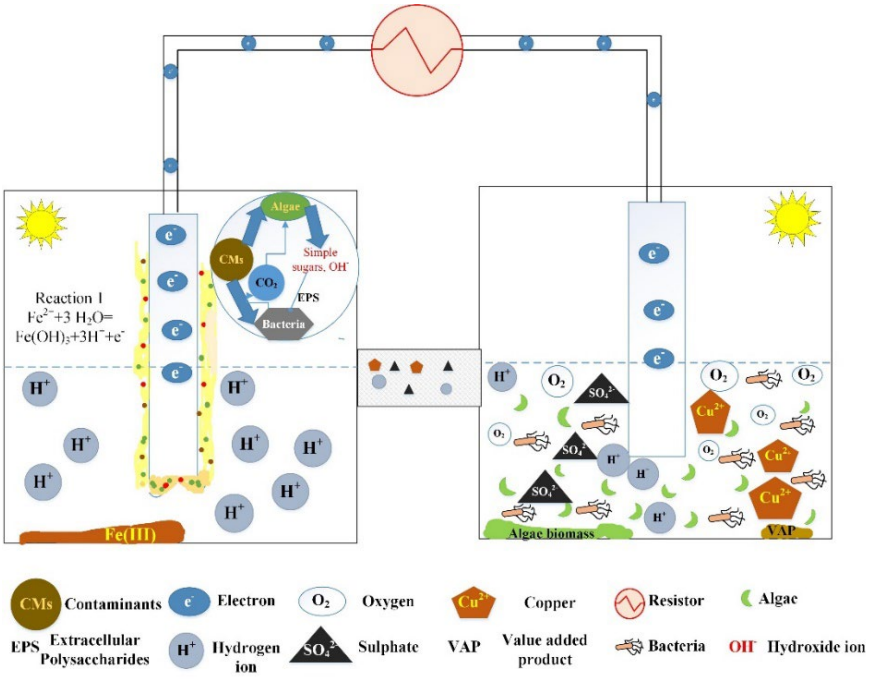

Fig. 2.2. MFC technology for its application in AMD bioremediation

The presence of other elements may affect the operation potential of MFCs by corroding the anode leading to lower output (Zhu and Logan 2014). The use of indigenous algal cells from AMD environment in the cathode cell may also help to reduce the oxygen input externally and can be a good electron acceptor as the oxygen production from photosynthesis is invariably higher. In addition, the use of microalgae in cathodic compartment also produces biomass which acts as substrate for the anodic compartment thereby reducing the substrate cost (Gajda et al. 2015). For instance, when fed with microalgal biomass in the anodic compartment as substrate, the maximum power density achieved was 1.9 W m^{-2} compared to acetate, and CO_2 produced is useful to cultivate algae in cathodic compartment (Cui et al. 2014). Nevertheless, Fe(II) oxidation controlled by the carbonate species at lower pH, and presence of hydroxides at higher pH indicate the involvement of CO_2 in oxidation of Fe(II) species (Song et al. 2013). The use of single chamber MFC or biocathodes instead of usual mode offers advantageous solutions. For instance, the removal of proton-exchange membrane for wastewater treatment increased the power density and reduced the cost of MFCs (Liu and Logan 2004). Lefebvre et al. (2012) observed reduction and reoxidation to hydroxyl precipitates of Fe(III) in membrane-bound cathodic cell consisting $FeCl_3$ solution mimicking the pH of AMD due to oxygen reduction and rise in pH by the cationic transfer. Luo et al. (2014a) using bipolar membrane in dual chambered MFC with applied voltage of 1 V recovered Cu^{2+}, Ni^{2+} and Fe^{2+} together with hydrogen production at cathode containing synthetic AMD. The bipolar membranes are

intended to produce 65–76% of H^+ and OH^- ions by splitting water (Ter Heijne et al. 2007). The use of reactive barrier with MFC produced sulfate reduction rates (33.1–51.2%) along with other heavy metal precipitation with various hydraulic rates (Tang et al. 2016).

It is also noteworthy that sulfate in AMD environment is very high, and its fate or participation in MFC needs more investigation. However, MFC application in sulfate containing wastewater was reported by Isosaari and Sillanpää (2017). In a two-chambered MFC, SRB bound in zeolite biofilm was able to produce a power density of 0.68 Wm^{-2} with elemental sulfur as the dominant oxidation product (Angelov et al. 2013). In another report, the consortia of SRB produced sulphide by reducing sulfate which was further utilized by respiring bacteria in biofilm for electricity generation in presence of organic carbon (Lee et al. 2012). While utilizing SRB-affiliated cathodic cell, the efficiency of sulfate removal was 49% and showed an 11-fold increase in electron generation rate under continuous flow mode (Luo et al. 2014b). A bacterium, *Rhodopseudomonas palustris*, was able to induce electron supply through nanofilaments in environments rich in iron oxide (Venkidusamy et al. 2015). Under acetate-fed conditions, this bacterium was able to produce a power density of 0.13 W m^{-2} with columbic efficiency of 46.7 ± 1.3% C (Venkidusamy and Megharaj 2016). Interestingly, use of MFC for recovery of heavy metals and nano iron particles is advantageous compared to other technologies (Cheng et al. 2011). The microbial nanofilaments form key for the futuristic approach in identification of strains as they tend to conduct electricity in distance. Proper identification of microorganisms which carry electrons to anodes is critical to the operation of MFC. Further delving MFC operation with modelling may yield and provide insights to optimize the higher product yield (Ortiz-Martínez et al. 2015). Thus, the potential of MFC technology involving microalgae and bacteria for the application in AMD remediation is seemingly high. Other criteria such as identification of suitable membrane and low cost substrates will help in making this technology sustainable. MFC technology with no drawbacks needs to be improved for effective AMD remediation in a larger scale. In this direction, new insights into the synthesis of nanofilaments and production of biofuel may also clinch a win-win approach.

2.6 Conclusions

Microalgae–bacteria synergy offers a striking approach to address the environmental challenges especially for AMD remediation. The mutual transfer of intermediates in metabolism such as proteins and carbohydrates, CO_2 uptake and O_2 production in AMDs make

microalgae–bacteria consortia unique and less energy intensive compared to other conventional methods. However, the bottleneck of this synergistic approach would lie within the exploratory mechanism for survival of the individual microorganism in order to facilitate the large-scale treatment. An insight into the metabolic activity of microalgal–bacterial biofilms using various OMICs tools may identify the expressed genes and delve unclear mechanisms for their adoption in AMD. Acclimated non-acidophilic microalgae together with their acidophilic counterparts in biofilms can enhance the performance of biofilms in continuous treatment of AMDs. Metabolic engineering of microalgae can improve their capabilities in uptake and accumulation of metals during bioremediation. Furthermore, the response of microalgal–bacterial biofilms under different modes of cultivation may provide an insight into their behaviour in AMD environments. Integrating microalgal–bacterial consortia in fuel cells is an attractive opportunity to remediate metal-contaminated wastewaters, recover energy and produce biomass.

2.7 References

ABS (2016) Australian Bureau of Statistics (ABS). Australian Environmental-Economic Accounts. Accessed 20.09.2016

Aguilera A, Manrubia SC, Gómez F, Rodríguez N, Amils R (2006) Eukaryotic community distribution and its relationship to water physicochemical parameters in an extreme acidic environment, Río Tinto (Southwestern Spain). Appl Environ Microbiol 72:5325−5330. doi:10.1128/AEM.00513-06

Amaral-Zettler LA (2012) Eukaryotic diversity at pH extremes. Front Microbiol 3:441. doi:10.3389/fmicb.2012.00441

Angelov A, Bratkova S, Loukanov A (2013) Microbial fuel cell based on electroactive sulfate-reducing biofilm. Energy Convers Manag 67:283−286. doi:10.1016/j.enconman.2012.11.024

Bahar MM, Megharaj M, Naidu R (2016) Influence of phosphate on toxicity and bioaccumulation of arsenic in a soil isolate of microalga *Chlorella* sp. Env Sci Poll Res 23:2663−2668. doi.10.1007/s11356-015-5510-7

Bahar MM, Megharaj M, Naidu R (2013) Toxicity, transformation and accumulation of inorganic arsenic species in a microalga *Scenedesmus* sp. isolated from soil. J Appl Phycol 25:913−917.doi.10.1007/s10811-012-9923-0

Baker BJ, Banfield JF (2003) Microbial communities in acid mine drainage. FEMS Microbiol Ecol 44:139−152. doi:10.1016/s0168-6496(03)00028-x

Baker BJ, Lutz MA, Dawson SC, Bond PL, Banfield JF (2004) Metabolically active eukaryotic communities in extremely acidic mine drainage. Appl Environ Microbiol 70:6264−6271. doi:10.1128/aem.70.10.6264-6271.2004

Balkos KD, Colman B (2007) Mechanism of CO_2 acquisition in an acid-tolerant *Chlamydomonas*. Plant Cell Environ 30:745−752. doi:10.1111/j.1365-3040.2007.001662.x

Becerra CA, López-Luna EL, Ergas SJ, Nüsslein K (2009) Microcosm-based study of the attenuation of an acid mine drainage-impacted site through biological sulfate and iron reduction. Geomicrobiol J 26:9−20. doi:10.1080/01490450802599250

Benner SG, Gould WD, Blowes DW (2000) Microbial populations associated with the generation and treatment of acid mine drainage. Chem Geol 169:435−448. doi:10.1016/S0009-2541(00)00219-9

Brock TD (1973) Lower pH limit for the existence of blue-green algae: evolutionary and ecological implications. Science 179:480-483

Butler TW (2007) Isotope geochemistry of drainage from an acid mine impaired watershed, Oakland, California. Appl Geochem 22:1416−1426. doi:10.1016/j.apgeochem.2007.01.009

Chen, L. 2013. Cooperative division of labor between quorum-sensing bacteria within marine self-organized biofilm. Master Scholar Thesis, Tsinghua University, Beijing, China.

Chen L-X, Li J-T, Chen Y-T, Huang L-N, Hua Z-S, Hu M, Shu W-S (2013) Shifts in microbial community composition and function in the acidification of a lead/zinc mine tailings. Environ Microbiol 15:2431−2444. doi:10.1111/1462-2920.12114

Cheng H, Hu Y, Luo J, Xu B, Zhao J (2009) Geochemical processes controlling fate and transport of arsenic in acid mine drainage (AMD) and natural systems. J Hazard Mater 165:13−26. doi:10.1016/j.jhazmat.2008.10.070

Cheng S, Dempsey BA, Logan BE (2007) Electricity generation from synthetic acid-mine drainage (AMD) water using fuel cell technologies. Environ Sci Technolnol 41:8149−8153. doi:10.1021/es0712221

Cheng S, Jang J-H, Dempsey BA, Logan BE (2011) Efficient recovery of nano-sized iron oxide particles from synthetic acid-mine drainage (AMD) water using fuel cell technologies. Water Res 45:303−307. doi:10.1016/j.watres.2010.07.054

Chia MA, Lombardi AT, Melão MdGG, Parrish CC (2017) Phosphorus levels determine changes in growth and biochemical composition of *Chlorella vulgaris* during cadmium stress. J Appl Phycol 29:1883−1891. doi:10.1007/s10811-017-1111-9

Cid C, Garcia-Descalzo L, Casado-Lafuente V, Amils R, Aguilera A (2010) Proteomic analysis of the response of an acidophilic strain of *Chlamydomonas* sp. (Chlorophyta) to natural metal-rich water. Proteomics 10:2026−2036. doi:10.1002/pmic.200900592

Cole M, Wrubel J, Henegan P, Janzen C, Holt J, Tobin T (2011) Development of a small-scale bioreactor method to monitor the molecular diversity and environmental impacts of bacterial biofilm communities from an acid mine drainage impacted creek. J Microbiol Meth 87:96−104. doi:10.1016/j.mimet.2011.07.015

Costa MC, Martins M, Jesus C, Duarte JC (2008) Treatment of acid mine drainage by sulphate-reducing bacteria using low cost matrices. Water Air Soil Pollut 189:149−162. doi:10.1007/s11270-007-9563-1

Cui Y, Rashid N, Hu N, Rehman MSU, Han J-I (2014) Electricity generation and microalgae cultivation in microbial fuel cell using microalgae-enriched anode and bio-cathode. Energy Convers Manag 79:674-680. doi:10.1016/j.enconman.2013.12.032

da Silveira AN, Silva R, Rubio J (2009) Treatment of acid mine drainage (AMD) in South Brazil: Comparative active processes and water reuse. Int J Mineral Process 93:103−109. doi:10.1016/j.minpro.2009.06.005

Diaz MM, Maberly SC (2009) Carbon-concentrating mechanisms in acidophilic algae. Phycologia 48:77−85. doi:10.2216/08-08.1

Dopson M, Johnson DB (2012) Biodiversity, metabolism and applications of acidophilic sulfur−metabolizing microorganisms. Environ Microbiol 14:2620−2631.

Dworjanyn SA, De Nys R, Steinberg PD (1999) Localisation and surface quantification of secondary metabolites in the red alga Delisea pulchra. Marine Biology 133(4):727-736.

Elliott P, Ragusa S, Catcheside D (1998) Growth of sulfate-reducing bacteria under acidic conditions in an upflow anaerobic bioreactor as a treatment system for acid mine drainage. Water Res 32:3724−3730. doi:10.1016/S0043-1354(98)00144-4.

Fang J, Hasiotis ST, Gupta SD, Brake SS, Bazylinski DA (2007) Microbial biomass and community structure of a stromatolite from an acid mine drainage system as determined by lipid analysis. Chem Geol 243:191−204. doi:10.1016/j.chemgeo. 2007 .06.001

Fergola P, Cerasuolo M, Pollio A, Pinto G, DellaGreca M (2007) Allelopathy and competition between *Chlorella vulgaris* and *Pseudokirchneriella subcapitata*: experiments and mathematical model. Ecol Model 208:205−214

Foucher S, Battaglia-Brunet F, Ignatiadis I, Morin D (2001) Treatment by sulfate-reducing bacteria of Chessy acid-mine drainage and metals recovery. Chem Eng Sci 56:1639−1645. doi:10.1016/S0009-2509(00)00392-4

Gajda I, Greenman J, Melhuish C, Ieropoulos I (2015) Self-sustainable electricity production from algae grown in a microbial fuel cell system. Biomass Bioenerg 82:87−93. doi:10.1016/j.biombioe.2015.05.017

Garbayo I, Torronteras R, Forján E, Cuaresma M, Casal C, Mogedas B, Ruiz-Domínguez MC, Márquez C, Vaquero I, Fuentes-Cordero JL, Fuentes R, González-del-Valle M, Vílchez C (2012) Identification and physiological aspects of a novel carotenoid-enriched, metal-resistant microalga isolated from an acidic river in Huelva (Spain). J Phycol 48:607−614. doi:10.1111/j.1529-8817.2012.01160.x

Gimmler H (2001) Acidophilic and Acidotolerant Algae. In: Rai LC, Gaur JP (eds) Algal adaptation to environmental stresses: Physiological, biochemical and molecular mechanisms. Springer Berlin, Heidelberg, pp 259−290. doi:10.1007/978-3-642-59491-5_9

Glombitza F (2001) Treatment of acid lignite mine flooding water by means of microbial sulfate reduction. Waste Manag 21:197−203. doi:10.1016/S0956-053X(00)00061-1

Gonçalves AL, Pires JCM, Simões M (2017) A review on the use of microalgal consortia for wastewater treatment. Algal Res 24:403-415

Gonzalez-Toril E, Santofimia E, Lopez-Pamo E, Garcia-Moyano A, Aguilera A, Amils R (2014) Comparative microbial ecol of the water column of an extreme acidic pit lake, Nuestra Senora del Carmen, and the Rio Tinto basin (Iberian Pyrite Belt). Int Microbiol 17:225−233.

Gross W (2000) Ecophysiology of algae living in highly acidic environments. Hydrobiologia 433:31−37.

Hallberg KB (2010) New perspectives in acid mine drainage microbiology. Hydrometallurgy 104:448−453. doi:10.1016/j.hydromet.2009.12.013

Hallberg KB, Johnson DB (2003) Novel acidophiles isolated from moderately acidic mine drainage waters. Hydrometallurgy 71:139−148. doi:10.1016/S0304-386X(03)00150-6

Halter D, Goulhen-Chollet F, Gallien S, Casiot C, Hamelin J, Gilard F, Heintz D, Schaeffer C, Carapito C, Van Dorsselaer A, Tcherkez G, Arsène-Ploetze F, Bertin PN (2012a) In situ proteo-metabolomics reveals metabolite secretion by the acid mine drainage bio-indicator, *Euglena mutabilis* ISME J 6:1391−1402. doi: 10.1038/ismej.2011.198

Halter D, Casiot C, Heipieper HJ, Plewniak F, Marchal M, Simon S, Arsène-Ploetze F, Bertin PN (2012b) Surface properties and intracellular speciation revealed an original adaptive mechanism to arsenic in the acid mine drainage bio-indicator *Euglena mutabilis.* Appl Microbiol Biotechnol 93:1735−1744. doi:10.1007/s00253-011-3493-y

Hao C, Wang L, Gao Y, Zhang L, Dong H (2010) Microbial diversity in acid mine drainage of Xiang Mountain sulfide mine, Anhui Province, China. Extremophiles 14:465−474. doi:10.1007/s00792-010-0324-5

Hao C, Zhang L, Wang L, Li S, Dong H (2012) Microbial community composition in acid mine drainage lake of Xiang Mountain sulfide mine in Anhui Province, China. Geomicrobiol J 29:886−895. doi:10.1080/01490451.2011.635762

Hao C-B, Zhang H-X, Bai Z-H, Hu Q, Zhang B-G (2007) A novel acidophile community populating waste ore deposits at an acid mine drainage site. J Environ Sci 19:444−450. doi:10.1016/S1001-0742(07)60074-6

Hard BC, Friedrich S, Babel W (1997) Bioremediation of acid mine water using facultatively methylotrophic metal-tolerant sulfate-reducing bacteria. Microbiol Res 152:65−73. doi:10.1016/S0944-5013(97)80025-0

Hirooka S, Higuchi S, Uzuka A, Nozaki H, Miyagishima SY (2014) Acidophilic green alga *Pseudochlorella* sp. YKT1 accumulates high amount of lipid droplets under a nitrogen-depleted condition at a low-pH. PLoS One 9:e107702. doi:10.1371/journal.pone.0107702

Hirooka S, Hirose Y, Kanesaki Y, Higuchi S, Fujiwara T, Onuma R, Era A, Ohbayashi R, Uzuka A, Nozaki H (2017) Acidophilic green algal genome provides insights into adaptation to an acidic environment. Proceedings of the National Academy of Sciences 114(39):E8304-E8313

Hubbard CG, Black S, Coleman ML (2009) Aqueous geochemistry and oxygen isotope compositions of acid mine drainage from the Río Tinto, SW Spain, highlight inconsistencies in current models. Chem Geol 265:321−334. doi:10.1016/ j.chemgeo. 2009.04.009

Isosaari P, Sillanpää M (2017) Use of sulfate-reducing and bioelectrochemical reactors for metal recovery from mine water. Separ Purif Rev 46:1−20. doi:10.1080/15422119.2016.1156548

Ivan Ň, Johnson D (2012) Acidophilic algae isolated from mine-impacted environments and their roles in sustaining heterotrophic acidophiles. Front Microbiol 3:325. doi:10.3389/fmicb.2012.00325

Jodeiri Shokri B, Doulati Ardejani F, Ramazi H (2016) Environmental geochemistry and acid mine drainage evaluation of an abandoned coal waste pile at the Alborz-Sharghi coal washing plant, NE Iran. Nat Resour Res 25:347−363. doi:10.1007/ s11 053-015-9289-5

Johnson DB (1995) Acidophilic microbial communities: Candidates for bioremediation of acidic mine effluents. Int Biodeter Biodegrad 35:41−58. doi:10.1016/0964-8305(95)00065-D

Johnson DB, Hallberg KB (2003) The microbiology of acidic mine waters. Res Microbiol 154:466−473. doi:10.1016/S0923-2508(03)00114-1

Johnson DB, Hallberg KB (2005) Acid mine drainage remediation options: a review. Sci Tot Environ 338:3−14. doi:10.1016/j.scitotenv.2004.09.002

Jönsson J, Jönsson J, Lövgren L (2006) Precipitation of secondary Fe(III) minerals from acid mine drainage. Appl Geochem 21:437−445. doi:10.1016/ j.apgeochem. 2005.12.008

Kalinowska R, Pawlik-Skowrońska B (2010) Response of two terrestrial green microalgae (Chlorophyta, Trebouxiophyceae) isolated from Cu-rich and unpolluted soils to copper stress. Environ Pollut 158:2778−2785. doi:10.1016/ j.envpol. 2010.03.003

Kamimura K, Okabayashi A, Kikumoto M, Manchur MA, Wakai S, Kanao T (2010) Analysis of iron- and sulfur-oxidizing bacteria in a treatment plant of acid rock drainage from a Japanese pyrite mine by use of ribulose-1,5-bisphosphate carboxylase/oxygenase large-subunit gene. J Biosci Bioeng 109:244−248. doi:10.1016/j.jbiosc.2009.08.007

Kamjunke N, Tittel J, Krumbeck H, Beulker C, Poerschmann J (2005) High heterotrophic bacterial production in acidic, iron-rich mining lakes. Microb Ecol 49:425−433. doi:10.1007/s00248-004-0270-9

Kassim MA, Meng TK (2017) Carbon dioxide (CO_2) biofixation by microalgae and its potential for biorefinery and biofuel production. Sci Tot Environ 584:1121−1129. doi:http://dx.doi.org/10.1016/j.scitotenv.2017.01.172

Kock D, Schippers A (2006) Geomicrobiological investigation of two different mine waste tailings generating acid mine drainage. Hydrometallurgy 83:167−175. doi:10.1016/j.hydromet.2006.03.022

Kosourov S, Seibert M, Ghirardi ML (2003) Effects of extracellular pH on the metabolic pathways in sulfur-deprived, H_2-producing *Chlamydomonas reinhardtii* cultures. Plant Cell Physiol 44:146−155. doi:10.1093/pcp/pcg020

Kouzuma A, Watanabe K (2015) Exploring the potential of algae/bacteria interactions. Current Opinion in Biotechnology 33(Supplement C):125-129 doi:https://doi.org/10.1016/j.copbio.2015.02.007

Leduc D, Leduc LG, Ferroni GD (2002) Quantification of bacterial populations indigenous to acidic drainage streams. Water Air Soil Pollut 135:1−21. doi:10.1023 /a: 1014778301817

Lee D-J, Lee C-Y, Chang J-S (2012) Treatment and electricity harvesting from sulfate/sulfide-containing wastewaters using microbial fuel cell with enriched sulfate-reducing mixed culture. J Hazard Mater 243:67−72. doi:10.1016/j.jhazmat. 2012.09.071

Lefebvre O, Shen Y, Tan Z, Uzabiaga A, Chang IS, Ng HY (2011) Full-loop operation and cathodic acidification of a microbial fuel cell operated on domestic wastewater. Bioresour Technol 102:5841−5848. doi:10.1016/j.biortech.2011.02.098

Lefebvre O, Neculita CM, Yue X, Ng HY (2012) Bioelectrochemical treatment of acid mine drainage dominated with iron. J Hazard Mater 241–242:411−417. doi:10.1016/j.jhazmat.2012.09.062

Lefticariu L, Walters ER, Pugh CW, Bender KS (2015) Sulfate reducing bioreactor dependence on organic substrates for remediation of coal-generated acid mine drainage: Field experiments. Appl Geochem 63:70−82. doi:10.1016/j.apgeochem.2015.08.002

Lessmann D, Fyson A, Nixdorf B (2000) Phytoplankton of the extremely acidic mining lakes of Lusatia (Germany) with pH ≤3. Hydrobiologia 433:123−128. doi:10.1023/a:1004018722898

Li MS (2006) Ecological restoration of mineland with particular reference to the metalliferous mine wasteland in China: A review of research and practice. Sci Tot Environ 357:38−53. doi:10.1016/j.scitotenv.2005.05.003

Liu H, Logan BE (2004) Electricity generation using an air-cathode single chamber microbial fuel cell in the presence and absence of a proton exchange membrane. Environ Sci Technol 38:4040−4046. doi:10.1021/es0499344

Logan BE, Rabaey K (2012) Conversion of wastes into bioelectricity and chemicals by using microbial electrochemical technologies. Science 337:686−690. doi:10.1126/science.1217412

López-Archilla AI, Marin I, Amils R (2001) Microbial community composition and ecology of an acidic aquatic environment: the tinto river, spain. Microb Ecol 41:20−35. doi:10.1007/s002480000044

Lucheta AR, Otero XL, Macías F, Lambais MR (2013) Bacterial and archaeal communities in the acid pit lake sediments of a chalcopyrite mine. Extremophiles 17:941−951. doi:10.1007/s00792-013-0576-y

Luo H, Liu G, Zhang R, Bai Y, Fu S, Hou Y (2014a) Heavy metal recovery combined with H_2 production from artificial acid mine drainage using the microbial electrolysis cell. J Hazard Mater 270:153−159. doi:10.1016/j.jhazmat.2014.01.050

Luo H, Fu S, Liu G, Zhang R, Bai Y, Luo X (2014b) Autotrophic biocathode for high efficient sulfate reduction in microbial electrolysis cells. Bioresour Technol 167:462−468. doi:10.1016/j.biortech.2014.06.058

Mahbub KR, Subashchandrabose SR, Krishnan K, Naidu R, Megharaj M (2017) Mercury alters the bacterial community structure and diversity in soil even at concentrations lower than the guideline values. Appl Microbio Biotechnol 101:2163−2175. https://doi.org/10.1007/s00253-016-7965-y

Mahmoud KK, Leduc LG, Ferroni GD (2005) Detection of *Acidithiobacillus ferrooxidans* in acid mine drainage environments using fluorescent in situ hybridization (FISH). J Microbiol Meth 61:33−45. doi:10.1016/j.mimet.2004.10.022

McGinness S, Barrie Johnson D (1993) Seasonal variations in the microbiology and chemistry if an acid mine drainage stream. Sci Tot Environ 132:27−41. doi:10.1016/0048-9697(93)90259-9

Mendoza-Cozatl D, Devars S, Loza-Tavera H, Moreno-Sanchez R (2002) Cadmium accumulation in the chloroplast of *Euglena gracilis.* Physiol Plant 115:276−283. doi: 10.1034/j.1399-3054.2002.1150214.x

Mendoza-Cózatl DG, Moreno-Sánchez R (2005) Cd^{2+} transport and storage in the chloroplast of *Euglena gracilis.* Biochim Biophys Acta - Bioener 1706:88−97. doi:10.1016/j.bbabio.2004.09.010

Moser M, Weisse T (2011) Combined stress effect of pH and temperature narrows the niche width of flagellates in acid mining lakes. J Plank Res 33:1023−1032. doi:10.1093/plankt/fbr014

Mueller RS, Dill BD, Pan C, Belnap CP, Thomas BC, VerBerkmoes NC (2011) Proteome changes in the initial bacterial colonist during ecological succession in an acid mine drainage biofilm community. Environ Microbiol 13:2279−2292. doi:10.1111/j.1462-2920.2011.02486.x

Montgomery K, Charlesworth J, LeBard R, Visscher P, Burns B (2013) Quorum Sensing in Extreme Environments. Life 3(1):131

Nancucheo I, Johnson DB (2010) Production of glycolic acid by chemolithotrophic iron- and sulfur-oxidizing bacteria and its role in delineating and sustaining acidophilic sulfide mineral-oxidizing consortia. Appl Environ Microbiol 76:461−467. doi:10.1128/aem.01832-09

Nevin KP, Lovley DR (2000) Lack of production of electron-shuttling compounds or solubilization of Fe(III) during reduction of insoluble Fe(III) oxide by *Geobacter*

metallireducens. Appl Environ Microbiol 66:2248−2251. doi: 10.1128/AEM.66.5.2248-2251.2000

Nishikawa K, Yamakoshi Y, Uemura I, Tominaga N (2003) Ultrastructural changes in *Chlamydomonas acidophila* (Chlorophyta) induced by heavy metals and polyphosphate metabolism. FEMS Microbiol Ecol 44:253−259. doi:10.1016/S0168-6496(03)00049-7

Nordstrom DK, Alpers CN, Ptacek CJ, Blowes DW (2000) Negative ph and extremely acidic mine waters from Iron Mountain, California. Environ Sci Technol 34:254−258. doi:10.1021/es990646v

Novis PM (2006) Taxonomy of *Klebsormidium* (Klebsormidiales, Charophyceae) in New Zealand streams and the significance of low-pH habitats. Phycologia 45:293−301. doi:10.2216/04-70.1

Okabayashi A, Wakai S, Kanao T, Sugio T, Kamimura K (2005) Diversity of 16S ribosomal DNA-defined bacterial population in acid rock drainage from Japanese pyrite mine. J Biosci Bioeng 100:644−652. doi:10.1263/jbb.100.644

Olsson S, Penacho V, Puente-Sánchez F, Díaz S, Gonzalez-Pastor JE, Aguilera A (2017) Horizontal Gene Transfer of Phytochelatin Synthases from Bacteria to Extremophilic Green Algae. Microbial ecology 73(1):50-60

Orandi S, Lewis DM (2013) Biosorption of heavy metals in a photo-rotating biological contactor − a batch process study. Appl Microbiol Biotechnol 97:5113−5123. doi:10.1007/s00253-012-4316-5

Orandi S, Yaghubpur A, Sahraei H, Behrouz M (2007) Influence of acid mine drainage on aquatic life at Sar Cheshmeh copper mine. Geochim Cosmochim Acta 71:A742

Orandi S, Lewis DM, Moheimani NR (2012) Biofilm establishment and heavy metal removal capacity of an indigenous mining algal-microbial consortium in a photo-rotating biological contactor. J Indust Microbiol Biotechnol 39:1321−1331. doi:10.1007/s10295-012-1142-9

Ortiz-Martínez VM, Salar-García MJ, de los Ríos AP, Hernández-Fernández FJ, Egea JA, Lozano LJ (2015) Developments in microbial fuel cell modeling. Chem Eng J 271:50−60. doi:10.1016/j.cej.2015.02.076

Paerl HW, Pinckney JL, Steppe TF (2000) Cyanobacterial−bacterial mat consortia: examining the functional unit of microbial survival and growth in extreme environments. Environ Microbiol 2:11−26. doi: 10.1046/j.1462-2920.2000.00071.x

Palma H, Killoran E, Sheehan M, Berner F, Heimann K (2017) Assessment of microalga biofilms for simultaneous remediation and biofuel generation in mine tailings water. Bioresour Technol 234:327−335. doi:http://dx.doi.org/10.1016/j.biortech.2017.03.063

Pfennig N, Widdel F, Trüper HG (1981) The dissimilatory sulfate-reducing bacteria. In: Starr MP, Stolp H, Trüper HG, Balows A, Schlegel HG (eds) The prokaryotes: A handbook on habitats, isolation, and identification of bacteria. Springer Berlin Heidelberg, pp 926−940. doi:10.1007/978-3-662-13187-9_74

Pinetown KL, Ward CR, van der Westhuizen WA (2007) Quantitative evaluation of minerals in coal deposits in the Witbank and Highveld Coalfields, and the potential impact on acid mine drainage. Int J Coal Geo 70:166−183. doi:10.1016/j.coal.2006.02.013

Puente-Sánchez F, Olsson S, Aguilera A (2016) Comparative transcriptomic analysis of the response of *Dunaliella acidophila* (Chlorophyta) to short-term cadmium and chronic natural metal-rich water exposures. Microbial Ecol 72:595−607. doi:10.1007/s00248-016-0824-7

Qureshi A, Maurice C, Öhlander B (2016) Potential of coal mine waste rock for generating acid mine drainage. J Geochem Expl 160:44−54. doi:10.1016/j.gexplo.2015.10.014

Rowe OF, Sanchez-Espana J, Hallberg KB, Johnson DB (2007) Microbial communities and geochemical dynamics in an extremely acidic, metal-rich stream at an abandoned sulfide mine (Huelva, Spain) underpinned by two functional primary production systems. Environ Microbiol 9:1761−1771. doi:10.1111/j.1462-2920. 2007. 01294.x

Sahinkaya E, Gunes FM, Ucar D, Kaksonen AH (2011) Sulfidogenic fluidized bed treatment of real acid mine drainage water. Bioresour Technol 102:683−689. doi:10.1016/j.biortech.2010.08.042

Sánchez España J, López Pamo E, Santofimia E, Aduvire O, Reyes J, Barettino D (2005) Acid mine drainage in the Iberian Pyrite Belt (Odiel river watershed, Huelva, SW Spain): Geochemistry, mineralogy and environmental implications. Appl Geochem 20:1320−1356. doi:10.1016/j.apgeochem.2005.01.011

Schönknecht G, Chen W-H, Ternes CM, Barbier GG, Shrestha RP, Stanke M (2013) Gene transfer from bacteria and archaea facilitated evolution of an extremophilic eukaryote. Science 339 doi:10.1126/science.1231707

Senko JM, Bertel D, Quick TJ, Burgos WD (2011) The influence of phototrophic biomass on Fe and S redox cycling in an acid mine drainage-impacted system. Mine Wat Environ 30:38−46. doi:10.1007/s10230-010-0123-3

Seufferheld MJ, Alvarez HM, Farias ME (2008) Role of polyphosphates in microbial adaptation to extreme environments. Applied and environmental microbiology 74(19):5867-5874

Sima M, Dold B, Frei L, Senila M, Balteanu D, Zobrist J (2011) Sulfide oxidation and acid mine drainage formation within two active tailings impoundments in the Golden Quadrangle of the Apuseni Mountains, Romania. J Hazard Mater 189:624−639. doi:10.1016/j.jhazmat.2011.01.069

Simate GS, Ndlovu S (2014) Acid mine drainage: Challenges and opportunities. J Environ Chem Eng 2:1785−1803. doi:10.1016/j.jece.2014.07.021

Søndergaard J, Elberling B, Asmund G (2008) Metal speciation and bioavailability in acid mine drainage from a high arctic coal mine waste rock pile: Temporal variations assessed through high-resolution water sampling, geochemical modelling and DGT. Cold Reg Sci Technol 54:89−96. doi:10.1016/j.coldregions.2008.01.003

Song W, Zhai L-F, Cui Y-Z, Sun M, Jiang Y (2013) Carbonate-mediated Fe(II) oxidation in the air-cathode fuel cell: A kinetic model in terms of Fe(II) speciation. J Phys Chem A 117:4627−4635. doi:10.1021/jp4014543

Souza-Egipsy V, Gonzalez-Toril E, Zettler E, Amaral-Zettler L, Aguilera A, Amils R (2008) Prokaryotic community structure in algal photosynthetic biofilms from extreme acidic streams in Rio Tinto (Huelva, Spain). Int Microbiol 11:251−260. doi:10.2436/20.1501.01.69

Spijkerman E (2005) Inorganic carbon acquisition by *Chlamydomonas acidophila* across a pH range. Can J Bot 83:872−878. doi:10.1139/b05-073

Spijkerman E (2007) Phosphorus acquisition by *Chlamydomonas acidophila* under autotrophic and osmo-mixotrophic growth conditions. J Exp Bot 58:4195−4202. doi:10.1093/jxb/erm276

Sracek O, Choquette M, Gélinas P, Lefebvre R, Nicholson RV (2004) Geochemical characterization of acid mine drainage from a waste rock pile, Mine Doyon, Québec, Canada. J Cont Hydrol 69:45−71. doi:10.1016/S0169-7722(03)00150-5

Stevens AE, McCarthy BC, Vis ML (2001) Metal content of *Klebsormidium*-dominated (Chlorophyta) algal mats from acid mine drainage waters in Southeastern Ohio. J Torrey Bot Soc 128:226−233. doi:10.2307/3088714

Subashchandrabose SR, Ramakrishnan B, Megharaj M, Venkateswarlu K, Naidu R (2011) Consortia of cyanobacteria/microalgae and bacteria: Biotechnological potential. Biotechnol Adv 29:896−907. doi:10.1016/j.biotechadv.2011.07.009

Subramaniyam V, Subashchandrabose SR, Thavamani P, Chen Z, Krishnamurti GSR, Naidu R, Megharaj M (2016) Toxicity and bioaccumulation of iron in soil microalgae. J Appl Phycol 28:2767−2776. doi:10.1007/s10811-016-0837-0

Tan G-L, Shu W-S, Hallberg KB, Li F, Lan C-Y, Zhou W-H, Huang L-N (2008) Culturable and molecular phylogenetic diversity of microorganisms in an open-dumped, extremely acidic Pb/Zn mine tailings. Extremophiles 12:657−664. doi:10.1007/s00792−008-0171-9

Tang H, Pu WC, Cai CF, Xu JP, He WJ (2016) Remediation of acid mine drainage based on a novel coupled membrane-free microbial fuel cell with permeable reactive barrier system. Pol J Environ Stud 25:107−112. doi:10.15244/pjoes/60891

Taylor BE, Wheeler MC, Nordstrom DK (1984) Stable isotope geochemistry of acid mine drainage: Experimental oxidation of pyrite. Geochim Cosmochim Acta 48:2669−2678. doi:10.1016/0016-7037(84)90315-6

Ter Heijne A, Hamelers HVM, Buisman CJN (2007) Microbial fuel cell operation with continuous biological ferrous iron oxidation of the catholyte. Environ Sci Technol 41:4130−4134. doi:10.1021/es0702824

Teplitski M, Rajamani S (2011) Signal and Nutrient Exchange in the Interactions Between Soil Algae and Bacteria. In: Witzany G (ed) Biocommunication in Soil Microorganisms. Springer Berlin Heidelberg, Berlin, Heidelberg, pp 413-426

Thiruvenkatachari R, Francis M, Cunnington M, Su S (2016) Application of integrated forward and reverse osmosis for coal mine wastewater desalination. Sep Pur Technol 163:181−188. doi: 10.1016/j.seppur.2016.02.034

Tsukamoto TK, Miller GC (1999) Methanol as a carbon source for microbiological treatment of acid mine drainage. Water Res 33:1365–1370. doi:10.1016/S0043-1354(98)00342-X

Valente T, Grande JA, de la Torre ML, Gomes P, Santisteban M, Borrego J, Sequeira Braga MA (2015) Mineralogy and geochemistry of a clogged mining reservoir affected by historical acid mine drainage in an abandoned mining area. J Geochem Explor 157:66−76. doi: 10.1016/j.gexplo.2015.05.016

Venkateswarlu K, Nirola R, Kuppusamy S, Thavamani P, Naidu R, Megharaj M (2016) Abandoned metalliferous mines: ecological impacts and potential approaches for reclamation. Rev Environ Sci Bio/Technol 15:327−354. doi:10.1007/s11157-016-9398-6

Venkidusamy K, Megharaj M (2016) A novel electrophototrophic bacterium, *Rhodopseudomonas palustris* strain RP2, exhibits hydrocarbonoclastic potential in anaerobic environments. Front Microbiol 7:1071. doi:10.3389/fmicb.2016.01071

Venkidusamy K, Megharaj M, Schroder U, Karouta F, Mohan SV, Naidu R (2015) Electron transport through electrically conductive nanofilaments in *Rhodopseudomonas palustris* strain RP2. RSC Adv 5:100790−100798. doi:10.1039/C5RA08742B

Verplanck PL, Nordstrom DK, Taylor HE, Kimball BA (2004) Rare earth element partitioning between hydrous ferric oxides and acid mine water during iron oxidation. Appl Geochem 19:1339−1354. doi:10.1016/j.apgeochem.2004.01.016

Yin H, Cao L, Qiu G, Wang D, Kellogg L, Zhou J, Dai Z, Liu X (2007) Development and evaluation of 50-mer oligonucleotide arrays for detecting microbial populations in acid mine drainages and bioleaching systems. J Microbiol Meth 70:165−178. doi: 10.1016/j.mimet.2007.04.011

Werner TP, Amrhein N, Freimoser FM (2007) Inorganic polyphosphate occurs in the cell wall of *Chlamydomonas reinhardtii* and accumulates during cytokinesis. BMC plant biology 7(1):51

Yin H, Cao L, Xie M, Chen Q, Qiu G, Zhou J, Wu L, Wang D, Liu X (2008) Bacterial diversity based on 16S rRNA and *gyrB* genes at Yinshan mine, China. Syst Appl Microbiol 31:302−311. doi: 10.1016/j.syapm.2008.05.003

Zeraatkar AK, Ahmadzadeh H, Talebi AF, Moheimani NR, McHenry MP (2016) Potential use of algae for heavy metal bioremediation, a critical review. J Environ Manage 181:817−831. doi:http://dx.doi.org/10.1016/j.jenvman.2016.06.059

Zhu X, Logan BE (2014) Copper anode corrosion affects power generation in microbial fuel cells. J Chem Technol Biotechnol 89:471−474. doi:10.1002/jctb.4156

Zhou J, Lyu Y, Richlen ML, Anderson DM, Cai Z (2016) Quorum Sensing Is a Language of Chemical Signals and Plays an Ecological Role in Algal-Bacterial Interactions. Critical Reviews in Plant Sciences 35(2):81-105 doi:10.1080/07352689.2016.1172461

Chapter 3 Sustainable production of biomass and biodiesel by acclimation of non-acidophilic microalgae to acidic conditions

3.1. Abstract

The overwhelming response towards algal biodiesel production has been very well-recognized recently as a sustainable alternative to conventional fuels. Most of the microalgae cannot grow well at acidic pH. The present study therefore investigated whether non-acidophilic microalgae *Desmodesmus* sp. MAS1 and *Heterochlorella* sp. MAS3 can be acclimated to extreme-acidic pH for sustainable production of biomass and biodiesel. Growth analysis indicated that both the microalgal strains possessed a passive uptake of CO_2 at pH 3.0 with a biomass production (g dry wt. L^{-1}) of 0.25 in *Desmodemus* sp. MAS1 and 0.45 in *Heterochlorella* sp. MAS3. Flow cytometry analysis for reactive oxygen species, membrane permeability and neutral lipids revealed the capabilities of both the strains to adapt to the stress imposed by acidic pH. Lipid production was doubled in both the strains when grown at pH 3.0. *In-situ* transesterification of biomass resulted in 13-15% FAME yield in the selected microalgae, indicating their great potential in biofuel production.

3.2. Introduction

Microalgae significantly contribute to the environment through CO_2 fixation, contaminant reduction and production of biomass as a promising feedstock for biofuel. As ubiquitous primary producers, microalgae are critical to the ecological biota. Recent research widely acknowledged the influence of extreme environments such as ocean acidification and acid mine drainage on microalgal communities (Sassenhagen et al., 2014; Hattich et al., 2017; Abinandan et al., 2018a). The most common phenomenon is the extent of pH that plays a critical role in algal growth dynamics. Several studies combined the effect of pH, nutrient starvation or cultivation modes for enhancing algal biomass preferably for increased biofuel production (Abinandan et al., 2018b). For instance, the addition of molasses (9.82 g L^{-1}) to serve as an organic carbon source at pH 6.7 resulted in higher yield (2 g L^{-1}) of microalgal biomass (Kose Engin et al., 2018). Cheirsilp and Torpee (2012) observed increased lipid content at a circumneutral pH upon exposure of microalgae to higher concentrations of glucose. Huang et al. (2017) demonstrated that microalgae turned the medium acidic with glucose when ammonium was predominantly present.

Most of the microalgae cannot survive at low pH (<6.0) as the transporters become inactive (Perez-Garcia et al., 2011). Several studies indicated that exogenous supply of pure CO_2 or flue

gas to enhance microalgal biomass productivity is favorable only at controlled pH maintained with bicarbonate availability (Ma et al., 2017). Jiang et al. (2012) reported that microalgae non-adapted to acidic conditions could not survive at pH 3.0, indicating that acid adaptation is imminent for survival. Likewise, *Chlorella* sp. KR-1 that was highly tolerant to CO_2 could not survive at a pH of 3.5 (Sung et al., 1999). Also, microalgae, when grown at pH 4.0, exhibited a drastic decline in the biomass, suggesting the significant toxicity of pH (Khalil et al., 2010). Interestingly, even pH 4.5 inhibited 50% of growth in acid-tolerant microalgae (Nalewajko et al., 1997). El-Ansari and Colman (2015) also reported that acid-tolerant microalgae could not grow at pH 3.0 due to a decrease in intracellular pH. Thus, acid-tolerant microalgae are also sensitive to low pH, implying that only acidophiles are capable of growth under such extreme conditions due to the gene inheritance through evolutionary response (Hirooka et al., 2017). Recently, the high potential of phytoplankton for phenotypic buffering was observed in response to ocean acidification (Hattich et al., 2017). Sassenhagen et al. (2014) also noted that microalgae could grow under a wide range of environmental conditions due to high phenotypic plasticity. An exogenous supply of carbon source (organic and inorganic) may be imminent for biofuel production (Kose Engin et al., 2018). Ma et al. (2017) suggested that pH of the medium (irrespective of carbon source) should be maintained at near neutral for microalgal cultivation. But, addition of hydroxides is required for maintenance of neutral pH and is not cost-effective (Abinandan et al., 2018b). However, available information suggests that non-acidophilic microalgae can withstand naturally-occurring acidic events such as ocean acidification by expressing high phenotypic plasticity or through adaptation process (Jiang et al., 2012; Hattich et al., 2017).

While perusing the literature on remediation of acid mine drainage (AMD) by microalgae–bacteria biofilms, it was hypothesized that acclimation of non-acidophilic microalgae to acidic conditions might be a better option than applying acidophilic counterparts for reclamation of AMDs (Abinandan et al., 2018a). This is because under different environmental pressures such as acidic conditions, only limited strains of non-acidophilic microalgae could phenotypically adjust to thrive and grow (Abinandan et al., 2018a). To validate this hypothesis, four microalgae isolated from natural habitats of soil and lake waters with near neutrality exposed to pH 3.0 to investigate the microalgal growth response to acclimation at this acidic condition. Subsequently, two microalgal strains capable of growth at pH 3.0 were selected to assess the potential for sustained production of biomass under the environmental pressures imposed by extreme acidic conditions following flow cytometry, and yield of biodiesel following FTIR-based microalgal fatty acid methyl esters (FAME) analysis. The present study reports for the

first time on acclimation of non-acidophilic microalgae to extreme acidic pH for the sustainable production of biomass and biodiesel.

3.3. Materials and methods

3.3.1.Microalgal strains and determination of growth rate

Microalgae were isolated from local soil and lake water samples by streaking onto agar with modified Bold's basal medium (BBM) with low phosphate. Cell sorting (BD FACSAria IIu) was done to obtain axenic cultures of the isolates. Briefly, log phase cells were sampled to measure chlorophyll dependent autofluorescence (FL3, 670 nm LP). The channel estimates at log scale and the sensitivity was set at 300 mV. Measurements of 10,000 events and 10^5 cells were sorted in sterile BBM and plated subsequently. The cells took nearly two weeks to develop axenic colonies. These isolates were grown at pH 3.0 (experimental) and pH 6.7 (control) in 30 mL BBM contained in 100 mL conical flasks under continuous illumination of 60 μmol m^{-2} s^{-1} at 23 ± 1ºC with 100 rpm shaking. The pH of the culture medium was monitored using LAQUA PC1100 pH meter (Horiba scientific, Japan).

Genomic DNA from algal strains was isolated using microbial DNA isolation kit (Mo Bio Laboratories, Inc.) as per the instructions provided. The DNA was amplified with 18S universal primers, the amplicons were cleaned using PCR and Gel kit (Bioline Laboratories, Inc.), and sequenced at Ramaciotti Centre, UNSW, Australia. The preliminary sequence identification was carried out for three isolates of microalgae using the NCBI Blast nucleotide search tool and a phylogenetic tree was constructed using MEGA 5.0 (Kumar et al., 2016). Phylogenetic analysis obtained from 1000 replicates as per the bootstrap test of clustal muscle alignment indicated that two of the microalgal isolates belong to the genus, *Desmodesmus*, with a slight difference of 3% similarity among nucleotides and hence designated as *Desmodesmus* sp. MAS1 and *Desmodesmus* sp. MAS2 (Fig. 3.1a). Since the third isolate is closely related to the genus, *Heterochlorella*, it has been designated as *Heterochlorella* sp. MAS3 (Fig. 3.1b). A well-studied *Chlorella* sp. MM3 (Ramadass et al., 2017; Subashchandrabose et al., 2017a, b; Ganeshkumar et al., 2018), obtained from in-house Phycology laboratory, was used in the present study as a reference microalga.

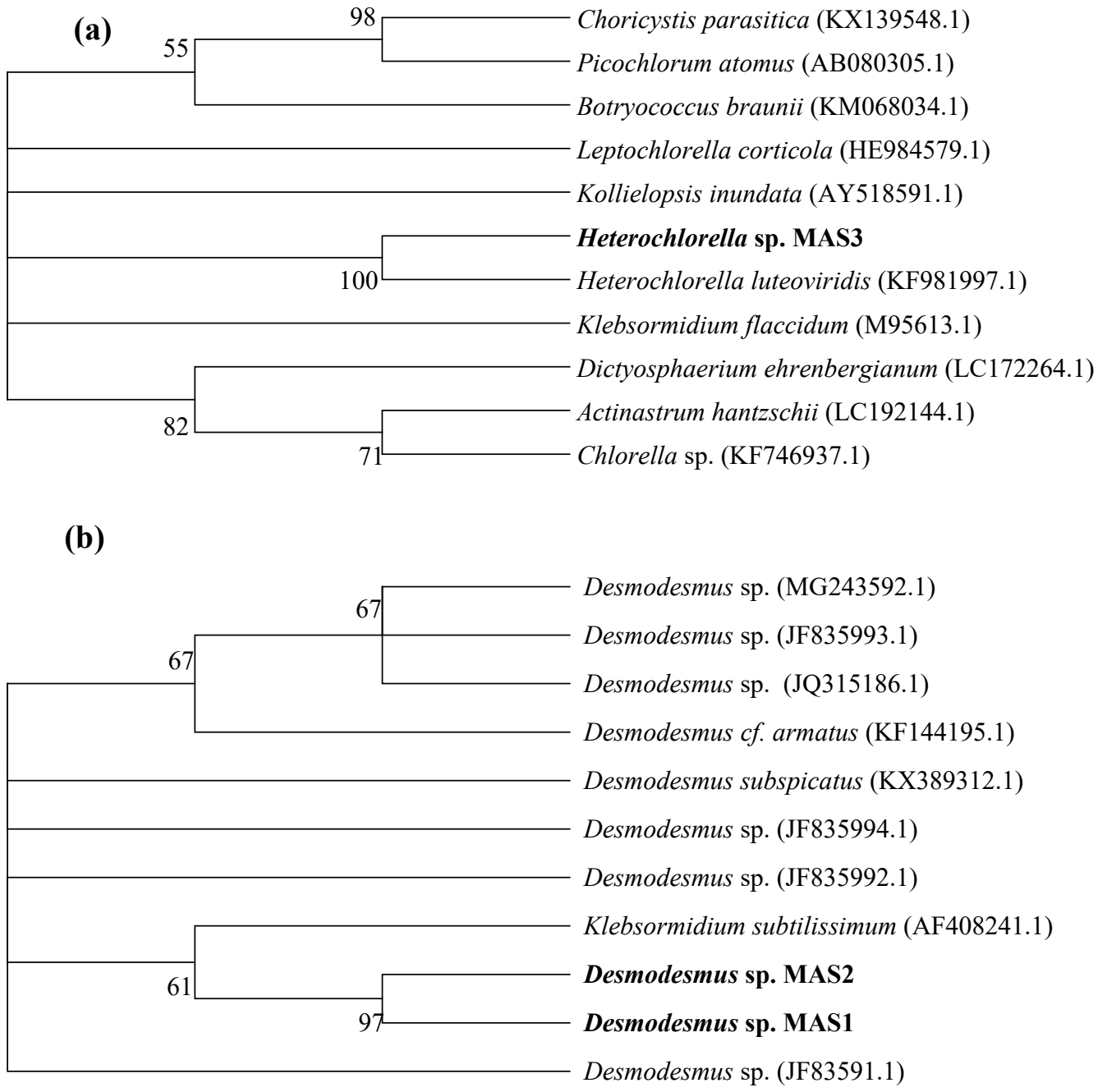

Fig. 3.1. Bootstrap consensus phylogenetic trees showing the evolutionary relationships of (a) *Desmodesmus* sp. MAS1 and *Desmodesmus* sp. MAS2, and (b) *Heterochlorella* sp. MAS3.

Microalgal growth, in terms of cell density, was determined in triplicate samples every alternate day using Neubauer hemocytometer (Bright line, Hausser Scientific, USA) under a light microscope (Olympus CX31, Japan). The growth rate was calculated using data at the exponential phase following the equation:

$$\mu = \frac{\ln N_1 - \ln N_0}{T_1 - T_0}$$

where, N_1, N_0 are the final and initial cell densities, and T_1, T_0 are the times taken, in days.

3.3.2. Determination of growth response

Triplicate samples from microalgal cultures were withdrawn every week for determining the activity of carbonic anhydrase (CA), chlorophyll, biomass and metabolic biomarkers such as carbohydrates, proteins and total lipids. After sonicating the microalgal cell suspension, the activity of CA was measured in terms of esterase activity (Ores et al., 2016), and expressed as U L^{-1}. One unit (U) of enzyme activity is defined as the quantity of enzyme needed to release 1 µmol of *p*-nitrophenol min^{-1} in the assay conditions. Total chlorophyll and carbohydrates were estimated after methanol extraction (Chen and Vaidyanathan, 2013). Bradford bioassay was carried out to determine proteins using Bio-Rad kit (Bio-Rad Protein Assay Dye Reagent Concentration; Protein Standard II), and the color intensity was read in a spectrophotometer (Orion AquaMate 7000, Thermofisher Scientific, USA). Chloroform from the extracts was dried before gravimetric analysis of total lipids. Chlorophyll, carbohydrates and total lipids are expressed as mg g^{-1} dry wt. respectively. Microalgal biomass, in triplicate samples, was determined by the gravimetric method and expressed as g dry wt. L^{-1}.

3.3.3. Assay of reactive oxygen species (ROS), membrane permeability and neutral lipids

Aqueous stock solution (0.5 mg mL^{-1}) of DCFH-DA (Sigma, USA) was used to determine ROS as described by Yilancioglu et al. (2014). Briefly, to 1 mL microalgal cell suspension, in triplicates withdrawn at desired intervals, 5 µL of dye solution was added and incubated for 20 min in the dark prior analysis. DCFH-DA, which is nonfluorescent, would pass inside the cells and converted into dichlorodihydrofluorescein (DCF) due to the activity of cellular esterase. Fluorescence of DCF formed was measured using a 488 nm laser and a 556LP 585/42 filter set on a BD FACSCanto Flow Cytometer.

Membrane permeability was measured using the staining dye, fluorescein diacetate (Sigma Aldrich, St. Louis, MO, USA), dissolved in acetone (1000 ppm, w/v) as per the method described by Chae et al. (2016). Intensities of fluorescein were measured in a BD FACSCanto Flow Cytometer fitted with a FITC filter (530/30), and the values were used to quantify cell permeability of each algal species. Non-stained cells were used as a negative control in both the channels to get the images for the samples stained. Data were evaluated using FlowJo Ver. 7.6.1 (Tree Star, Inc.).

Harvested microalgal suspensions were stained with 15 mM Nile Red (Sigma) to determine neutral lipids following a modified protocol of Dempster and Sommerfeld (1998). Aliquots of 50 µL solution of NR in acetone (0.1 mg mL^{-1}) were added to 1.0 mL suspension with gentle vortexing and incubated for 10 min at 37 °C in the dark. The uptake of NR in triplicate samples was monitored using a BD FACSCanto Flow Cytometer (Becton Dickinson Instruments) equipped with a 488 nm argon laser. The optical system used in the flow cytometer collects yellow and orange light (560-640 nm) that corresponds to neutral lipids. For the flow cytometry analysis, a positive control (heat-killed algal cells treated with the dye) and a negative control (untreated algal cells) were used, and the data were expressed in terms of fluorescence intensity as well as cell count.

3.3.4. FAME analysis

Analysis of FTIR-based FAME (Mathimani et al., 2015) from microalgal biomass was carried out by *in-situ* transesterification (Laurens et al., 2015) followed by gravimetric quantification. In brief, algal biomass in triplicates, harvested after three weeks was dried overnight at 40 °C and transesterified using 0.3 mL of HCl-MeOH blend (5%, v/v) for one h at 85 °C. The mixture was washed with water and chloroform to allow debris to be separated in the methanol layer and biodiesel in chloroform layer. Controls were maintained without the algal biomass. FT-IR spectroscopy was employed through Agilent Technologies Cary 660 FT-IR system working in mid-IR energy range (4000-400 cm^{-1}) in ATR mode to determine FAME. All the measurements were made through multi-bounce ZnSE ATR prism by placing FAME dissolved in chloroform. Solvent alone served as control. A total of 16 scans obtained for each sample were co-averaged to improve signal-to-noise ratio at a resolution of 8 cm^{-1} using air-cooled DTGS detector. All the spectra acquired are processed through Agilent IR Resolutions Pro software. Simultaneously, triplicate samples were analyzed for the yield of total lipids to make a comparison with the FAME yield.

3.3.5. Statistical analysis

The averages and standard deviations of the experimental data were identified using Graphpad Prism 7 software, and the statistical significance of means was determined by t-test using IBM SPSS Statistical Software (ver.24).

3.4. Results and discussion

3.4.1. Growth response of non-acidophilic microalgae to acidic pH

Initially, three different cell densities (1×10^4, 1×10^5, 5×10^5 cells mL^{-1}) of all the four microalgal strains were used to screen for assessment of tolerance and growth at pH 3.0. All the four microalgae at both the cell densities of 1×10^4 and 1×10^5 cells mL^{-1} could not survive after 12 days (Fig 3.2).

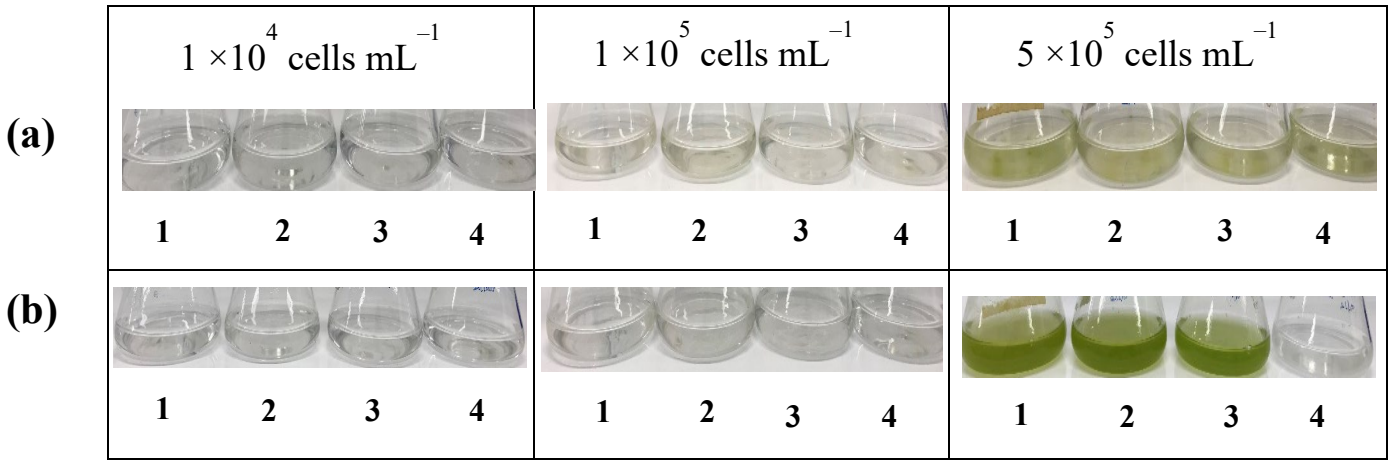

Fig. 3.2. Microalgal cultures (a) at day 0, and (b) after 12 days. (1) *Desmodesmus* sp. MAS1; (2) *Desmodesmus* sp. MAS2; (3) *Heterochlorella* sp. MAS3; (4) *Chlorella* sp. MM3 (control).

However, *Desmodesmus* sp. MAS1, *Desmodesmus* sp. MAS2 and *Heterochlorella* sp. MAS3 at the cell density of 5×10^5 cells mL^{-1} grew well during this incubation period. Interestingly, *Chlorella* sp. MM3 that was used as a control did not survive even at this higher cell density. Thus, these results clearly indicate that *Desmodesmus* sp. MAS1, *Desmodesmus* sp. MAS2 and *Heterochlorella* sp. MAS3 with good phenotypic plasticity could withstand acidic conditions (Sassenhagen et al., 2015; Abinandan et al., 2016). Such a tolerance in non-acidophiles to stress mediated by acidic conditions is unique since most of the microalgae are reported to be neutrophils as they grow ideally at circumneutral pH (Hirooka et al., 2017). Furthermore, *Desmodesmus* sp. MAS2 exhibited more than ten days of lag phase (data not shown) when compared to other two microalgae, confirming that the strain MAS2 is distinct from MAS1 (Fig. 3.1b). Based on these observations, only two cultures, viz., *Desmodesmus* sp. MAS1 and *Heterochlorella* sp. MAS3, were used for further studies on growth and metabolic activities. The maximum specific growth rates for *Heterochlorella* sp. MAS3 and

Desmodesmus sp. MAS1 at pH 6.7 were 0.20 and 0.15 day^{-1}, and 0.19 and 0.13 day^{-1} at pH 3.0, respectively (Fig. 3.3).

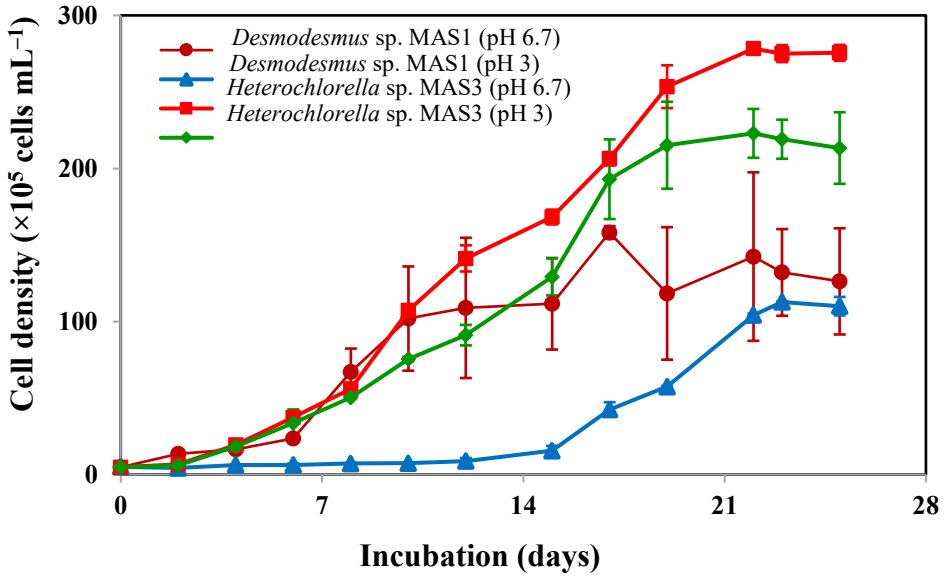

Fig. 3.3. Growth of *Desmodesmus* sp. MAS1 and *Heterochlorella* sp. MAS3 at pH 6.7 and 3.0. Error bars represent standard deviation (n = 3).

Similarly, an acidophilic microalga, *Coccomyxa onubensis*, achieved an approximate growth rate of 0.16 day^{-1} at pH 2.5 under light intensity of 50 µmol m^2 s^{-1} (Vaquero et al., 2014). On the other hand, the doubling times when grown at pH 6.7 for *Heterochlorella* sp. MAS3 and *Desmodesmus* sp. MAS1 were 3.4 and 4.6 days, respectively, and the corresponding values at pH 3.0 were 3.6 and 5.5 days. Thus, the growth rates observed for both the microalgal strains are much lower than those reported for other microalgae found growing abundantly in acidic pH environment (Sassenhagen et al., 2015), suggesting that the microalgae used in the present study are non-acidophiles that grow normally at circumneutral conditions. The possible reason for the lower growth rate in non-acidophilic microalgae could be due to culture conditions and low-level expression of proteins under acidic conditions (Hirooka et al., 2017). Since microbial acid tolerance is indicative of an adaptive response that results in enhanced tolerance to pH 3.0 (Lund et al., 2014), both the microalgae used in the present study can be considered as 'acid-tolerant' strains. Again, *Heterochlorella* sp. MAS3 is a better acid-tolerant strain than *Desmodesmus* sp. MAS1.

The response of the two microalgae to acidic conditions (pH 3.0) was studied employing three growth parameters such as the activity of CA, chlorophyll content and biomass production. The growth of microalgae in autotrophic conditions is primarily dependent on carbon concentration mechanisms (CCMs) through CA activity and passive diffusion uptake

of CO_2. The activity of CA depends upon the presence of bicarbonate ions (HCO_3^-) in the culture medium that regulates overall microalgal growth. Since CA activity can serve as an indicator of growth in photoautotrophs, this enzyme was also considered to assess the response of selected microalgal strains to acidic pH. In general, CA activity in the present study significantly declined when both the strains were grown for three weeks at pH 6.7 (Fig. 3.4a). Thus, the reduction in enzyme activity in *Heterochlorella* sp. MAS1 was 53% while it was 21% in the case of *Desmodesmus* sp. MAS3. A similar trend in decline of CA activity was observed in the cultures grown at pH 3.0. However, particularly after two weeks of growth at pH 3.0, the enzyme activity increased by 31 and 247% in *Heterochlorella* sp. MAS3 and *Desmodesmus* sp. MAS1, respectively, over the activities of CA observed at pH 6.7. This differential activity of CA over incubation period indicates that CCM is species-dependent (Van Hille et al., 2014). Also, the increase in CA activity corresponds to the bicarbonate transport, which is probably active as growth precedes with an increase in pH (Moroney and Ynalvez, 2007). Furthermore, this observed trend of increase in CA activity may be due to the adaptive response to the bicarbonate availability in microalgae (Yadav et al., 2014).

The present observation also suggests that both the microalgae survived in the first week at pH 3.0 through passive diffusion uptake of CO_2 rather than CA activity. Similarly, El-Ansari and Colman (2015) observed that an acid-tolerant microalga, *Chlorella kessleri*, grew well at pH 4 under continuous illumination (50 µmol m^{-2} s^{-1}) by maintaining near neutral internal pH through passive diffusion of CO_2. The passive diffusion of CO_2 is seemingly more in *Heterochlorella* sp. MAS3 than in *Desmodesmus* sp. MAS1. Thus, *Heterochlorella* sp. MAS3 must have maintained growth at acidic pH similar to that at pH 6.7 through the accumulation of CO_2 in high concentrations at the active site of Rubisco as suggested by El-Ansari and Colman (2015). Interestingly, both the strains showed low CA activity after three weeks probably due to increase in pH by triggering carbonate (CO_3^{2-}) synthesis from HCO_3^- (Van Hille et al., 2014). In all, the above results indicate that the two microalgae grew at pH 6.7 through CCM involving CA activity while both the mechanisms (passive diffusion uptake of CO_2 followed by CA activity) were used at pH 3.0.

The chlorophyll content in *Heterochlorella* sp. MAS3 grown at pH 6.7 for one week was 8.08 mg g^{-1} whereas the corresponding value in *Desmodesmus* sp. MAS1 was 9.08 mg g^{-1} (Fig. 3.4b). Interestingly, chlorophyll decreased significantly after three weeks of incubation and reached a concentration of 4.05 mg g^{-1}. Such a decrease in chlorophyll content is expected since nitrogen depletion even at pH 6.6 after 20 days may impair the photosynthetic activity thereby decrease the pigments like chlorophyll as in case of a red microalga, *Porphyridium*

cruentum (Zhao et al., 2017). Overall, the growth response in terms of chlorophyll content at pH 3.0 was also like that observed with biomass productivity. However, there was a drastic decrease (9-fold) in chlorophyll of *Desmodesmus* sp. MAS1 at pH 3.0 after the first week, indicating impairment of photosystem and the contribution of nitrogen pool mostly for survival rather than chlorophyll metabolism (Jiang et al., 2011). But, the concentration of chlorophyll increased from 0.33 mg g^{-1} (dry wt.) to 3.48 mg g^{-1} in strain MAS1 after three weeks of incubation at pH 3.0. Vaquero et al. (2014) showed that microalgae growing at pH 2.5 with a high inoculum density and light intensity of 400 µmol photons m^{-2} s^{-1} accumulated higher concentrations of lutein rather than chlorophyll without compromising biomass productivity. When grown at pH 3.0 for one week, there was no change in biomass of *Heterochlorella* sp. MAS3 while a significant decrease was evident in *Desmodesmus* sp. MAS1 (Fig. 3.4c). Thus, the reduction in biomass of the strain MAS1 after one week of growth at pH 3.0, when compared with that at pH 6.7, was 50% and was 43% at the end of two weeks. However, after three weeks of incubation at pH 3.0, the decrease of biomass in *Desmodesmus* sp. MAS1 was 40%, whereas the reduction in case of *Heterochlorella* sp. MAS3 was only 28% during this period. Jian et al. (2012) also observed >1-fold decrease in biomass production in non-adapted *Scenedemus dimorphus* grown at pH 3.0. Similarly, Eibl et al. (2014) reported low biomass production (0.5 g L^{-1}) even in acidophilic microalgae after 35 days. However, the overall yield of biomass in *Heterochlorella* sp. MAS3 decreased in acidic medium continuously for three weeks, while there was a significant increase in biomass of *Desmodesmus* sp. MAS1, clearly suggesting that the acclimation response in the latter strain was higher when compared with the former strain. However, the data also indicate that both the microalgal strains produced higher biomass at pH 3.0 when compared with those acidophilic microalgae grown in the presence of 15-20% CO_2 (Neves et al., 2018), suggesting that microalgae potential for biomass production even in hostile environments such as AMDs.

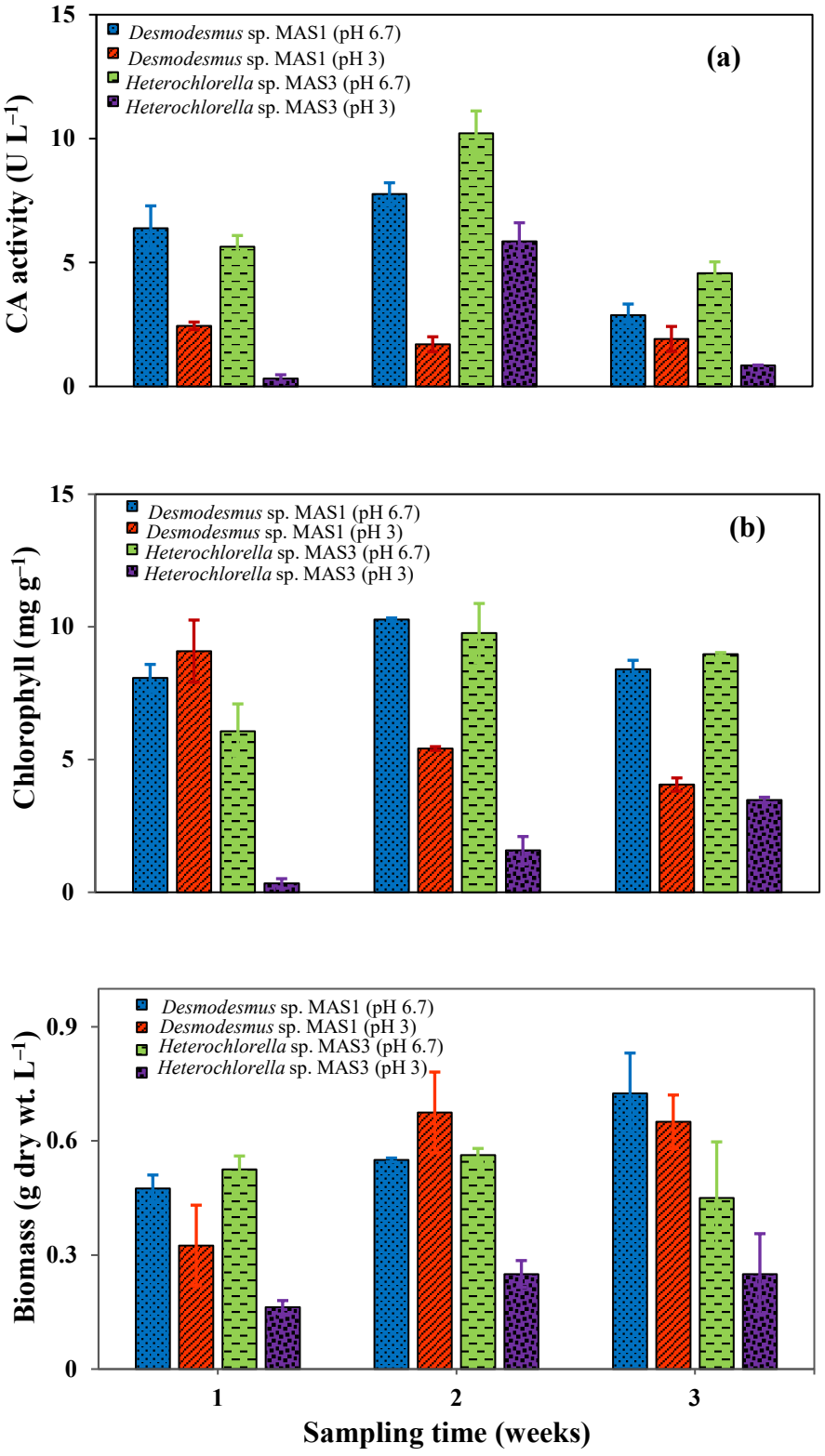

Fig. 3.4. (a) Carbonic anhydrase (CA) activity, (b) Chlorophyll and (c) Biomass in *Heterochlorella* sp. MAS3 and *Desmodesmus* sp. MAS1 after growth at pH 6.7 and 3.0. Error bars represent standard deviation (n = 3).

3.4.2. Biochemical and stress response in microalgae to acidic pH

The impact of acidic pH on biochemicals, viz., total proteins, carbohydrates and lipids in microalgae are very crucial in understanding the changes in metabolism. *Heterochlorella* sp. MAS3 accumulated high concentrations (nearly 3-fold) of carbohydrates while *Desmodesmus* sp. MAS1 recorded a significant decrease (23%) (Fig. 3.5a) when grown at pH 6.7 for three weeks. Such a differential response among the microalgal strains even at neutral pH could be due to sharp changes in nutrient status of the medium. For instance, Rizza et al. (2017) observed low levels of carbohydrates in *Scenedesmus* sp. under limited conditions of nitrogen. Although carbohydrate accumulation in *Heterochlorella* sp. MAS3 decreased by 50% at pH 3.0 after one week; there was >5 and >7-fold increase at the end of two and three weeks of incubation, respectively. On the other hand, the accumulation of carbohydrates increased by 48% in *Desmodesmus* sp. MAS1 after two weeks when grown at pH 3.0, but significantly decreased (2-fold) after three weeks. Khalil et al. (2009) also reported such a decrease in *Dunaliella bardawil* and *Chlorella ellipsoidea* since endogenous carbohydrates are used for survival at pH 4.0. Contrary to the response of carbohydrates, the extent of protein accumulation in the selected microalgae was entirely different. Thus, even at pH 6.7, the protein increases in *Desmodesmus* sp. MAS1 after a week was 3.5-fold when compared with *Heterochlorella* sp. MAS3 (Fig. 3.5b). Interestingly, there was a significant decrease over time in strain MAS1 and increase in strain MAS3. The observed decline in *Desmodesmus* sp. MAS1 could be ascribed to nitrogen limitation since Yilancioglu et al. (2014) perceived that certain microalgae shift to accumulate higher lipid and less protein especially under nitrogen starvation at a near neutral pH. It has been well established in the literature that the response to limitation and consequent depletion of nitrogen results in a decrease in photosynthetic pigment as well as protein content and an increase in lipid content of microalgae (Tan et al., 2016; Vo et al., 2018).

Overall, protein accumulation significantly increased after three weeks in both the strains when grown at pH 3.0. Thus, the increase in protein content after three weeks in *Heterochlorella* sp. MAS3 was 34% as against to 58% enhancement in *Desmodesmus* sp. MAS1, indicating that protein-coding genes may have been upregulated in acidic pH as reported in the case of *C. ellipsoidea* by Khalil et al. (2009). The total lipids increased significantly in *Desmodesmus* sp. MAS1 as compared to *Heterochlorella* sp. MAS3 after one week at pH 6.7 (Fig. 3.5c). Incubation of the strain MAS1 for two weeks at pH 3.0 significantly increased (119%) the protein content, but the increase declined to only 15% at the end of three weeks. Some reports indicated that nitrogen deprivation caused lipid induction even in acidic

algae (Hirooka et al., 2014; 2016). Eibl et al. (2014) observed a three-week lag phase and appearance of green to yellow color in microalgae isolated from mine environment (pH 3.0) and correlated this change to the synthesis of lipids. There was a two-fold increase in lipid content of *Desmodemsus* sp. MAS1 at pH 3.0 while the increase was only one-fold in *Heterochlorella* sp. MAS3 after two weeks of incubation. The above results indicate that *Desmodesmus* sp. MAS1 yields proteins and total lipids better than *Heterochlorella* sp. MAS3 under acidic conditions.

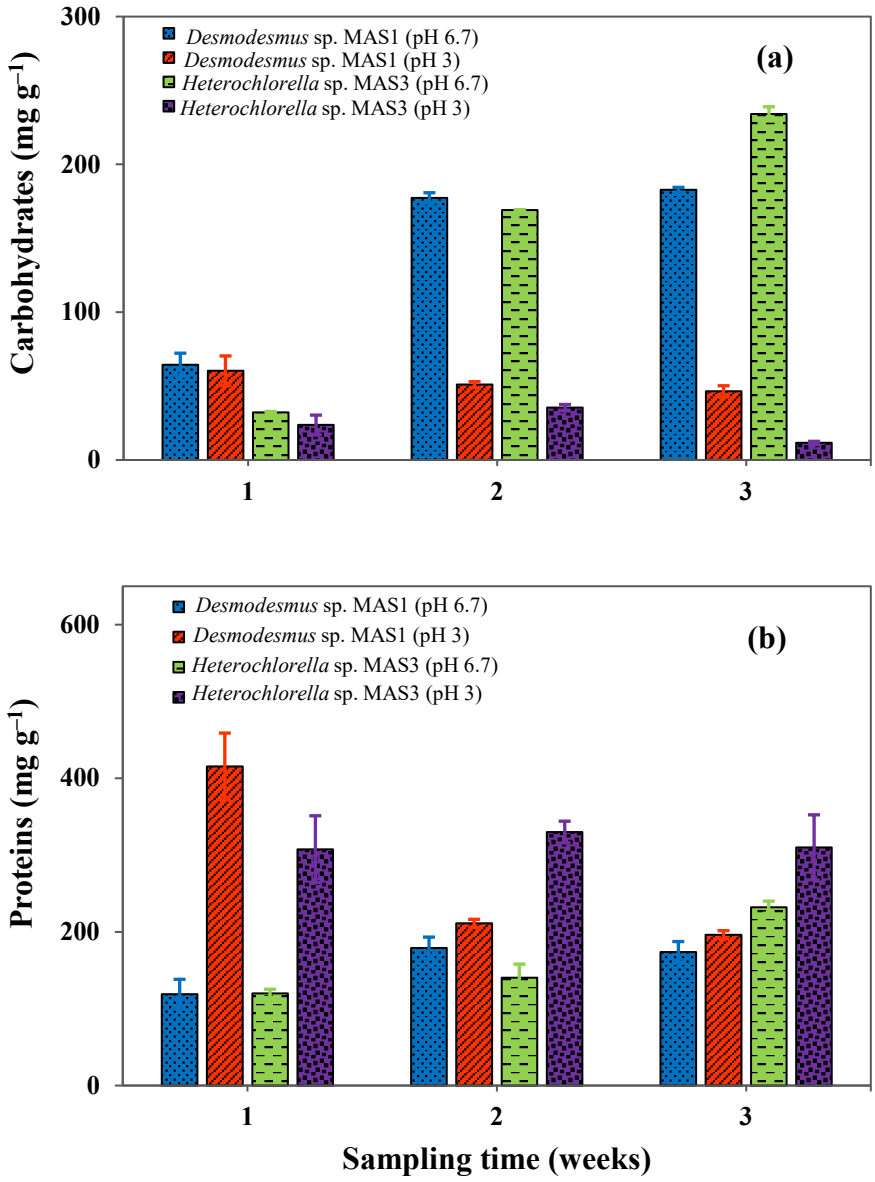

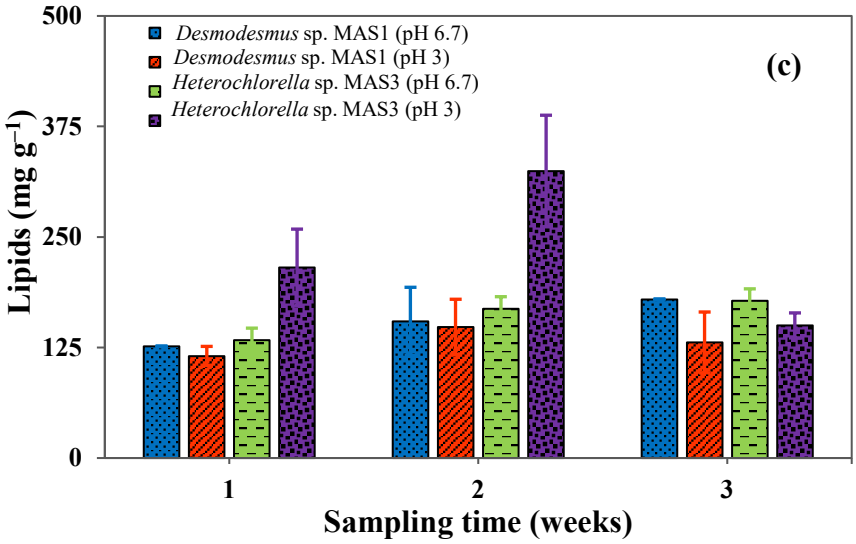

Fig. 3.5. (a) Carbohydrates, (b) Proteins, and (c) Lipids in *Heterochlorella* sp. MAS3 and *Desmodesmus* sp. MAS1 after growth at pH 6.7 and 3.0. Error bars represent standard deviation (n = 3).

Since it is also essential to understand the stress response to extreme environmental fluctuations (Hyka et al., 2013), advocates for the use of flow cytometry analysis in the present study. Thus, ROS, membrane permeability and neutral lipids were used as the criteria for stress response in microalgae. The ROS (Fig. 3.6a) profile showed that the stress was apparent only in *Desmodesmus* sp. MAS1. After the first week, there was a 2-fold increase in ROS at pH 3.0 but dropped at the end of the second week, and the microalga was relieved entirely from stress after three weeks. Eibl et al. (2014) also observed identical pattern of increased stress after one week in an acidophilic microalga, *Scenedesmus* sp. Lig 290, isolated from a waterbody with pH 4.5. On the contrary, there was no stress in *Heterochlorella* sp. MAS3 even after two weeks, indicating its high potential in adapting quickly to the changed pH. The data presented in Fig. 3.6b indicate changes in the membrane permeability of the non-acidophilic microalgae when grown in acidic conditions. *Desmodesmus* sp. MAS1 exhibited a significant (>2-fold) decrease in fluorescence signal at pH 3.0 when compared to its growth at neutral pH, indicating the low permeability of the dye into the cells in acidic conditions. However, the fluorescence signal gradually increased in *Heterochlorella* sp. MAS3 upon growth at pH 3.0. These differences in membrane permeability observed because of structural and physiological changes in both the strains grown at pH 3.0 corroborate with the results on ROS. Similarly, neutral lipid profile (Fig. 3.6c) indicates a tremendous increase in fluorescence intensity in *Desmodesmus* sp. MAS1 is grown at pH 3.0. Thus, the observed 3.3-fold increase in neutral lipids in the first

week corroborates with the enhancement of membrane permeability and ROS production noticed during this period. This increase in lipid was also observed even after two weeks, which may be due to the limitation of nutrients, especially nitrogen. Yao et al. (2016) also found an increasing trend in the lipid content of *Dunaliella salina* under osmotic shock through Nile red fluorescence. Thus, the present results on neutral lipids in *Desmodesmus* sp. MAS1 suggest that the microalga during acclimation to extreme acidic conditions changed its metabolic pathway to protein and lipid, especially higher neutral lipid faction, synthesis resulting in decreased carbohydrate reserves. In contrast, *Heterochlorella* sp. MAS3 did not show significant changes in lipid profile, a response similar in case of ROS production.

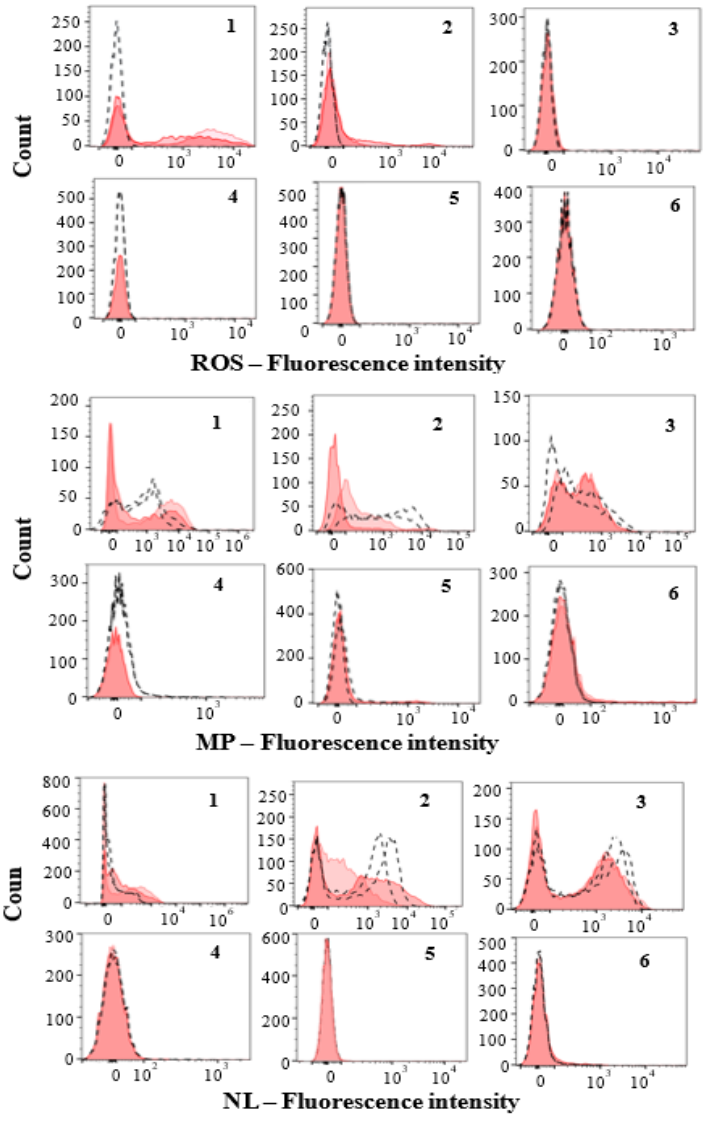

Fig. 3.6. Three-week response of (a) Reactive oxygen species (ROS), (b) Membrane permeability (MP), and (c) Neutral lipids (NL) in *Desmodesmus* sp. MAS1 (1-3); and *Heterochlorella* sp. MAS3 (4-6) after growth at pH 6.7 (- -) and pH 3.0 ( ).

3.4.3. Biodiesel production in microalgae at acclimated acidic pH

Since FTIR-based microalgal FAME (biodiesel) analysis is considered as a rapid method compared to the conventional techniques (Mathimani et al., 2015), and this approach employed in the study to monitor the biofuel production from algal biomass through *in-situ* transesterification. FTIR spectral analysis of FAME exhibit strong peak areas as suggested for the presence of ester molecules and the characterization of biodiesel from microalgae (Table 3.1).

Table 3.1. Microalgal FAME-FTIR characteristics

Wave number (cm^{-1})	**Vibration**	**Functional group**	**Reference**
2943-2945	ν_{as}, ν_s (CH_2)	Aliphatic fatty acid hydrocarbon chains	Leong et al. (2016)
2835	ν(C−H)	Methoxy chain in oil residue	Manthey (2006)
1730-1743	ν_s (C=O)	Triglyceride and free fatty acid esters	Sitthithanaboon et al. (2015)
1650-1652	δ_{as} (C=C)	Disubstituted and unsatutrated *cis*-olefins	Timilsena et al. (2017)
1450-1454	δ_s (CH_2; CH_3)	Methyl and methylene groups	Mahesar et al. (2011)
1232-1236	ν_{as} (PO_2^-) ν_{as} (C–O)	Phosphorylated molecules, e.g. nucleic acids/ester group	Dao et al. (2017)
1106-1114 1019-1025	ν_{as} (C–O) ν (C–O–C)	Carbonyl esters/Carbohydrates	Silva et al. (2014)

ν – vibrational stretch, ν_{as} – asymmetric vibrational stretch, ν_s – symmetric vibrational stretch, δs – symmetric vibrational bend, δas – asymmetric vibrational bend.

The appearance of peaks in the region of 1730-1743 cm^{-1} is due to C=O stretching vibrations from the mixture of carboxylic acid esters, indicating the conversion of triglycerides (Viêgas et al., 2015). Again, the peak region at 1106-1114 cm^{-1} is due to asymmetric vibrational stretching of esters group arising from methyl C-O, confirming that the biodiesel is predominantly a monoalkyl ester (Sitthithanaboon et al., 2015). Furthermore, the bending vibrational frequency of C-O as evident in the region 1232-1236 cm^{-1} confirms the presence of ester molecules as has been established for a fatty acid ester derived from hydrothermal liquefaction of *Dunaliella teriolecta* biomass by Zou et al. (2009). The occurrence of rich aliphatic hydrocarbons in the present samples, as evident at 2835 cm^{-1} and 2943-2945 cm^{-1} through $–CH_2$/$-CH_3$ symmetric and asymmetric stretching vibrations, respectively, indicates the good quality of biodiesel (Mathimani et al., 2015). Interestingly, another peak has also been observed at 1650-1652 cm^{-1} that corresponds to the C=C stretching vibration arising from *cis*-olefins, suggesting a degree of unsaturation that is found in vegetable oils (Timilsena et al., 2017). The 3D-IR image analysis for the region 1700-1800 cm^{-1} after deconvolution of the peaks as shown in Fig 3.7. confirms the proper transesterification in both the microalgal strains. It also proves that the conversion of triglyceride to ester is high in biomass samples collected at pH 3.0 when compared to those grown at pH 6.7.

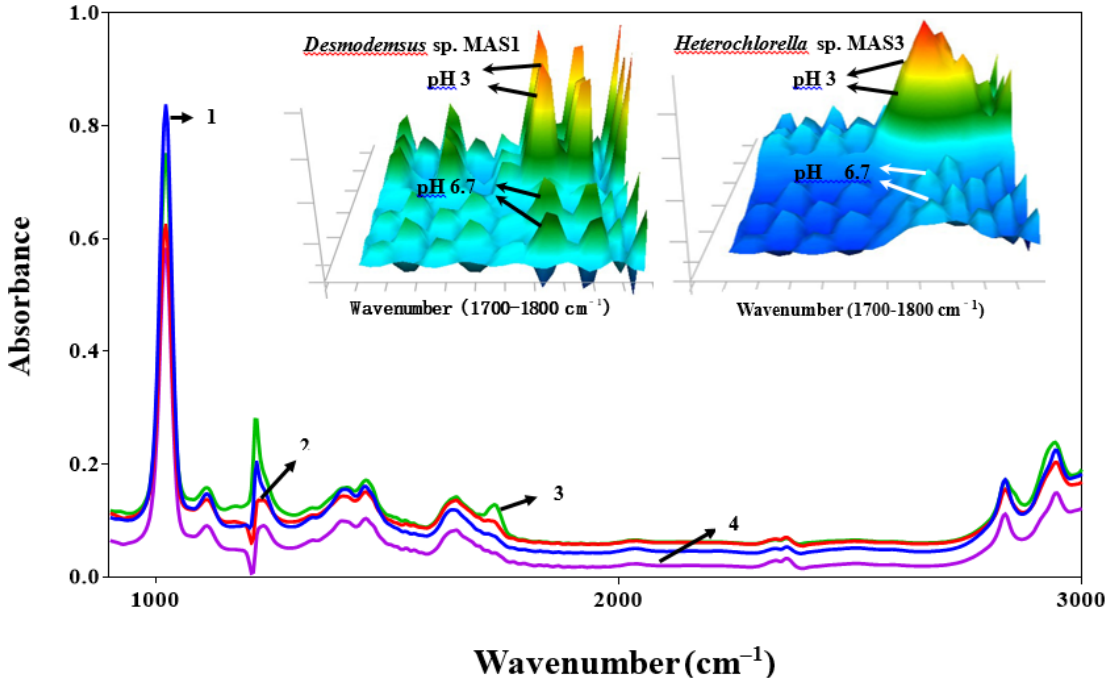

Fig. 3.7. FAME-FTIR spectra of *Desmodesmus* sp. MAS1 grown at (1) pH 6.7 and (2) pH 3.0, and *Heterochlorella* sp. MAS3 at (3) pH 6.7 and (4) pH 3.0. The inset data correspond to the spectra at 1700-1800 cm^{-1}.

The yield of FAME was 11 and 13% from *Desmodesmus* sp. MAS1 when grown at pH 6.7 and 3.0, respectively, and the corresponding values for FAME yield in *Heterochlorella* sp. MAS3 were 7 and 15% (Fig. 3.8).

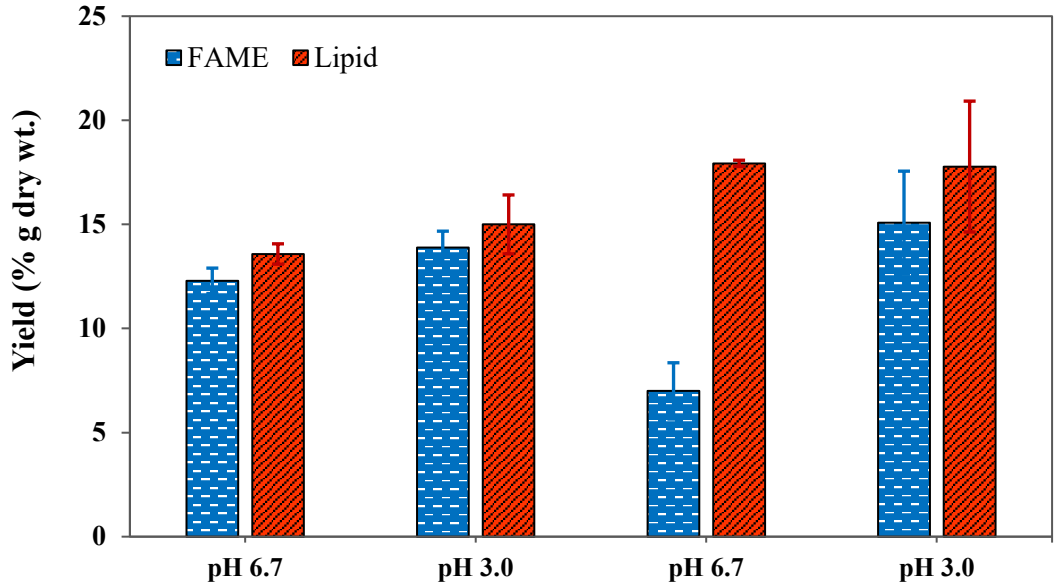

Fig. 3.8. Yield (% dry wt.) of FAMEs and lipids in *Desmodesmus* sp. MAS1 and *Heterochlorella* sp. MAS3 when grown at pH 6.7 and 3.0. Error bars represent standard deviation (n = 3).

While Laurens et al. (2012) reported 9-10% yield of FAME in *Chlorella vulgaris* and *Nannochloropsis* sp. under normal growth conditions, Tang et al. (2016) observed a FAME yield of 10% (on a dry weight basis) in *Nannochloropsis* sp. The results indicate that the FAME yield in both the microalgal strains when acclimated to acidic conditions is higher than those reported in the literature. Recently, Souza et al. (2017) reported a 15% oil yield in *Chlamydomonas acidophila* LAFIC-004 grown under acidic conditions. In general, the lipid to FAME yield was low in both the microalgae acclimated to acidic pH. Similarly, Ruiz-Dominguez et al. (2015) observed that lipid to FAME yield was low even in acidophilic microalgae. The FAME yield in *Heterochlorella* sp. MAS3 at pH 6.7 was low probably because of non-optimization of lipid to oil conversion (Ehimen et al., 2010). However, *Heterochlorella* sp. MAS3 gave a higher yield of lipids and FAME than *Desmodesmus* sp. MAS1 at pH 3.0. Likewise, Eibl et al. (2014) observed that acidophilic microalgae are growing at optimum pH of 4.0 accumulated higher lipids relative to those grown at pH 7.0. Hirooka et al. (2016) also found that red algae assimilated higher lipid in medium depleted with nitrogen source in acidic pH. Pick and Avidan (2017) showed that microalgae under nitrogen limitation assimilated

neutral lipids made from C allocation. The present observation of a significant increase in lipids and FAME indicates the stress mediated by both acidic pH and nutrient depletion, with the former occurring initially and the latter in the third week of microalgal growth. Such a sequential stress response was observed earlier in acidophilic microalgae wherein they accumulated more lipids under nitrogen limited conditions at a pH range of 3-5 (Hirooka et al., 2014). The efficiency in conversion of lipid to biodiesel was relatively higher in *Desmodesmus* sp. MAS1 than in *Heterochlorella* sp. MAS3, indicating the accumulation of tranesterifiable lipids (triacylglycerols, TAGs) due to the stress induced by acidic conditions. Based on the results, *Desmodesmus* sp. MAS1 and *Heterochlorella* sp. MAS3 is designated as acid tolerant strain.

3.4.4. Practical applications and prospects of the present findings

Very recent report from NASA (Global Climate Change, 2018) indicates that anthropogenic activities resulted in a relative 93% increase in atmospheric CO_2 during the last 12 yrs. Also, the European Union dedicated to cut CO_2 and other greenhouse gas emissions based on the UN Framework using microalgae (CORDIS, 2013). Sequestration of CO_2 by microalgae is often limited due to mass transfer in raceway ponds and requires the specific design of photobioreactors to produce biomass for revenue generation (Abinandan et al., 2018b). Furthermore, CO_2 reacts with water to form carbonic acid resulting in very acidic pH necessitating the addition of hydroxides to maintain the required bicarbonate for microalgal growth (Van Den Hende et al., 2012). These factors cause more capital and energy investments, thus always underestimating the promising values of the microalgal technology for biomass production. It is imperative to explore and identify the microalgae as a primary indicators/tools to sequester at least the CO_2 emission from industrial activities such as flue gas that contributes about 10-20% CO_2 (Sakarika and Kornaros 2016). However, the flue gas reaction with water creates a very acidic environment suggesting that the acidophilus microalgae are a possible alternative for CO_2 sequestration (Neves et al., 2018).

The stress for acidophilic microalgae in acidic conditions is much less compared to non-acidophiles and it reflects in less biofuel production by the former group. Hence, non-acidophilic microalgae should be bio-prospected for biomass and biodiesel production under extreme acidic environments. Several studies that exploited microalgae to produce biofuel relied mostly on nutrient stress and varying other growth conditions such as phototrophy, mixotrophy and heterotrophy (Cheirsilp and Torpee, 2012; Huang et al. 2017; Ma et al., 2017; Kose Engin et al., 2018). However, while acclimating non-acidophilic microalgae for lipid

production, their response to varying nutrients needs to be thoroughly understood. In fact, this approach would be especially beneficial in many developing countries such as Vietnam, Laos, Cambodia and Myanmar for alleviating the levels of excess nutrients in wastewaters and probable effluents from mine sites (Reichl et al., 2018). For instance, wastewaters from shrimp farming in Vietnam generate high amounts of nitrogen (159 kg^{-1} ha^{-1} $crop^{-1}$) and phosphates (19.6 kg^{-1} ha^{-1} $crop^{-1}$) that can be utilized for microalgal biofuel production (Vo et al., 2018). Also, reports suggest that acid-tolerant microalgae produce carotenoids and lutein in response to stress implying their applications for producing commercial nutraceuticals (Vaquero et al., 2014). Interestingly, acidophilic microalgae found in such extreme environments as AMDs develop tolerance to survive rather than remediating the contaminants (Abinandan et al., 2018a). Hence, consortia of acidophilic microalgae and acid-tolerant microalgae obtained from non-acidophilic environments can be the best candidates for remediation of AMDs. Future research must include a wide array of non-acidophilic microalgae to establish their greater potential in production of biomass and biofuel under extreme acidic conditions.

3.5. Conclusions

Present investigation demonstrated that selective non-acidophilic microalgae can grow well under acidic conditions through passive diffusion of CO_2. This acclimation could be ascribed to downregulation of carbohydrate-pathway and upregulation of protein and lipid-pathways as evidenced in *Desmodesmus* sp. MAS1 and to a lesser extent in *Heterochlorella* sp. MAS3. The FAME yield during acclimation was relatively high in both the strains compared to neutral conditions, indicating the biofuel potential. This study provides a proof-of-the-concept that non-acidophilic microalgae can acclimated to acidic conditions for the potential use in the sustainable production of biomass and biodiesel under extremely acidic conditions as exist in AMDs.

3.6. References

Abinandan, S., Shanthakumar, S., 2016. Evaluation of photosynthetic efficacy and CO_2 removal of microalgae grown in an enriched bicarbonate medium. 3 Biotech 6, 9.

Abinandan, S., Subashchandrabose, S.R., Venkateswarlu, K., Megharaj, M., 2018a. Microalgae–bacteria biofilms: a sustainable synergistic approach in remediation of acid mine drainage. Appl. Microbiol. Biotechnol. 102, 1131–1144.

Abinandan, S., Subashchandrabose, S.R., Venkateswarlu, K., Megharaj, M., 2018b. Nutrient removal and biomass production: advances in microalgal biotechnology for wastewater treatment. Crit. Rev. Biotechnol. 38, 1244 –1260.

Chae, Y., Kim, D. and An, Y.J., 2016. Effect of fluoride on the cell viability, cell organelle potential, and photosynthetic capacity of freshwater and soil algae. Environ. Pollut. 219, 359–367.

Cheirsilp, B., Torpee, S., 2012. Enhanced growth and lipid production of microalgae under mixotrophic culture condition: Effect of light intensity, glucose concentration and fed-batch cultivation. Bioresour. Technol. 110, 510–516.

Chen, Y., Vaidyanathan, S., 2013. Simultaneous assay of pigments, carbohydrates, proteins and lipids in microalgae. Anal. Chim. Acta 776, 31–40.

CORDIS, 2013. https://cordis.europa.eu/news/rcn/35593_en.html (Accessed 19.09.2018).

Dempster, A., Sommerfeld, R., 1998. Effects of environmental conditions on growth and lipid accumulation in *Nitzschia communis* (Bacillariophyceae). J. Phycol. 34, 712–721.

Eibl, J.K., Corcoran, J.D., Senhorinho, G.N., Zhang, K., Hosseini, N.S., Marsden, J., Laamanen, C.A., Scott, J.A. and Ross, G.M., 2014. Bioprospecting for acidophilic lipid-rich green microalgae isolated from abandoned mine site water bodies. AMB Exp, 4, 7.

Ehimen, E.A., Sun, Z.F., Carrington, C.G., 2010. Variables affecting the in situ transesterification of microalgae lipids. Fuel 89, 677–684.

El-Ansari, O., Colman, B. 2015. Inorganic carbon acquisition in the acid-tolerant alga *Chlorella kessleri*. Physiol. Plantar. 153, 175–182.

Ganeshkumar, V., Subashchandrabose, S.R., Dharmarajan, R., Venkateswarlu, K., Naidu, R., Megharaj, M., 2018. Use of mixed wastewaters from piggery and winery for nutrient removal and lipid production by *Chlorella* sp. MM3. Bioresour. Technol. 256, 254–258.

Global Climate Change, NASA, 2018. https://climate.nasa.gov/vital-signs/carbon-dioxide (Accessed 19.09.2018).

Hattich, G.S.I., Listmann, L., Raab, J., Ozod-Seradj, D., Reusch, T.B.H., Matthiessen, B., 2017. Inter- and intra-specific phenotypic plasticity of three phytoplankton species in response to ocean acidification. Biol. Lett. 13, 20160774.

Hirooka, S., Higuchi, S., Uzuka, A., Nozaki, H. and Miyagishima, S.Y., 2014. Acidophilic green alga *Pseudochlorella* sp. YKT1 accumulates high amount of lipid droplets under a nitrogen-depleted condition at a low-pH. PLoS One 9, 107702.

Hirooka, S., Miyagishima, S.Y., 2016. Cultivation of acidophilic algae *Galdieria sulphuraria* and *Pseudochlorella* sp. YKT1 in media derived from acidic hot springs. Front. Microbiol. 7, 2022.

Hirooka, S., Hirose, Y., Kanesaki, Y., Higuchi, S., Fujiwara, T., Onuma, R., Era, A., Ohbayashi, R., Uzuka, A., Nozaki, H., Yoshikawa, H., Miyagishima, S.Y., 2017. Acidophilic green algal genome provides insights into adaptation to an acidic environment. Proc. Natl. Acad. Sci. USA 114, E8304–E8313.

Huang, A., Sun, L., Wu, S., Liu, C., Zhao, P., Xie, X., Wang, G., 2017. Utilization of glucose and acetate by *Chlorella* and the effect of multiple factors on cell composition. J. Appl. Phycol. 29, 23–33.

Hyka, P., Lickova, S., Přibyl, P., Melzoch, K., Kovar, K., 2013. Flow cytometry for the development of biotechnological processes with microalgae. Biotechnol. Adv. 31, 2–16.

Jiang, Y., Peng, X., Zhang, W., Liu, T., 2012. Enhancement of acid resistance of *Scenedesmus dimorphus* by acid adaptation. J. Appl. Phycol. 24, 1637–1641.

Jiang, L., Luo, S., Fan, X., Yang, Z. Guo, R., 2011. Biomass and lipid production of marine microalgae using municipal wastewater and high concentration of CO_2. Appl. Energy 88, 3336–3341.

Jin, J., Dupré, C., Legrand, J. and Grizeau, D., 2016. Extracellular hydrocarbon and intracellular lipid accumulation are related to nutrient-sufficient conditions in pH-controlled chemostat cultures of the microalga *Botryococcus braunii* SAG 30.81. Algal Res. 17, 244–252.

Khalil, Z.I., Asker, M.M., El-Sayed, S. and Kobbia, I.A., 2010. Effect of pH on growth and biochemical responses of *Dunaliella bardawil* and *Chlorella ellipsoidea*. World J. Microbiol. Biotechnol. 26, 1225–1231.

Kose Engin, I., Cekmecelioglu, D., Yücel, A.M., Oktem, H.A., 2018. Enhancement of heterotrophic biomass production by *Micractinium* sp. ME05. Waste Biomass Valori. 9, 811–820.

Kumar S., Stecher G., Tamura, K., 2016. MEGA7: Molecular evolutionary genetics analysis version 7.0 for bigger datasets. Mol. Biol. Evol. 33,1870–1874.

Laurens, L.M.L., Nagle, N., Davis, R., Sweeney, N., Van Wychen, S., Lowell, A., Pienkos, P.T., 2015. Acid-catalyzed algal biomass pretreatment for integrated lipid and carbohydrate-based biofuels production. Green Chem. 17, 1145–1158.

Laurens, L.M.L., Quinn, M., Van Wychen, S., Templeton, D.W., Wolfrum, E.J., 2012. Accurate and reliable quantification of total microalgal fuel potential as fatty acid methyl esters by in situ transesterification. Anal. Bioanal. Chem. 403(1), 167–178.

Lund, P., Tramonti, A., De Biase, D., 2014. Coping with low pH: molecular strategies in neutralophilic bacteria, FEMS Microbiol. Rev. 38, 1091–1125.

Ma, M., Yuan, D., He, Y., Park, M., Gong, Y., Hu, Q. 2017. Effective control of *Poterioochromonas malhamensis* in pilot-scale culture of *Chlorella sorokiniana* GT-1 by maintaining CO_2-mediated low culture pH. Algal Res. 26, 436–444.

Mathimani, T., Uma, L., Prabaharan, D., 2015. Homogeneous acid catalysed transesterification of marine microalga *Chlorella* sp. BDUG 91771 lipid – An efficient biodiesel yield and its characterization. Renew. Energy 81, 523–533.

Moroney, J.V., Ynalvez, R.A., 2007. Proposed carbon dioxide concentrating mechanism in *Chlamydomonas reinhardtii.* Eukaryot. Cell., 6, 1251–1259.

Neves, F.D.F., Hoinaski, L., Rörig, L.R., Derner, R.B. and de Melo Lisboa, H., 2018. Carbon biofixation and lipid composition of an acidophilic microalga cultivated on treated wastewater supplied with different CO_2 levels. Env. Technol. https://doi.org/10.1080/09593330.2018.1471103.

Nalewajko, C., Colman, B. and Olaveson, M., 1997. Effects of pH on growth, photosynthesis, respiration, and copper tolerance of three *Scenedesmus* strains. Environ. Exp. Bot. 37(2-3), 153–160.

Ores, J.d.C., Amarante, M.C.A.D., Kalil, S.J., 2016. Co-production of carbonic anhydrase and phycobiliproteins by *Spirulina* sp. and *Synechococcus nidulans*. Bioresour. Technol. 219, 219–227.

Perez-Garcia, O., Escalante, F.M.E., de-Bashan, L.E., Bashan, Y. 2011. Heterotrophic cultures of microalgae: Metabolism and potential products. Water Res. 45, 11–36.

Pick, U. and Avidan, O., 2017. Triacylglycerol is produced from starch and polar lipids in the green alga *Dunaliella tertiolecta*. J. Exp. Bot. 68,4939–4950.

Reichl, C., Schatz, M. and Zsak, G., 2018. World mining data. Minerals Production International Organizing Committee for the World Mining Congresses, 32.1-261.

Ramadass, K., Megharaj, M., Venkateswarlu, K., Naidu, R., 2017. Toxicity of diesel water accommodated fraction toward microalgae, *Pseudokirchneriella subcapitata* and *Chlorella* sp. MM3. Ecotoxicol. Environ. Saf. 142, 538–543.

Ruiz-Domínguez, M.C., Vaquero, I., Obregón, V., de la Morena, B., Vílchez, C. and Vega, J.M., 2015. Lipid accumulation and antioxidant activity in the eukaryotic acidophilic microalga *Coccomyxa* sp.(strain onubensis) under nutrient starvation. J. Appl. Phycol. 27(3), 1099–1108.

Sassenhagen, I., Wilken, S., Godhe, A., Rengefors, K., 2015. Phenotypic plasticity and differentiation in an invasive freshwater microalga. Harmful Algae 41, 38–45.

Sakarika, M., Kornaros, M., 2016. Effect of pH on growth and lipid accumulation kinetics of the microalga *Chlorella vulgaris* grown heterotrophically under sulfur limitation. Bioresour. Technol., 219, 694–701.

Sitthithanaboon, W., Reddy, H.K., Muppaneni, T., Ponnusamy, S., Punsuvon, V., Holguim, F., Dungan, B., Deng, S., 2015. Single-step conversion of wet *Nannochloropsis gaditana* to biodiesel under subcritical methanol conditions. Fuel 147, 253–259.

Souza, L.D.S., Simioni, C., Bouzon, Z.L., Schneider, R.D.C.D.S., Gressler, P., Miotto, M.C., Rossi, M.J. and Rörig, L.R., 2017. Morphological and ultrastructural characterization of the acidophilic and lipid-producer strain *Chlamydomonas acidophila* LAFIC-004 (Chlorophyta) under different culture conditions. Protoplasma 254, 1385–1398.

Subashchandrabose, S.R., Logeshwaran, P., Venkateswarlu, K., Naidu, R., Megharaj, M., 2017. Pyrene degradation by *Chlorella* sp. MM3 in liquid medium and soil slurry: Possible role of dihydrolipoamide acetyltransferase in pyrene biodegradation. Algal Res. 23, 223–232.

Subashchandrabose, S.R., Wang, L., Venkateswarlu, K., Naidu, R., Megharaj, M., 2017. Interactive effects of PAHs and heavy metal mixtures on oxidative stress in *Chlorella* sp. MM3 as determined by artificial neural network and genetic algorithm. Algal Res. 21, 203–212.

Sung, K.D., Lee, J.S., Shin, C.S., Park, S.C., 1999. Isolation of a new highly CO_2 tolerant fresh water microalga *Chlorella* sp. KR-1. Renew. Energy 16, 1019–22.

Tan, K.W.M., Lin, H., Shen, H., Lee, Y.K., 2016. Nitrogen-induced metabolic changes and molecular determinants of carbon allocation in *Dunaliella tertiolecta*. Sci. Rep., 6, 37235.

Tang, Y., Zhang, Y., Rosenberg, J., Betenbaugh, M., Wang, F., 2016. Optimization of one-step in situ transesterification method for accurate quantification of EPA in *Nannochloropsis gaditana*. Appl. Sci., 6, 343.

Timilsena, Y.P., Vongsvivut, J., Adhikari, R., Adhikari, B., 2017. Physicochemical and thermal characteristics of Australian chia seed oil. Food Chem. 228, 394–402.

Van Hille, R., M. Fagan, L., Pott, B.R., 2014. A modified pH drift assay for inorganic carbon accumulation and external carbonic anhydrase activity in microalgae. J. Appl. Phycol. 26, 377–385.

Van Den Hende, S., Vervaeren, H. and Boon, N., 2012. Flue gas compounds and microalgae: (bio-)chemical interactions leading to biotechnological opportunities. Biotechnol. Adv. 30, 1405–1424.

Vaquero, I., Mogedas, B., Ruiz-Domínguez, M.C., Vega, J.M. and Vílchez, C., 2014. Light-mediated lutein enrichment of an acid environment microalga. Algal Res., 6, 70–77.

Viêgas, C.V., Hachemi, I., Freitas, S.P., Mäki-Arvela, P., Aho, A., Hemming, J., Smeds, A., Heinmaa, I., Fontes, F.B., da Silva Pereira, D.C., Kumar, N., Aranda, D.A.G., Murzin, D.Y., 2015. A route to produce renewable diesel from algae: Synthesis and characterization of biodiesel via in situ transesterification of *Chlorella* alga and its catalytic deoxygenation to renewable diesel. Fuel 155, 144–154.

Vo, H.N.P., Bui, X.T., Nguyen, T.T., Nguyen, D.D., Dao, T.S., Cao, N.D.T., Vo, T.K.Q., 2018. Effects of nutrient ratios and carbon dioxide bio-sequestration on biomass growth of *Chlorella* sp. in bubble column photobioreactor. J. Environ. Manage. 219, 1–8.

Yadav, R.R., Krishnamurthi, K., Shekh, A.Y., Mudliar, S.N., Devi, S.S., Chakrabarti, T., 2014. Activity enhancement of carbonic anhydrase in *Chlamydomona*s sp. for effective CO_2 sequestration. Clean. Technol. Environ. 16, 1827–1833.

Yao, S., Lu, J., Sárossy, Z., Baggesen, C., Brandt, A., An, Y., 2016. Neutral lipid production in *Dunaliella salina* during osmotic stress and adaptation. J. Appl. Phycol. 28, 2167–2175.

Yilancioglu, K., Cokol, M., Pastirmaci, I., Erman, B. and Cetiner, S., 2014. Oxidative stress is a mediator for increased lipid accumulation in a newly isolated *Dunaliella salina* strain. PLoS One 9, e91957.

Zhao, L.S., Li, K., Wang, Q.M., Song, X.Y., Su, H.N., Xie, B.B., Zhang, X.Y., Huang, F., Chen, X.L., Zhou, B.C. and Zhang, Y.Z., 2017. Nitrogen starvation impacts the photosynthetic performance of *Porphyridium cruentum* as revealed by chlorophyll a fluorescence. Sci. Rep. 7, 8542.

Zou, S., Wu, Y., Yang, M., Li, C., Tong, J. 2009. Thermochemical catalytic liquefaction of the marine microalgae *Dunaliella tertiolecta* and characterization of bio-oils. Energy Fuels 23, 3753–3758.

Chapter 4a Potential of acid-tolerant microalgae, *Desmodesmus* sp. MAS1 and *Heterochlorella* sp. MAS3, in heavy metal removal and biodiesel production at acidic pH

4a.1. Abstract

Metals in traces are vital for microalgae but their occurrence at high concentrations in habitats is a serious ecological concern. We investigated the potential of two acid-tolerant microalgae, *Desmodesmus* sp. MAS1 and *Heterochlorella* sp. MAS3, isolated from neutral environments, for simultaneous removal of heavy metals such as copper (Cu), iron (Fe), manganese (Mn) and zinc (Zn), and production of biodiesel when grown at pH 3.5. Excepting Cu, the selected metals at concentrations of 10-20 mg L^{-1} supported good growth of both the strains. Cellular analysis for metal removal revealed the predominance of intracellular mechanism in both the strains resulting in 40-80 and 40-60% removal of Fe and Mn, respectively. *In-situ* transesterification of biomass indicated enhanced biodiesel yield with increasing concentrations of metals suggesting that both these acid-tolerant microalgae may be the suitable candidates for simultaneous remediation and biodiesel production in environments like metal-rich acid mine drainages.

4a.2. Introduction

Microalgae, the photosynthetic organisms that thrive in various habitats including extreme environments (Perera et al., 2018), have been well recognized for their great potential in CO_2 fixation, bioremediation and biofuel production(Abinandan et al., 2018a,b). Optimal growth conditions are vital to achieve efficient large-scale cultivation of microalgae for biomass and biofuel production (Umamaheswari and Shanthakumar, 2016; Kropat et al., 2011). Although the use of wastewaters for production of microalgal biomass and biofuel in commercial scale is quite promising, better insights are still essential into various aspects such as strain selection, pH, and macro- and micro-nutrients (Abinandan et al., 2018a). Nutrient stress induced especially by carbon and nitrogen in microalgae plays a crucial role in microalgal growth for biotechnological applications (Ji et al., 2013; Ji et al., 2014). The available promising strains of microalgae should therefore be intially screened for their response to different envrionmental settings in a systematic way since this step is imminent in scaling up the production of biomass/biofuel (Ji et al., 2015).

Metal such as copper (Cu), iron (Fe), manganese (Mn) and zinc (Zn), although available in trace amounts as micronutrients, are crucial for photosynthesis and other metabolic pathways

in microalgae (Sunda et al., 2005). Song et al. (2012) optimized Fe, Mn, nickel and molybdenum for enhancing hydrocarbon production in microalgae. Saha et al. (2013 demonstrated that synergistic stress imposed by nitrogen limitation and micronutrients enhance carotene production in *Dunaliella salina*. Kwak et al. (2016) reported that synergistic effect of multiple stress conditions enhances microalgal lipid productivity, implying that it can be an efficient strategy for production of algal biofuels with high quality and economic feasibility. Also, Hanifzadeh et al. (2018) reported a three-fold increase in lipid productivity of microalgae without compromising growth by optimizing micronutrients. Indeed, the toxicity studies involving microalgae have been conducted at near neutral pH where the bioavailability of metals is very much limited because they form complexes with phosphates and chelating agents such as EDTA (Prochazkova et al., 2014; Subashchandrabose et al., 2015). However, higher concentrations of metals are available in environments like acid mine drainage (AMD) due to prevailing extreme acidic conditions (Palma et al., 2017). Although certain microalgae can withstand acidic pH due to their phenotypic plasticity (Sassenhagen et al., 2015; Hattich et al., 2017) and yet it is very hard for all the non-acidophilic microalgae to tolerate the extreme acidic conditions in metal-laden environments as exist in AMD (Abinandan et al., 2018b).

It is clear from the perused literature that the response of microalgae to metals in acidic pH has been poorly understood and leaves a wide research gap in identifying potential microalgal strains for bioremediation of environments like AMDs (Abinandan et al., 2018b). Very recently, we reported for the first time on acclimation of two acid-tolerant microalgae, viz., *Desmodesmus* sp. MAS1 and *Heterochlorella* sp. MAS3, to extreme acidic pH of 3.0 for sustainable production of biomass and biodiesel (Abinandan et al., 2019). Such an established biotechnological potential of microalgae can be exploited in situations like AMDs if these strains perform equally well in the presence of metals (Abinandan et al., 2018b). The main intent of this further study was therefore to investigate the response of the above two strains of acid-tolerant microalgae at pH 3.5, in terms of growth and biodiesel production, to different concentrations of metals such as Cu, Fe, Mn and Zn that are likely to be available in extreme environments as in AMDs. This approach is novel because the recent techno-economic report on microalgal cultivation systems suggests that biodiesel production is the best plausible strategy to make use of metal-laden biomass (Xin et al., 2016). We followed *in-situ* transesterification and FTIR-based fatty acid methyl esters (FAME) analysis for biodiesel recovery from microalgal biomass (Abinandan et al., 2019). The present study thus provides a cost-effective approach that has a potential application in simultaneous reclamation of metal-rich AMDs and biodiesel production by acid-tolerant microalgae.

4a.3. Materials and methods

4a.3.1. Microalgal strains and metals

Desmodesmus sp. MAS1 and *Heterochlorella* sp. MAS3 were maintained in 30 mL of modified Bold's basal medium (BBM), originally composed of heavy metals such as Cu, Fe, Mn and Zn at a concentration of 0.02, 1.0, 0.50 and 0.11 mg L^{-1}, respectively, at pH 3.5 in 100 mL conical flasks under continuous illumination (60 µmol m^{-2} s^{-1}) at 23 ± 1ºC and shaking (100 rpm). Low phosphate (1/10th of the original concentration) was used in the culture medium to avoid the formation of phosphate complexes and to make the metals bioavailable (Subashchandrabose et al., 2015). Stock solutions (500 mg L^{-1}) of Cu, Fe, Mn, and Zn were prepared in ultrapure water and filtered through a sterile 0.22 µm disposable sterile syringe filter.

4a.3.2. Effect of metals on microalgal growth

Ten millilitres of the culture medium (BBM), used for the maintenance of the microalgae, were taken in 40 mL sterile glass vials and supplemented with the heavy metals. The concentrations of Cu, Mn and Zn added to the BBM were in the range of 0.5-20 mg L^{-1}, while Fe was in the range of 5-50 mg L^{-1}. These ranges were used keeping in view the likely metal concentrations in AMDs that vary with geology and mining practices. Table 4a.1 presents the data on speciation of metals supplemented at different concentrations in BBM at pH 3.5 as determined by Visual MINTEQ modelling. Portions of the culture medium with no added metals served as controls. Exponentially-growing cultures were centrifuged at 6000 ×*g* for 7 min, and the cell suspensions were used to inoculate aliquots of culture medium containing metal micronutrients to provide an initial population density of 5×10^5 cells mL^{-1} in each treatment. Each experiment was replicated thrice, and duplicate samples were withdrawn at 2-day intervals up to 16 days for assaying chlorophyll content and analysis of metals.

Table 4a.1. Species distribution of metals supplemented in culture medium as determined by Visual MINTEQ modelling.

Metal	Metal species (%)	Concentration used (mg L^{-1})					
		0.5	1	2	5	10	20
Cu	Cu^{2+}	0.002395	–	–	–	–	–
	$CuSO_{4\ (aq)}$	0.00729	–	–	–	–	–
	$CuEDTA^{2-}$	0.243885	–	–	–	–	–
	$CuHEDTA^{-}$	0.234785	–	–	–	–	–
	$CuH_2EDTA_{\ (aq)}$	0.011615	–	–	–	–	–
Fe	Fe^{2+}	–	–		0.881	2.0058	4.3488
	$FeSO_{4\ (aq)}$	–	–	0.00132	2.8166	6.3901	13.7546
	$FeH_2PO_4^{+}$	–	–	1.42244	0.05915	0.1337	0.285
	$FeEDTA^{2-}$	–	–	0.55708	0.945	1.1173	1.2236
	$FeHEDTA^{-}$	–	–	0.0083	0.2977	0.352	0.3856
Mn	Mn^{2+}	–	–	–	2.2539	5.0196	10.7556
	$MnCl^{+}$	–	–	–	0.00085	0.0019	0.004
	$MnSO_{4\ (aq)}$	–	–	–	1.6232	3.6063	7.6894
	$MnNO_3^{+}$	–	–	–	0.00505	0.0112	0.024
	$MnEDTA^{2-}$	–	–	–	0.6863	0.8362	0.938
	$MnHEDTA^{-}$	–	–	–	0.4306	0.5246	0.5882
Zn	Zn^{2+}	–	–	0.06862	1.41485	3.8533	8.7752
	$ZnH_2EDTA_{\ (aq)}$	–	–	0.00378	0.0043	0.0044	0.0044
	$ZnCl^{+}$	–	–	-	0.0015	0.0042	0.0094
	$ZnSO_{4\ (aq)}$	–	–	0.06132	1.2625	3.4303	7.775
	$Zn(SO_4)^{2-}$	–	–	0.00994	0.2042	0.5535	1.2486
	$ZnNO_3^{+}$	–	–	0.00024	0.0051	0.0139	0.0316
	$ZnEDTA^{2-}$	–	–	1.2339	1.4011	1.4229	1.433
	$ZnHEDTA^{-}$	–	–	0.62212	0.70645	0.7174	0.7226

–; Not determined

4a.3.3. Microalgal growth determination and analysis of metals

Microalgal growth in different treatments was determined in terms of chlorophyll content by measuring autofluorescence (Podevin et al., 2015). In brief, 100 µL of samples were taken in 96-well microplate and measured at an excitation wavelength (440 nm) and an emission wavelength (690 nm) using fluorescence plate reader (Perkin Elmer). The data obtained as relative fluorescence units (RFUs) were converted to log values for developing growth curves and calculating specific growth rates of the two strains under the influence of selected metals.

For determination of metals accumulated within the cells, the procedure described earlier by literatures was adapted (Krishnamurti et al., 2015, Subramaniyam et al., 2016; Subashchandrabose et al., 2017). In brief, 5-mL culture suspensions were centrifuged and washed twice with 0.025 M EDTA to remove metals adsorbed onto the cell surface and to determine extracellular accumulation. The cell pellet was dried overnight at 40 °C, treated with 0.5 mL HNO_3 and diluted with 9.5 mL sterile ultrapure water to determine intracellular accumulation of metals. The contents of metals were determined using Inductively Coupled Plasma Mass Spectrometer (ICPMS) (Agilent 7500C), and total removal of metals were calculated following the formula:

$$Total\ removal\ (\%) = \frac{Intial\ conc.\ (mg\ L^{-1}) - Final\ conc.\ (mg\ L^{-1})}{Intial\ conc.\ (mg\ L^{-1})} \times 100$$

4a.3.4. FAME synthesis and characterization

FAME from microalgal biomass were obtained by *in situ* transesterification (Laurens et al., 2015) and quantified following a gravimetric method. In brief, moisture from the algal biomass was removed by drying overnight at 40 °C, and was subjected to transesterification using 300 µL of HCl-MeOH (5%, v/v) blend for one h at 85 °C. The distinct layers formed were washed with water to collect debris in methanol layer and biodiesel in chloroform layer. Controls without algal biomass were used to determine biodiesel gravimetrically. ATR-FTIR approach was followed to analyze FAME partitioned in solvent layer using control samples as blanks as described earlier (Abinandan et al., 2019). The spectra acquired on FTIR Spectroscopy (Agilent Technologies) were scanned in mid IR range of 400-4000 cm^{-1}. For each sample withdrawn after 16 days of incubation, in duplicate, a total of 16 scans were performed to improve signal noise ratio and mean values were used for data analysis.

4a.3.5. Statistical analysis

The standard deviations for the averages of experimental data were calculated using Graphpad Prism 7 software, and the statistical significance of means was determined by t-test using IBM SPSS Statistical Software (ver.24).

4a.4. Results and discussion

4a.4.1. Growth response of Desmodesmus sp. MAS1 and Heterochlorella sp. MAS3 in presence of metals

The data on growth response, in terms of specific growth rate derived from chlorophyll fluorescence units, of *Desmodesmus* sp. MAS1 and *Heterochlorella* sp. MAS3 under the influence of various concentrations of Cu, Fe, Mn and Zn at pH 3.5 for 16 days are presented in Figs. 4a.1 and 4a.2. Both the microalgal strains could survive and grow well at 0.5 mg L^{-1} of Cu when compared with the control cultures (Fig. 4a.1). The specific growth rates of *Desmodesmus* sp. MAS1 and *Heterochlorella* sp. MAS3 when grown in BBM (pH 3.5) were 0.27 and 0.28 d^{-1}, respectively, while the corresponding μ values in the presence of 0.5 mg L^{-1} of Cu at pH 3.5 were 0.37 and 0.40 d^{-1}, respectively. Recently, Rugnini et al. (2017) showed that strains of *Desmodesmus* sp. and *Chlorella* sp. exhibited specific growth rate of 0.078 and 0.11 d^{-1}, respectively, even at Cu concentration of 2 mg L^{-1} added to BG11 medium at pH 7.4. The present observation clearly indicates that the selected strains MAS1 and MAS3 can grow rapidly even if the concentration of Cu increases 25-fold than it is present in BBM at pH 3.5. However, all the other higher concentrations of Cu used were algicidal. Although microalgae tend to compromise growth at high concentrations of Cu under neutral pH conditions due to membrane lipid peroxidation (Jiang et al., 2016), exposure of the two strains at concentrations of 1 and 2 mg L^{-1} at pH 3.5 seemed to be lethal. The lowered phosphate concentration ($1/10^{th}$) used in BBM may also have contributed to the increased sensitivity of the microalgal strains to the higher concentrations of Cu at acidic conditions (Hall et al., 1989). On the other hand, *Desmodesmus* sp. MAS1 could tolerate and grow at all the concentrations, excepting 50 mg L^{-1}, of Fe whereas *Hetreochlorella* sp. MAS3 tolerated all the concentrations of Fe used (5-50 mg L^{-1}). Thus, the specific growth rates for the strains MAS1 and MAS3 under the influence of different concentrations of Fe were 0.26-0.37 and 0.36-0.40 d^{-1}, respectively. Earlier, Concas et al. (2014) reported higher growth rates at near neutral pH in *Chlorella vulgaris* due to the absence of dissolved iron concentration (Fe^{2+}). However, Kona et al. (2017) observed that the presence of Fe-EDTA improved chlorophyll content and growth in *Chlorella* sp. at

near neutral pH whereas its absence decreased biomolecules. Our results suggest that both the microalgal strains could tolerate 20 to 50-fold higher concentrations of Fe than its level in BBM, highlighting their potential in tolerating Fe at acidic pH.

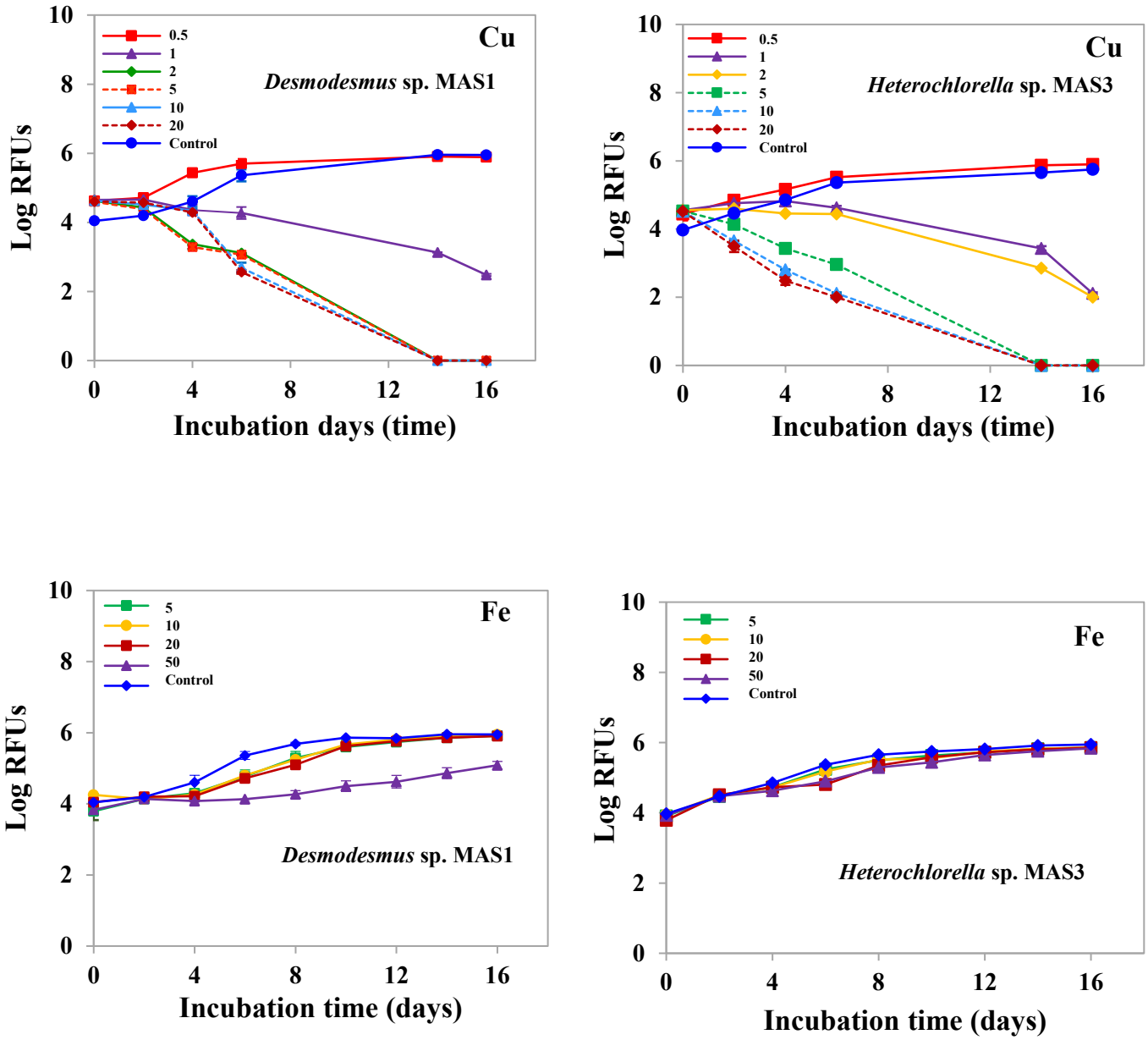

Fig. 4a.1. Growth response, in terms of relative fluorescence units (RFUs), in *Desmodesmus* sp. MAS1 and *Heterochlorella* sp. MAS3 to Cu and Fe at different concentrations at pH 3.5.

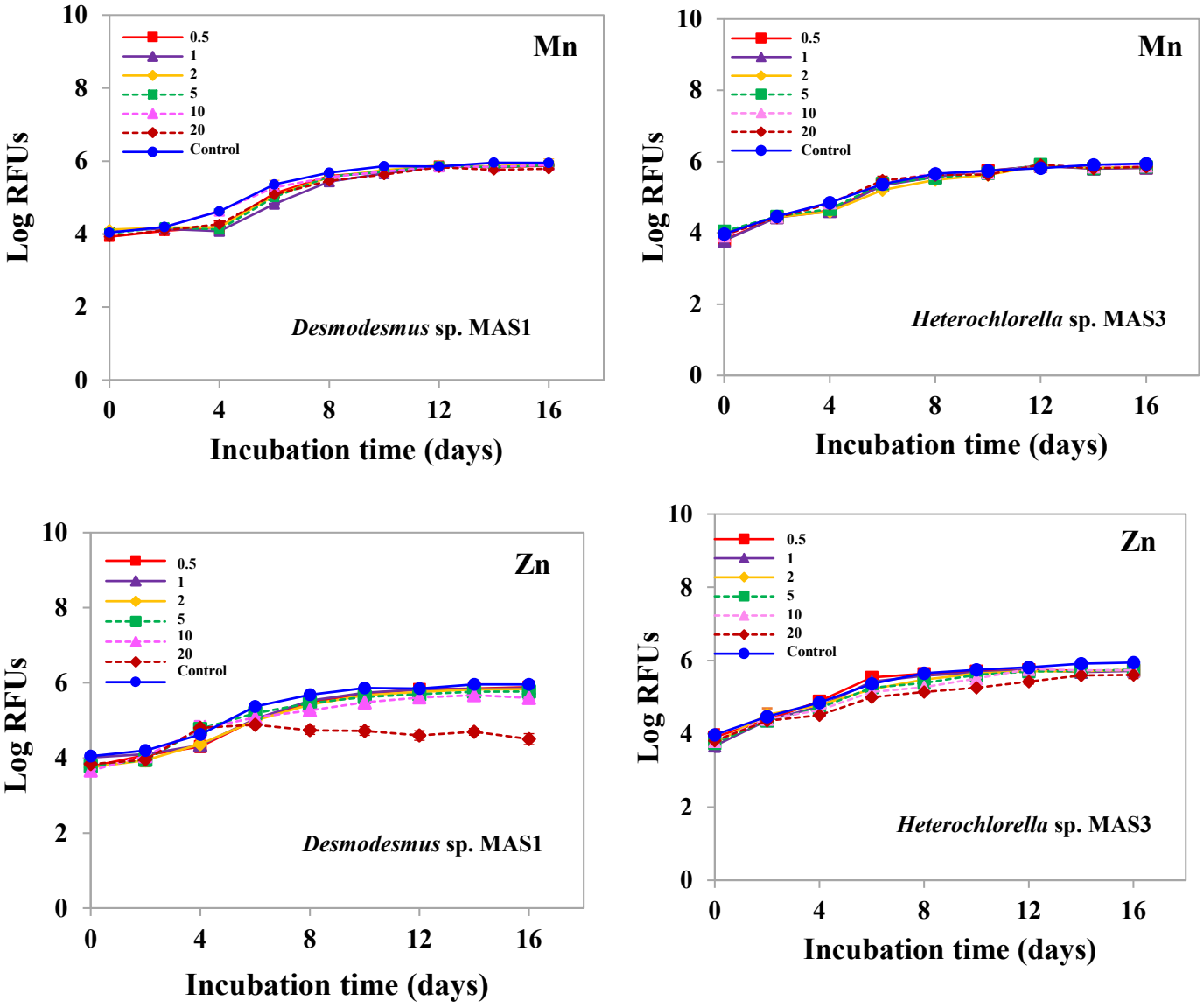

Fig. 4a.2. Growth response, in terms of relative fluorescence units (RFUs), in *Desmodesmus* sp. MAS1 and *Heterochlorella* sp. MAS3 to Mn and Zn at different concentrations at pH 3.5.

Even highest concentration of 20 mg L^{-1} of Mn used in the present study was not inhibitory to growth of both the microalgal strains at pH 3.5 (Fig. 4a.2). The specific growth rates for the strains MAS1 and MAS3 in presence of Mn at different concentrations were in the range of 0.26-0.36 d^{-1} and 0.36-0.40 d^{-1}, respectively. Although the selected strains of microalgae grow well in BBM by supplementing with 0.5 mg L^{-1} of Mn, the present observations indicate that they could withstand concentrations of this metal up to 20 mg L^{-1}. Only 20 mg L^{-1} of Zn was toxic to *Desmodesmus* sp. MAS1, but not to *Heterochlorella* sp. MAS3. The possible stress mediated by metals due to nutrient limitation especially phosphorus (Gao et al., 2016) was not

evident from growth of both the strains in medium supplemented with any of the metals. So far, the available studies in the literature investigated the influence of metal concentrations on microalgae at near neutral pH. Thus, Yang et al. (2015) showed that Zn concentration of 2-6 mM was inhibitory to *Chlorella minutissima* in medium that contained 1% of free ion at near neutrality. Hamed et al. (2017) observed 59% reduction of chlorophyll content in *Scenedesmus acuminatus* at 0.6 mM Zn with a decrease in growth rates. Also, Liu et al. (2017) whereas high concentrations were not conducive. As such, this is the first study to demonstrate the great potential of acid-tolerant microalgal strains, originally isolated from near neutral environments, to withstand and grow at higher concentrations of Cu, Fe, Mn and Zn.

4a.4.2. Metal removal and bioaccumulation in Desmodesmus sp. MAS1 and Heterochlorella sp. MAS3

The total of both external and internal accumulation of metals has been considered to express the extent of total metal removal by the two strains of microalgae (Fig. 4a.3). When grown in presence of 0.5 mg L^{-1} Cu, *Desmodesmus* sp. MAS1 removed 27% of the metal while *Heterochlorella* sp. MAS3 could remove 43%. Most of Cu^{2+} (75%) accumulated intracellularly in *Heterochlorella* sp. MAS 3 while vice versa trend of extracellular accumulation (>75%) was observed in *Desmodesmus* sp. MAS1 of the total metal removal. The intracellular accumulation of Cu may have been in polyphosphate bodies or complexed with phytochelatin as observed in other microalgae (Jiang et al., 2016; Abboud et al., 2013). Bossuyt and Janssen (2004) observed a high intracellular accumulation of Cu in *Pseudokirchneriella subcapitata* rather than extracellular accumulation at pH 7.8. A marine unicellular alga, *Tetraselmis chuii*, was found to be the most tolerant strain that accumulated high Cu concentrations at pH 8 compared to other strains (Bossuyt et al., 2004). No accumulation in both the strains was expected, as there was no growth at higher concentrations of Cu used in the present study. Increasing concentrations of Fe at pH 3.5 effected an increase in removal by *Desmodesmus* sp. MAS1. Thus, growth of the microalga in presence of Fe at concentrations of 5, 10 and 20 mg L^{-1} resulted in 79, 82 and 86% removal, respectively, after 16 days, while the corresponding percent removal by *Heterochlorella* sp. MAS3 was 40, 38 and 30 during this incubation period. Growth of the selected microalgal strains in presence of 5 and 10 mg L^{-1} Fe resulted mostly in intracellular accumulation (97–99%) of the total Fe removal (79%-82%) as shown in Fig.2. *Desmodesmus* sp. MAS1 accumulated 98% of 20 mg L^{-1} Fe as compared to 75% accumulation in *Heterochlorella* sp. MAS3 of total metal removal 85%, 29% respectively. Subramaniyam et al. (2016) observed similar differential sensitivity of various algal species such as

Chloroccoccum sp., *Chlamydomonas* sp. and *Chlorella* sp. toward Fe at pH 6.8. Sutak et al. (2012) proposed two mechanisms for iron uptake: surface binding of iron in the cells, and uptake of both ferric and ferrous irrespective of reductase mechanism. The addition of EDTA in mineral media is required to retain Fe in the solution rather than precipitation (Sunda et al., 2005). In our study, the complexation of Fe ions with phosphate and EDTA in *Desmodesmus* sp. MAS1 was less with $FeSO_4$ and Fe^{2+} as free ions possibly resulting in lower overall reduction but better metal accumulation. However, *Heterochlorella* sp. MAS3 showed a better reduction (>4.5 fold) than strain MAS1 indicating that Fe complex could also have been taken up by MAS3. This is attributed to chelated Fe through dissociation and chelation will be available as unchelated inorganic Fe ions (Shaked et al., 2005). Recently, Fe complex was found to act with humic acids in the same mechanism with EDTA justifying the uptake of complexes in microalgae (Orlowska et al., 2017).

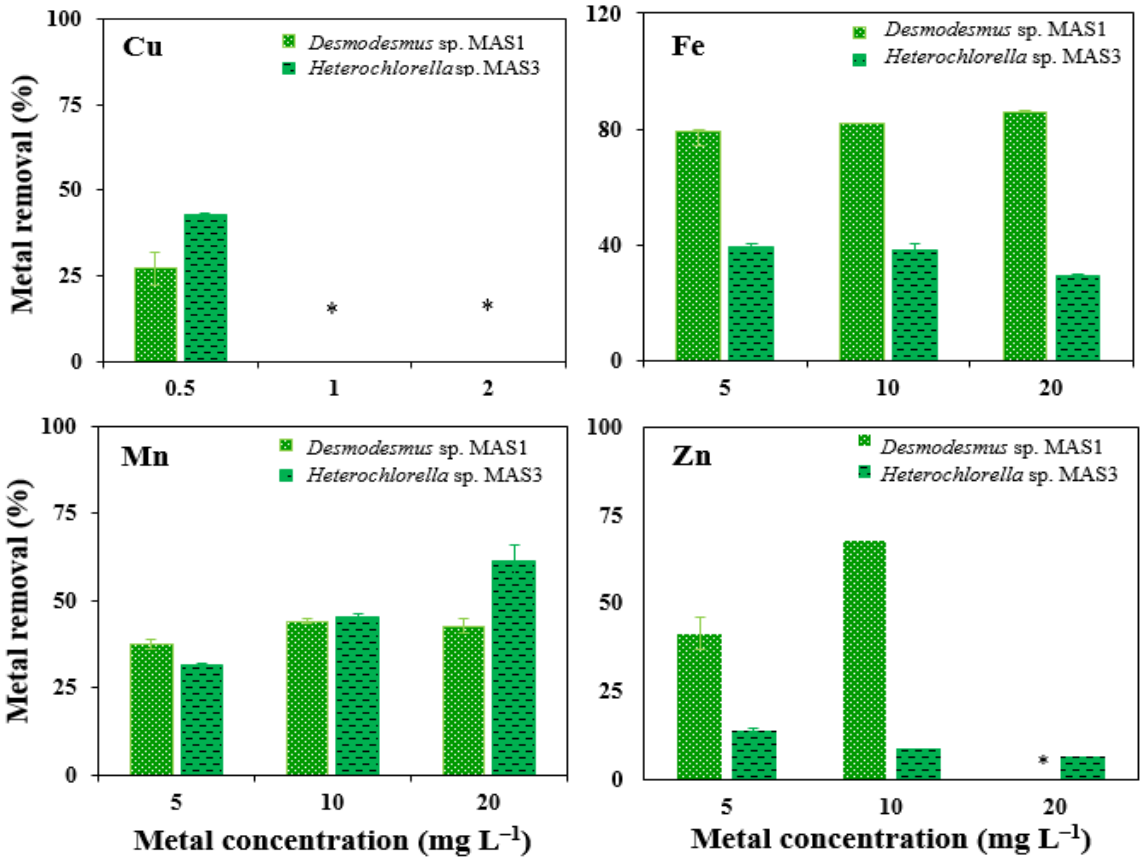

Fig. 4a.3 Per cent total removal of Cu, Fe, Mn and Zn by *Desmodesmus* sp. MAS1 and *Heterochlorella* sp. MAS3 grown in presence of different concentrations at pH 3.5. * = No growth.

The total removal pattern of Mn was similar in the two strains of microlagae. In fact, growth in BBM with increased concentrations of Mn enhanced the per cent removal of Mn. *Desmodesmus* sp. MAS1 removed 37-43% of 5-20 mg L^{-1} Mn whereas the range in per cent removal of these concentrations by *Heterochlorella* sp. MAS3 was 32 to 61. Thus, *Heterochlorella* sp. MAS3 seems to be efficient in removing Mn under acidic conditions. Likewise, both the species exhibited better internal and external accumulation of Mn. The external sorption of Mn was 61% of 5 mg L^{-1} by *Desmodesmus* sp. MAS1 while it was even 84% of 10 mg L^{-1} in *Heterochlorella* sp. MAS3 of total metal removal. Very recently, Saavedra et al. (2018) observed >99% removal of Mn by microalgae at pH 7.0 with reduced rates of removal at acidic pH <5.5. Palma et al. (2017) showed that indigenous biofilm from mine removed 26% of Mn with an initial concentration of 22 mg L^{-1}. Our results clearly indicate that both the strains of acid-tolerant microalgae have great potential in removing even 20 mg L^{-1} of Mn at pH 3.5, signifying their remediation potential. *Desmodesmus* sp. MAS1 removed 68% of 10 mg L^{-1} Zn after 16 days, but the total removal percentage was only 23 during this incubation. On the other hand, the percent removal of 10 and 20 mg L^{-1} Zn was 9 and 7, respectively, by *Heterochlorella* sp. MAS3. At the highest Zn concentration of 20 mg L^{-1} used under acidic conditions, the strain MAS1 could not survive. At 5 and 10 mg L^{-1} Zn concentration, the external sorption was >60% in *Desmodesmus* sp.MAS1 and >50% in *Heterchlorella* sp.MAS3 of total metal removal. According to Areco et al. (2018), Zn precipitates in microalgae, rather than accumulating, at pH 5.5. Bácsi et al. (2015) observed that *Monoraphidium* sp. removed 84.8, and 52.8% of 10 and 20 mg L^{-1} respectively at pH 7-7.5. The availability of Zn (Table 4a.1) tends to improve better along with sulfate and chloride rather than complexing with EDTA indicating the possibilities of Zn transport through other channels. At pH 3, the indigenous biofilm was shown to remove Zn up to 10% in the presence of other metals suggesting competitive adsorption into the surface of the communities (Orandi and Lewis, 2013). We observed here that the microalgal strains tend to accumulate Zn intracellularly (75-85%) rather than external adsorption in the presence of other elements.

4a.4.3. Impact of metals on biodiesel production in acid-tolerant microalgae

FTIR interpretation of biodiesel production from microalgae is the simple and most accessible approach. *In-situ* transesterification of biodiesel conversion from direct biomass was performed for the two strains and the data are presented in Fig. 4a.4. The displayed band regions of the FTIR spectra (data not shown), obtained from *in-situ* transesterification of algal biomass, as aliphatic C-H stretching vibration (3000-2800 cm^{-1}), bending vibration at (1500-

1600 cm^{-1}) and C=O with intense absorption bands (1746-1654 cm^{-1}) are indicative of biodiesel production by microalgal samples withdrawn after 16 days (Difusa et al., 2016). Since these regions are an indicator of aliphatic hydrocarbon chains/long hydrocarbon chains, the present results suggest that biodiesel produced is rich in monoalkyl esters. Similar results of biodiesel were recorded from microalgal biomass obtained after two-stage transesterification process (Kumar et al., 2014). Furthermore, the presence of C-O bending vibrations at the region 1232-1236 cm^{-1} endorses the presence of esters as has been reported earlier in algal biomass obtained after liquefaction process (Zou et al., 2009).

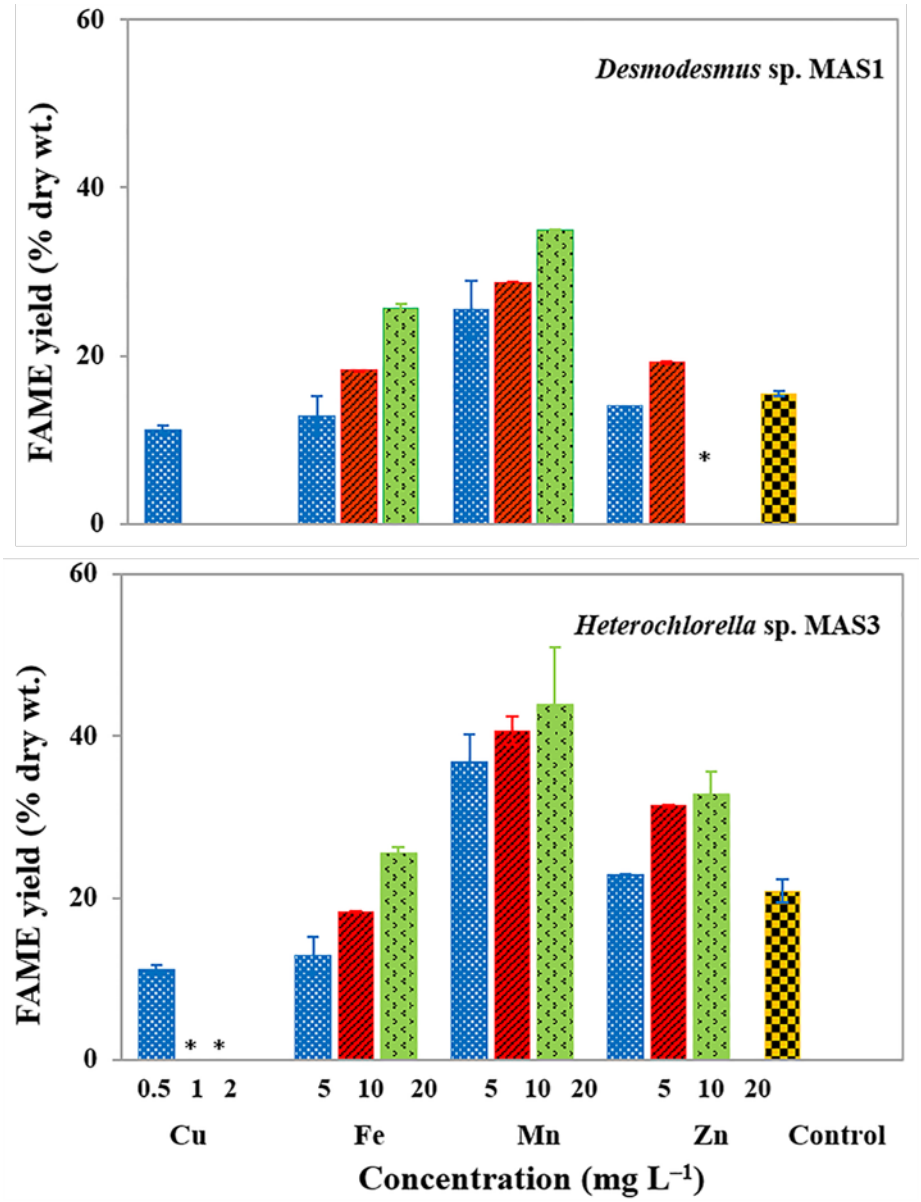

Fig. 4a.4. FAME yield in *Desmodesmus* sp. MAS1 and *Heterochlorella* sp. MAS3 as influenced by different concentrations of metals. * = No growth.

Even 0.5 mg L^{-1} of Cu at pH 3.5 inhibited biodiesel production by 4.5% in *Desmodesmus* sp. MAS1. However, the biodiesel yield by this strain increased with increasing concentration of Fe and Mn. Thus, the range in per cent yield of biodiesel by the microalga when grown in presence of Fe was 12.8-25.6 while it was 25.5-35 for Mn. The biofilms in response to tailing water contaminated with metals accumulated long chain fatty acids due to metal load, especially Mn (Palma et al., 2017). The concentration of 10 mg L^{-1} Zn slightly enhanced the biodiesel production, and 20 mg L^{-1} yielded no biodiesel as this concentration totally inhibited the growth. As with the strain MAS1, *Heterochlorella* sp. MAS3 also responded, in terms of biodiesel production, to the exposure of Fe and Mn. Interestingly, growth of the strain MAS3 in presence of Zn at all the concentrations of 5, 10 and 20 mg L^{-1} resulted in enhanced yield of biodiesel. Likewise, the per cent biodiesel production at these concentrations of Zn ranged from 22.9 to 32.9 as against 11% yield in control culture. Available data on biodiesel production by microalgae in presence of metals is related only to near neutral pH. To mention a few, Abd El Baky et al. (2012) reported accumulation of 28.12% higher lipids when *Scenedesmus obliquus* was grown in presence of 10-20 mg Fe^{3+} L^{-1} at pH 7. The influence of metals such as Mn and cobalt were shown to induce total fatty acids >40% but reduced saturated fatty acids (Battah et al., 2015). Kona et al. (2017) found that microalgae could produce higher amounts of unsaturated fatty acids when grown at 8 mg L^{-1} of iron but not at lower concentrations. Liu et al. (2017) showed that *Chlorella* sp. was able to accumulate biodiesel at 46% with 5 mg L^{-1} Mn. Yang et al. (2015) observed that *Chlorella mintussima* achieved a better yield of biodiesel when exposed to 6 mM Mn at a neutral pH. Another microalga, *Chlorella* sp., showed maximum accumulation of TAG only at a higher concentration (5.05 mg L^{-1}) of Zn (Liu et al., 2017). Yang et al. (2015) reported that higher concentration (6 mM) of Zn increased TAG content. Overall, it is apparent from the data that individual metal and its concentration significantly improved FAME yield in both the species of microalgae.

The interactions between metal types, metal concentrations and microalgal strains on per cent metal removal and biodiesel yield are presented by three-way ANOVA analysis (Table 4a.2). The metal removal and biodiesel yield significantly varied (P<0.05) for all the metal types and concentrations tested for both the microalgal strains. One-way effects of the above parameters revealed higher order of significance on metal removal and FAME yield (P<0.05).

Table 4a.2 Interaction effects of factors on metal removal and FAME yield.

Source	DF	Adj SS	Adj MS	*F*	*P*
		Metal removal (%)			
Metals	3	15759.5	5253.16	132.27	0.000
Conc.	2	2124.5	219.38	5.52	0.011
Species	1	5180.1	5180.12	130.44	0.000
Metals × Conc.	6	4038.0	673.0	16.95	0.000
Metals × Species	3	4995.5	1665.18	41.93	0.000
Conc × Species	2	328.4	164.18	4.13	0.029
Metals × Conc × Species	6	1425.4	237.57	5.98	0.001
Error	24	953.1	39.71		
Total	47	33118.8			
R^2, 0.97; R^2(pred), 0.94					
		FAME yield (% dry wt.)			
Metals	3	5131.94	1710.65	643.38	0.000
Conc.	2	105.93	52.97	19.92	0.000
Species	1	1551.04	1551.04	583.35	0.000
Metals × Conc.	6	1643.15	273.86	103.00	0.000
Metals × Species	3	168.42	56.14	21.11	0.000
Conc × Species	2	45.15	22.58	8.49	0.002
Metals×Conc.× Species	8	179.03	29.84	11.22	0.000
Error	24	63.81	2.66		
Total	47	8888.49			
R^2, 0.99; R^2 (pred), 0.99					

F is the statistical value that refers to the variation between sample means/variation within the samples. *P* is the ≤ α value that indicates statistical significance.

The total metal removal was very high in the order of Cu, Fe, Mn and Zn at initial concentrations. The strains exhibited similar trend in Fe removal at almost all the concentrations tested. However, there was a decrease in the metal removal at increasing concentrations of metal (P<0.011) and in two different strains (P<0.029) throughout. At high

concentration, there was no growth of the strains in presence of Cu, and both the microalgae showed a poor response to Zn removal at very high concentrations. In fact, *Desmodesmus* sp. MAS1 showed better metal removal rates as compared to *Heterochlorella* sp. MAS3 except for Zn. The metal removal in response to the metals, their concentrations and the microalgal strains was strongly correlated (R^2, 0.99) and was statistically significant (P<0.01). Furthermore, there was a significant influence of metals and concentrations on FAME yield (P<0.01), and highest yield of biodiesel was obtained at higher levels of metals which could be attributed to the stress induced. Among the metals tested, Mn ranked best and achieved a biodiesel yield (30-40%) which is two-fold higher than in control cultures. Battah et al. (2015) showed that Mn at high concentrations benefits in accumulating high lipid when compared to cobalt in *Chlorella vulgaris.* Furthermore, *Desmodesmus* sp. MAS1 exhibited >50% metal removal whereas *Heterochlorella* sp. MAS3 showed approximately 30% less removal at all concentrations of metals. This indicates a significant interaction among the microalgal species and different metal concentrations (P<0.02). Hamed et al. (2017) observed two different mechanisms of antioxidant activity to alleviate Cu stress induced in microalgae, *Scenedesmus acuminatus* and *Chlorella sorokiniana*. Overall, the stress induced by metals at various concentrations was strongly correlated (R^2, 0.99) but resulted in significant (P<0.05) FAME yield. Thus, the present findings clearly substantiate that both the strains together can be excellent candidates not only for remediating metal-rich environments with acidic pH as exist in AMDs but also for producing good quality biodiesel.

4a.5. Conclusion

In the present study, we demonstrated that two acid-tolerant microalgae, despite the higher degree of free ion availability of metals at pH 3.5, exhibited good growth by doubling their population quickly. FTIR analysis indicated that the yield of FAME rich in aliphatic hydrocarbons was >20-40% in metal-grown cultures than control cultures. Based on the linear model interaction plot, *Desmodesmus* sp. MAS1 showed better metal removal than *Heterochlorella* sp. MAS3 although both the strains together accounted for 20-50% metal removal. Our data indicate that heavy metal-laden biomass could be a valuable source of biodiesel production, contributing to cost-effective green and sustainable technology.

4a.6. References

Abboud, P., Wilkinson, K.J., 2013. Role of metal mixtures (Ca, Cu and Pb) on Cd bioaccumulation and phytochelatin production by *Chlamydomonas reinhardtii*. Environ. Pollut. 179, 33–8.

Abd El Baky, H.H., El-Baroty, G.S., Bouaid, A., Martinez, M., Aracil, J., 2012. Enhancement of lipid accumulation in *Scenedesmus obliquus* by optimizing CO_2 and Fe^{3+} levels for biodiesel production. Bioresour. Technol. 119, 429–32.

Abinandan, S., Subashchandrabose, S.R., Venkateswarlu, K., Megharaj, M., 2018a. Nutrient removal and biomass production: advances in microalgal biotechnology for wastewater treatment. Crit. Rev. Biotech. 38, 1–17.

Abinandan, S., Subashchandrabose, S.R., Venkateswarlu, K., Megharaj, M., 2018b. Microalgae–bacteria biofilms: a sustainable synergistic approach in remediation of acid mine drainage. Appl. Microbiol. Biotechnol. 102, 1131–44.

Abinandan, S., Subashchandrabose. S.R., Cole, N., Dharmarajan, R., Venkateswarlu, K., Megharaj, M., 2019. Sustainable production of biomass and biodiesel by acclimation of non-acidophilic microalgae to acidic conditions. Bioresour. Technol. 271, 316–24.

Areco, M.M., Haug, E., Curutchet, G., 2018. Studies on bioremediation of Zn and acid waters using *Botryococcus braunii*. J. Environ. Chem. Eng. 6, 3849–59.

Bácsi, I., Novák, Z., Jánószky, M., B-Béres, V., Grigorszky, I., Nagy, S.A., 2015. The sensitivity of two *Monoraphidium* species to zinc: their possible future role in bioremediation. Int. J. Environ. Sci. Technol. 12, 2455–6.

Battah, M., El-Ayoty, Y., Abomohra, A.E.F., El-Ghany, S.A., Esmael, A., 2015. Effect of Mn^{2+}, Co^{2+} and H_2O_2 on biomass and lipids of the green microalga *Chlorella vulgaris* as a potential candidate for biodiesel production. Annal. Microbiol. 651, 55–62.

Bossuyt, B.T.A., Janssen, C.R., 2004. Long-term acclimation of *Pseudokirchneriella subcapitata* (Korshikov) Hindak to different copper concentrations: changes in tolerance and physiology. Aquat. Toxicol. 68, 61–74.

Concas, A., Steriti, A., Pisu, M., Cao, G., 2014. Comprehensive modeling and investigation of the effect of iron on the growth rate and lipid accumulation of *Chlorella vulgaris* cultured in batch photobioreactors. Bioresour. Technol. 153, 340–50.

Difusa, A., Mohanty, K., Goud, V.V., 2016. The chemometric approach applied to FTIR spectral data for the analysis of lipid content in microalgae cultivated in different nitrogen sources. Biomass Conv. Bioref. 6, 27–33.

Gao, C., De Schamphelaere, K.A.C., Smolders, E., 2016. Zinc toxicity to the alga *Pseudokirchneriella subcapitata* decreases under phosphate limiting growth conditions. Aquat. Toxicol. 173, 74–82.

Hall, J., Healey, F.P., Robinson, G.G.C., 1989. The interaction of chronic copper toxicity with nutrient limitation in two chlorophytes in batch culture. Aquat. Toxicol. 14, 1–13.

Hamed, S.M., Selim, S., Klöck, G., AbdElgawad, H., 2017. Sensitivity of two green microalgae to copper stress: Growth, oxidative and antioxidants analyses. Ecotox. Environ. Safe. 144, 19–25.

Hamed, S.M., Zinta, G., Klöck, G., Asard, H., Selim, S., AbdElgawad, H., 2017. Zinc-induced differential oxidative stress and antioxidant responses in *Chlorella sorokiniana* and *Scenedesmus acuminatus*. Ecotox. Environ. Safe. 140, 256–63.

Hanifzadeh, M., Garcia, E.C., Viamajala, S., 2018. Production of lipid and carbohydrate from microalgae without compromising biomass productivities: role of Ca and Mg. Renew. Energy 127, 989–97.

Hattich, G.S.I., Listmann, L., Raab, J., Ozod-Seradj, D., Reusch, T.B.H., Matthiessen, B., 2017. Inter- and intraspecific phenotypic plasticity of three phytoplankton species in response to ocean acidification. Biol. Lett. 13, 20160774.

Ji, F., Liu, Y., Hao, R., Li, G., Zhou, Y., Dong, R., 2014. Biomass production and nutrients removal by a new microalgae strain Desmodesmus sp. in anaerobic digestion wastewater. Bioresour. Technol. 161, 200–207.

Ji, F., Hao, R., Liu, Y., Li, G., Zhou, Y., Dong, R., 2013. Isolation of a novel microalgae strain Desmodesmus sp. and optimization of environmental factors for its biomass production. Bioresour. Technol. 148, 249–254.

Ji, F., Zhou, Y., Pang, A., Ning, L., Rodgers, K., Liu, Y., Dong, R., 2015. Fed-batch cultivation of Desmodesmus sp. in anaerobic digestion wastewater for improved nutrient removal and biodiesel production. Bioresour. Technol. 184, 116–122.

Jiang, Y., Zhu, Y., Hu, Z., Lei, A., Wang, J., 2016. Towards elucidation of the toxic mechanism of copper on the model green alga *Chlamydomonas reinhardtii*. Ecotoxicology 25, 1417–25.

Kona, R., Hemalatha, M., Venu Srivastav, K., Venkata Mohan S., 2017. Regulatory effect of Fe-EDTA on mixotrophic cultivation of *Chlorella* sp. towards biomass growth and metabolite production. Bioresour. Technol. 244, 1227–34.

Krishnamurti, G.S., Subashchandrabose, S.R., Megharaj, M. and Naidu, R., 2015. Assessment of bioavailability of heavy metal pollutants using soil isolates of *Chlorella* sp. Environ Sci Pollut Res. 22(12), 8826–8832.

Kropat, J., Hong-Hermesdorf, A., Casero, D., Ent, P., Castruita, M., Pellegrini, M., 2011. A revised mineral nutrient supplement increases biomass and growth rate in *Chlamydomonas reinhardtii*. Plant J. 66, 770–80.

Kumar, V., Muthuraj, M., Palabhanvi, B., Ghoshal, A.K., Das, D., 2014. Evaluation and optimization of two stage sequential in situ transesterification process for fatty acid methyl ester quantification from microalgae. Renew. Energy 68, 560–9.

Kwak, H.S., Kim, J.Y.H., Woo, H.M., Jin, E., Min, B.K., Sim, S.J., 2016. Synergistic effect of multiple stress conditions for improving microalgal lipid production. Algal Res. 19, 215–24.

Laurens, L.M.L., Nagle, N., Davis, R., Sweeney, N., Van Wychen, S., Lowell, A et al., 2015. Acid-catalyzed algal biomass pretreatment for integrated lipid and carbohydrate-based biofuels production. Green Chem. 17, 1145–58.

Liu, Y., Zhan, J.J., Hong, Y., 2017. Effects of metal ions on the cultivation of an oleaginous microalga *Chlorella* sp. Environ. Sci. Pollut. Res. 24, 26594–604.

Orandi, S., Lewis, D.M., 2013. Biosorption of heavy metals in a photo-rotating biological contactor--a batch process study. Appl. Microbiol. Biotechnol. 97, 5113–23.

Orlowska, E., Roller, A., Pignitter, M., Jirsa, F., Krachler, R., Kandioller, W et al., 2017. Synthetic iron complexes as models for natural iron-humic compounds: Synthesis, characterization and algal growth experiments. Sci. Tot. Environ. 577, 94–104.

Palma, H., Killoran, E., Sheehan, M., Berner, F., Heimann, K., 2017. Assessment of microalga biofilms for simultaneous remediation and biofuel generation in mine tailings water. Bioresour. Technol. 234, 327–35.

Perera, I., Subashchandrabose, S.R., Venkateswarlu, K., Naidu, R., Megharaj, M., 2018 Consortia of cyanobacteria/microalgae and bacteria in desert soils: an underexplored microbiota. Appl. Microbiol. Biotechnol. 102, 7351–7363.

Podevin, M., De Francisci, D., Holdt, S.L., Angelidaki, I., 2015. Effect of nitrogen source and acclimatization on specific growth rates of microalgae determined by a high-throughput in vivo microplate autofluorescence method. J. Appl. Phycol. 27, 1415–23.

Procházková, G., Brányiková, I., Zachleder, V., Brányik, T., 2014. Effect of nutrient supply status on biomass composition of eukaryotic green microalgae. J. Appl. Phycol. 26,1359–77.

Rugnini, L., Costa, G., Congestri, R., Bruno, L., 2017. Testing of two different strains of green microalgae for Cu and Ni removal from aqueous media. Sci. Tot. Environ. 601-602, 959–67.

Saavedra, R., Muñoz, R., Taboada, M.E., Vega, M., Bolado, S., 2018. Comparative uptake study of arsenic, boron, copper, manganese and zinc from water by different green microalgae. Bioresour. Technol. 263, 49–57.

Saha, S.K., Moane, S., Murray, P., 2013. Effect of macro- and micro-nutrient limitation on superoxide dismutase activities and carotenoid levels in microalga *Dunaliella salina* CCAP 19/18. Bioresour. Technol. 147, 23–8.

Sassenhagen, I., Wilken, S., Godhe, A., Rengefors, K., 2015. Phenotypic plasticity and differentiation in an invasive freshwater microalga. Harmful Algae 41, 38–45.

Shaked, Y., Kustka, A.B., Morel, F.M.M., 2005. A general kinetic model for iron acquisition by eukaryotic phytoplankton. Limnol. Oceanogr. 50, 872–82.

Song, L., Qin, J.G., Su, S., Xu, J., Clarke, S., Shan, Y., 2012. Micronutrient requirements for growth and hydrocarbon production in the oil producing green alga *Botryococcus braunii* (Chlorophyta). PLoS ONE 7, e41459.

Subashchandrabose, S.R., Megharaj, M., Venkateswarlu, K., Naidu, R., 2015. Interaction effects of polycyclic aromatic hydrocarbons and heavy metals on a soil microalga, *Chlorococcum* sp. MM11. Environ. Sci. Pollut. Res. 22, 8876–89.

Subashchandrabose, S.R., Wang, L., Venkateswarlu, K., Naidu, R., Megharaj, M., 2017. Interactive effects of PAHs and heavy metal mixtures on oxidative stress in *Chlorella* sp. MM3 as determined by artificial neural network and genetic algorithm. Algal Res. 21, 203–12.

Subramaniyam, V., Subashchandrabose, S.R., Kumar, V.G., Thavamani, P., Chen, Z., Naidu, R., Megharaj, M., 2016. Cultivation of *Chlorella* on brewery wastewater and nano-particle biosynthesis by its biomass. Bioresour. Technol. 211, 698–703.

Subramaniyam, V., Subashchandrabose, S.R., Thavamani, P., Chen, Z., Krishnamurti, G.S.R., Naidu, R. and Megharaj, M., 2016. Toxicity and bioaccumulation of iron in soil microalgae. J Appl Phycol. 28(5), 2767–2776.

Sunda, W.G., Price, N.M., Morel, F.M., 2005. Trace metal ion buffers and their use in culture studies. Algal Cult. Techn. 4, 35–63.

Sutak, R., Botebol, H., Blaiseau, P.L., Léger, T., Bouget, F.Y., Camadro, JM et al., 2012. A comparative study of iron uptake mechanisms in marine microalgae: iron binding at the cell surface is a critical step. Plant Physiol. 160, 2271–84.

Umamaheswari, J., Shanthakumar, S., 2016. Efficacy of microalgae for industrial

Chapter 4b Macromolecular changes in acid-tolerant microalgae, *Desmodesmus* sp. MAS1 and *Heterochlorella* sp. MAS3, induced by heavy metals at pH 3.5

4b.1. Abstract

The biomolecular response of two acid-tolerant strains of microalgae, *Desmodesmus* sp. MAS1 and *Heterochlorella* sp. MAS3, grown at pH 3.5 under the stress of varying concentrations of heavy metals that serve as micronutrients like copper, iron, manganese and zinc, was investigated following the attenuated total reflectance (ATR)-Fourier transform infrared (FTIR) spectroscopy. The ATR-FTIR spectra revealed significant changes in carbohydrates, proteins and lipids in both the strains of microalgae. Symmetric vibrational stretch observed for amide I region (1650-1670 cm^{-1}) increased with increasing concentrations of metals in *Desmodesmus* sp. MAS1, but not in *Heterochlorella* sp. MAS3. However, the symmetric and asymmetric vibrational stretches characteristic of carboxylic esters (1735-1750 cm^{-1}) and methylene groups (2925 and 2960 cm^{-1}) of lipids were significant in strain MAS3 than in strain MAS1. The observed data on biomolecular changes were validated following chemometric approach involving principal component analysis and orthogonal partial least square regression.

4b.2. Introduction

Heavy metals (HMs) are outsourced to the environment by anthropogenic and industrial activities, volcanic eruptions, and geological distribution. Most HMs that occur commonly in the habitats like acid mine drainages (AMDs) are copper (Cu), cadmium (Cd), zinc (Zn), manganese (Mn), arsenic (As), iron (Fe), aluminum (Al), nickel (Ni), lead (Pb), and chromium (Cr) (Yen et al. 2017). Higher concentrations of HMs are toxic and disrupt the biota leading to ecological imbalance (Abinandan et al. 2019a). However, such phytoplankton as microalgae developed several strategies to survive under the stress during evolution (Pereira et al. 2013). On the contrary, HMs such as Cu, Zn, Mn and Fe play a vital role as essential micronutrients in humans and aquatic organisms including microalgae. In microalgae, metal-rich and membrane-bound organelles such as chloroplasts and mitochondria use Cu, Zn, Mn and Fe for photosynthetic and metabolic activities (Merchant et al. 2006). As active non-protein cofactors for stabilizing protein structures, these metals also participate in enzymatic reactions in microalgae (Hänsch and Mendel 2009). Iron, mostly occurring as Fe^{3+} oxides, is insoluble under aerobic environments at neutral pH (Terauchi et al. 2010). Under Fe-deficient conditions,

microalgae tend to produce lipids with abundant saturated fatty acids besides losing certain enzymes (Urzica et al. 2013). In *Chalmydomonas reinhardtii*, Fe deficiency triggered the expression of stress-related protein synthesis (Höhner et al. 2013). Especially, Zn deficiency affects the pathways of carbon concentration and copper signaling (Malasarn et al. 2013). Cu is crucially involved not only in protein–protein interactions but also in iron transport mediated by multicopper ferroxidase (Blaby-Haas and Merchant 2012). Also, under Cu-deficient conditions, microalgae tend to replace Cu allocation from plastocyanin to enzyme cytochrome c oxidase (Kropat et al. 2015). Since Cu and Fe are unchelated redox metal ions that generate reactive oxygen species in microalgae, the metabolic pathways involved in synthesizing important cellular macromolecules are modified under deficient conditions of these ions (Hsieh et al. 2013).

Most of the microalgal biomass (>70%) consists of important macromolecules such as carbohydrates, proteins and lipids that serve as building blocks in the cells (Bataller and Capareda 2018). These macromolecules also have a variety of commercial applications from nutraceuticals to biofuels (Markou and Nerantzis 2013). The impact of stress imposed by higher concentrations of those HMs that serve as micronutrients on increased production of carbohydrates, proteins and lipids in microalgae has been investigated only at neutral pH conditions (Battah et al. 2015; Rocha et al. 2016; Kona et al. 2017; Liu et al. 2017; Palma et al. 2017). But, the toxicity of any metal toward microalgae is higher in acidic pH rather than neutral pH and has been ascribed to the predominance of free and hydrated metal ions (Wilde et al. 2006; Abinandan et al. 2019a). It was reported that Cu and Zn imposed predominant toxicity in *Scenedesmus quadricauda* at an acidic pH of 4.5 rather than near neutral pH of 6.5 (Starodub et al. 1987). Acidophilic microalgae are commonly found in extreme environments such as AMDs that contain dissolved heavy metals in surplus amounts due to low pH because they develop tolerance mechanisms through several physiological and metabolic adaptations (Souza-Egipsy et al. 2011; Abinandan et al. 2018). Very recently, we assessed the potential of two acid-tolerant microalgal strains, *Desmodesmus* sp. MAS1 and *Heterochlorella* sp. MAS3, originally isolated from neutral habitats (Abinandan et al. 2019b), for removal of HMs such as Cu, Fe, Mn and Zn as well as yield of biodiesel when grown at pH 3.5 (Abinandan et al. 2019a). Subsequent application attenuated total reflection-Fourier transform infrared (ATR-FTIR) spectroscopy (Dao et al. 2017), a robust approach with veracity in obtaining relevant IR spectra than the conventional mode of measurements, together with chemometric analysis (Gurbanov et al. 2018). The main intent of the present study was to further determine for the first time the changes in macromolecules such as carbohydrates, proteins and lipids in *Desmodesmus* sp.

MAS1 and *Heterochlorella* sp. MAS3 when grown in presence of varying concentrations of HMs like Cu, Fe, Mn and Zn at pH 3.5. Although some habitats such as AMDs contain alarmingly higher levels of HMs in bioavailable forms, it is not clearly understood as to what extent these concentrations exert biomolecular changes in microalgae at acidic conditions. Overall, the purpose is to further use these strains of microalgae to test whether they can sustain in AMDs by synthesizing the essential biomolecules while remediating such acidic habitats.

4b.3. Materials and methods

4b.3.1. Microalgal strains and growth in presence of heavy metals

Exponentially-growing cultures of two acid-tolerant microalgae, *Desmodesmus* sp. MAS1 and *Heterochlorella* sp. MAS3, were inoculated into Bold's basal medium (BBM) in presence of varying concentrations (mg L^{-1}) of Cu, Fe, Mn and Zn at pH 3.5, and grown for 16 days under constant illumination as described earlier (Abinandan et al. 2019a, b). The selection of metal concentrations, viz., Cu (0.5, 1 and 2 mg $L^{-1)}$, Fe and Mn (5, 10 and 20 mg L^{-1}), and Zn (0.5, 1, 2 and 5 mg L^{-1}) to grow microalgae was based on our earlier observations on toxicity of these HMs to both the strains of microalgae (Abinandan et al. 2019a). The selected concentrations of the HMs and their corresponding designations used in the study are presented in Table 4b.1.

Table 4b.1 Concentrations of heavy metals used to grow the microalgal strains and the corresponding designations.

Microalga	**Heavy metal**	**Concentration (mg L^{-1})**		
		A	B	C
Desmodesmus sp. MAS 1	Cu	0.5	1	2
	Fe	5	10	20
	Mn	5	10	20
	Zn	2	5	10
Heterochlorella sp. MAS 3	Cu	0.5	1	2
	Fe	5	10	20
	Mn	5	10	20
	Zn	5	10	20

4b.3.2. ATR-FTIR spectroscopy

Samples (2 mL), with cell densities of ~10^7 cells mL^{-1}, were withdrawn from each culture (n=3) after 16 days and centrifuged at 8000 ×*g* for 10 min to obtain microalgal biomass. The biomass was washed with sterile pure water twice to remove cell debris and resuspended in BBM. The samples were then placed on a horizontal plane ATR (HATR) trough prism made of ZnSe crystal (Refractive index 2.4) for IR measurements (PIKE PN: 022-2010-45). The trapezoid-shaped specific accessory with dimensions of 8 mm long, 1 cm wide and 4 cm thick had 450 internal critical reflection angle and capable of multiple reflections up to 10 times. It was incorporated into the HATR base assembly (PIKE PN: 022-1213). All the microalgal samples were placed onto this ZnSe trough plate and held tightly through a pressing accessory (PIKE PN: 022-3052) using a HATR pressure clamp (PIKE PN: 022-3050) for maximum contact. A working matrix without microalgal samples was employed to obtain background spectrum. All the spectra were scanned using Agilent Technologies Cary 660 FTIR spectrometer system by placing HATR accessory inside the sample compartment. Spectral scans were done in the mid-IR energy range (4000-400 cm^{-1}) taking into consideration the spectral cut-off for ZnSe prism with resolution of 8 cm^{-1} and co-averaging 16 scans for each sample using Agilent IR Resolutions Pro software. The DTGS detector of the spectrophotometer was air-cooled at room temperature for optimizing the sensitivity levels of the measurements. Since all the spectral data were further processed through chemometrics datasets, no ATR corrections were performed.

4b.3.3. Processing of spectra and multivariate analysis

The spectra obtained were processed through spectroscopy skin in SIMCA 15 software (Umetrics, Sweden), and the dataset exported in .csv format from Agilent Resolution's Pro software was averaged and assigned into primary variable id, primary observation id (unique identifier), secondary observation Id, X and Y variables before importing to SIMCA dataset. Spectral filters were applied under control filters tab to obtain spectra of standard normal variate (SNV) transformation. Since the spectroscopic data were multivariate that make the difference among group interpretation to be difficult (Dao et al. 2017), the principal component analysis (PCA) was performed through PCA Tab by auto fitting option for the second derivative spectra that helped to account for most variation in the data. Score plots were used to visualize the clustering of data and variation among them. The important macromolecular composition of microalgae cells (Table 4b.2) that varies from 900-3000 cm^{-1} was taken into consideration for data analysis. To improve the prediction error of the data acquired from

spectral filterings such as SNV and derivatives, a partial least square regression called orthogonal partial least square (OPLS) regression was employed in the analysis since OPLS distinguishes the variations in another way compared to PLS although both tend to possess the same predictive properties. One advantage of OPLS is that the model created will be easier to interpret data from a spectroscopic point of view. For OPLS regression, the X and Y variables assigned for the dataset were selected and processed under the OPLS tab of spectroscopy skin. On processing, all the data were transformed to avoid error and center-scaled to derive the prediction data set.

4b.4. Results and discussion

4b.4.1. Evaluation of heavy metal-grown microalgae for macromolecules through ATR-FTIR

Both physiological and biochemical changes are the immediate responses to abiotic stresses in microalgae. Therefore, the biochemical response, in terms of macromolecular composition, is a prerequisite to monitor immediate changes under environmental stresses in microalgal cells. The data on FTIR spectral peak areas related to important macromolecules such as carbohydrates, proteins and lipids in two microalgal strains, *Desmodesmus* sp. MAS1 and *Heterochlorella* sp. MAS3 grown in presence of varying concentrations of HMs that serve as micronutrients, are presented in Fig. 4b.1. The bands assigned for these three biochemicals were predominantly found in the regions 900-1200, 1300-1650 and 2850-2960 cm^{-1} (Fig. 4b.2) as described in the literature (Laurens and Wolfrum 2011; Vongsvivut et al. 2013; Dao et al. 2017). Similar distinct spectral patterns were reported among various species of microalgae under different experimental conditions (Laurens and Wolfrum 2011; Dao et al. 2017). The observed changes at 1500-1600 cm^{-1} clearly indicate the impact of HMs on *Desmodesmus* sp. MAS1 but not on *Heterochlorella* sp. MAS3. Moreover, the second derivative spectra obtained (Figs.4b.3) as well as the changes in the raw spectra could not unravel any useful information (Dao et al. 2017). But, the importance of second derivative spectra is to remove baseline and replace maxima bands in raw spectra to minima for highlighting the differences (Karpinska 2012; Dao et al. 2017). Thus, the carbohydrates, proteins and lipids identity has been confirmed based on the corresponding major peaks in the FTIR spectra (Table 4b.2). The significant changes of the biochemicals are thus related to the negative scores in the second derivative spectra.

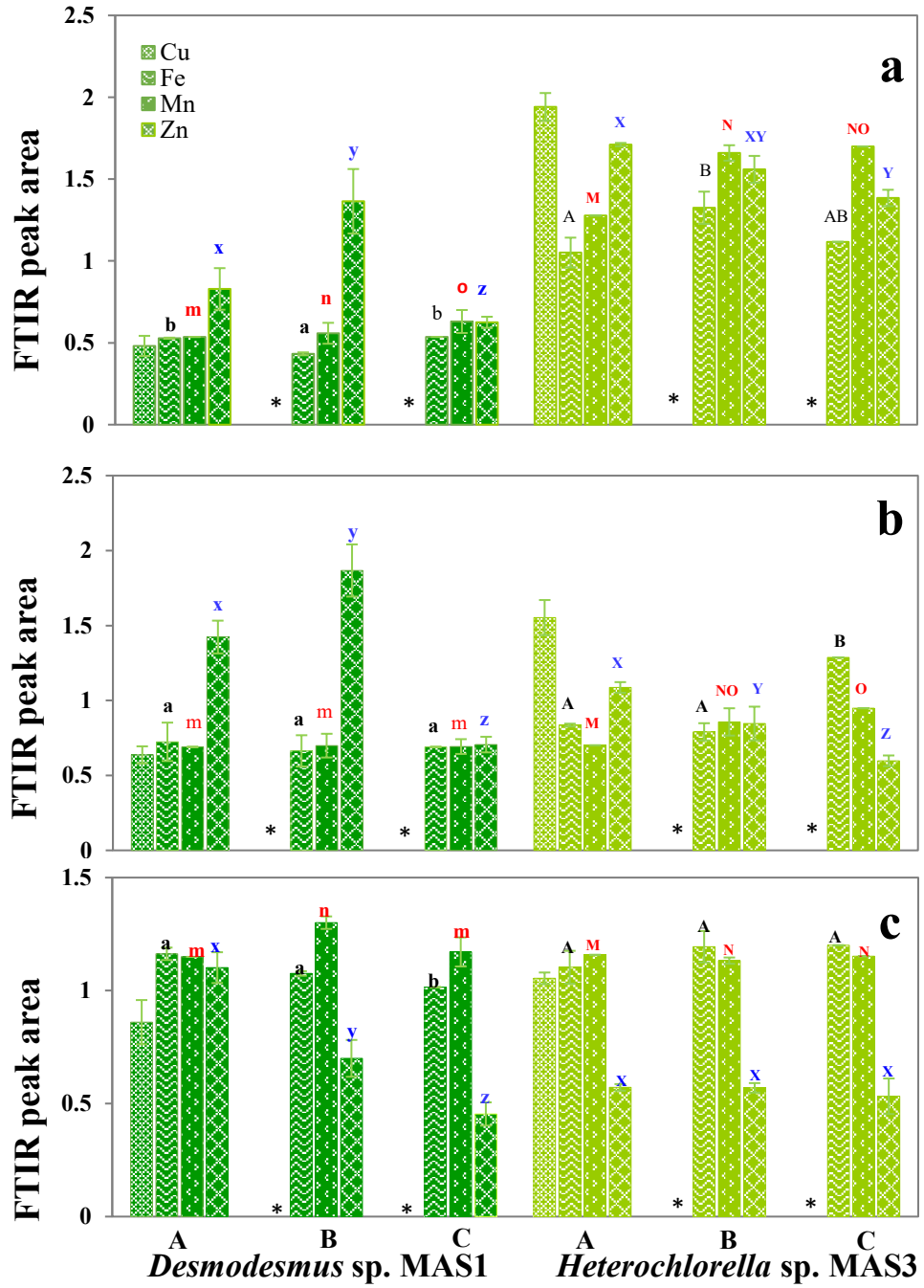

Fig. 4b.1 Changes in (a) carbohydrates, (b) proteins and (c) lipids as revealed by FTIR spectra in *Desmodesmus* sp. MAS1 and *Heterochlorella* sp. MAS3 when grown in presence of Cu, Fe, Mn and Zn at varying concentrations. Refer to the Table 4b.1 for the concentrations that correspond to A, B and C of a metal. All the experimental values of spectral peak area are presented in relation to a control value of 1.0. *Indicates that Cu at concentrations of 1 and 2 mg L^{-1} was lethal. Error bars signify standard deviations (n = 3). Data mean related to a heavy metal used for a microalgal strain sharing the same letter on top of the bars are in significantly dissimilar ($P \leq 0.05$) according to DMRT.

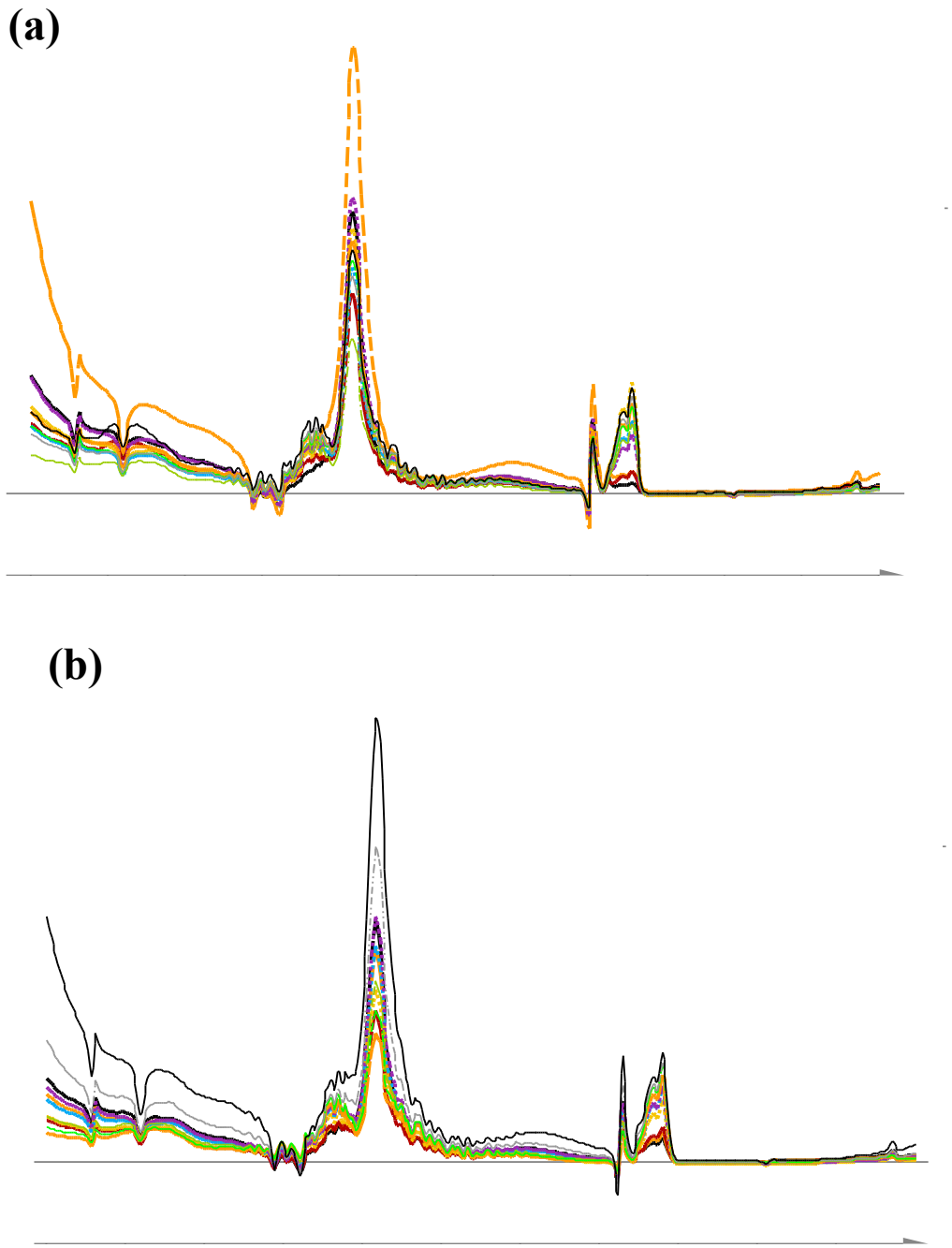

Fig. 4b.2. FTIR spectral raw data for acid-tolerant microalgae: (a) *Desmodesmus* sp. MAS1 and (b) *Heterochlorella* sp. MAS3. Refer to the Table 1 for the concentrations that correspond to A, B and C of a metal.

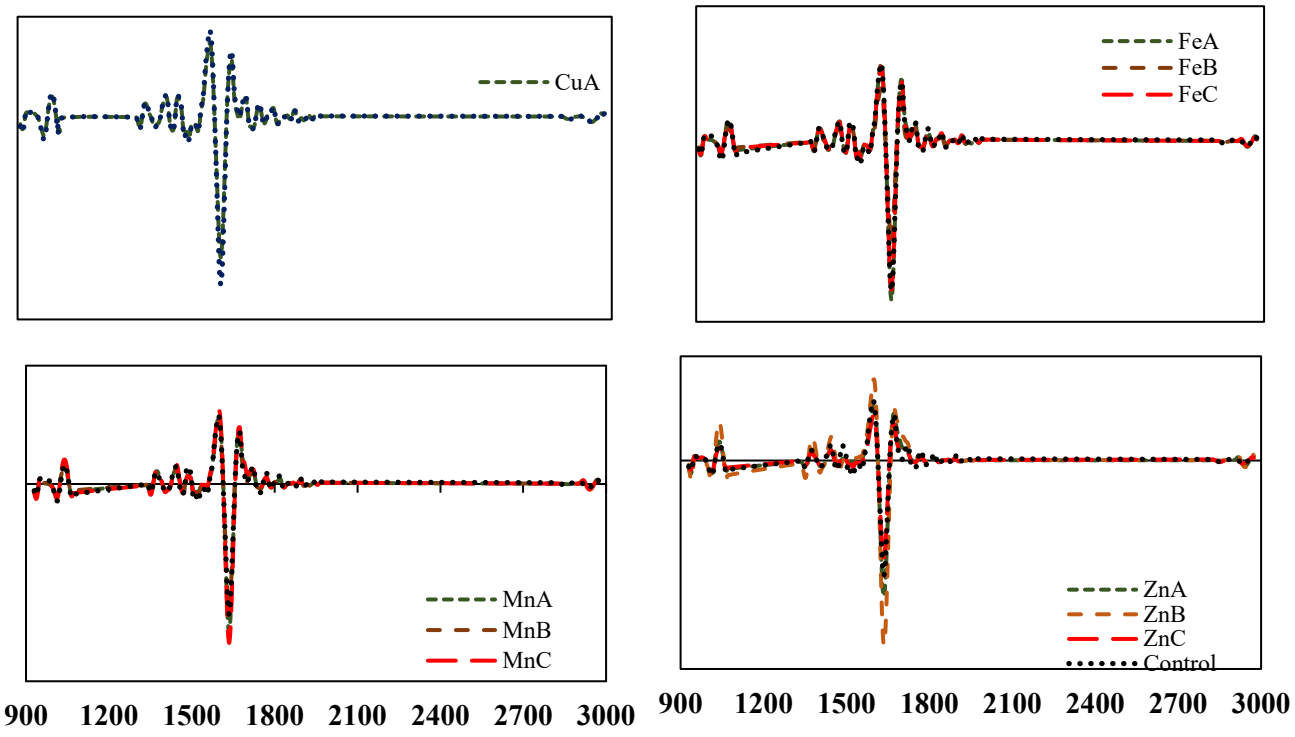

Fig. 4b.3a. Second derivative spectra for *Desmodesmus* sp. MAS1 grown in presence of different concentrations of metals at pH 3.5. Refer to the Table 1 for the concentrations that correspond to A, B and C of a metal.

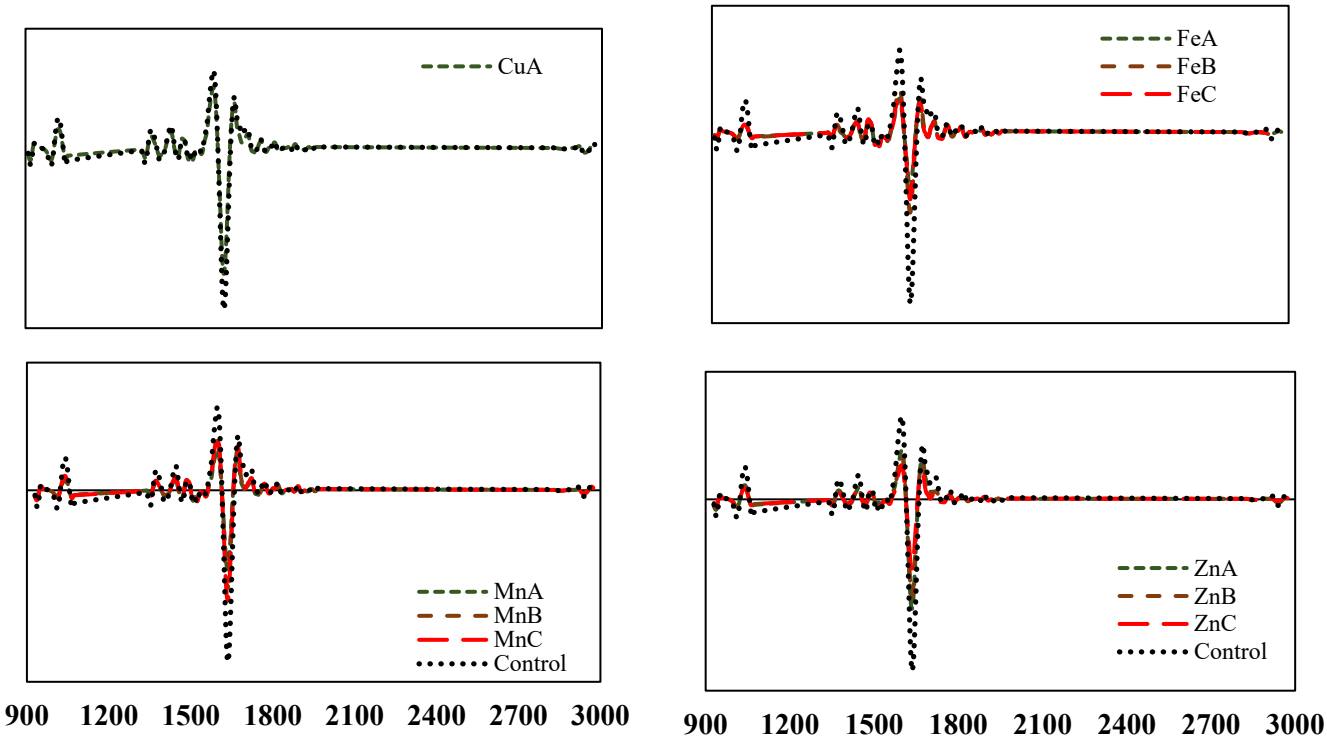

Fig. 4b.3b. Second derivative spectra for *Heterochlorella* sp. MAS3 grown in presence of different concentrations of metals at pH 3.5. Refer to the Table 1 for the concentrations that correspond to A, B and C of a metal.

Table 4b.2 Identity of biomolecules based on the major peaks in the FTIR spectra obtained from microalgal cultures grown in presence of heavy metals.

Biomolecule (wavelength range, cm^{-1})	Wave number/range (cm^{-1})	Vibration	Functional group	Reference
Carbohydrates (900-1236)	992	γ(=CH)	Phosphate vibration from RNA	(Vongsvivut et al., 2013)
	920-950 1019-1070 1106-1114	ν (C–O) ν (C–O–C) ν_{as} (C–O)	Carbonyl esters/Carbohydrates	(Abinandan et al., 2019c)
	1232-1236	ν_{as} (PO_2^-) ν_{as} (C–O)	Phosphorylated molecules, e.g. nucleic acids/ester group	(Abinandan et al., 2019c; Dao et al., 2017)
	2925, 2960	ν_{as}, ν_s (C−H)	Methyl and methylene groups in lipids	(Vongsvivut et al., 2013)
Proteins (1400-1670)	1400	ν_s (COO^-)	Protein methyl groups	(Vongsvivut et al., 2013)
	1450-1454	δ_s (CH_2; CH_3)	Methyl and methylene groups in DNA and RNA	(Abinandan et al., 2019c)
	1514,1550	δ (N−H) ν(C−N)	Amide II Protein (perpendicular modes of α helix and β sheet)	(Vongsvivut et al., 2013)
	1650-1670	ν_s (C=O)	Amide I Protein (α helix)	(Dao et al., 2017)
Lipids (1717-1750) (2835-2960)	1717	ν(C=O)	Free fatty acids, unsaturated fatty acid esters	(Vongsvivut et al., 2013)
	1735-1750	ν_s (C=O)	Triglyceride and free fatty acid esters	(Dao et al., 2017)
	2835	ν(C−H)	Methoxy chain in oil residue	(Abinandan et al., 2019c)
	2925, 2960	ν_{as}, ν_s (C−H)	Methyl and methylene groups in lipids	(Vongsvivut et al., 2013)

ν – vibrational stretch; ν_{as} – asymmetric vibrational stretch; ν_s – symmetric vibrational stretch; δs – symmetric vibrational bend; δas – asymmetric vibrational bend; γ – out of plane deformation.

4b.4.2. Carbohydrates

Carbohydrates are considered as biomolecules of energy storage in microalgal cells. HMs-grown *Heterochlorella* sp. MAS3 exhibited higher intensities in the regions 936, 1013 and 1065 cm^{-1} while the corresponding intensities were at 936, 1011 and 1067 cm^{-1} in *Desmodesmus* sp. MAS1 (Table 4b.2), possibly due to vibrational stretching frequencies of carbohydrates. Both the microalgal strains exhibited tolerance up to 0.5 mg L^{-1} of Cu (Fig. 4b.1a), while higher concentrations of the metal were algicidal (Abinandan et al. 2019a). Furthermore, a significant overlapping of the vibrational frequencies at these regions was observed in case of *Desmodesmus* sp. MAS1, but not in *Heterochlorella* sp. MAS3. Similar spectral patterns for carbohydrates were also observed in *Selenastrum gracile* grown at pH 7 in presence of copper (Rocha et al. 2016). Interestingly, higher concentrations of Cu were shown to upregulate several transcripts in an acidophilic microalga, *Chlamydomonas acidophila* (Olsson et al. 2015). Higher concentrations of Fe used to grow microalgae at pH 3.5 resulted in either increase or decrease of carbohydrates in *Heterochlorella* sp. MAS3 while these biomolecules were downregulated in *Desmodesmus* sp. MAS1. The reason for the observed synthesis of low amounts of carbohydrates in microalgal cultures grown in presence of higher concentrations of Fe could be due to the formation of Ferric-EDTA at acidic pH (Rizwan et al. 2017). On the contrary, the carbohydrate accumulation in microalgae *Chlorella* sp. increased even upon formation of Ferric-EDTA at pH 7.1 (Kona et al. 2017). Similarly, *Heterochlorella* sp. MAS3 when grown in medium supplemented with Mn or Zn exhibited enhanced accumulation of carbohydrates at increasing concentrations, especially at 936 and 1063 cm^{-1} due to vibrational symmetric stretching of C-O and C-C of glucosyl units (Wiercigroch et al. 2017). However, a significant reduction in carbohydrates was observed with varying concentrations of Mn in *Desmodesmus* sp. MAS1 as reported in acidophilic algal biofilms dominated by *Chlorella* sp. used for treating mine drainages (Palma et al. 2017).

4b.4.3. Proteins

Like carbohydrates, proteins are also an important macromolecular component of microalgae, and especially metals such as Cu, Fe, Mn and Zn act as essential non-protein cofactors in the enzymes (Blaby-Haas and Merchant 2017). The most prominent spectral bands observed at 1463, 1518, 1548 and 1630 cm^{-1} are characteristic of symmetrical vibration bend of methyl groups, amide II proteins and the vibrational stretch of amide I proteins (Table 4b.2). When both the microalgal strains were grown in presence of Cu, a significant overlapping was found at 1463, 1518 and 1548 cm^{-1}, an observation similar to the controls (Figs. 4b.3). However,

growth with Cu resulted in increased protein synthesis only in *Heterochlorella* sp. MAS3 (Fig. 4b.1b). The spectrum for amide I provides information about the secondary structure of the proteins which include C=O (80%), C–N (10%) and N–H (10%) (Ami et al. 2014; Dao et al. 2017). Under replete conditions, Cu content in plastocyanin and Cytochrome c oxidase increases with increase in growth (Kropat et al. 2015). The increase in proteins observed here is consistent with the increased photosynthetic efficiency in terms of chlorophyll *a* in *Heterochlorella* sp. MAS3 (Abinandan et al. 2019a). Similarly, growth in presence of higher concentration of Fe (20 mg L^{-1}) increased the protein content in *Heterochlorella* sp. MAS3 but not in *Desmodesmus* sp. MAS1. In microalgal cells, most of the iron is concentrated in chloroplast as it is an important cofactor for photosynthesis (Terauchi et al. 2010). However, under iron-limiting conditions protein involved in plastocyanin was greatly reduced (Hsieh et al. 2013). Another micronutrient, Mn, is actively involved in PSII of photosynthetic apparatus in microalgae. The bands of symmetric vibrational methylene groups and amide II stretch observed in *Desmodesmus* sp. MAS1 revealed no significant changes when grown in higher concentrations of Mn (Fig. 4b.1b). The amide I region exhibited increased spectral absorbance due to symmetric vibrational stretch from C=O group present in the proteins of *Desmodesmus* sp. MAS1 (Figs. 4b.3a and 4b.3b). However, no such stretching and bending vibrations of C=O, C-N, N-H of methyl groups, and amide I and amide II proteins were observed in *Heterochlorella* sp. MAS3 at increasing concentration of Mn. In PSII, two redox tyrosine residues are involved in membrane protein complexes and is dominated by symmetrical vibrational stretch recorded between 1620-1720 cm^{-1} that advocates for the Mn influence in case of *Desmodesmus* sp. MAS1 (Berthomieu and Hienerwadel 2005). When grown in presence of Zn, all the protein assigned vibrational bands (Table 4b.2) in *Heterochlorella* sp. MAS3 decreased when compared with the relative control. However, *Desmodesmus* sp. MAS1 exhibited a decrease at 5 mg L^{-1}. Notably, the amide I band with stretching vibration increased in mid concentration (2 mg L^{-1}) and subsequently decreased at 5 mg L^{-1} of Zn. It appears that higher concentrations of Zn tend to cause protein denaturation and correspondingly decreased Zn-binding sites in microalgae (Bácsi et al. 2015).

4b.4.4. Lipids

Lipids and fatty acids play a significant role in cellular function such as metabolism, energy storage and membrane activities (Bi et al. 2014). The critical spectral bands that represent microalgal lipids and fatty acids in microalgal strains grown in presence of four metals were found at 1745-1750, 2850 and 2940 cm^{-1} (Table 4b.2). In both the algal strains, Cu exerted less

impact on lipid profile (Fig. 4b.1c) although Cu is expected to induce oxidative stress at specific concentrations by triggering lipid accumulation (Hsieh et al. 2013). Similarly, Fe enhanced lipid accumulation as evidenced from the peak area in both the strains, particularly in *Heterochlorella* sp. MAS3. In *Desmodesmus* sp. MAS1, the spectral peak at 2940 cm^{-1} revealed the occurrence of both symmetric & asymmetric vibrational stretches of methyl and methylene groups of lipids (Figs. 4b.3a and 4b.3b). However, the symmetrical vibrational stretch of carboxylic esters observed at the region 1750 cm^{-1} decreased in Fe-grown cultures. On the other hand, increased accumulation of triglycerides, as indicated from the vibrational trend of C=O at 1750 cm^{-1}, and a decrease in the acyl chains of fatty acids at 2950 cm^{-1} were observed in *Heterochlorella* sp. MAS3. Under iron-replete conditions, no lipid droplets were observed in *Chlamydomonas* sp. (Urzica et al. 2013). Other studies indicated the positive influence of Fe in lipid enrichment in microalgae (Ren et al. 2014; Rizwan et al. 2017). An increase in symmetric and asymmetric vibrational stretches at 2950 cm^{-1} under increased metal concentrations of Mn was observed in *Desmodesmus* sp. MAS1, while an increased vibrational stretch of C=O was apparent in *Heterochlorella* sp. MAS3. This trend was even supported by the peak area ratio of both the strains at higher concentrations of Mn. Yang et al. (2015) observed that metal stress induced lipid accumulation without interfering with the growth mechanism. Growth with Zn at lower concentration resulted in higher lipid accumulation in *Desmodesmus* sp. MAS1 while all the concentrations tested were inhibitory to lipid synthesis in *Heterochlorella* sp. MAS3. The observed lipid accumulation at lower concentration of Zn in MAS1 could be ascribed to metal stress (Hamed et al. 2017). Although both Zn and Mn deficiencies cause hyper-accumulation of triacylglycerol in microalgae (Hsieh et al. 2013; Malasarn et al. 2013), we observed increased lipid accumulation in microalgae under the influence of higher concentrations at pH 3.5. The present results on lipid composition are consistent with our earlier observation of higher biodiesel production in *Heterochlorella* sp. MAS3 than in *Desmodesmus* sp. MAS1 at pH 3.5 when grown in presence of Cu, Fe, Mn and Zn (Abinandan et al. 2019a).

4b.4.5. Chemometric analysis for validating the data

Principal component analysis (PCA) applied to asses the similarity and variation between metals and their concentrations, and responses of both the microalgal strains, *Desmodesmus* sp. MAS1 and *Heterochlorella* sp. MAS3. PCA score plots were constructed using the variables in the second derivative spectra (Fig. 4b.4a). The maximum variation was quite high in *Desmodesmus* sp. MAS1 with PC1 (76%) followed by PC2 (21%) while the corresponding

values for PC1 and PC2 in *Heterochlorella* sp. MAS3 were 84.5 and 14.2%, respectively. In *Desmodesmus* sp. MAS1, the score plots revealed the clustering of various concentrations of the metals as well as the controls excepting Zn (Fig. 4b.4a). Although the control group was not clustered with the metals in *Heterochlorella* sp. MAS3, scattering of variables exhibited the impact of metals and their concentrations (Fig. 4b.4b). Similarly, Dao et al. (2017) observed variation on the impact of lead in two microalgae. Though metals are essential in microquantities, changes in macromolecules is immient in microalgae under metal-deficient or replete conditions (Hsieh et al. 2013). The results obtained from OPLS calibration, in terms of R^2 and root mean square error of cross-validation (RMSEcv) for the spectral filters such as raw, SNV, and its derivatives are presented in Table 4b.3. The OPLS models built for FTIR spectra of *Desmodesmus* sp. MAS1 and *Heterochlorella* sp. MAS3 exhibited R^2 values >0.99, especially for second derivative spectra advocating the precision of the obtained data.

Table 4b.3 Validation of the spectral data by the orthogonal partial least square (OPLS) regression.

Species	Spectrum	R^2 X (Cum)	R^2 Y (Cum)	Q_2	RMSEcv
Desmodesmus sp. MAS1	Raw	0.997	0.897	0.823	0.519
	SNV	0.851	0.776	0.643	0.737
	First derivative	0.999	0.927	0.871	0.443
	Second derivative	0.997	0.897	0.846	0.484
Heterochlorella sp. MAS3	Raw	0.997	0.897	0.962	0.519
	SNV	0.851	0.776	0.95	0.737
	First derivative	0.999	0.927	0.853	0.443
	Second derivative	0.997	0.897	0.86	0.484

Cum – Cumulative; RMSEcv – Root mean square error cross validation; X and Y – Variables; R^2 – Regression coefficient; Q_2 – Estimate of predictive ability of the model; SNV – Standard normal variate.

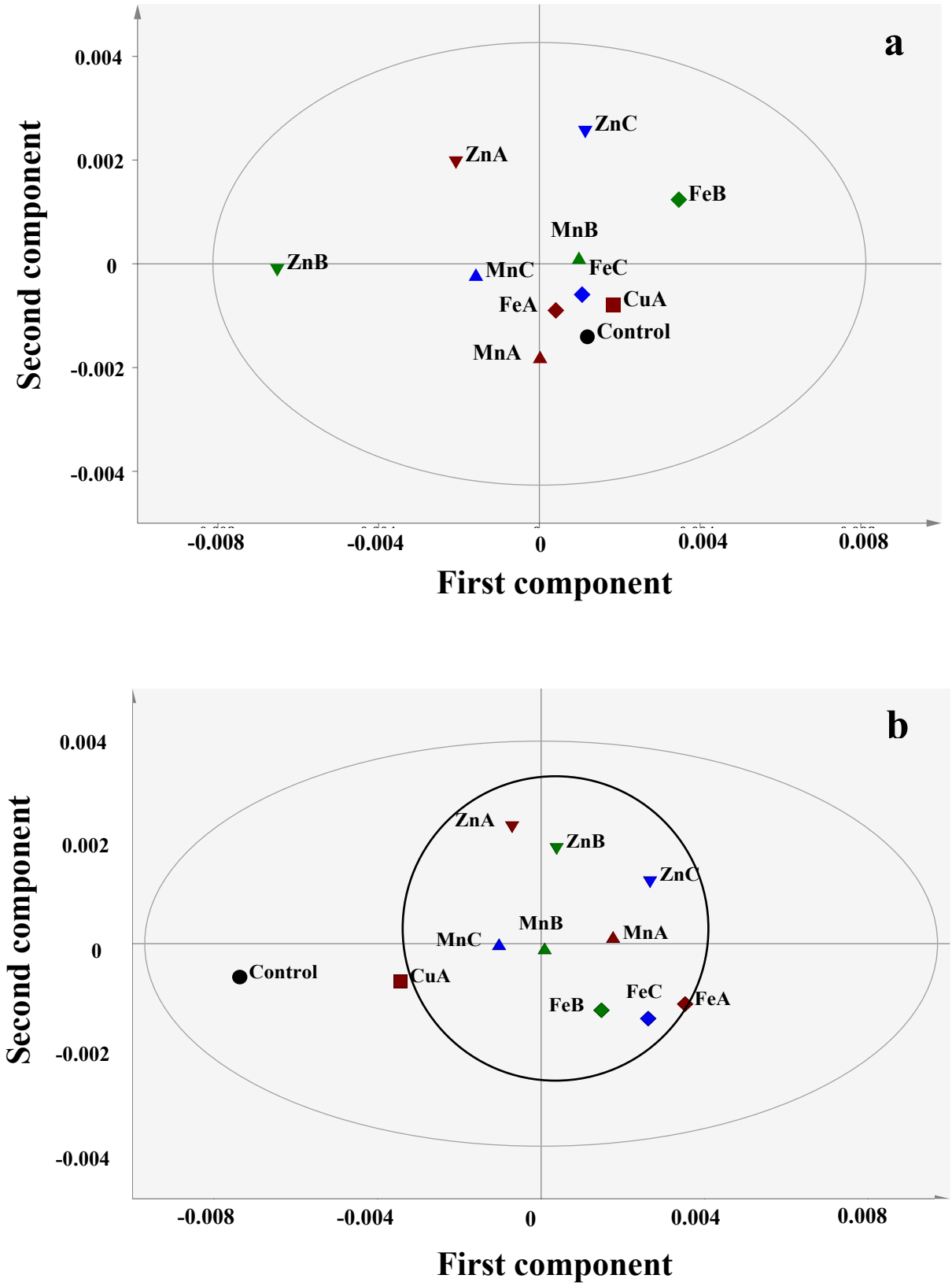

Fig. 4b.4 PCA of the experimental data. (a) *Desmodesmus* sp. MAS1 and (b) *Heterochlorella* sp. MAS3 grown at pH 3.5 in presence of different concentrations of metal**s.**

4b.5. Conclusion

The present approach of ATR-FTIR spectroscopy revealed that varying concentrations of the chosen HMs caused differential response on the accumulation of carbohydrates in acid-tolerant microalgal strains at pH 3.5. Vibrational stretches characteristic of proteins of amide I and carboxylic esters in lipids were the apparent responses to the increasing metal concentrations. The data were validated by PCA and OPLS regression and found statistically significant (R^2 >0.95). Since both the selected microalgae can sustain the heavy metal stress at pH 3.5 by synthesizing the essential biomolecules, these strains could be the potential candidates for bioremediation of such extreme habitats as AMDs.

4b.6. References

Abinandan S, Subashchandrabose SR, Venkateswarlu K, Megharaj M (2018) Microalgae–bacteria biofilms: a sustainable synergistic approach in remediation of acid mine drainage. Appl Microbiol Biotechnol 102:1131−1144.

Abinandan S, Subashchandrabose SR, Pannerselvan L, Venkateswarlu K, Megharaj M (2019a) Potential of acid-tolerant microalgae, *Desmodesmus* sp. MAS1 and *Heterochlorella* sp. MAS3 in heavy metal removal and biodiesel production at acidic pH. Bioresour Technol 278:9–16.

Abinandan S, Subashchandrabose SR, Cole N, Dharmarajan R, Venkateswarlu K, Megharaj M (2019b) Sustainable production of biomass and biodiesel by acclimation of non-acidophilic microalgae to acidic conditions. Bioresour Technol 271:316–324.

Abinandan S, Subashchandrabose SR, Venkateswarlu K, Perera IA, Megharaj M (2019c) Acid-tolerant microalgae can withstand higher concentrations of invasive cadmium and produce sustainable biomass and biodiesel at pH 3.5. Bioresour Technol 281:469–473

Ami D, Posteri R, Mereghetti P, Porro D, Doglia SM, Branduardi P (2014) Fourier transform infrared spectroscopy as a method to study lipid accumulation in oleaginous yeasts. Biotechnol Biofuels 7:12.

Bácsi I, Novák Z, Jánószky M, B-Béres V, Grigorszky I, Nagy SA (2015) The sensitivity of two *Monoraphidium* species to zinc: their possible future role in bioremediation. Int J Environ Sci Technol 12:2455–2466.

Bataller BG, Capareda SC (2018) A rapid and non-destructive method for quantifying biomolecules in *Spirulina platensis* via Fourier transform infrared–attenuated total reflectance spectroscopy. Algal Res 32:341–352.

Battah M, El-Ayoty Y, Abomohra AE-F, El-Ghany SA, Esmael A (2015) Effect of Mn^{2+}, Co^{2+} and H_2O_2 on biomass and lipids of the green microalga *Chlorella vulgaris* as a potential candidate for biodiesel production. Ann Microbiol 65:155–162.

Berthomieu C, Hienerwadel R **(**2005) Vibrational spectroscopy to study the properties of redox-active tyrosines in photosystem II and other proteins. Biochim Biophys Acta 1707: 51–66.

Bi R, Arndt C, Sommer U (2014) Linking elements to biochemicals: effects of nutrient supply ratios and growth rates on fatty acid composition of phytoplankton species. J Phycol 50: 117–130.

Blaby-Haas CE, Merchant SS (2012) The ins and outs of algal metal transport. Biochim Biophys Acta Mol Cell Res 1823:1531–1552.

Blaby-Haas CE, Merchant SS (2017) Regulating cellular trace metal economy in algae. Curr Opin Plant Biol 39:88–96.

Dao L, Beardall J, Heraud P **(**2017) Characterisation of Pb-induced changes and prediction of Pb exposure in microalgae using infrared spectroscopy. Aquat Toxicol 188:33–42.

Gurbanov R, Gozen AG, Severcan F (2018) Rapid classification of heavy metal-exposed freshwater bacteria by infrared spectroscopy coupled with chemometrics using supervised method. Spectrochim Acta A 189:282–290.

Hamed SM, Zinta G, Klöck G, Asard H, Selim S, AbdElgawad H (2017) Zinc-induced differential oxidative stress and antioxidant responses in *Chlorella sorokiniana* and *Scenedesmus acuminatus*. Ecotoxicol Environ Saf 140:256–263.

Hänsch R, Mendel RR (2009) Physiological functions of mineral micronutrients (Cu, Zn, Mn, Fe, Ni, Mo, B, Cl). Curr Opin Plant Biol 12:259–266.

Höhner R, Barth J, Magneschi L, Jaeger D, Niehues A, Bald T, Grossman A, Fufezan C, Hippler M (2013) The metabolic status drives acclimation of iron deficiency responses in *Chlamydomonas reinhardtii* as revealed by proteomics based hierarchical clustering and reverse genetics. Mol Cell Proteomics M113:029991.

Hsieh SI, Castruita M, Malasarn D, Urzica E, Erde J, Page MD, Yamasaki H, Casero D, Pellegrini M, Merchant, SS, Loo JA (2013) The proteome of copper, iron, zinc, and manganese micronutrient deficiency in *Chlamydomonas reinhardtii*. Mol Cell Proteomics 12:65–86.

Karpinska J (2012) Basic principles and analytical application of derivative spectrophotometry. Macro to nano spectroscopy, Jamal Uddin, IntechOpen, DOI: 10.5772/37673.

Kona R, Hemalatha M, Venu Srivastav K, Venkata Mohan S (2017) Regulatory effect of Fe-EDTA on mixotrophic cultivation of *Chlorella* sp. towards biomass growth and metabolite production. Bioresour Technol 244:1227–1234.

Kropat J, Gallaher SD, Urzica EI, Nakamoto SS, Strenkert D, Tottey S, Mason AZ, Merchant SS (2015) Copper economy in *Chlamydomonas*: prioritized allocation and reallocation of copper to respiration vs. photosynthesis. Proc Natl Acad Sci USA 112: 2644–2651.

Laurens LML, Wolfrum EJ (2011) Feasibility of spectroscopic characterization of algal lipids: chemometric correlation of NIR and FTIR spectra with exogenous lipids in algal biomass. BioEnergy Res 4:22–35.

Liu B, Liu J, Chen T, Yang B, Jiang Y, Wei D, Chen F (2015) Rapid characterization of fatty acids in oleaginous microalgae by near-infrared spectroscopy. Int J Mol Sci 16: 7045.

Malasarn D, Kropat J, Hsieh SI, Finazzi G, Casero D, Loo JA, Pellegrini M, Wollman FA, Merchant SS (2013) Zinc deficiency impacts CO_2 assimilation and disrupts copper homeostasis in *Chlamydomonas reinhardtii*. J Biol Chem 288:10672–10683.

Markou G, Nerantzis E (2013) Microalgae for high-value compounds and biofuels production: a review with focus on cultivation under stress conditions. Biotechnol Adv 31:1532–1542.

Merchant SS, Allen MD, Kropat J, Moseley JL, Long JC, Tottey S, Terauchi AM (2006) Between a rock and a hard place: Trace element nutrition in *Chlamydomonas*. Biochim Biophys Acta Molec Cell Res 1763:578–594.

Olsson S, Puente-Sánchez F, Gómez MJ, Aguilera A (2015) Transcriptional response to copper excess and identification of genes involved in heavy metal tolerance in the extremophilic microalga *Chlamydomonas acidophila*. Extremophiles 19:657–672.

Palma H, Killoran E, Sheehan M, Berner F, Heimann K (2017) Assessment of microalga biofilms for simultaneous remediation and biofuel generation in mine tailings water. Bioresour Technol 234:327–335.

Pereira M, Bartolomé MC, Sánchez-Fortún S (2013) Bioadsorption and bioaccumulation of chromium trivalent in Cr(III)-tolerant microalgae: a mechanisms for chromium resistance. Chemosphere 93:1057–1063.

Ren HY, Liu BF, Kong F, Zhao L, Xie GJ, Ren NQ (2014) Enhanced lipid accumulation of green microalga *Scenedesmus* sp. by metal ions and EDTA addition. Bioresour Technol 169:763–767.

Rizwan M, Mujtaba G, Lee K **(**2017) Effects of iron sources on the growth and lipid/carbohydrate production of marine microalga *Dunaliella tertiolecta*. Biotechnol Bioprocess Eng 22:68–75.

Rocha GS, Parrish CC, Lombardi AT, Melão M (2016) Copper affects biochemical and physiological responses of *Selenastrum gracile* (Reinsch). Ecotoxicology 25:1468–1477.

Souza-Egipsy V, Altamirano M, Amils R, Aguilera A (2011) Photosynthetic performance of phototrophic biofilms in extreme acidic environments. Environ Microbiol 13:2351–8.

Starodub ME, Wong PTS, Myfield IC, Chaud YK (1987) Influence of complexation and pH on individuals and combined heavy metal toxicity to freshwater green algae. Can J Fish Aquat Sci 44:1173–1180.

Terauchi AM, Peers G, Kobayashi MC, Niyogi KK, Merchant SS (2010) Trophic status of *Chlamydomonas reinhardtii* influences the impact of iron deficiency on photosynthesis. Photosyn Res 105:39–49.

Urzica EI, Vieler A, Hong-Hermesdorf A, Page MD, Casero D, Gallaher SD, Kropat J, Pellegrini M, Benning C, Merchant SS (2013) Remodeling of membrane lipids in iron starved *Chlamydomonas*. J Biol Chem 113:490425.

Vongsvivut J, Heraud P, Gupta A, Puri M, McNaughton D, Barrow CJ (2013) FTIR microspectroscopy for rapid screening and monitoring of polyunsaturated fatty acid production in commercially valuable marine yeasts and protists. Analyst 138:6016–6031.

Wiercigroch E, Szafraniec E, Czamara K, Pacia MZ, Majzner K, Kochan K, Kaczor A, Baranska M, Malek K (2017) Raman and infrared spectroscopy of carbohydrates: a review. Spectrochim Acta A185:317–335.

Wilde KL, Stauber JL, Markich SJ, Franklin NM, Brown PL (2006) The effect of pH on the uptake and toxicity of copper and zinc in a tropical freshwater alga (*Chlorella* sp.). Arch Environ Cont Toxicol 51:174–185.

Yang J, Cao J, Xing G, Yuan H (2015) Lipid production combined with biosorption and bioaccumulation of cadmium, copper, manganese and zinc by oleaginous microalgae *Chlorella minutissima* UTEX2341. Bioresour Technol 175:537–544.

Yen HW, Chen PW, Hsu CY, Lee L (2017) The use of autotrophic *Chlorella vulgaris* in chromium (VI) reduction under different reduction conditions. J Taiwan Inst Chem Eng 74: 1–6.

Chapter 4c Acid-tolerant microalgae can withstand higher concentrations of invasive cadmium and produce sustainable biomass and biodiesel at pH 3.5

4c.1. Abstract

In this study, two acid-tolerant microalgae, *Desmodesmus* sp. MAS1 and *Heterochlorella* sp. MAS3, originally isolated from non-acidophilic environment, was tested to withstand high concentrations of an invasive heavy metal, cadmium (Cd), at an acidic pH of 3.5 and produce biomass rich in biodiesel. The growth analysis, in terms of chlorophyll, revealed that strain MAS1 was tolerant even to 20 mg L^{-1} of Cd while strain MAS3 could withstand only up to 5 mg L^{-1}. When grown in the presence of 2 mg L^{-1}, a concentration which is 400-fold higher than that usually occurs in the environment, the microalgal strains removed >58% of Cd from culture medium at pH 3.5. FTIR analysis of Cd-laden biomass indicated production of significant amounts of biodiesel rich in fatty acid esters. This is the first study that demonstrates the ability of acid-tolerant microalgae to grow well and remove Cd at acidic pH.

4c.2. Introduction

Industrial and anthropogenic activities have been significantly contributing to the release of copious amounts of different metals into the environment. Only certain heavy metals (copper, zinc, manganese and iron), at trace amounts, are essential to the biota while other non-essential heavy metals pose a threat to the organisms of ecological significance. Amongst the latter, cadmium (Cd) is the highly toxic invasive heavy metal that enters the environment through mining activities, disposal of batteries, treatment of wastewaters, etc. Estimates also indicate that 15% of the total of 6.4 tons of Cd released into the aquatic environment is from wastewater treatment plants (Samdani et al., 2018). In extreme habitats such as acid mine drainages (AMDs), Cd concentrations are in the range of 300-5000 µg L^{-1} together with the predominant occurrence of sulfur ions (Cui et al., 2012). Environmentally relevant concentrations of Cd range from 0.011 to 25 µg L^{-1} of non-polluted and slightly polluted waters in China (Yu et al., 2018). Vig et al. (2003) proposed that Cd readily associates with other elemental species such as chlorides, hydroxyl, sulfhydryls and thiols, and determines the fate of any biological activity. Thus, bioaccumulation of Cd is a serious concern to the ecosystem as this invasive metal is highly dangerous to cellular functions and tends to enter the food web

through microalgae, which serve as a primary producer. However, microalgae can be useful for removal of Cd at neutral pH by sorption mechanisms (Yang et al., 2015).

It has been reported that Cd even at low concentrations can be very toxic to microalgae at neutral pH (Chia et al., 2013, 2017). The presence of EDTA, organic matter, phosphates in media act as chelating agents that tend to reduce the bioavailability of "free metal ions" in microalgae (Subashchandrabose et al., 2015). The toxicity of a heavy metal depends on its speciation at low pH rather than the presence of other chelating agents (Vig et al., 2003). Xu et al. (2012) observed that low pH even in the presence of complexing agents affected the growth of marine phytoplankton, indicating that acidic pH can be used as an actual "tool" to test for a metal tolerance studies of microalgae. However, only certain strains can tolerate extreme acidic conditions in metal-laden environments as exist in AMDs (Abinandan et al., 2018). Samadani et al. (2018) observed that an acid-tolerant microalga, *Chlamydomonas* CPCC 121, originally isolated from Cu-contaminated mine site, could tolerate higher concentrations of Cd at pH 4 due to exclusion of the metal at the cell wall surface, while a non-acidophilic strain of *C. reinhardtii* showed a higher accumulation of Cd only at pH 7.

As such, there are no studies on Cd removal and biomass production by acid-tolerant strains of microalgae at acidic pH (Abinandan et al., 2018). Very recently, two non-acidophilic microalgae, *Desmodesmus* sp. MAS1 and *Heterochlorella* sp. MAS3, are acid-tolerant and have the potential for sustainable production of biomass and biodiesel at acidic pH of 3 was demonstrated (Abinandan et al., 2019a). Furthermore, it has been established that the above two strains of microalgae can remove copper, iron, manganese and zinc, and produce biodiesel when grown at pH 3.5 (Abinandan et al., 2019b). Both these two microalgal strains were tested in the present study whether they could tolerate and remove higher concentrations of Cd when grown at pH of 3.5, an acidic condition that generally prevails in AMDs. Also, the impact of Cd-induced stress on the yield of biodiesel from Cd-laden microalgal biomass was assessed following *in-situ* transesterification and FTIR-based fatty acid methyl esters (FAME) analysis. This is the first study that demonstrates the sustainable biomass and biodiesel production by acid-tolerant microalgae while withstanding higher concentrations of Cd, the invasive heavy metal, at an acidic pH.

4c.3. Materials and methods

4c.3.1. Microalgae and growth with Cd

Heterochlorella sp. MAS3 and *Desmodesmus* sp. MAS1, originally isolated from natural habitats of soil and lake waters with near neutrality, were acclimated to pH 3.0 (Abinandan et al., 2019a). These acid-tolerant strains were maintained in modified Bold's basal medium (BBM) with low phosphate ($1/10^{th}$ of the original concentration) at pH 3.5 in conical flasks under continuous illumination (60 µmol photons m^{-2} s^{-1}) with shaking (100 rpm) at 23±1 ^{o}C. Cd stock solution (100 mg L^{-1}) was prepared from $CdNO_3$ in Milli Q water and filtered through a sterile 0.22 µm disposable syringe filter. Varying concentrations (0.5, 1, 2, 5, 10 and 20 mg L^{-1} which correspond to 4.45, 8.9, 17.8, 44.5, 88.9 and 177.9 µM, respectively) of Cd were added to 10 mL of low phosphate BBM contained in 40 mL sterilized glass vials. Aliquots of the culture medium with no added Cd served as controls. Logarithmically-grown cultures were pelleted by centrifugation at 6000 ×*g* for 7 min, cells were resuspended in fresh medium and used as inoculum to attain an initial density of 5×10^5 cells mL^{-1}. Triplicates of all the treatments were incubated as described above.

4c.3.2.Analysis of chlorophyll and Cd accumulation

In duplicate samples of each treatment, growth of the microlagal cultures, in terms of chlorophyll, was determined at regular intervals of 2 days by monitoring autofluorescence, and the average data values for each treatment were expressed as relative fluorescence units (RFUs), and growth rates determined (Abinandan et al., 2019b). The amount of Cd accumulated in microalgal cells was determined by following the procedure described for other heavy metals (Abinandan et al., 2019b). The total accumulation includes internally accumulated cadmium obtained after acid digestion and externally bound cadmium after EDTA wash of microalgae biomass after 16 days incubation, and the values were expressed as mg g^{-1}.

4c.3.3.Biochemical response and biodiesel yield

The algal biomass was used for biochemical analysis following attenuated total reflection-Fourier-transform infrared (ATR-FTIR) spectroscopy (Abinandan et al., 2019b). Biodiesel from Cd-laden algal biomass was obtained by *in-situ* transesterification and quantified by the gravimetric method (Abinandan et al., 2019a, b). ATR-FTIR spectroscopy was also followed to analyze biodiesel using appropriate controls (Abinandan et al., 2019b).

The spectra acquired by FTIR spectroscopy (Agilent Technologies) were scanned in mid IR range (400-4000 cm^{-1}). For duplicate samples, a total of 16 scans were performed to improve signal noise ratio, and the mean data values were used for analysis (Abinandan et al., 2019b).

4c.3.4.Statistical analysis

The means and standard deviations of the experimental data were determined using Graphpad Prism 7 software. Statistical significance of the means was determined using t-test following IBM SPSS Statistical Software (ver.24).

4c.4. Results and discussion

4c.4.1. Growth of acid-tolerant microalgae in the presence of Cd at pH 3.5

The growth of *Desmodesmus* sp. MAS1 in the presence of Cd at concentrations of 0.5 to 5 mg L^{-1} at the end of 16 days was almost the same as that observed in control culture (Fig. 4c.1a). Thus, the growth rates of the strain MAS1 were 0.348, 0.356, 0.352, 0.344 and 0.332 d^{-1} in the presence of 0, 0.5, 1, 2 and 5 mg L^{-1} of Cd, respectively. However, the microalgal growth rate at higher concentrations of 10 and 20 mg L^{-1} were 0.31and 0.27 d^{-1}. These data indicate that the microalgal strain MAS1 can grow well up to a concentration of 5 mg L^{-1} of Cd and tolerate this heavy metal up to a concentration of 20 mg L^{-1}. On the other hand, *Heterochlorella* sp. MAS3 was sensitive even to 5 mg L^{-1} of Cd, and other higher concentrations used were toxic to this microalga (Fig. 4c.1b). The growth rates of the strain MAS3 in the presence of Cd up to 2 mg L^{-1} were like those observed for the strain MAS1. In fact, 20 mg L^{-1} of Cd eliminated the strain MAS3 by the end of 16 days.

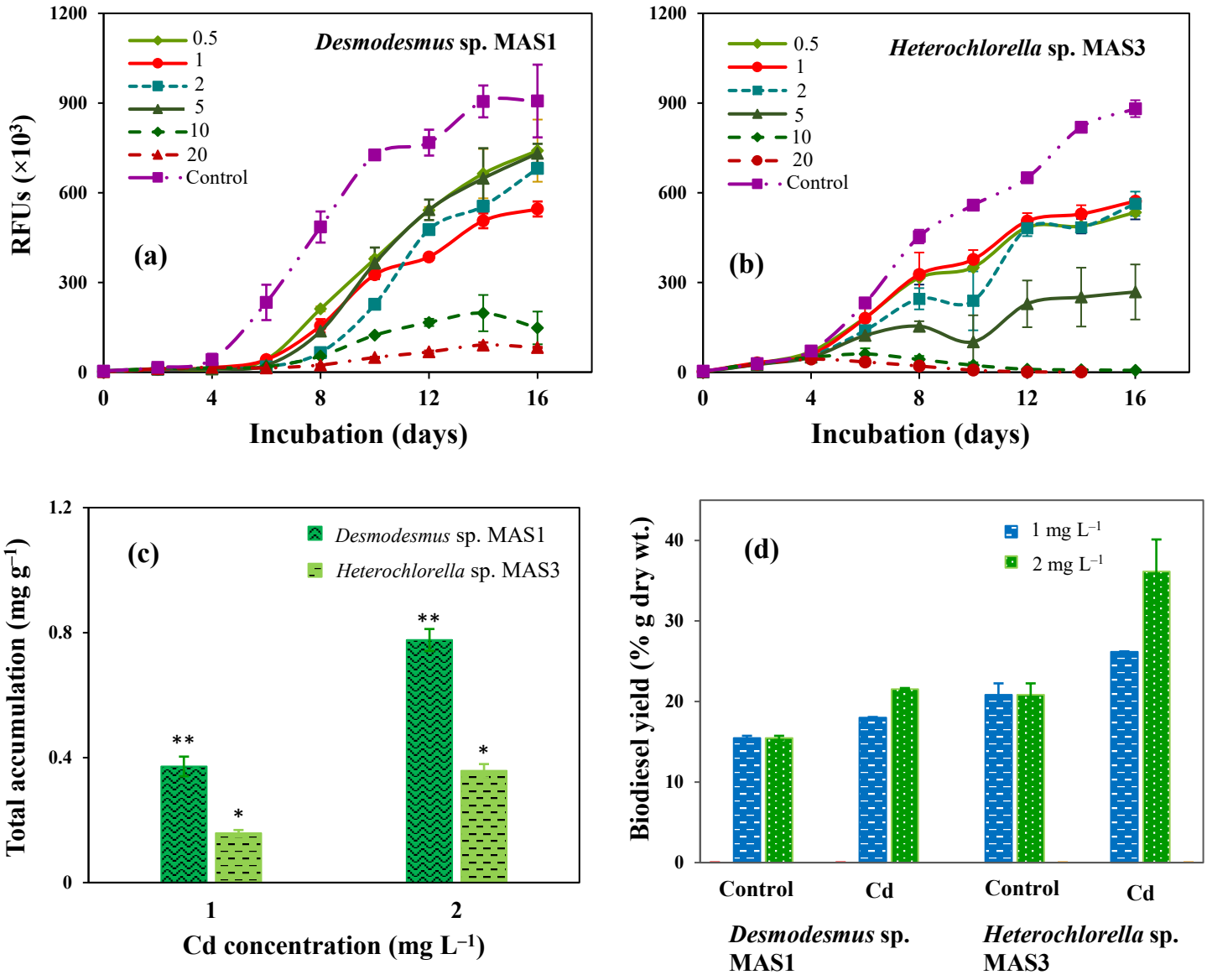

Fig. 4c.1 Response of the two acid-tolerant microalgal strains to the stress imposed by different concentrations (mg L−1) of Cd at pH 3.5. Growth, in terms of relative fluorescence units (RFUs), in (a) *Desmodesmus* sp. MAS1, (b) *Heterochlorella* sp. MAS3; (c) Total Cd accumulation after 16 days (*P < 0.05; **P < 0.01); and (d) Biodiesel yield after 16 days. Error bars represent standard deviation (n=3).

In acidic pH, heavy metals like Cd, copper, zinc complex with other ions preferably chlorides and sulphates (Vig et al., 2003; Krishnamurti et al., 2004). Since metals, as free ions and even complexes, are internalized into the cells, Cd speciation was determined at pH 3.5 using Visual MINTEQ software (Abinandan et al., 2019b). The data indicated that Cd free ion (Cd^{2+}) together with other ions increased with increasing concentrations (Table 4c). Similarly, Samdani et al. (2018) reported that Cd^{2+} availability increased from 12 to 51% with a change

in pH of the medium from 7 to 4. However, the occurrence of these ions is not directly proportional to the concentration of Cd. Even though complexation of Cd with EDTA accounted for >99% up to 2 mg L^{-1} of Cd, the extent of Cd-EDTA complex formation was consistent with higher levels of 5-20 mg L^{-1}, which might be due to the limited concentration of EDTA used in the culture medium. On the other hand, the toxicity observed at higher concentrations of Cd may be ascribed to the combined effect of Cd-EDTA complex and Cd^{2+} mostly available at pH 3.5. Virtually, there was no complex formation with phosphates, probably because of the low ($1/10^{th}$ of the original concentration in BBM) level of phosphate used in the medium. Webster et al. (2011) reported a reduction in the growth of microalgae in the presence of Cd (25 nM free Cd) and 10 µM of phosphate at neutral pH since both inorganic and organic phosphates precipitated with Cd^{2+} and eventually became less bioavailable. It was also found that growth was reduced upon exposure to 25 nM free Cd and was very high in low phosphate concentration of 0.01 mM (Webster et al., 2011). In comparison, the present data indicate that the selected acid-tolerant microalgae could withstand Cd^{2+} at levels as high as 2.652 µM even in the presence of 17 µM phosphate at pH 3.5.

Table 4c.1. Speciation of Cd in BBM at pH 3.5 based on Visual MINTEQ modelling

Cd species	**Cd concentration (mg L^{-1})**					
	0.5	1	2	5	10	20
Cd species concentration (mg L^{-1})						
Cd^{2+}	0.000545	0.00141	0.00538	0.29815	1.2895	3.3238
$CdCl^{+}$	0.00171	0.0044	0.00036	0.01945	0.084	0.2162
$CdSO_4$ (aq)	0	0.00041	0.01682	0.9296	4.012	10.295
$Cd(SO_4)^{2-}$	0	0.00105	0.00402	0.22205	0.9562	2.4426
$CdNO_3^{+}$	0	0	0	0.0024	0.0104	0.0268
$CdEDTA^{2-}$	0.307145	0.61333	1.21882	2.17915	2.2528	2.2816
$CdHEDTA^{-}$	0.18656	0.37254	0.74032	1.32365	1.3684	1.386
CdH_2EDTA (aq)	0.00359	0.00717	0.01424	0.0255	0.0263	0.0266
Total EDTA complex	0.497295	0.99304	1.97338	3.5283	3.6475	3.6942

Table 4c.2. Relative concentrations of Cd and its ions in culture medium at pH 3.5

Cd (mg L^{-1})	Cd (µM)	Cd and other ions (µM)		
		Cd free ion	Other ions	EDTA complex
0.5	4.45	0.005	0.019	4.421
1	8.9	0.013	0.048	8.835
2	17.8	0.048	0.188	17.555
5	44.5	2.652	10.440	31.388
10	88.9	11.471	45.030	32.450
20	177.9	29.568	115.470	32.870

Free ion, Cd^{2+}

Other ions: $CdCl^{+}$; $CdSO_{4(aq)}$; $Cd(SO_4)^{2-}$; $CdNO_3^{+}$

EDTA complex: $CdEDTA^{2-}$; $CdHEDTA^{-}$; $CdH_2EDTA_{(aq)}$

4c.4.2. Cd accumulation by acid-tolerant microalgae at pH 3.5

Since microalgal growth was unaffected by Cd at concentrations of 0.5-2 mg L^{-1}, the extent of total accumulation (combination of external and internal accumulation) of the invasive heavy metal was determined from the biomass obtained after 16 days in the presence of 1 and 2 mg L^{-1} of Cd at pH 3.5. In fact, both the microalgal strains showed significant accumulation of Cd (Fig. 4c.1c), which corroborates the observations made by Pokora et al. (2014) in a strain of *Desmodesmus armatus* grown at neutral pH. *Desmodesmus* sp. MAS1 accumulated 0.37-0.77 mg g^{-1} of 1-2 mg L^{-1} Cd added to the modified BBM. However, the corresponding range for the total accumulation in case of *Heterochlorella* sp. MAS3 was 0.16-0.36 mg g^{-1}. Most of the studies available in the literature reported either accumulation/removal of Cd by microalgal strains grown at neutral pH or by acidophilic microalgae at acidic pH. Two strains of *D. armatus* accumulated 159-341 µg g^{-1} of Cd from 93 µM CdCl supplemented at pH 7 (Pokora et al., 2014). Yang et al. (2015) stated that microalgal biomass could remove ~74% of 200 µM (22 µg mL^{-1}) $CdNO_3$ at pH 7 and the rate of removal decreased rapidly with increasing concentrations. However, Santiago-Martínez et al. (2015) observed 50-75% accumulation of 2-25 µM CdCl by an acidophilic microalga, *Euglena gracili*s, cultivated at pH 3.5. By comparison, the present results indicate that *Desmodesmus* sp. MAS1 and *Heterochlorella* sp. MAS3 accumulated about 500 and 347 µg g^{-1} of Cd, respectively, even

under extremely acidic conditions. Moreover, substantial amounts of Cd were removed by both the acid-tolerant microalgae at pH 3.5. Since the environmentally relevant concentrations of Cd have been reported to be in the range of 4.92-49.2 μg L^{-1} (Yu et al., 2018), the present data suggest that the two selected strains have the great potential in withstanding even the higher concentrations of Cd (300-5000 μg L^{-1}) that prevail in acidic environments such as AMDs. Thus, both *Desmodesmus* sp. MAS1 and *Heterochlorella* sp. MAS3 can serve as suitable candidates for metal removal of aqueous environments like AMDs polluted with Cd.

4c.4.3.Biochemical response in microalgae grown in presence of Cd

FTIR spectra showing biochemical changes in *Desmodesmus* sp. MAS1 and *Heterochlorella* sp. MAS3 after their growth in the presence of Cd are presented (Fig 4c.2). Various biochemical such as carbohydrates, proteins, lipids/esters, alkynes and lipids corresponding to the peaks resolved at 900–1200, 1550 and 1650, 1728–1745, 2250 and 2855–2925 cm^{-1} in the spectra were identified (Wagner et al., 2010). Carbohydrates that serve as energy reserves as well as proteins of amide I and amide II were the predominant macromolecules in control cultures of both the strains. But, these biochemicals along with lipids/esters were present at higher concentrations in *Heterochlorella* MAS3 grown without Cd. By comparison, all the biochemicals identified were affected in cultures of *Heterochlorella* MAS3 grown in the presence of Cd than those of *Desmodesmus* sp. MAS1. A perusal of literature indicates the impact of Cd on the yield of various biochemical in microalgae cultures grown at neutral pH. Also, phosphate depletion and Cd stress were reported to increase the carbohydrate content in *C. vulgaris* (Chia et al., 2017).

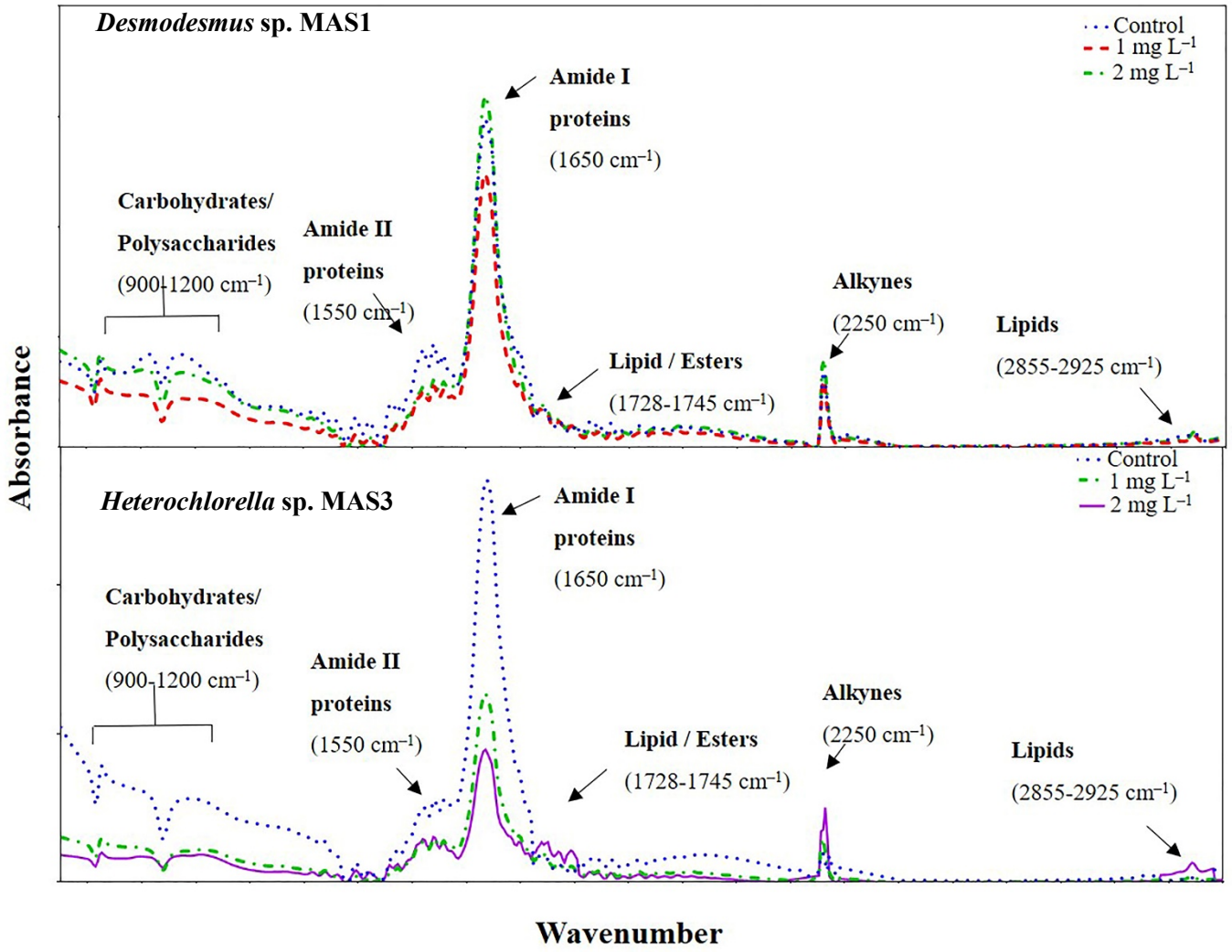

Fig. 4c.2. ATR-FTIR spectra showing different biochemicals in *Desmodesmus* sp. MAS1 and *Heterochlorella* sp. MAS3 when grown at pH 3.5 in presence of different concentrations of Cd.

The cellular proteins identified in the microalgal cultures used in the present study are of amide I (resolved at 1650 cm^{-1} due to bending of N–H functional group rather than carbon bonds) and amide II (1550 cm^{-1}) category. In general, the concentration of amide I proteins is rich in *Heterochlorella* MAS3 while amide II proteins are more in *Desmodesmus* sp. MAS1. Surprisingly, the levels of amide I proteins increased in the strain MAS1 when grown at 2 mg L^{-1} of Cd. Both the categories of proteins were significantly affected in Cd-grown *Heterochlorella* MAS3. Chia et al. (2017) observed that *C. vulgaris* was able to accumulate proteins under phosphate limitation and Cd-stress. Furthermore, an acidophilic alga, *Euglena gracilis*, accumulated less protein when exposed to Cd (Santiago-Martínez et al., 2015).

The peak in the region 2250 cm^{-1} can be attributed to the separation of alkyne (C=C)/ nitrile (C=N), and the concentration is higher in Cd-grown cultures than in controls of both the strains. Lipids, another important biochemical crucial in determining end value of the algal biomass predominantly produced, resolved strongly at ~1740 cm^{-1} and with weak bonds of CH_2 group at 2855-2925 cm^{-1}. Interestingly, the accumulation of lipids was significant in both the strains when grown at higher concentrations of Cd than in control cultures. Chia et al. (2017) also showed accumulation of lipids at 600 μM concentration of Cd and phosphate limitation in microalgae *C. vulgaris* grown at pH 7. Interestingly, the increase in ester group (1740 cm^{-1}) of lipids in *Heterochlorella* sp. MAS3 under the impact of Cd exposure revealed the dominance of C_{16} and C_{18} fatty acids as observed in *C. vulgaris* by Chia et al. (2013). In case of energy limitation, the accumulated lipids act as energy sources (Hu et al., 2008). Also, enhanced lipid accumulation increases the cellular redox homeostasis and alleviates oxidative stress developed due to metal exposure (Mock and Kroon, 2002).

4c.4.4.Biodiesel from Cd-laden biomass of acid-tolerant microalgae

The data on biodiesel obtained from Cd-laden microalgal biomass through *in-situ* transesterification are presented (Fig. 4c.1d). The approach used for FTIR interpretation of biodiesel production from the same microalgae under the influence of metals that serve as micronutrients (Abinandan et al., 2019b) has been followed in the present study. Interestingly, both the strains when grown at pH 3.5 in the presence of Cd produced high amounts of biodiesel. Several investigations reported production of biodiesel under the influence of metals only by growing microalgae at neutral pH. Palma et al. (2017) suggested that microalgal biofilms that remediate mine tailings water are good candidates for biodiesel production. Enhanced biodiesel production observed in the present study indicated improved conversion

of lipids to triglycerides and free fatty acid esters as evident from the FTIR spectrum at 1724-1745 cm^{-1} and aliphatic fatty acid hydrocarbons at 2855-2925 cm^{-1} (Mathimani et al., 2015). Mathimani et al. (2015) reported microalgal production of biodiesel rich in monoalkyl esters, while Kumar et al. (2014) observed more of aliphatic long-chain hydrocarbons in biodiesel. In all, these results indicate that the selected acid-tolerant strains of microalgae produce biodiesel rich in both the categories of lipids under stress imposed by high concentrations of Cd. Thus, in the present data on Cd together with the earlier findings with other heavy metals such as copper, iron, manganese and zinc (Abinandan et al., 2019b) clearly suggest that both *Desmodesmus* sp. MAS1 and *Heterochlorella* sp. MAS3 have great potential in remediating metal-rich environments with acidic conditions as exist in AMDs besides producing sustainable biomass for the yield of biodiesel abundant in FAME.

4c.5. Conclusion

The present study demonstrates that two acid-tolerant microalgal strains, MAS1 and MAS3 can withstand Cd at concentrations higher than those available in the ecosystem, and bioaccumulate substantial amounts at pH 3.5. The yield of microalgal biomass was significant containing increased amounts of biochemicals and FAME rich in triglycerides and aliphatic fatty acid hydrocarbons. The selected strains of microalgae could be used for removal of Cd from contaminated environments and subsequent biodiesel production. Future pilot-scale investigations concerning mixed metal influence on growth, Cd removal and biodiesel production will greatly help in exploiting the full potential of the selected acid-tolerant microalgal strains.

4c.6. References

Abinandan, S., Subashchandrabose, S. R., Venkateswarlu, K., Megharaj, M., 2018. Microalgae–bacteria biofilms: a sustainable synergistic approach in remediation of acid mine drainage. Appl. Microbiol. Biotechnol. 102, 1131–1144.

Abinandan, S., Subashchandrabose, S. R., Cole, N., Dharmarajan, R., Venkateswarlu, K., Megharaj, M., 2019a. Sustainable production of biomass and biodiesel by acclimation of non-acidophilic microalgae to acidic conditions. Bioresour. Technol. 271, 316–324.

Abinandan, S., Subashchandrabose, S. R., Pannerselvan, L., Venkateswarlu, K., Megharaj, M., 2019b. Potential of acid-tolerant microalgae, *Desmodesmus* sp. MAS1 and *Heterochlorella* sp.

MAS3, in heavy metal removal and biodiesel production at acidic pH. Bioresour. Technol. 278, 9–16.

Chia, M. A., Lombardi, A. T., Melão, M.D. G. G., Parrish, C. C., 2013. Lipid composition of *Chlorella vulgaris* (Trebouxiophyceae) as a function of different cadmium and phosphate concentrations. Aquat. Toxicol. 128–129, 171–182.

Chia, M. A., Lombardi, A. T., Melão, M. D. G. G., Parrish, C. C., 2017. Phosphorus levels determine changes in growth and biochemical composition of *Chlorella vulgaris* during cadmium stress. J. Appl. Phycol. 29, 1883–1891.

Cui, M., Jang, M., Cho, S.-H., Khim, J., Cannon, F. S., 2012. A continuous pilot-scale system using coal-mine drainage sludge to treat acid mine drainage contaminated with high concentrations of Pb, Zn, and other heavy metals. J. Hazard. Mat. 215–216, 122–128.

Hu, Q., Sommerfeld, M., Jarvis, E., Ghirardi, M., Posewitz, M., et al., 2008. Microalgal triacylglycerols as feedstocks for biofuel production: perspectives and advances. Plant J. 54, 621–639.

Krishnamurti, G. S. R., Megharaj, M., Naidu, R., 2004. Bioavailability of cadmium-organic complexes to soil alga – an exception to the free ion model. J. Agr. Food Chem. 52, 3894–3899.

Kumar, V., Muthuraj, M., Palabhanvi, B., Ghoshal, A. K., Das, D., 2014. Evaluation and optimization of two stage sequential in situ transesterification process for fatty acid methyl ester quantification from microalgae. Renew. Energy 68, 560–569.

Mathimani, T., Uma, L., Prabaharan, D., 2015. Homogeneous acid catalysed transesterification of marine microalga *Chlorella* sp. BDUG 91771 lipid – an efficient biodiesel yield and its characterization. Renew. Energy 81, 523–533.

Mock, T., Kroon, B.M.A., 2002. Photosynthetic energy conversion under extreme conditions – I: important role of lipids as structural modulators and energy sink under N-limited growth in Antaric sea ice diatoms. Phytochemistry 61, 41–51.

Palma, H., Killoran, E., Sheehan, M., Berner, F., Heimann, K., 2017. Assessment of microalga biofilms for simultaneous remediation and biofuel generation in mine tailings water. Bioresour. Technol. 234, 327–335.

Pokora, W., Bascik-Remisiewicz, A., Tukaj, S., Kalinowska, R., Pawlik-Skowronska, B., Dziadziuszko, M., Tukaj, Z., 2014. Adaptation strategies of two closely related *Desmodesmus*

armatus (green alga) strains contained different amounts of cadmium: A study with light-induced synchronized cultures of algae. J. Plant Physiol. 171, 69–77.

Samadani, M., Perreault, F., Oukarroum, A., Dewez, D., 2018. Effect of cadmium accumulation on green algae *Chlamydomonas reinhardtii* and acid-tolerant *Chlamydomonas* CPCC 121. Chemosphere 191, 174–182.

Santiago-Martínez, M. G., Lira-Silva, E., Encalada, R., Pineda, E., Gallardo-Perez, J. C., Zepeda-Rodriguez, A., Moreno-Sanchez, R., Saavedra, E., Jasso-Chavez, R., 2015. Cadmium removal by *Euglena gracilis* is enhanced under anaerobic growth conditions. J. Hazard. Mat. 288, 104–112.

Subashchandrabose, S.R., Megharaj, M., Venkateswarlu, K., Naidu, R., 2015. Interaction effects of polycyclic aromatic hydrocarbons and heavy metals on a soil microalga, *Chlorococcum* sp. MM11. Environ. Sci. Pollut. Res. 22, 8876–8889.

Vig, K., Megharaj, M., Sethunathan, N., Naidu, R., 2003. Bioavailability and toxicity of cadmium to microorganisms and their activities in soil: a review. Adv. Environ. Res. 8, 121–135.

Wagner, H., Liu, Z., Langner, U., Stehfest, K., Wilhelm, C., 2010. The use of FTIR spectroscopy to assess quantitative changes in the biochemical composition of microalgae. J. Biophotonics 3, 557-566.

Webster, R. E., Dean, A. P., Pittman, J. K., 2011. Cadmium exposure and phosphorus limitation increases metal content in the freshwater alga *Chlamydomonas reinhardtii*. Environ. Sci. Technol. 45, 7489–7496.

Xu, Y., Shi, D., Aristilde, L. Morel, F.M., 2012. The effect of pH on the uptake of zinc and cadmium in marine phytoplankton: possible role of weak complexes. Limnol. Oceanogr. 57, 293–304.

Yang, J., Cao, J., Xing, G., Yuan, H., 2015. Lipid production combined with biosorption and bioaccumulation of cadmium, copper, manganese and zinc by oleaginous microalgae *Chlorella minutissima* UTEX2341. Bioresour. Technol. 175, 537–544.

Yu, Z., Wei, H., Hao, R., Chu, H., Zhu, Y., 2018. Physiological changes in *Chlamydomonas reinhardtii* after 1000 generations of selection of cadmium exposure at environmentally relevant concentrations. Environ. Sci. Process Impacts 20, 923–933.

Chapter 5 Sustainable iron recovery and biodiesel yield by acid-adapted microalgae, *Desmodesmus* sp. MAS1 and *Heterochlorella* sp. MAS3, grown in synthetic acid mine drainage

5.1. Abstract

Sustainable resource recovery is the key to manage the overburden of various waste entities of mining practices. The present study demonstrates for the first time a novel approach for iron recovery and biodiesel yield from two acid-adapted microalgae, *Desmodesmus* sp. MAS1 and *Heterochlorella* sp. MAS3, grown in synthetic acid mine drainage (SAMD). Virtually, there was no difference in growth of the strain MAS3 both in Bold's basal medium (control) and SAMD. Using IC_{50} level (200 mg L^{-1}) and a lower concentration (50 mg L^{-1}) of iron in SAMD, the cell granularity, exopolysaccharide (EPS) secretion, iron recovery, and biodiesel were assessed in both the strains. Both cell granularity and accumulation of EPS were significantly altered under metal stress in SAMD, resulting in an increase in total accumulation of iron. Growth of the microalgal strains in SAMD yielded 12-20% biodiesel, with no traces of heavy metals, from the biomass. The entire amount of iron, accumulated intracellularly, was recovered in the residual biomass. Our results on the ability of the acid-adapted microalgal strains in iron recovery and yield of biodiesel when grown in SAMD indicate that they could be the potential candidates for use in bioremediation of extreme habitats like AMD.

5.2. Introduction

The heavy global demand for minerals over the years led to the depletion of their resources, and the intensive mining resulted in several hazards from derelict mines.[1,2] The environmental challenges from the mining process are also of great concern.[3] The acidic effluent produced from the rock interaction or oxidation of iron sulfide (FeS_2), termed as acid mine drainage (AMD), is the most hazardous form of post-mining activity.[4] The environmental impact of AMD is very high, contributing to the bioavailability of heavy metals (HMs) principally in water and soils. Because of the widespread occurrence of AMD, nearly 19,000 km of streams and 72,000 ha of lakes and reservoirs are affected throughout the world.[3] The water from Maurliden mine in Sweden contains high concentrations of iron (400 mg L^{-1}) and zinc (450 mg L^{-1}) besides the presence of other metals such as Mn and Cd in trace concentrations.[5] In South Africa, the iron concentration in acidic effluents (pH 2.1-3.1) from coal and gold mines was >800 mg L^{-1}.[6] At the mining-impacted area of Iberian pyrite belt in Spain, iron concentration in water samples collected at different locations varied from 21.8 to

2000 mg L^{-1}. [7] The above reports imply that iron is the most predominant metal in AMD irrespective of the conditions at geological strata of the mining areas.

Current mining waste management practices are aligned towards linear economic thinking (take-make-waste), necessitating the implementation of sustainable approaches to reuse and efficiently manage the resources.[8] The recovery of metals like iron from AMD is a valuable approach to meet their discharge limits while maintaining sustainable economic approach.[9] Limestone drains, open limestone channels and limestone diversion wells are the standard options in the passive treatment AMD.[3] Hammarstrom et al.[10] reported that the use of pulsed limestone bed systems for treating AMD reduced the formation of coatings besides hindering treatment efficiency. On the other hand, the active treatment processes generate copious sludge volumes enriched with various metals thus requiring further treatment.[9] Also, the recovery of metals from AMD using chemical precipitation produces sludge, and the metal recycling is not a sustainable process.[11] Adsorption[12], coagulation[13], chemical precipitation[14], and integrated filtration and chemical precipitation[15] are some of the other techniques used for iron recovery from AMD. Though biological methods for recovery of metals through passive bioreactors are promising viable alternatives, they require electron donors or substrates to promote and sustain the process.[16,17] Microalgae that thrive in any extreme habitats from desert to AMD by their ability to tolerate harsh environmental conditions are implicated in a wide array of biotechnological applications.[18-21] Most studies on metal recovery from synthetic solutions used dead algal biomass as adsorbent,[22,23] but the potential of acidophilic microalgae in metal recovery from AMD has not been understood so far. The approach of biofuel production, especially as an alternative to other fossil fuels, cannot compete with the conventional technology due to the costs associated with the yield of biomass and biofuel.[24,25] However, the 'green technology' involving microalgae is significant in circular economy related to bioremediation, resource recovery and generation of value-added products.[19] Very recently, we identified two strains of acid-tolerant microalgae, *Desmodesmus* sp. MAS1 and *Heterochlorella* sp. MAS3, that can grow well at pH 3.5, and remove HMs and sustainably produce biomass for the yield of biodiesel.[26-28] In the present study, for the first time, we tested whether these acid-tolerant microalgal strains upon prolonged adaptation for over 100 generations to acidic conditions at pH 3.5 have the potential for sustainable iron recovery and biodiesel production when grown in a synthetic AMD (SAMD).

5.3. Experimental section

5.3.1. Microalgae and analysis of growth response

The acid-tolerant microalgal strains, *Desmodesmus* sp. MAS1 and *Heterochlorella* sp. MAS3, initially maintained in Bold's basal medium (BBM), were adapted to acidic conditions for more than 100 generations by growing in BBM at pH 3.5 under the culture conditions described earlier.[26,27] The microalgal cells growing at log phase were centrifuged at 8000 ×*g* for 10 min and washed with ultra-pure water twice, and the pellet was re-suspended either in BBM or SAMD (Table 1). The composition of metals used in SAMD is based on our earlier studies related to toxicity and uptake of HMs, [26,27] and wherever necessary the concentrations of HMs in SAMD were changed. The microalgal suspension was added to 20 mL of sterilized BBM or SAMD samples contained in 50 mL Erlenmeyer flasks to obtain a final density of 5 $\times 10^5$ cells mL^{-1} for initially determining the relative growth. Varying concentrations of Fe were prepared using a stock solution of $FeSO_4.7H_2O$ (Sigma Aldrich, USA) in ultrapure water and passed through a sterile 0.22 µm disposable syringe filter. Initially, the microalgae were tested for their survival in SAMD composed of higher concentrations of HMs than those in AMD since they exhibited tolerance to Mn, Cu, Zn and Cd, but not Fe.[27,28] Subsequently, iron concentrations ranging from 25 to 800 mg L^{-1} were included in SAMD to determine IC_{50} (the concentration of iron required for 50% growth inhibition) values for iron in both the strains. Finally, to determine microalgal growth and their potential in iron recovery and yield of biodiesel, concentrations of only 50 and 200 mg L^{-1} of iron that correspond to a lower and IC_{50} value, respectively, were used. Each treatment was replicated thrice, and all the flasks were incubated under constant illumination (60 µmol m^{-2} s^{-1}) with 100 rpm shaking at 25 °C.[26]

The microalgal growth was determined, in terms of relative fluorescence units (RFUs) of chlorophyll, in a microplate reader using 100 µL aliquots of the cultures withdrawn at desired intervals as described earlier.[26,27] After 96 h of growth at pH 3.5, IC_{50} values for iron were determined by referring to the dose-response curve (inhibition) following nonlinear regression and using Graphpad prism software (version 8, USA). The content of exopolysaccharides (EPS) in the strains were analyzed by ATR-FTIR technique at a wave region of 900-1200 cm^{-1} following FTIR spectroscopy (Agilent Technologies, USA), and the peak area was calculated using Resolutions pro software (Agilent Technologies). Cell granularity was measured by flow cytometry using side scatter signal (SSC) collected through autofluorescence laser (695/40 nm band pass filter) in a BD FACS Canto flow cytometer (Becton Dickinson Instruments) as described previously.[26]

5.3.2. Iron and biodiesel analysis

Ten mL of the microalgal cultures, in triplicates, from each treatment were withdrawn for iron analysis only after 96h for iron analysis. Iron content in the samples was analyzed in Inductively Coupled Plasma-Optical Emission Spectrometer (ICP-OES, Agilent technologies, USA) as described earlier.[27,28] The total, intracellular, and extracellular concentrations of iron accumulated in the biomass were determined to account for the extent of iron recovery from SAMD, and the values were expressed as mg g^{-1} of biomass (dry wt.).

For analysis of biodiesel after 96h, 10-mL culture suspensions were centrifuged and washed twice with 0.025 M EDTA to remove EPS together with metals adsorbed onto the cell surface. Following solvent extraction using HCl-MeOH mixture and in situ transesterification, biodiesel was then extracted with hexane. The hexane layer was removed for quantification of biodiesel gravimetrically, and the yield values were expressed as percentages based on dry wt. of biomass[28]. The leftover aqueous phase together with the residual biomass was then concentrated in a vacufuge concentrator (Eppendorf) at 60 °C for 2 h. The biomass pellet was digested and the digest was diluted ten times with 5% nitric acid, and used for iron analysis in ICP-Mass spectrometer (ICPMS, Agilent technologies, USA). The biodiesel obtained was also analyzed for iron after diluting with 5% nitric acid. The values for iron partitioned in biodiesel and the residual biomass were expressed as percentages.

5.3.3. Statistical analysis

The standard deviations for the experimental data means (n = 3) were calculated using Graphpad Prism V.8 software, and the statistical significance ($P \leq 0.05$) of the means was determined following one-way ANOVA analysis and Duncan's multiple range (DMR) test using IBM SPSS statistical software (version 24, USA).

5.4. Results and Discussion

5.4.1. Growth of acid-adapted microalgae in SAMD

The The acid-adapted microalgae, *Desmodesmus* sp. MAS1 and *Heterochlorella* sp. MAS3, were grown in SAMD that contained 50% of phosphates originally present in AMD (Table 5.1). In fact, this reduction in phosphates in SAMD is to avoid complexation in the culture medium and increase iron bioavailability as determined by Visual MINTEQ modelling (Table 5.2). Initially, growth of the microalgal strains in BBM and SAMD, in terms of chlorophyll, was compared (Fig. 5.2a).

Table 5.1. Characteristics of AMD and synthetic AMD (SAMD)

Characteristic	AMD[a]	SAMD[b]
pH	3.0±0.1	3.5±0.2
Iron (Fe)	208.0±9.95	1±0.02
Manganese (Mn)	14.48±0.16	20±0.1
Copper (Cu)	0.052±0.002	0.5±0.02
Zinc (Zn)	0.0151±0.004	0.5±0.01
Cadmium (Cd)	0.005±0	0.5±0.1
Nitrate (NO_3^-)	129.65±0.61	90±1.5
Total phosphate (PO_4^{3-})	6.77±1.07	3.3±0.2

[a]n = 5; [b]n = 3. The concentrations are in mg L^{-1}

Table 5.2. Species distribution of iron supplemented in SAMD as determined by Visual MINTEQ modelling

Metal species (%)	**Fe concentration (mg L^{-1})**		
	SAMD	SAMD + 50 mg Fe L^{-1}	SAMD + 200 mg Fe L^{-1}
Fe^{2+}	0.23611	12.141	68.205
$FeCl^+$	0.0001	0.005	0.03
$FeSO_{4\ (aq)}$	0.7604	37.6935	181.115
$FeH_2PO_4^+$	0.00339	0.16	0.65

Overall, growth of the strain MAS1 in SAMD was significantly more than that of the strain MAS3. The calculated doubling time for the strain MAS1 was two-fold higher in BBM compared to SAMD. Interestingly, no such difference in generation time was observed for the strain MAS3, indicating its better tolerance to the elevated concentrations of metals in SAMD. The growth inhibition in the microalgal strains in SAMD could be due to the competition between H^+ and metal ions for cell surface binding sites, especially under acid pH.[29] In presence of a mixture of metals such as Cu and Ni and standard BG11 phosphates, Rugnini et al.[30]

reported significant inhibition in the photosynthetic activity of *Desmodesmus* sp. and *Chlorella vulgaris*. Under balanced growth conditions at pH 2.6, the energy balance, based on amount of absorbed energy, and the pigment content per cell were reduced in an acidophilic microalga, *Chalmydomonas acidophila*, due to changes in the environmental conditions that force the microalga to adapt by reorganizing photosynthetic apparatus and metabolic pathways.[31] Concentration-dependent growth inhibition observed at the end of 96 h by using Fe concentrations ranging from 25 to 800 mg L^{-1} in both the microalgal strains revealed an IC_{50} value of 200 mg L^{-1} (R^2 = 0.94; 0.97 for MAS1 and MAS3, respectively) (Fig. 5.1). Spijkerman[32] suggested that high concentrations of iron in the medium tend to limit the phosphate uptake that is essential for acidophilic algae. Especially higher concentrations of iron decrease the bioavailable fraction of phosphates by complexation or lowering P uptake rates due to adsorption process, a phenomenon that is common in iron-rich acidic lakes.[33] Also, ferric ion concentration exceeding five mmol L^{-1} was too toxic for phytoplankton in an acidic river in Spain leading the algae to consume more ATP resulting in growth inhibition.[32,34] Moreover, Visual MINTEQ data (Table 5.2) revealed that iron complexation with phosphates is about 0.26 and 0.32% at 50 and 200 mg L^{-1}, respectively. Based on the above observations, only the two concentrations, 50 and 200 mg L^{-1}, were used in further experimentation.

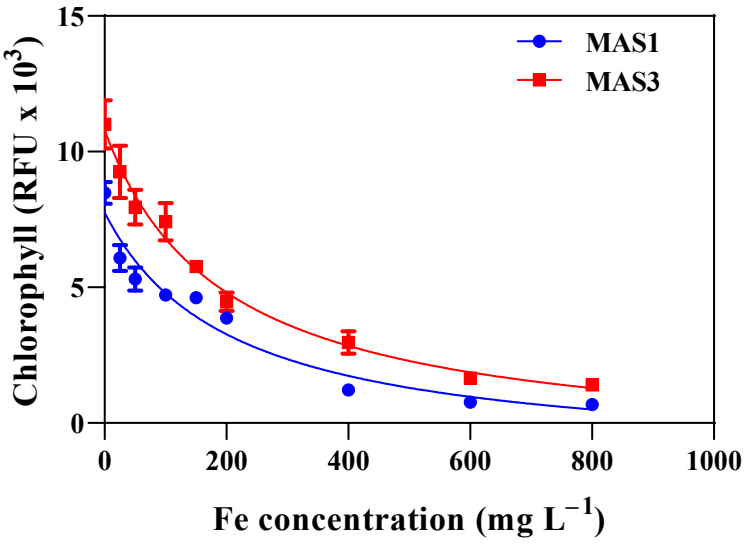

Fig 5.1. Determination of IC_{50} values following growth inhibition, in terms of relative fluorescence units (RFUs) of chlorophyll, in strains of MAS1, MAS3 at various iron concentrations in SAMD.

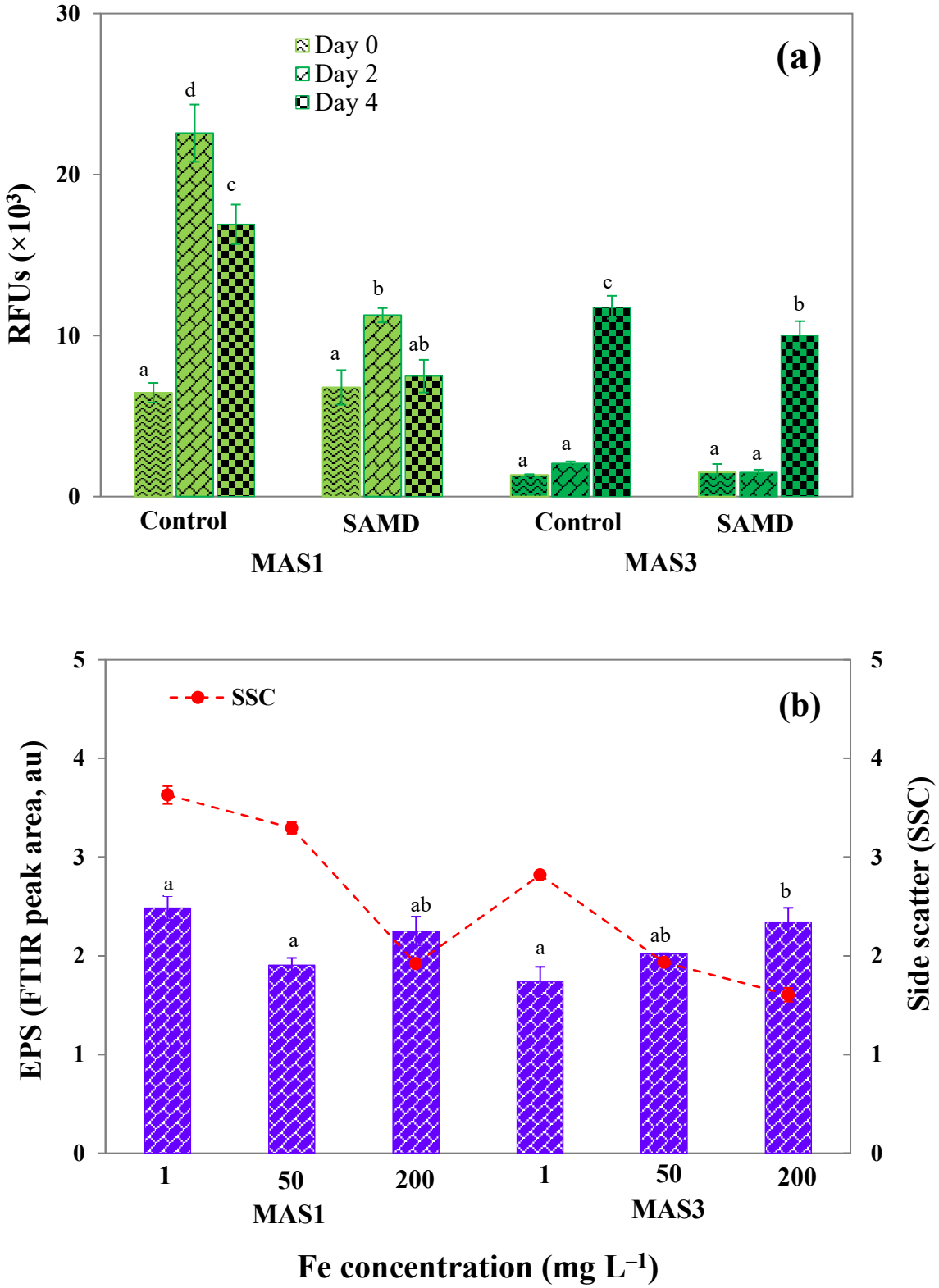

Fig. 5.2. (a) Response, in terms of relative fluorescence units (RFUs) of chlorophyll in strains MAS1 and MAS3 grown in BBM and SAMD; (b) Exopolysaccharides (EPS) and Cell granularity in strains MAS1 and MAS3 grown in SAMD at 1, 50 and 200 mg Fe L^{-1}. The mean

values (n = 3), related to a microalgal strain, carrying the same letter on the bars are not significantly ($P \leq 0.05$) different from each other according to Duncan's multiple range (DMR) test.

5.4.2. Microalgal response to iron levels in SAMD

Cell granularity, measured through side scatter (SSC) following flow cytometry, and EPS accumulation by FTIR spectroscopy were determined to assess the microalgal response to iron at 1 mg L^{-1} as contained in SAMD (Table 5.1) and higher supplemental levels of 50 and 200 mg L^{-1} (Fig. 5.2b). The cell granularity, attributed mostly to intracellular changes under stress, was very less when the microalgal strains were grown in SAMD that contained 1 mg L^{-1} of iron. Increased iron concentrations in SAMD (50 and 200 mg L^{-1}) decreased the SSC signal in both the strains, indicating significant intracellular changes. However, the change in granularity was significant in strain MAS3 as compared to strain MAS1. Such a decrease in cell granularity in response to metals such as Cu and Ni was also observed in a microalga, *Chlorococcum infusionum*.[35] Metals in high concentrations alter the cell membrane by increasing permeability leading to enlargement of cells due to accumulation of photosynthetic products.[36] Also, increased cellular granularity may be due changes in the ultrastructure as observed in *Chlamydomonas reinhardtii* when exposed to Cd.[29] At high concentrations of Zn (4.4 mM) in presence of Mn and Ni at pH 3.5, *Ulothrix* sp., an acidophilic alga isolated from AMD, exhibited completely disoriented thylakoids in chloroplasts.[37] The secretion of EPS, as determined from FTIR peak area (arbitrary units, au) increased at higher concentrations of iron in both the strains of microalgae (Fig. 5.2b). The strain MAS3 exhibited 5-10% increase in EPS accumulation at 50-200 mg L^{-1} of Fe than MAS1. Notably, MAS1 showed a significant reduction (20%) in EPS accumulation at 50 mg Fe L^{-1} as compared to 1 mg L^{-1}, but was increased subsequently at higher Fe concentrations (Fig. 5.2b). Strains of microalgae are known to produce more EPS under stress conditions imposed by environmental pollutants, especially HMs,[38] thus corroborating with the present results observed at 200 mg L^{-1}. Likewise, Palma et al.[39] reported an enhanced EPS secretion in *Chlorella* sp. when grown in mine tailing water contaminated with HMs wherein the iron concentration was less than 1mg L^{-1}, indicating the influence of other metal like Mn

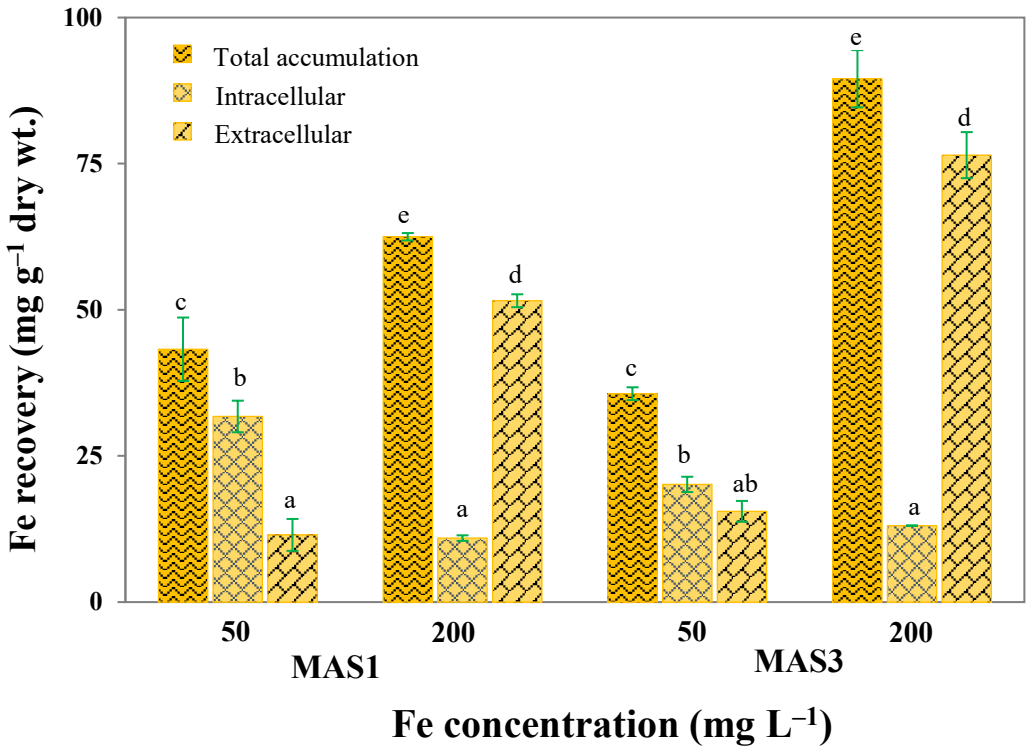

Fig. 5.3. Iron recovery (mg Fe g^{-1} dry wt. of biomass), in terms of accumulation (total, extracellular and intracellular), by strains MAS1 and MAS3 grown in presence of 50 and 200 mg Fe L^{-1} in SAMD for 96h. The mean values (n = 3), related to a microalgal strain, carrying the same letter on the bars are not significantly ($P \leq 0.05$) different from each other according to DMR test.

5.4.3. Sustainable iron recovery and biodiesel yield by microalgae

Total accumulation (both external and internal) was considered for the extent of iron recovery by the microalgal strains grown in SAMD supplemented with 50 or 200 mg L^{-1} of iron. Increased Fe concentrations enhanced its total accumulation in both the strains of MAS1 and MAS3 (Fig. 5.3). While the extent of iron uptake is less, the intracellular accumulation was higher which accounted for 80% of the total accumulated iron, at 50 mg Fe L^{-1} in strain MAS1. However, the extracellular accumulation was very significant (90% of the total) when this strain was grown in presence of 200 mg L^{-1} of Fe. The increase in total accumulation of iron in strain MAS1 when iron concentration in SAMD increased from 50 to 200 mg L^{-1} was 3-fold whereas the corresponding increase in MAS3 was only 1.2-fold. Interestingly, the extracellular accumulation of iron was significantly higher in strain MAS3 grown in presence of 50 or 200 mg L^{-1} of iron in SAMD. The mode of adsorption and accumulation of iron is not understood although iron uptake in microalgae is likely to include one of the two pathways (i)

active surface adsorption and passive intracellular accumulation, or (ii) passive surface adsorption and active intracellular accumulation.[41] In presence of Fe and Zn that are essentially involved in photosynthesis, *Euglena gracilis* (an acidophilic alga) accumulated 60% of Cd in chloroplasts[40], but Ni accumulation was limited in the presence of other essential divalent metals such as Zn, Mn, Cu.[42] Nearly 80% of total accumulated iron accounted for extracellular accumulation in MAS1 grown in SAMD with 200 mg L^{-1} of iron. In fact, higher EPS secretion associated with elevated concentrations of iron (Fig. 5.2b) resulted in increased external accumulation of iron. García-Meza et al.[42] also observed significant extracellular metal accumulation in photosynthetic biofilms from mine tailings facilitated by more EPS secretion. Similarly, in AMD environments that contained mixed metals, the increased accumulation of EPS was attributed to the alleviation of metal toxicity in microalgae present in biofilms[39]

Biodiesel was extracted after *in situ* transesterification of the biomass collected from the microalgal cultures grown in BBM (control) and SAMD containing 1, 50 or 200 mg Fe L^{-1} (Fig 5.4a). In all, the biodiesel yield increased significantly when the strains were grown in SAMD. Among three concentrations of iron included in SAMD, 50 mg L^{-1} was significantly effective in yielding biodiesel. Again, it is quite interesting to note that particularly 50 mg L^{-1} of iron in SAMD significantly enhanced biodiesel yield in strain MAS1. Thus, the per cent biodiesel yield in strain MAS1 grown in 1, 50 and 200 mg Fe L^{-1} was 13, 20 and 15, while the corresponding values for MAS3 were 12, 16 and 14. Evidently, there was an 18-25% decrease in biodiesel production in cultures grown in SAMD supplemented with 200 mg L^{-1} of iron when compared with the concentration of 50 mg L^{-1}. Laurens et al.[43] observed that the biodiesel yield determined following *in situ* transesterifcation in *Chlorella* and *Nannochloropsi*s was only 9-10% of the biomass (based on dry wt.). Lipids, primarily triacylglycerols (TAGs) are synthesized under unfavorable conditions as energy storage molecules in microalgae.[44] The significant enhancement in intracellular accumulation of iron and increased biodiesel production in MAS1 when grown in presence of 50 mg Fe L^{-1} clearly support the likely triggered accumulation of TAGs which are the precursors for biodiesel enhancement.[27] Also, we observed earlier that the same strains MAS1 and MAS3 when grown in BBM supplemented with 20 mg L^{-1} of Fe at pH 3.5, the yield of fatty acid methyl esters (FAME) was ~25% on dry wt. basis.[27] Concas et al.[45] suggested that increased iron concentration could trigger oxidative stress in microalgal species resulting in enhanced accumulation of lipids. Also, Ren et al.[46] reported that higher iron concentrations in the culture medium induced lipid synthesis through metabolic alteration in *Chlorella vulgaris*.

Although iron was supplemented even at 200 mg L^{-1} in SAMD, no traces of iron or any other HM were detected in biodiesel obtained from both the microalgal strains, indicating that the biodiesel is of good quality and can be safely used as an energy source. Raikova et al.[47] determined bio-oil production by hydrothermal liquefaction from metal-grown *Spirulina* biomass and observed that metals were accumulated in biomass residue than in oil. Similarly, biodiesel obtained from microalgal biomass cultivated in metal-contaminated flue gas showed no traces of metals.[48] Interestingly, a major portion of iron that accumulated inside the microalgal cells remained in the residual biomass recovered after extraction of biodiesel (Fig. 5.4b). In fact, iron content in residual biomass collected from both the cultures grown in presence of 50 mg L^{-1} was significantly more as compared to the higher concentration used in SAMD. For instance, the recovery of iron from the residual biomass was 75% of the amount accumulated intracellularly in strain MAS1 grown in SAMD with 50 mg Fe L^{-1}, and the corresponding value for strain MAS3 was 98%. Our data demonstrate that most of the iron accumulated in microalgal strains could be recovered from the residual biomass left after extraction of biodiesel. Also, the present study indicates the great potential of the two acid-tolerant microalgae in resource recovery and biodiesel production while remediating an AMD.

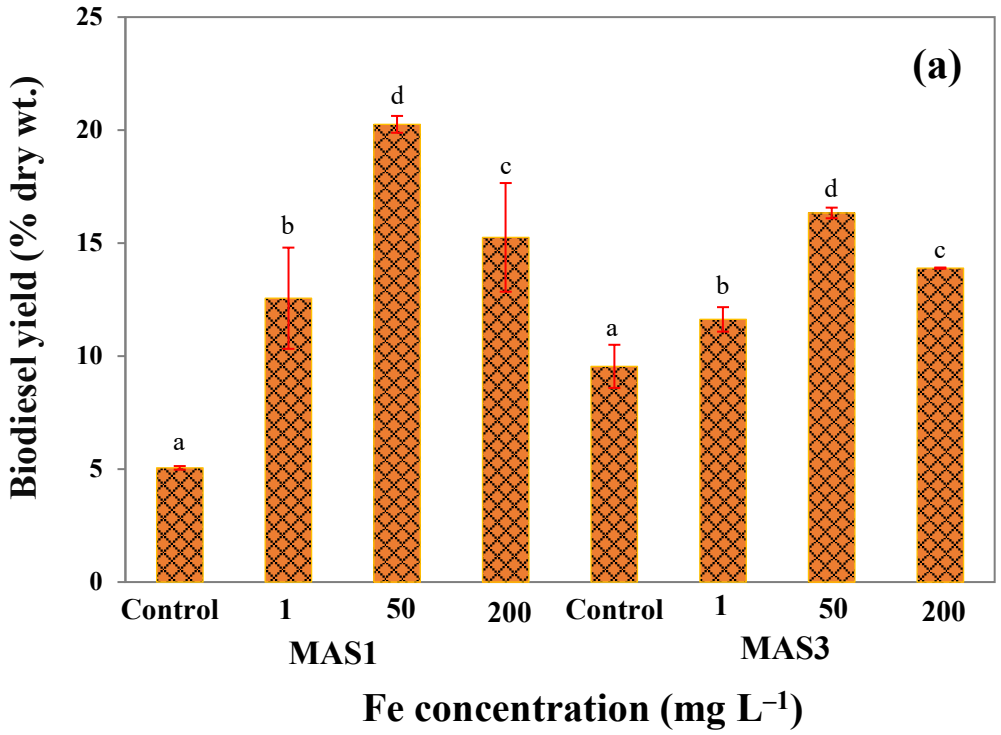

.

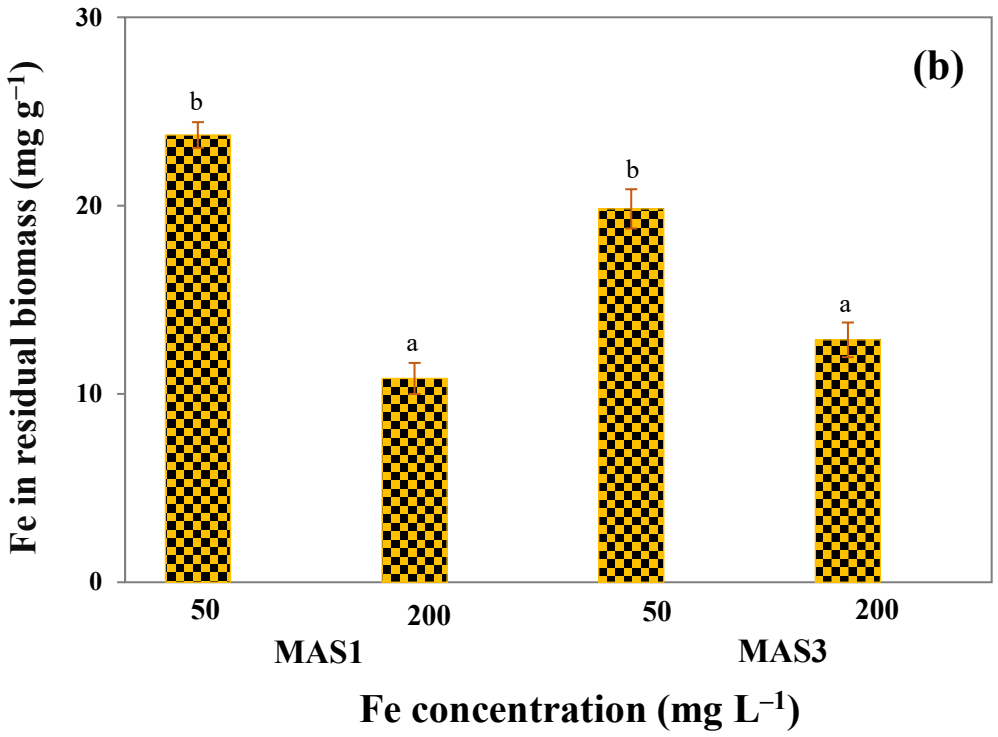

Fig. 5.4. (a) Biodiesel yield (% dry wt. of biomass) in strains MAS1 and MAS3 grown in BBM (control) and SAMD at concentrations of 1, 50 and 200 mg Fe L^{-1} for 96h; (b) Iron recovery (mg Fe g^{-1} dry wt.) from residual biomass obtained after extracting biodiesel. The mean values (n = 3), related to a microalgal strain, carrying the same letter on the bars are not significantly ($P \leq 0.05$) different from each other according to DMR test.

5.5. Conclusions

Identifying suitable microorganisms for metal recovery and biodiesel yield is of utmost importance in bioremediation of extreme habitats like AMD. Two acid-tolerant strains of microalgae, *Desmodesmus* sp. MAS1 and *Heterochlorella* sp. MAS3, grew well in SAMD samples that contained iron at 200 mg L^{-1}, a concentration close to that present in real AMD. While growing in SAMD with higher concentrations of iron (200 mg L^{-1}), both the strains could remove significant amounts of the metal and this recovery was directly related to the altered cellular granularity and increased secretion of EPS under the conditions of stress imposed by metals. Growth of both the strains at 200 mg Fe L^{-1} resulted in an enhanced extracellular accumulation of iron facilitated by increased production of EPS. *In situ* transesterification of metal-enriched biomass yielded 12-20% biodiesel at high concentrations of iron in SAMD. The entire amount of iron in the biomass was recovered from the residual biomass left after solvent extraction for biodiesel. This is the first study that demonstrated the

great potential of acid-tolerant microalgae in sustainable recovery of iron and biodiesel yield when grown in extreme conditions as exist in AMD, thus paving for the green circular economy.

5.6. References

(1) Giurco, D.; Littleboy, A.; Boyle, T.; Fyfe, J.; White, S., Circular economy: questions for responsible minerals, additive manufacturing and recycling of metals. *Resources* **2014**, 3 (2), 432−453.

(2) Venkateswarlu, K.; Nirola, R.; Kuppusamy, S.; Thavamani, P.; Naidu, R.; Megharaj, M., Abandoned metalliferous mines: ecological impacts and potential approaches for reclamation. *Rev. Env. Sci. Bio/Tech.* **2016**, *15* (2), 327−354.

(3) Johnson, D. B.; Hallberg, K. B., Acid mine drainage remediation options: a review. *Sci. Total Environ*. **2005**, *338* (1–2), 3−14.

(4) Simate, G. S.; Ndlovu, S., Acid mine drainage: challenges and opportunities. *J. Environ. Chem. Eng.* **2014**, *2* (3), 1785−1803.

(5) Hedrich, S.; Johnson, D. B., Remediation and selective recovery of metals from acidic mine waters using novel modular bioreactors. *Environ. Sci. Technol*. **2014**, *48* (20), 12206−12212.

(6) Kefeni, K. K.; Msagati, T. M.; Mamba, B. B., Synthesis and characterization of magnetic nanoparticles and study their removal capacity of metals from acid mine drainage. *Chem. Eng. J.* **2015**, *276*, 222−231.

(7) Valente, T.; Grande, J. A.; de la Torre, M. L.; Santisteban, M.; Cerón, J. C., Mineralogy and environmental relevance of AMD-precipitates from the Tharsis mines, Iberian Pyrite Belt (SW, Spain). *Appl. Geochem*. **2013**, *39*, 11−25.

(8) Kinnunen, P. H. M.; Kaksonen, A. H., Towards circular economy in mining: opportunities and bottlenecks for tailings valorization. *J .Clean. Prod.* **2019**, *228*, 153−160.

(9) Wei, X.; Roger C. Viadero , J.; Buzby, K. M., Recovery of iron and aluminum from acid mine drainage by selective precipitation. *Environ. Eng. Sci.* **2005**, *22* (6), 745−755.

(10) Hammarstrom, J. M.; Sibrell, P. L.; Belkin, H. E., Characterization of limestone reacted with acid-mine drainage in a pulsed limestone bed treatment system at the Friendship Hill National Historical Site, Pennsylvania, USA. *Appl. Geochem*. **2003**, *18* (11), 1705−1721.

(11) Chen, T.; Yan, B.; Lei, C.; Xiao, X., Pollution control and metal resource recovery for acid mine drainage. *Hydrometallurgy* **2014**, *147–148*, 112−119.

(12) Mohan, D.; Chander, S., Removal and recovery of metal ions from acid mine drainage using lignite – a low cost sorbent. *J. Hazard. Mat.* 2006, 137 (3), 1545−1553.

(13) Menezes, J. C. S. S.; Silva, R. A.; Arce, I. S.; Schneider, I. A. H., Production of a poly-ferric sulphate chemical coagulant by selective precipitation of iron from acidic coal mine drainage. *Mine Water Environ*. **2009**, *28* (4), 311.

(14) de Almeida Silva, R.; Menezes, J. C. S. d. S.; Lopes, F. A.; Kirchheim, A. P.; Schneider, I. A. H., Synthesis of a goethite pigment by selective precipitation of iron from acidic coal mine drainage. *Mine Water Environ*. **2017**, *36* (3), 386−392.

(15) Ryan, M. J.; Kney, A. D.; Carley, T. L., A study of selective precipitation techniques used to recover refined iron oxide pigments for the production of paint from a synthetic acid mine drainage solution. *Appl. Geochem*. **2017**, *79,* 27−35.

(16) Bai, H.; Kang, Y.; Quan, H.; Han, Y.; Sun, J.; Feng, Y., Treatment of acid mine drainage by sulfate reducing bacteria with iron in bench scale runs. *Bioresour. Technol.* **201**3, *128*, 818−822.

(17) Ayala-Parra, P.; Sierra-Alvarez, R.; Field, J. A., Treatment of acid rock drainage using a sulfate-reducing bioreactor with zero-valent iron. *J. Hazard. Mat.* **2016**, *308*, 97−105.

(18) Abinandan, S.; Subashchandrabose, S. R.; Venkateswarlu, K.; Megharaj, M., Microalgae–bacteria biofilms: a sustainable synergistic approach in remediation of acid mine drainage. *Appl. Microbiol. Biotechnol.* **2018**, *102* (3), 1131−1144.

(19) Abinandan, S.; Subashchandrabose, S. R.; Venkateswarlu, K.; Megharaj, M., Nutrient removal and biomass production: advances in microalgal biotechnology for wastewater treatment. *Crit. Rev. Biotechnol.* **2018**, *38* (8), 1244−1260.

(20) Perera, I.; Subashchandrabose, S. R.; Venkateswarlu, K.; Naidu, R.; Megharaj, M., Consortia of cyanobacteria/microalgae and bacteria in desert soils: an underexplored microbiota. *Appl. Microbiol. Biotechnol.* **2018**, *102* (17), 7351−7363.

(21) Abinandan, S.; Subashchandrabose, S. R.; Venkateswarlu, K.; Megharaj, M., Soil microalgae and cyanobacteria: the biotechnological potential in the maintenance of soil fertility and health. *Crit. Rev. Biotechnol.* **2019**, *39* (8), 981−998.

(22) Furuhashi, Y.; Honda, R.; Noguchi, M.; Hara-Yamamura, H.; Kobayashi, S.; Higashimine, K.; Hasegawa, H., Optimum conditions of pH, temperature and preculture for biosorption of europium by microalgae *Acutodesmus acuminatu*s. *Biochem. Eng. J.* **2019**, *143*, 58−64.

(23) Pradhan, D.; Sukla, L. B.; Mishra, B. B.; Devi, N., Biosorption for removal of hexavalent chromium using microalgae *Scenedesmus* sp. *J. Clean. Prod*. **2019**, *209,* 617−629.

(24) Anto, S.; Mukherjee, S.S.; Muthappa, R.; Mathimani, T.; Deviram, G.; Kumar, S.S.; Verma, T.N.; Pugazhendhi, A., Algae as green energy reserve: Technological outlook on biofuel production. *Chemosphere* **2020**, *242*, 125079.

(25) Deviram, G.; Mathimani, T.; Anto, S.; Ahamed, T.S.; Ananth, D.A.; Pugazhendhi, A., Applications of microalgal and cyanobacterial biomass on a way to safe, cleaner and a sustainable environment. *J. Clean. Prod.* **2019,** *253,* 119770.

(26) Abinandan, S.; Subashchandrabose, S. R.; Cole, N.; Dharmarajan, R.; Venkateswarlu, K.; Megharaj, M., Sustainable production of biomass and biodiesel by acclimation of non-acidophilic microalgae to acidic conditions. *Bioresour. Technol.* **2019**, *271*, 316−324.

(27) Abinandan, S.; Subashchandrabose, S. R.; Panneerselvan, L.; Venkateswarlu, K.; Megharaj, M., Potential of acid-tolerant microalgae, *Desmodesmus* sp. MAS1 and *Heterochlorella* sp. MAS3, in heavy metal removal and biodiesel production at acidic pH. *Bioresour. Technol.* **2019**, *278*, 9−16.

(28) Abinandan, S.; Subashchandrabose, S. R.; Venkateswarlu, K.; Perera, I. A.; Megharaj, M., Acid-tolerant microalgae can withstand higher concentrations of

invasive cadmium and produce sustainable biomass and biodiesel at pH 3.5. *Bioresour. Technol.* **2019**, *281*, 469−473.

(29) Samadani, M.; Perreault, F.; Oukarroum, A.; Dewez, D., Effect of cadmium accumulation on green algae *Chlamydomonas reinhardtii* and acid-tolerant *Chlamydomonas* CPCC 121. *Chemosphere* **2018**, *191*, 174−182.

(30) Rugnini, L.; Costa, G.; Congestri, R.; Bruno, L., Testing of two different strains of green microalgae for Cu and Ni removal from aqueous media. *Sci. Total Environ*. **2017**, *601−602*, 959−967.

(31) Langner, U. W. E.; Jakob, T.; Stehfest, K.; Wilhelm, C., An energy balance from absorbed photons to new biomass for *Chlamydomonas reinhardtii* and *Chlamydomonas acidophila* under neutral and extremely acidic growth conditions. *Plant Cell Environ*. **2009**, *32* (3), 250−258.

(32) Spijkerman, E.; Barua, D.; Gerloff-Elias, A.; Kern, J.; Gaedke, U.; Heckathorn, S. A., Stress responses and metal tolerance of *Chlamydomonas acidophila* in metal-enriched lake water and artificial medium. *Extremophiles* **2007**, *11* (4), 551−562.

(33) Spijkerman, E., Phosphorus limitation of algae living in iron-rich, acidic lakes. *Aquat. Microb. Ecol.* **2008**, *53* (2), 201−210.

(34) Rowe, O. F.; Sanchez-Espana, J.; Hallberg, K. B.; Johnson, D. B., Microbial communities and geochemical dynamics in an extremely acidic, metal-rich stream at an abandoned sulfide mine (Huelva, Spain) underpinned by two functional primary production systems. *Environ. Microbiol.* **2007**, *9* (7), 1761−71.

(35) Nam, S.-H.; An, Y.-J., Cell size and the blockage of electron transfer in photosynthesis: Proposed endpoints for algal assays and its application to soil alga *Chlorococcum infusionum*. *Chemosphere* **2015**, *128*, 85−95.

(36) Debelius, B.; Forja, J. M.; DelValls, Á.; Lubián, L. M., Toxicity and bioaccumulation of copper and lead in five marine microalgae. *Ecotoxicol. Environ. Saf.* **2009**, *72* (5), 1503−1513.

(37) Massocato, T. F.; Ramos, J. C.; Bascuñan, V. L. F.; Simioni, C.; Rörig, L. R.; Bonomi Barufi, J., Tolerance of *Ulothrix* sp. LAFIC 010 (Chlorophyta) against high

concentration of metals from acid mine drainage. *Ecotoxicol. Environ. Saf.* **2018**, *157*, 227−234.

(38) Zhang, W.; Tan, N. G. J.; Fu, B.; Li, S. F. Y., Metallomics and NMR-based metabolomics of *Chlorella* sp. reveal the synergistic role of copper and cadmium in multi-metal toxicity and oxidative stress. *Metallomics* **2015**, *7* (3), 426−438.

(39) Palma, H.; Killoran, E.; Sheehan, M.; Berner, F.; Heimann, K., Assessment of microalga biofilms for simultaneous remediation and biofuel generation in mine tailings water. *Bioresour. Technol.* **2017**, *234*, 327−335.

(40) Mendoza-Cózatl, D. G.; Moreno-Sánchez, R., Cd^{2+} transport and storage in the chloroplast of *Euglena gracilis*. *Biochim. Biophys. Acta - Bioenergetics* **2005**, *1706* (1–2), 88−97.

(41) Subramaniyam, V.; Subashchandrabose, S.R.; Thavamani, P.; Chen, Z.; Krishnamurti, G.S.R.; Naidu, R.; Megharaj, M., Toxicity and bioaccumulation of iron in soil microalgae. *J. Appl. Phycol.* **2016**, *28*, 2767−2776.

(42) García-Meza, J. V.; Barrangue, C.; Admiraal, W., Biofilm formation by algae as a mechanism for surviving on mine tailings. *Environ. Toxicol. Chem.* **2005**, *24* (3), 573−581.

(43) Laurens, L.M.; Quinn, M.; Van Wychen, S.; Templeton, D.W.; Wolfrum, E.J., Accurate and reliable quantification of total microalgal fuel potential as fatty acid methyl esters by in situ transesterification. *Anal. Bioanal. Chem.* **2012**, *403*, 167−178.

(44) Kona, R.; Hemalatha, M.; Venu Srivastav, K.; Venkata Mohan, S., Regulatory effect of Fe-EDTA on mixotrophic cultivation of *Chlorella* sp. towards biomass growth and metabolite production. *Bioresour. Technol.* **2017**, *244*, 1227−1234.

(45) Concas, A.; Steriti, A.; Pisu, M.; Cao, G., Comprehensive modeling and investigation of the effect of iron on the growth rate and lipid accumulation of *Chlorella vulgaris* cultured in batch photobioreactors. *Bioresour. Technol.* **2014**, *153*, 340−350.

(46) Ren, H.-Y.; Liu, B.-F.; Kong, F.; Zhao, L.; Xie, G.-J.; Ren, N.-Q., Enhanced lipid accumulation of green microalga *Scenedesmus* sp. by metal ions and EDTA addition. *Bioresour. Technol.* **2014**, *169*, 763−767.

(47) Raikova, S.; Smith-Baedorf, H.; Bransgrove, R.; Barlow, O.; Santomauro, F.; Wagner, J. L.; Allen, M. J.; Bryan, C. G.; Sapsford, D.; Chuck, C. J., Assessing hydrothermal liquefaction for the production of bio-oil and enhanced metal recovery from microalgae cultivated on acid mine drainage. *Fuel Process Technol*. **2016**, *142*, 219−227.

(48) Hess, D.; Quinn, J. C., Impact of inorganic contaminants on microalgal biofuel production through multiple conversion pathways. *Biomass Bioenergy* **2018**, *119,* 237−245

Chapter 6 Acid-adapted microalgae exhibit phenotypic changes for their survival in acid mine drainage samples

6.1. Abstract

Phenotypic plasticity or genetic adaptation in an organism provides phenotypic changes when exposed to the extreme environmental conditions. The resultant physiological and metabolic changes greatly enhance the organism's potential for its survival in such harsh environments. In the present novel approach, we tested the hypothesis whether acid-adapted microalgae, initially isolated from non-acidophilic environments, can survive and grow in acid-mine-drainage (AMD) samples. Two acid-adapted microalgal strains, *Desmodesmus* sp. MAS1 and *Heterochlorella* sp. MAS3, were tested individually or in combination (co-culture) for phenotypic changes during their growth in samples collected from AMD. The acid-adapted microalgae in AMD exhibited a two-fold increase in growth when compared with those grown at pH 3.5 in BBM up to 48h and then declined. Furthermore, oxidative stress triggered several alterations such as increased cell size, granularity, and enhanced lipid accumulation in AMD-grown microalgae. Especially, the apparent limitation of phosphate in AMD inhibited the uptake of copper and iron in the cultures. Interestingly, growth of the acid-adapted microalgae in AMD downregulated amino acid metabolic pathways as a survival mechanism. This study demonstrates for the first time that acid-adapted microalgae can survive under extreme environmental conditions as exist in AMD by effecting significant phenotypic changes.

6.2. Introduction

Activities of mining and mineral resource industries play a crucial role in the economy by offering jobs and revenues in terms of royalties, taxes and exports of minerals in several developing and developed countries (Reichl *et al.* 2016). On the other hand, mining activities significantly contribute to the release of contaminants and environmental degradation of mined areas and their surroundings (Venkateswarlu *et al.* 2016; Abinandan *et al.* 2018). Acid mine drainage (AMD) or acid rock drainage is generated due to oxidation of pyrite present in most of the metallic ore beds (Gray 1998; Gerson *et al.* 2019). The main characteristic feature of AMD is its lower pH (1.5-4.0) and the presence of sulfates and several heavy metals and metal(loids) (Nordstrom *et al.* 2000). Furthermore, AMDs are the habitats for predominant species of acidophilic microorganisms especially archaea and bacteria favoring for redox transformations of sulfur as well as removal of metals (Dopson and Johnson 2012). Hence, remedial approaches involving bioreactors were widely used as passive treatment processes

based on the naturally-occurring mechanisms such as oxidation of Fe, sulfur and nitrates (Chen *et al.* 2015; Jones and Johnson 2016). However, higher concentrations of Fe^{3+} (>60 mg L^{-1}) inhibited population of sulfate-reducing bacteria (SRB) in the bioreactors due to competition of iron-reducing bacteria with SRB or deposition of iron sulfide on cell surface of SRB resulting in growth inhbition (Deng and Lin 2013; Deng *et al.* 2013). Therefore, selective microbial strains must be used in the effective passive bioremediation approaches (Jones and Johnson 2016). Interestingly, various studies indicate the presence of naturally-occurring eukaryotic microorganisms such as microalgae exhibiting symbiotic interactions in the biofilms especially in AMDs (Aguilera *et al.* 2006; Thavamani *et al.* 2017; Abinandan *et al.* 2018). Acid tolerance and supply of nutrients to other microbes by acidophilic microalgae are the bases for their implication in remediation of AMDs (Johnson 2012; Abinandan *et al.* 2018). However, acidophilic microalgae in biofilms removed less amounts of metals (Orandi *et al.* 2012; Orandi and Lewis 2013), probably due to the nonavailablity of nutrients such as phosphates required for their survival and growth (Dean *et al.* 2019). Both innate tolerance capacity and metal resistance in acidophilic microalgae are derived through adaptation as compared to neutrophilic ancestors. For instance, Hirooka *et al*. (2017) reported higher expression of heat shock protein, H-ATPase, metabolic loss and acquisition of metal detoxifying genes in an acidophilic microalga, *Chlamydomonas eustigma*, when compared with a neutrophilic relative, *Chlamydomonas reinhardtii*. Thus, neutrophilic microalgae are also known to respond to any environmental perturbations like metal accumulation, grazing, nutrient stress, climate change through phenotypic alterations (Merila and Hendry 2014; Zhu *et al*. 2015; Subashchandrabose *et al*. 2015; Zhu *et al*. 2016).

For instance, phenotypic plasticity is the ability of an individual genotype to produce different phenotypes in response to environmental conditions or the immediate response to the environmental changes that allow living beings to cope with the stress induced (Lande *et al.* 2009; Bonamour *et al.* 2019). Also, plasticity is often regarded as a rapid response mechanism in an organism to survive during environmental fluctuations; but, in some instances it can also be maladaptive or neutral (Fox *et al.* 2019). However, plasticity in phenotypes helps in adaptation and population survival only if they are adaptive (Bonamour *et al.* 2019). Merila and Hendry (2014) also suggested that the induction of plasticity in response to the environmental conditions like climate change strongly contributes to phenotypes. Thus, phenotypic changes through plasticity is generally linked to the relative fitness of an organism and may alter or modify physiology, morphology and biochemistry for its survival in a new environment (Agrawal 2001). Ghalambor *et al*. (2007) distinguished plasticity into non-

adaptive and adaptive based on the phenotypic response to stressful environments to achieve optimum adaptive divergence among populations. We recently hypothesized that acid-tolerant microalgae obtained from non-acidophilic environments, upon adaptation to acidic conditions, could be a viable option for effective AMD bioremediation (Abinandan *et al.* 2018). Subsequently, two non-acidophilic microalgae, *Desmodesmus* sp. MAS1 and *Heterochlorella* sp. MAS3, were acclimated to acidic conditions to demonstrate their plasticity to grow at pH 3 with a minimal cell density of 5×10^5 cells mL^{-1} (Abinandan *et al.* 2019a). These strains were shown to a have a great potential in sustainable production of biomass and biodiesel besides accumulating high concentrations of heavy metals such as copper (Cu), iron (Fe), manganese (Mn), cadmium (Cd) and zinc (Zn) even at pH 3.5 (Abinandan *et al.* 2019b, c, d; Abinandan *et al*. 2020).

Both the microalgal strains MAS1 and MAS3, isolated from the local environmental matrices such as soil and water, survived at pH 3 than other non-acidophilic strains, but their growth rates were very low compared to those at pH 6.7 (Abinandan *et al.* 2019a). Therefore, these microalgal strains were grown repeatedly at pH 3.5 for about 100 generations to negate the pH effects, if any, in AMD samples (Abinandan *et al.* 2020). The present novel approach is thus to verify whether inoculation of acid-adapted microalgal strains into AMD samples, either alone or in combination, could bring about any phenotypic changes and survive in such harsh environment. In this study, phenotypic changes in the microalgal cultures grown in AMD samples were determined by assaying growth, in terms of optical density and chlorophyll content, reactive oxygen species (ROS), lipids, heavy metals and nutrients, all to serve as indicators of their sustained survival in AMD. Metabolomic approach has also been followed to identify the changes in metabolites of both the microalgal strains exposed to AMD samples. To our knowledge, this is the first novel study that demonstrated the significant phenotypic changes in acid-adapted microalgae for their survival in extreme acidic environments such as AMDs.

6.3. Materials & Methods

6.3.1. Acid adaptation of microalgal strains

Two acid-tolerant microalgal strains, *Desmodesmus* sp. MAS1 and *Heterochlorella* sp. MAS3, were initially maintained in modified Bold's basal medium (BBM) continuously under constant illumination (60 µmol m^{-2} s^{-1}) at 25 °C with 100 rpm shaking as described previously (Abinandan et al. 2019a). We observed earlier that an optimal density of 5×10^5 cells mL^{-1} was

required for these acid-tolerant strains to survive at pH 3 (Abinandan et al. 2019a), indicating that the low pH itself as the bottleneck for their survival. Hence, each microalgal strain, in triplicate samples, was subsequently adapted to acidic conditions by repeated subculturing in BBM at pH 3.5 using a population density of 5 $\times 10^5$ cells mL^{-1} for over 100 generations, and by ensuring axenic nature of the cultures each time (Abinandan et al. 2019a). The cells were counted at each transfer using Haemocytometer to determine specific growth rate, and the number of generations was calculated according to the following formulae (Padfield et al. 2016):

$$\mu = \frac{\ln\left(\frac{C}{C_0}\right)}{\Delta T} \quad (1)$$

where ΔT is the time interval (d), C is the final cell density (cells mL^{-1}) and C_0 is the initial cell density (cells mL^{-1}), and

$$g = \frac{\Delta T}{(\ln\ (2)/\mu)} \quad (2)$$

where ΔT is the time interval of the transfer (d), μ is the specific growth rate (d^{-1}), ln (2)/μ is the doubling time (d).

6.3.2. Exposure of microalgal strains to AMD samples

Samples of AMD (pH 3.5), collected from a local coal mining site, contained Fe, Mn, Cu, Zn and Cd at 200, 14.5, 0.05, 0.02 and 0.01 mg L^{-1}, respectively. Nitrates and phosphates in AMD samples were at the concentrations of 129.7 and 6.8 mg L^{-1}, respectively. These samples were straightaway used to grow the acid-adapted microalgal strains. Exponentially-growing microalgal cultures were harvested by centrifugation (7000 ×*g* for 7 min), washed twice with sterile distilled water, and the cells were suspended in AMD samples. Required aliquots of these suspensions were used to provide a final cell density (5 × 10^5 cells mL^{-1}) in a total volume of 100 mL AMD contained in 250 mL Erlenmeyer flasks. The cultures with the same cell density of 5 × 10^5 cells mL^{-1} were grown in BBM at pH 3.5 to serve as the controls. Co-culturing was done by combing 2.5 ×10^5 cells mL^{-1} of each culture together to provide the same final density of 5 ×10^5 cells mL^{-1}. This approach was to verify whether microalgal growth was effective with the use of individual or combined cultures for their sustainability in AMD samples. Five independent replicates were included for each treatment (6 treatments × 5 replicates = 30 flasks) to avoid pseudo-replication and incubated for four days under the same culture conditions described above.

6.3.3. *Assessing phenotypic changes in microalgae*

a) Growth determinations

Samples were withdrawn at desired intervals for determining growth, in terms of optical density ($OD_{750\ nm}$) of the culture medium or total chlorophyll, up to four days of incubation. Aliquots (100 µL) of microalgal cultures were added to a 96-well Nunc® microplate (Thermofisher scientific) to measure the absorbance in a microplate reader (Perkin Elmer, Inc). Total chlorophyll in culture suspensions was determined by measuring autofluorescence at an excitation wavelength (440 nm) and an emission wavelength (690 nm) using fluorescence plate reader (Perkin Elmer), and expressed as relative fluorescence units (RFUs) (Abinandan et al. 2019b).

b) Physiological changes in microalgae

Oxidative stress, in terms of ROS and lipids in microalgal cultures were measured after staining with 2',7'-dichlorodihydrofluorescein diacetate (DCFH-DA) and Nile red (NR), respectively. Cell morphology and granularity were determined by forward scatter (FSC) and side scatter (SSC) signals, respectively, following flow cytometry after 96 h of incubation. In brief, 1.0 mL aliquots of samples, in triplicates, were subjected to flow cytometry analysis with 5 µL of DCFH-DA (0.5 mg mL^{-1}), NL (15 mM) involving both positive and negative controls. Both FSC and SSC signals were collected through auto fluorescence laser (695/40 nm band pass filter) in a BD FACS Canto flow cytometer (Becton Dickinson Instruments, USA) as described earlier (Abinandan *et al.* 2019a). The morphological changes, if any, in the cultures grown in AMD samples were observed under a light microscope (100×), and fixed using Olympus IMMOIL solution.

c) Analysis for uptake of nutrients and metals

Microalgal cell suspensions were harvested after 48 and 96 h by centrifugation at 8000 ×*g* for 7 min, and the supernatant was used to determine nitrates and phosphates. The metal uptake by microalgal cells was determined in inductively coupled plasma mass spectrophotometer (ICP-MS, Agilent technologies, USA) (Abinandan *et al.* 2019b). In brief, supernatants were diluted appropriately to 10 mL using concentrated nitric acid to obtain a final concentration of 5% (v/v). Likewise, calibration standards and internal standard metal concentrations were maintained for quality control. In addition, automatic continuing calibration verification (CCV) and continuing calibration blank (CCB) were included in between the samples for routine ICP-MS quality check. Nitrates and total phosphates were

estimated following the standard methods (APHA 2005). Finally, the uptake of metals, nitrates and phosphates was calculated and expressed as percentages.

d) Nuclear magnetic resonance (NMR)-based metabolome analysis

Biochemicals from the microalgal cells grown in BBM or AMD samples were extracted as per the method of Zhang *et al*. (2015) with slight modifications. In brief, after 96 h of growth the cultures were centrifuged, quenched and freeze-dried immediately. The dried biomass obtained was suspended in pre-chilled chloroform:methanol:water (10:2:1) and sonicated at least three times at 40 Hz for 5 min under ice, and centrifuged at 8000 ×*g* for 7 min. The aqueous phase was then concentrated in a vacufuge concentrator (Eppendorf) at 60 °C for 2 h. The extracts containing metabolites were resuspended in phosphate buffer (0.1 M in 100% D_2O) containing 0.5 mM 4,4-dimethyl-4-silapentane-1-sulfonic acid (DSS), pH adjusted to 7.4 using sodium deuteroxide (Sigma Aldrich), and transferred to 5 mm NMR tubes. ^{1}H-NMR-based metabolomics analysis was carried out in 600 MHz NMR spectrometer (Bruker BioSpin Avance III, USA). The sample temperature was 298 K (25 °C) and was left for few min to attain a thermal equilibration. Further, the spectrometer frequency was locked to deuterium arising from solvent with sample shimming perfumed using automated method. NMR spectroscopy was set up with pulse sequence to attain 30 deg pulse angle, 10 kHz spectral width with processing parameters of spectra (128 scans). The raw spectra were imported to Chenomx software for the removal of water peaks, phase correction and baseline correction. The final peak list obtained was normalized against DSS followed by log transformation and auto-scaling using Metaboanalyst (v.4) for principal component analysis, heat map construction, and pathway analysis (Chong *et al.* 2018). The top 25 highly significant (P<0.05) metabolites in heat map were tentatively identified using Chenomx software, biological magnetic resonance data bank and other data available in the literature (Kim *et al.* 2010; Zhang *et al.* 2014; Zhang *et al.* 2018; Ma *et al.* 2018).

6.3.4. Statistical analysis

The statistical significance ($P \leq 0.05$) of the means ($n = 5$) was determined following one-way ANOVA followed by Duncan's multiple range (DMR) test using IBM SPSS statistical software (version 24, USA). Also, linear mixed effect models (LME) were analyzed through nlme package, and random effects were included for day and treatment (flask) to account for the temporal pseudo-replication for chlorophyll response in microalgae after their growth in AMD samples as followed earlier by Scheuerl and Stelzer (2013). Furthermore, to address

autocorrelation, multiple comparisons for gls models were performed using emmeans package according to Tukey post hoc analysis (Scheuerl et al. 2019).

6.4. Results

6.4.1. Phenotypic changes in acid-adapted microalgae grown in AMD samples

Acid-adapted *Desmodesmus* sp. MAS1 and Heterochlorella sp. MAS3 grew steadily in BBM maintained at pH 3.5 (Fig. 6.1a). Co-culture growth in AMD samples was less after four days of incubation as compared to individual cultures. On the other hand, growth of the acid-adapted microalgae, either alone or in co-culture, was significantly rapid until two days and then declined rapidly (Fig. 6.1b). Thus, the reduction in growth of the strain MAS1, MAS3 and co-culture in AMD samples, as compared to growth in BBM, was 41, 34 and 55% at the end of four days. However, the strain MAS1 grew well when compared with the strain MAS3 or the co-culture. The specific growth rate (μ) of the strains MAS1 and MAS3 in BBM was about 0.29 while the corresponding value for the co-culture was only 0.20. Thus, the range in doubling time when the strains were grown alone in BBM was 2.35-2.40 days whereas it was 3.4 days in case of co-culturing. On the other hand, the growth rates in AMD samples for the strains MAS1, MAS3 and co-culture were 0.71, 0.57 and 0.51, and the generation times were 0.97, 1.22 and 1.37 days, respectively.

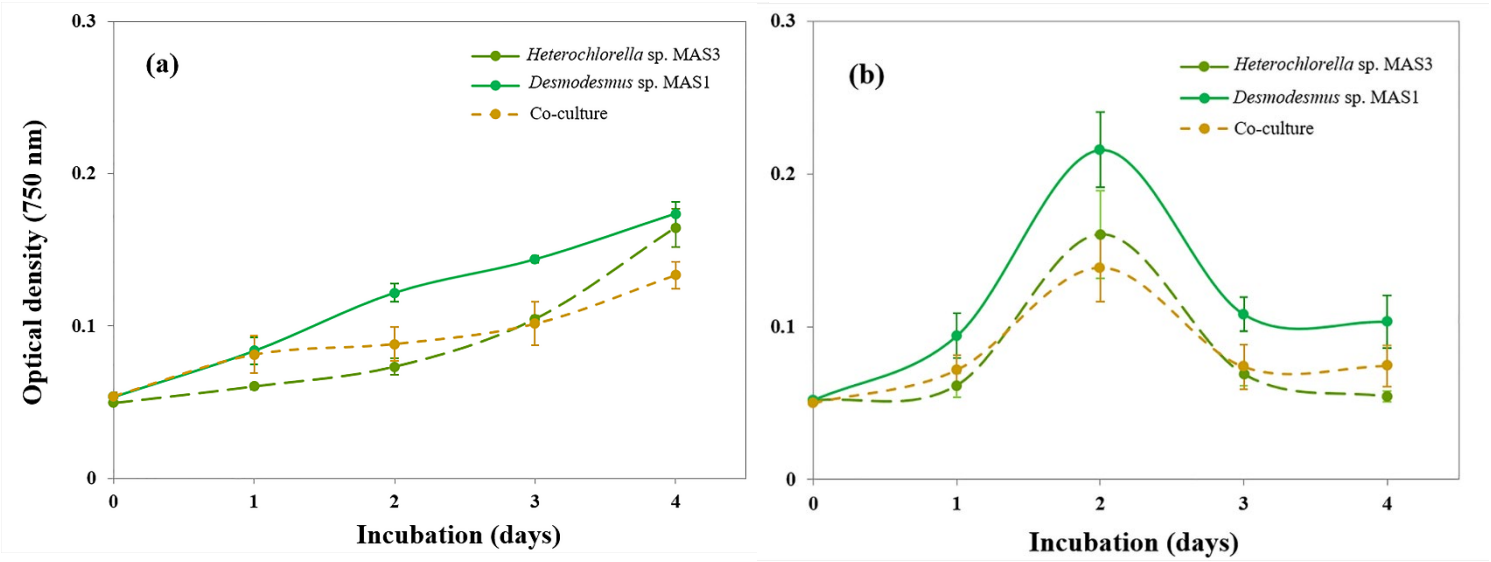

Fig. 6.1 Growth response (OD_{750} nm) of *Desmodesmus* sp. MAS1, *Heterochlorella* sp. MAS3, and co-culture in (a) Control (BBM-grown) and (b) AMD-grown samples after 4 days of incubation. Error bars represent standard deviations (n = 5).

The data obtained after four days for chlorophyll, measured in terms of RFUs, were similar with a significant two-fold decrease (P<0.05, 0.01) in all AMD-grown cultures when compared with those grown in BBM (Fig. 6.2, Table 6.1). Interestingly, chlorophyll content was almost of the same level in microalgal strains grown alone in AMD samples up to two days. Also, the incubation time (day) was an important factor (F = 10.275; P<0.05), as evident from the fixed effect model and ANOVA (Table 6.2), towards chlorophyll in all the treatments. However, strain MAS1, MAS3 or co-culture exhibited differential chlorophyll response upon exposure to AMD samples for varying incubation periods (F = 1.291; P =0.391).

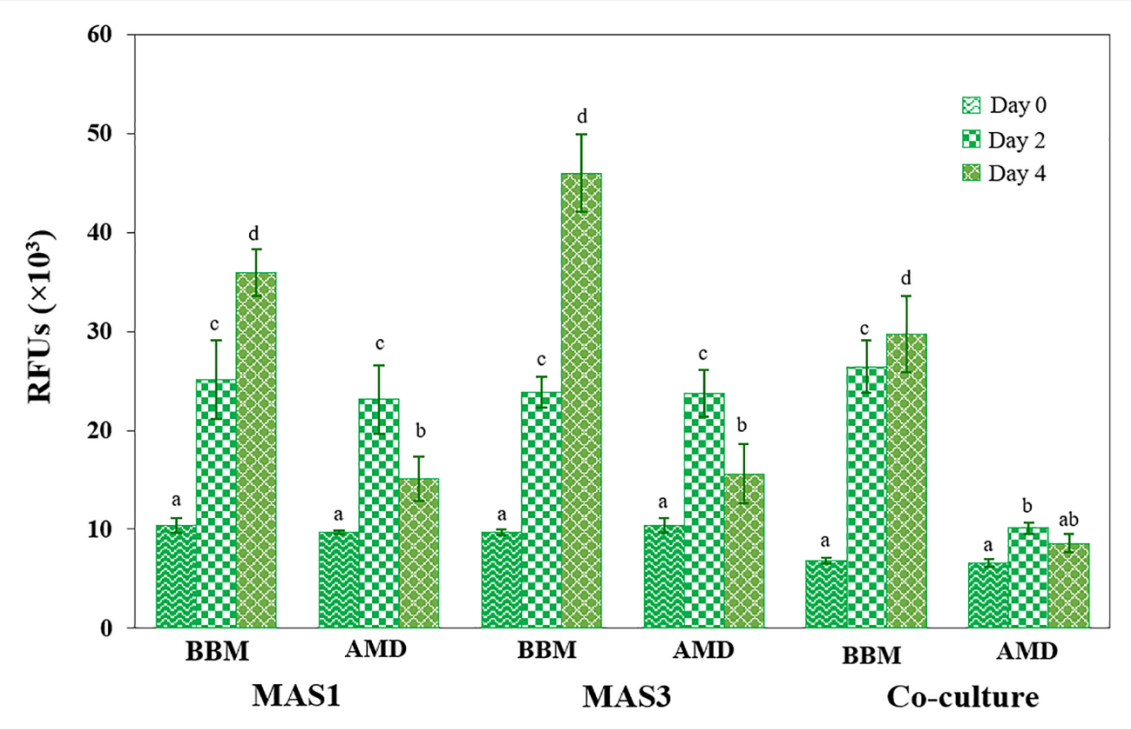

Fig. 6.2. Chlorophyll, in terms of relative fluorescence units, in *Desmodesmus* sp. MAS1, *Heterochlorella* sp. MAS3 and co-culture grown in Control (BBM-grown at pH 3.5) and AMD samples. Error bars represent standard deviation (n = 5). Means related to a microalgal inoculations carrying the same letter on the bars are not significantly different ($P \leq 0.05$) according to Duncan's multiple range (DMR) test

Table 6.1 One-way ANOVA and post hoc multiple comparisons for chlorophyll data of MAS1, MAS3 and Co-culture.

Strains	Parameters	Sum of Squares	df	Mean Square	F	Sig.
MAS1	Between Groups	2558276439.844	5	511655287.969	79.366	.000
	Within Groups	154723077.424	24	6446794.893		
	Total	2712999517.268	29			
MAS3	Between Groups	4536186723.500	5	907237344.700	166.219	.000
	Within Groups	130994284.994	24	5458095.208		
	Total	4667181008.493	29			
Co-culture	Between Groups	2752670579.430	5	550534115.886	141.458	.000
	Within Groups	93404857.830	24	3891869.076		
	Total	2846075437.260	29			

Table 6.2 Results of the linear mixed effects model of day flask (treatment) and Anova analysis based on random effects of day and flask on chlorophyll response

Fixed effects: Chlorophyll ~ Day * Flask	**numDF**	**Std. error**	**denDF**	**t-value**	**P-value**
Intercept	11323.913	3005.19	82	3.768136	0.0003
Day	7839.665	2811.25	82	2.7886	0.0066
Flask	-199.520	771.662	4	-0.2585	0.8087
Day: Flask	-1110.858	721.864	82	-1.538	0.1277

ANOVA	**numDF**	**denDF**	**F-value**	***P* -value**
Intercept	1	82	119.7543	<0.0001
Day	1	82	10.2745	0.0019
Flask	1	4	1.29142	0.3193
Day: Flask	1	82	2.3681	0.1277

Changes in microalgae, in terms of cell size, intracellular granularity, oxidative stress, and lipid accumulation, were examined through forward scatter (FSC) and side scatter (SSC) profile and flow cytometry (Fig. 6.3). A clear increase in fluorescence intensity was observed in strain MAS1, MAS3 or co-culture grown in AMD samples compared to those grown in BBM. The geometric mean intensity values of FSC in microalgal strains grown in AMD samples increased by 2.5-fold when compared with those of the control cultures, and the increase followed the order: MAS3 > co-culture > MAS1. Again, the geometric intensity values of SSC for AMD samples were higher compared to the FSC values and followed the same order: MAS3 > co-culture > MAS1. Light microscopic observations revealed substantial intracellular changes in strain MAS3 than in MAS1 when grown in AMD samples (Fig. 6.4), thus corroborating with the SSC profile.

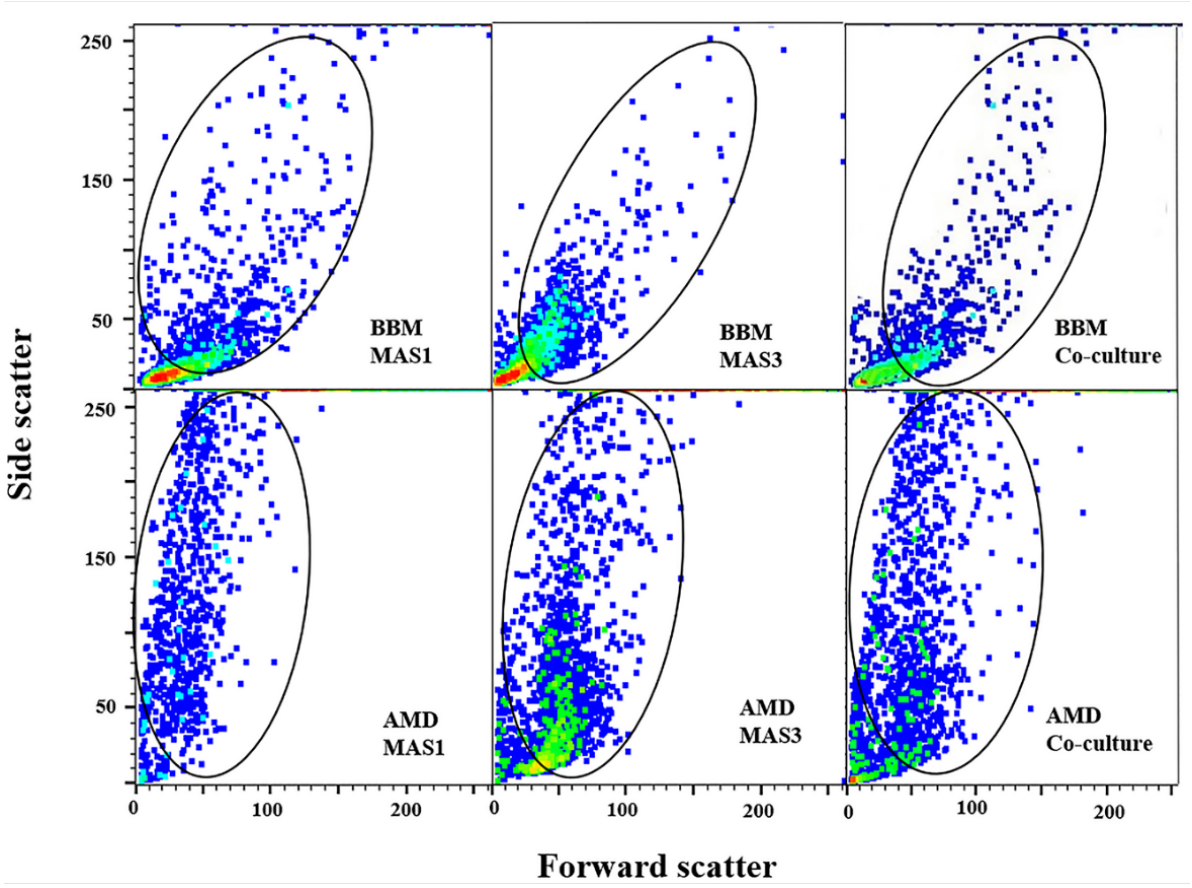

Fig. 6.3. Flow cytometry analysis for cell morphology and granularity by forward and side scatter profile after four days of incubation. Top panel: Control (BBM-grown at pH 3.5) samples – strain MAS1, strain MAS3 and Co-culture; Bottom panel: AMD-grown samples – strain MAS1, strain MAS3 and Co-culture.

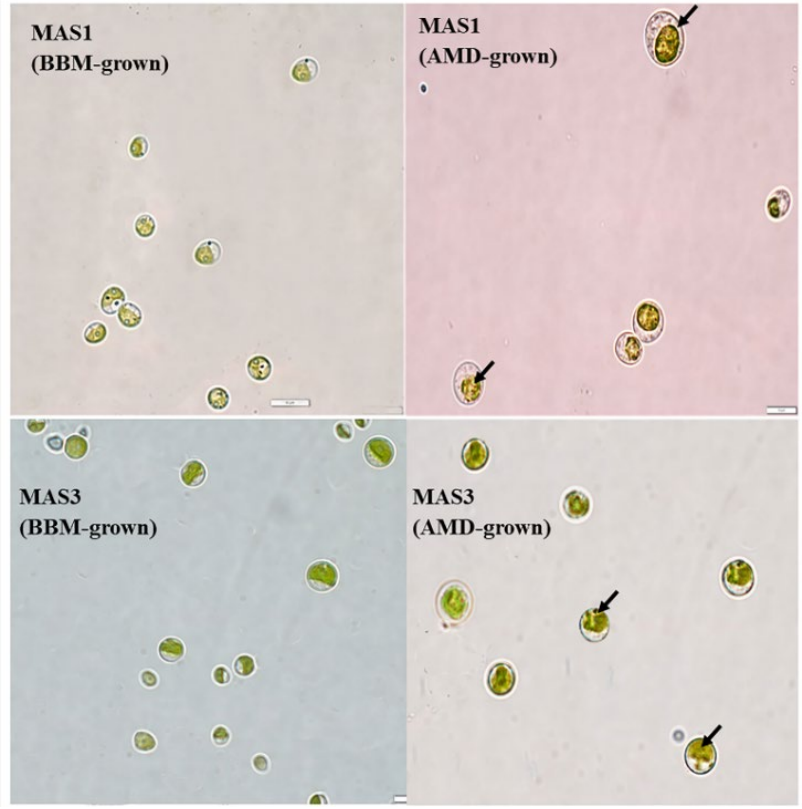

Fig. 6.4. Morphological changes observed under light microscope (100×) in MAS1 and MAS3 after four days of incubation.

The geometric mean intensity value for ROS increased by 15-20-fold in AMD-grown cultures (Fig. 6.5a) indicating the significant (P<0.05) increase in oxidative stress imposed by AMD samples. Also, the geometric mean intensity value of lipid accumulation was higher in AMD-exposed microalgal cultures (Fig. 6.5b). Thus, the increase in lipid when grown in AMD samples was 130 and 269% in strain MAS3 and MAS1, respectively. Although the oxidative stress was relatively higher in co-culture grown in AMD samples than that in BBM-grown samples, there was no parity in lipid accumulation. Overall, the oxidative stress and lipid accumulation in AMD-grown microalgae were significantly correlated and were in the increasing order: MAS3 > MAS1 > co-culture.

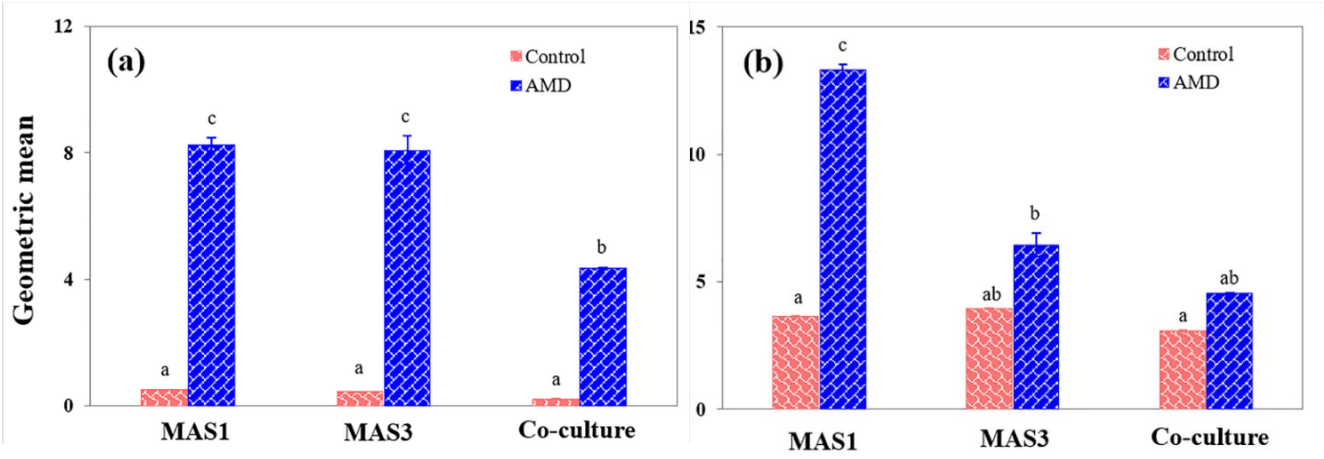

Fig. 6.5. Flow cytometry analysis for (a) oxidative stress (ROS), and (b) Lipids in control (BBM-grown) and AMD-grown samples after four days of incubation. Error bars represent standard deviation (n = 5). Means carrying the same letters on the bars are not significantly different ($P \leq 0.05$) according to Duncan's multiple range test.

Nitrate uptake in all the treatments increased significantly with time (P =0.001, Table 6.4) however, the increase was more in BBM-grown cultures when compared with AMD-grown microalgae (Fig. 6.6a). Again, no significant differences in nitrate uptake were observed among three cultures (MAS1, MAS3 and co-culture) when grown in BBM either for 2 or 4 days. This was true with the cultures grown in AMD samples for 2 days. But, the uptake of nitrate was significantly higher with AMD-grown MAS1 as compared to other two cultures. In contrast with the nitrate uptake, totally a distinct scenario was evident in the uptake of phosphate (Fig. 6.6b). Though there was no significant change in phosphate uptake in all the three cultures grown in BBM at the end of two days, the increased uptake of this nutrient observed after 4 days was differential among the cultures (P =0.002, Table 6.3). Thus, the increase in phosphate uptake by the cultures grown in BBM at the end of 4 days followed the order: MAS1 > co-culture > MAS3. Interestingly, the uptake of phosphate by AMD-grown cultures after 2 days was significantly more when compared with that observed in cultures grown in BBM. Thus, the increase in uptake of phosphate by AMD-grown MAS1, MAS33 and co-culture was 2-, 7- and 3-fold during the first 2 days of incubation. However, the nutrient uptake after 4 days was significantly less (10-15%) in cultures grown in the presence of AMD samples. Overall, uptake of phosphate was higher than that of nitrate during AMD exposure, while a reverse trend was evident in BBM-grown (pH 3.5) samples.

Table 6.3 A generalized estimated equation model to observe the incubation time effect on nitrate and phosphate uptake.

Parameter	Contrast	Estimate	Standard error (SE)	df	t. ratio	*P*-value
Nitrate uptake (%)	Day 2-4	-12.8	3.7	58	-3.458	0.001*
Phosphate uptake (%)	Day 2-4	-10.3	3.29	58	-3.122	0.0028*

*Significant (P<0.05)

The ICP-MS analysis indicated that the uptake of heavy metals contained in the AMD samples by the three cultures significantly increased with the incubation time (Table 6.4). The invasive heavy metal, Cd, and Zn were completely taken up by all the three cultures even after two days of incubation. The range in per cent uptake of Cu, Fe and Mn by the cultures after four days of their growth in AMD samples was 50-65, 29-37 and 19-23, respectively. Thus, metal uptake from AMD samples among the microalgae was in the order: co-culture > MAS1 > MAS3.

Table 6.4 Metal uptake capacity (%) in *Desmodesmus* sp. MAS1 and *Heterochlorella* sp. MAS3 from AMD samples

Incubation time (day)	Metal	MAS1	MAS3	Co-culture
2	Cu	31.1±4.7	9.5±5.2	31.2±12.5
	Cd	100	100	100
	Fe	25.2±1.8	21.9±0.8	26.7±1.5
	Mn	14.2±4.0	18.3±1.6	15.8±4.1
	Zn	100	100	100
4	Cu	60.2±8.8	41.9±5.1	65.3±3.7
	Cd	100	100	100
	Fe	29.1±1.2	34.6±1.3	36.7±2.1
	Mn	19.2±0.8	22.7±7.2	20.9±0.9
	Zn	100	100	100

*Data are the means (n=5) with standard deviation and statistically significant based on Duncan's multiple range test (P <0.01)

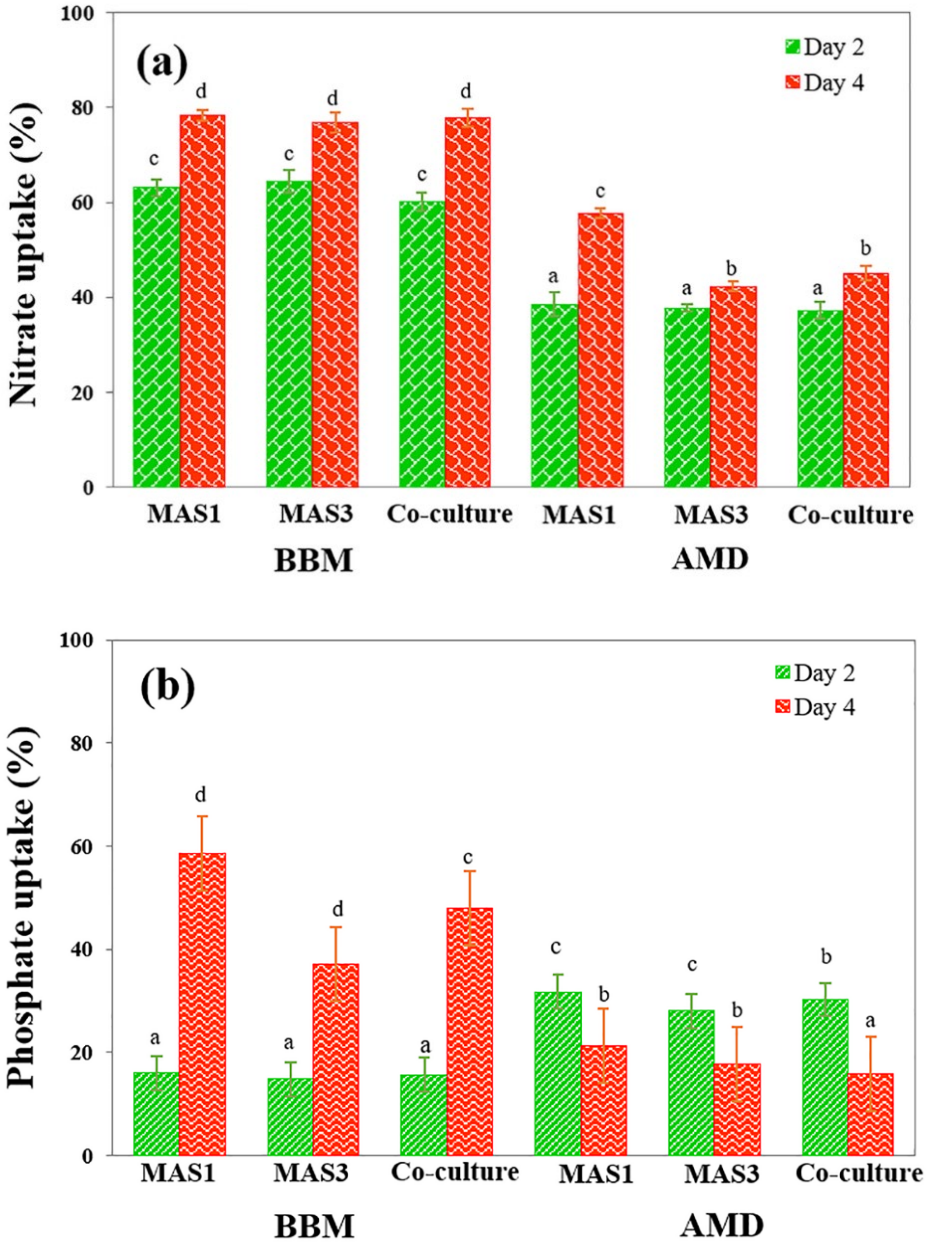

Fig. 6.6 Per cent nutrient uptake by *Desmodesmus* sp. MAS1, *Heterochlorella* sp. MAS3 and Co-culture in Control (BBM-grown at pH 3.5) and AMD-grown samples after four days of incubation. (a) Nitrate uptake, and (b) Phosphate uptake.

6.4.2. Metabolome changes in acid-adapted microalgae after growth in AMD samples.

^{1}H-NMR spectral analysis of polar extracts obtained from cultures grown in BBM or AMD samples showed significant common signals with new and increased peak areas at low frequency region (δ 0.7-4.7 ppm) and high frequency region (δ 5-9.6 ppm) indicating the presence of branched amino acids, organic acids and organic osmolytes, and aromatic amino acids and energy storage compounds, respectively. The combined first component and second component following the plot of orthogonal projections to latent structures discriminant analysis (OPLS-DA) revealed 42% of the total variance among the genotypes (Fig. 6a). The

cells of both the BBM- and AMD-grown cultures were clearly distinct and clustered into significant groups (P <0.05). Mainly, cells of the strain MAS1 grown in BBM or AMD samples exhibited slight overlap, indicating the upregulation of metabolites in the presence of heavy metals. However, the microalgal strains when grown alone or as a co-culture in AMD samples showed substantial differences in metabolic activities when compared to their growth in BBM (Fig. 6b). The data presented in Fig. 6c show the significant changes in biosynthesis of major metabolites, as evident at high frequency region (δ 7.5-8.5 ppm) and low frequency region (δ 1-2 ppm), in microalgal strains grown in BBM and AMD samples either alone or in combination as a co-culture. The metabolites that upregulated in strain MAS1 and co-culture and downregulated in strain MAS3 when grown in AMD samples were D-allose, D-aspartate, α-lipoamide, nicotinate, nicotinuric acid, tryptophan, inosine monophosphate, citrate and isonicotinamide. The metabolites that were downregulated in AMD-grown strain MAS1 and co-culture include proline, N-acetyl L-aspartic acid, alanine, valine, 3-phosphono-DL-alanine, L-alanine, L-adenylhomocysteine and 1-kestose (Fig. 6c). In strain MAS3, 1-methyl-L-histidine was upregulated while reduced L-glutathione and s-(5'-adenosyl)-L-methionine were downregulated in both MAS3 and co-culture grown in AMD samples.

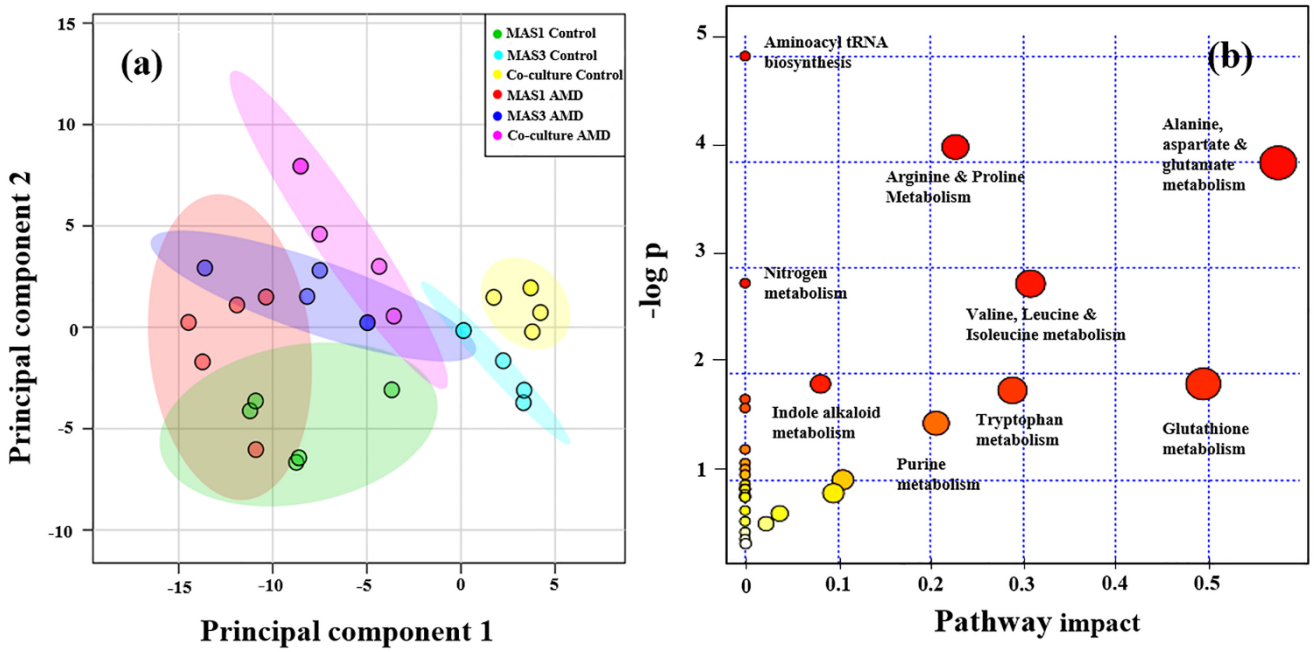

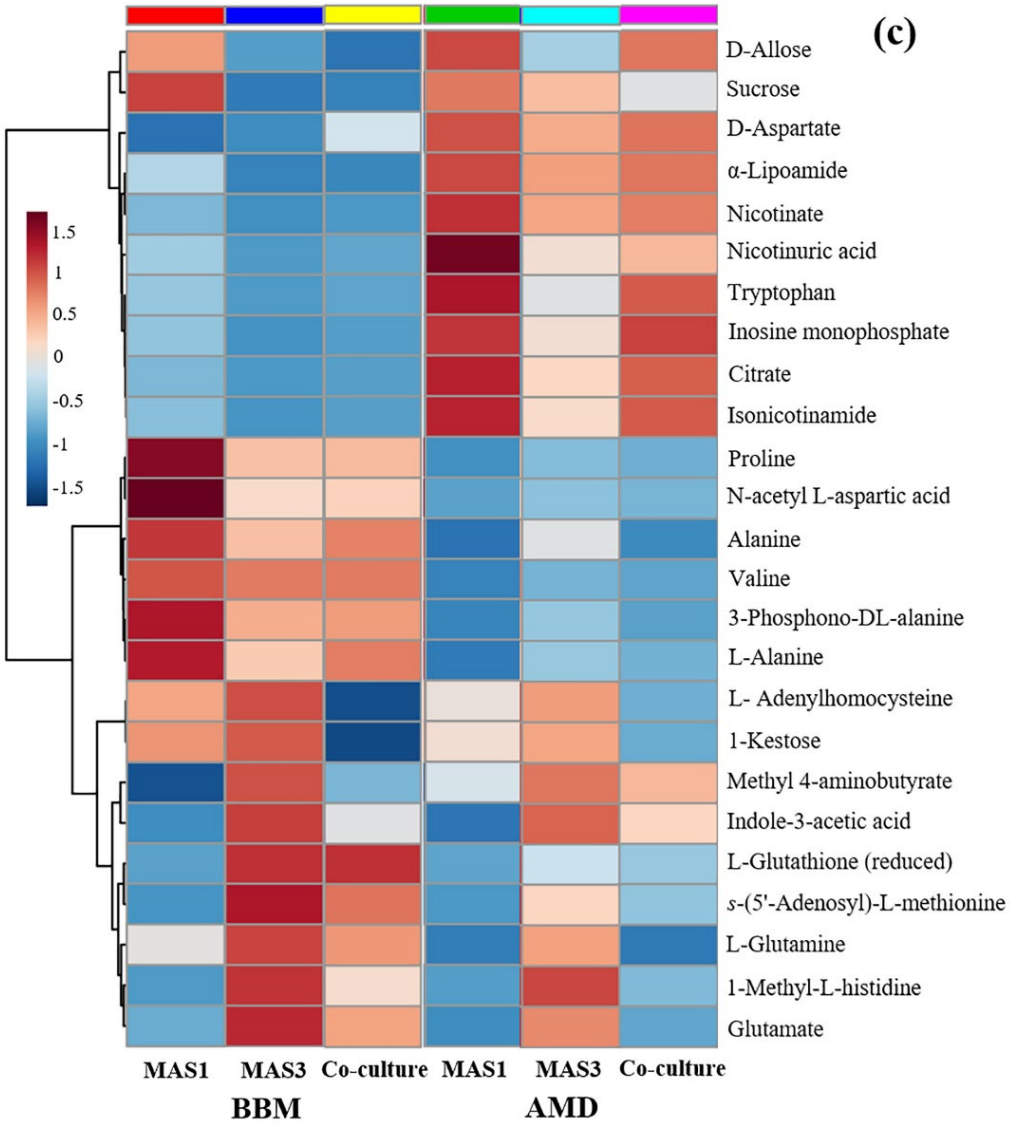

Fig 6.7. Metabolome analysis using ^{1}H-NMR spectroscopy in *Desmodesmus* sp. MAS1, *Heterochlorella* sp. MAS3 and Co-culture in Control (BBM-grown at pH 3.5) and AMD-grown samples after four days of incubation using Metaboanalyst software (v 4.0). (a) Orthogonal Partial Least Square -Discriminant Analysis (OPLS-DA), (b) Pathway impact, and (c) Heat map of major 25 statistically significant ($P \leq 0.05$) metabolites.

6.5. Discussion

Phenotypic changes are one of the primary mechanisms in response to the environmental fluctuations (Lande 2009). In the present study, the impact of metals and other contaminants present in AMD samples on acid-adapted microalgae was tested since the effect of pH was overcome through their adaptation to acidic pH for over 100 generations. In our study, the extent of phenotypic changes was assessed in acid-adapted microalgal strains individually and as a co-culture when grown in AMD samples obtained from local mines.

Although the microalgal strains were isolated from two different locations, their growth response was similar in presence of AMD samples. Microalgal growth, in terms of absorbance of the cultures, increased up to 48 h and decreased by the end of 96 h in presence of AMD samples. Moreover, the growth rates were two-fold higher in AMD-grown cultures as compared to those grown in BBM (pH 3.5), indicating the impact of plasticity in response to the extreme conditions. Interestingly, the increase in growth of the strains under the impact of AMD samples that contained higher heavy metal concentrations was >50%, and this result is significant when compared with that reported earlier by Abinandan et al. (2019a, b). Gerloff-Elias et al. (2005) also reported such a trend in growth of a *Chlamydomonas* sp. that is closely related to an acidophilic microalga, *Chlamydomonas acidophila*. Similarly, Dean et al. (2019) observed a higher level of chlorophyll in an acid-tolerant microalgal strain, *Chlamydomonas* sp. PM01, isolated from an AMD, with increased concentrations of Cu in the culture medium, but the concentrations of chlorophyll were higher only at lower levels of Cd and Zn. The decrease in chlorophyll content after two days of growth observed in the present study (Fig. 2) could be due to the toxicity of essential or non-essential metals, present in AMD samples at higher levels, towards the photosystems. García-García et al. (2018) also reported that the presence of essential metals, in excess, inhibited mitochondrial respiratory activity and deformation of thylakoid structure that eventually led to disruption of photosynthesis. In fact, essential metals such as Ni, Co and Cu induce autophagy by displacing cognate metals like Fe and Mn in binding sites of photosystem (Pérez-Martín et al. 2015). Also, Zn which is an essential metal when present alone at elevated concentrations disrupts photosynthesis by replacing Mg^{2+} ions in chlorophyll. Exposure to Ni in Ankistrodesmus falcatus causes morphological changes through cell wall deformation (Martínez-Ruiz and Martínez-Jerónimo 2015). According to flow cytometry data, cell morphology and granularity was significantly different in AMD than control. The increase in cell size of microalgal strains could be due to the adaptive phenotypic plasticity in response to stress as observed by Zhu et al. (2015) in a microalga, Scenedesmus obliques, during grazer-induced defence. Microscopic observation of cell surface in both the microalgal strains showed encrustation of iron during their growth in AMD samples which could be due to the presence of extracellular polysaccharides (Fig. 6.4). A similar observation was reported in Tribonema sp. growing in a river water contaminated with coal mine drainage (Mori et al. 2015). This mucilaginous layer on the surface of microalgae acts as a barrier in preventing the toxicity of heavy metals (Lombardi et al. 2002). The advantage of microalgae for AMD remediation is their higher metal sorption sites on the cell wall that results in complexation of metals and reduction in metal toxicity (Drewniak et al.

2016). Also, metal complexation on algal surface is yet another advantage for microbial iron cycling since iron–organic matter complexes can accelerate the metal removal process (Kügler et al. 2019).

With elevated concentrations of metals accumulated in acidophiles in AMD environments, an overexpression of ROS can occur (Sánchez-Thomas et al. 2016; García-García et al. 2018). The significant accumulation of lipids in the cultures due to the oxidative stress induced by AMD samples followed the order: MAS3 > MAS1 > co-culture. Among the ROS, the levels of hydroxyl radical significantly correlated with lipid accumulation as reported earlier by Menon et al. (2013). Growth of the cultures in AMD samples resulted in reduced phosphate uptake together with an increased metal uptake compared to those grown in BBM. Subsequently, nitrate was preferred under low metal concentration as observed in BBM-grown cultures. Furthermore, multiple comparisons based on Tukey's test confirmed that phosphate ($P = 0.0028$; Table 6.3) played a pivotal role than nitrate ($P = 0.001$; Table 6.3) during phenotypic response of microalgal strains grown in AMD. Under acidic conditions, phosphate ions strongly bind to hydrolyzed species of Fe(III) and Al(III) thereby limit free phosphorus and affect the primary production in microalgae of AMDs (DeNicola and Lellock, 2015). Since phosphates play a crucial role in chlorophyll production, and the scarcity of free phosphates in AMD could result in the decreased amount of chlorophylls in cultures grown in AMD samples. Spijkerman et al. (2018) reported that higher Fe^{3+} concentrations in acidic water reduced the uptake of phosphorus which resulted in a higher ratio of cellular iron to phosphorus in Chlamydomonas acidophila. Since phosphate concentration in AMD samples (8 mg L^{-1}) is higher than that present in BBM (~5 mg L^{-1}), phosphates are not a limiting factor. However, the enhanced phosphate uptake (Fig. 6.6b) observed in microalgal strains grown in AMD samples could be ascribed to the higher heavy metal uptake during the stress imposed (Table 6.4). Our findings corroborate with Webster et al. (2011) who observed that under P-limiting conditions and mixed metal environments, Cd which is a non-essential and invasive metal induced the accumulation of essential metals such as Cu, Fe and Zn but not Mn in *Chlamydomonas reinhardtii*. Especially, co-culture grown in AMD showed considerably higher metal uptake than the individual cultures, probably due to less chlorophyll content despite no significant changes in phosphate uptake. Due to antagonistic interactions that affect phosphate metabolism, especially cadmium toxicity was observed in microalgae (Chia et al. 2017). On the other hand, the negative effects of P-limitation and high metal uptake observed in the present study may be ascribed to over allocation of resources inside the cell or exceeding the cell quota that hamper chlorophyll synthesis (Zhu et al. 2016).

^{1}H-NMR-based metabolome analysis revealed that eight pathways related to amino acid synthesis as well as nitrogen and purine metabolic pathways were altered in AMD-grown microalgae. According to Fishers test, the perturbations observed in the microalgal strains grown in AMD samples were significant in biosynthesis of aminoacyl t-RNA involved in L-glutamine, L-valine, L-alanine, L-tryptophan, L-proline and L-glutamic acid; arginine and proline metabolism which involves L-proline, S-adenosylmethionine, L-glutamine and L-glutamic acid; and alanine, aspartate and glutamate synthesis that includes L-alanine, L-glutamine and L-glutamic acid (Fig. 6.6c). Under conditions of oxidative stress, proline that notably serves as a metal chelator, osmoprotectant and scavenger of free radicals with antioxidant properties was significantly downregulated in all the cultures grown in AMD samples. Through in situ proteo-metabolomic approach, Halter et al. (2012) showed that Euglena mutabilis secreted high concentrations of proline as a mechanism of adaptation to AMD environments. Zhang et al. (2014) observed significant decrease in alanine and glutamate in *Chlorella* sp. as a result of high Cu^{2+} exposure that led to impairment of photosynthesis. Thus, the present observation of reduction in the content of amino acids suggests the possible switch over to mechanisms that alleviate the metal toxicity induced by AMD samples in microalgae. Our results support that adaptation of microalgae to acid pH 3 would allow them to survive in extreme environments such as acid mine drainage. Despite the presence of oxidative stress on exposure to AMDs, microalgae acquired phenotypic plasticity through physiological alterations such as cell size and granularity with enhanced lipid accumulation. The P limited conditions induced the metal toxicity in microalgae disrupting the photosynthetic activity. Further, metabolic pathway especially, the downregulation of intracellular amino acid metabolism seems to be a major survival strategy to cope with metal toxicity in microalgae exposed to AMDs. Upregulation of sugar metabolites and metal uptake in microalgae makes them as valuable candidates for metal remediation in AMDs.

6.6. Conclusion

Our results indicate the fact that the acid-adapted microalgal strains exhibit phenotypic changes to survive in extreme environments such as AMD. The alterations included cell size and granularity with enhanced lipid accumulation as observed through flow cytometry. Interestingly, enhanced P uptake was observed initially under the influence of heavy metals present in AMD samples which subsequently created P-limiting environment and induced metal toxicity by disrupting the photosynthetic activity. Furthermore, the downregulation of intracellular amino acid metabolism seems to be a major survival strategy in microalgae to

cope with the metal toxicity exerted by AMD samples. Upregulation of sugar metabolites and metal uptake in the selected microalgae under oxidative stress conditions make them to serve as valuable candidates in bioremediation of AMDs. Although co-culturing of both the strains in presence of AMD was expected to perform better than individual cultures, growth and chlorophyll content in co-culture were relatively low. Interestingly, the AMD stress was less in co-culture, resulting in higher metal uptake than in individual strains possibly due to synergism, a viable mechanism necessary for remediation. These acid-adapted microalgal strains can also be exploited as filters in biofilms at pilot-scale investigations concerning bioremediation of heavy metal-contaminated wastewaters. In cases where AMDs have phosphate limitation, addition of a suitable low-cost phosphate source could be a viable option during heavy metal removal.

References

Abinandan S, Subashchandrabose SR, Venkateswarlu K, Megharaj M. Microalgae–bacteria biofilms: a sustainable synergistic approach in remediation of acid mine drainage. *Appl Microbiol Biotechnol* 2018;**102**:1131−1144.

Abinandan S, Subashchandrabose SR, Cole N *et al.* Sustainable production of biomass and biodiesel by acclimation of non-acidophilic microalgae to acidic conditions. *Bioresour Technol* 2019a;**271**:316−324.

Abinandan S, Subashchandrabose SR, Pannerselvan L *et al.* Potential of acid-tolerant microalgae, *Desmodesmus* sp. MAS1 and *Heterochlorella* sp. MAS3, in heavy metal removal and biodiesel production at acidic pH. *Bioresour Technol* 2019b;**278**:9−16.

Abinandan S, Subashchandrabose SR, Venkateswarlu K *et al.* Acid-tolerant microalgae can withstand higher concentrations of invasive cadmium and produce sustainable biomass and biodiesel at pH 3.5. *Bioresour Technol* 2019c**;281:**469−473.

Abinandan S, Subashchandrabose SR, Venkateswarlu K *et al.* Sustainable iron recovery and biodiesel yield by acid-adapted microalgae, *Desmodesmus* sp. MAS1 and *Heterochlorella* sp. MAS3, Grown in Synthetic Acid Mine Drainage. *ACS omega* 2020;**5:**6888−6894.

Agrawal AA. Phenotypic plasticity in the interactions and evolution of species. *Science* 2001;**294**:321−326.

Aguilera A, Manrubia SC, Gómez F *et al.* Eukaryotic community distribution and its relationship to water physicochemical parameters in an Extreme Acidic Environment, Río Tinto (Southwestern Spain). *Appl Environ Microbio*l 2006;**72**:5325−5330.

APHA. American Public Health Association. Standard Methods for the Examination of Water and Wastewater. 21st ed. American Public Health Association, Washington DC, 2005, 1220p.

Arora N, Dubey D, Sharma M, Patel A *et al.* NMR-Based metabolomic approach to elucidate the differential cellular responses during mitigation of arsenic (III, V) in a green microalga. *ACS Omega* 2018;**3**:11847−11856.

Ayala-Parra P, Sierra-Alvarez R, Field JA. Algae as an electron donor promoting sulfate reduction for the bioremediation of acid rock drainage. *J Hazard Mater* 2016;**317**:335−343.

Barranguet C, Plans M, Van Der Grinten E, Sinke JJ, Admiraal W. Development of photosynthetic biofilms affected by dissolved and sorbed copper in a eutrophic river. *Environ Toxicol Chem* 2002;**21**:1955−1965.

Bonamour S, Chevin LM, Charmantier A, Teplitsky C, Phenotypic plasticity in response to climate change: the importance of cue variation. *Phil Trans R Soc B* 2019;**374**:20180178.

Caldana C, Degenkolbe T, Cuadros-Inostroza A, *et al.* High-density kinetic analysis of the metabolomic and transcriptomic response of *Arabidopsis* to eight environmental conditions. *Plant J* 2011;**67**:869−84.

Casiot C, Egal M., Elbaz-Poulichet F, *et al.* Hydrological and geochemical control of metals and arsenic in a Mediterranean river contaminated by acid mine drainage (the Amous River, France); preliminary assessment of impacts on fish (*Leuciscus cephalus*). *Appl Geochem* 2009;**24**:787−799.

Chen LX, Li JT, Chen YT *et al.* Shifts in microbial community composition and function in the acidification of a lead/zinc mine tailings. *Environ Microbiol* 2013;**15**:2431−2444.

Chen LX, Hu M, Huang LN *et al.* Comparative metagenomic and metatranscriptomic analyses of microbial communities in acid mine drainage. *ISME J* 2015;**9**:1579−1592.

Chia, MA, Lombardi AT, Melão MDGG, Parrish CC. Phosphorus levels determine changes in growth and biochemical composition of *Chlorella vulgaris* during cadmium stress. *J Appl Phycol* 2017;**29**:1883−1891.

Chokshi K, Pancha I, Ghosh A, Mishra S. Nitrogen starvation-induced cellular crosstalk of ROS-scavenging antioxidants and phytohormone enhanced the biofuel potential of green microalga *Acutodesmus dimorphus*. *Biotechnol Biofuels* 2017;**10**:60.

Chong J, Soufan O, Li C *et al.* MetaboAnalyst 4.0: towards more transparent and integrative metabolomics analysis. *Nucl Acids Re*s 2018;**46**:486−494.

Dani VD, Simpson AJ, Simpson MJ. Analysis of earthworm sublethal toxic responses to atrazine exposure using ^{1}H nuclear magnetic resonance (NMR)-based metabolomics. *Environ Toxicol Chem* 2018;**37**:473−480.

Dao L, Beardall J, Heraud P. Characterisation of Pb-induced changes and prediction of Pb exposure in microalgae using infrared spectroscopy. *Aquat Toxicol* 2017;**188**;33−42.

Debelius B, Forja JM, DelValls Á, Lubián LM. Toxicity and bioaccumulation of copper and lead in five marine microalgae. *Ecotoxicol Environ Saf* 2009;**72**:1503−1513.

Deng D, Lin LS. Two-stage combined treatment of acid mine drainage and municipal wastewater. *Water Sci Technol* 2013;**67**:1000−1007.

Deng D, Weidhaas JL, Lin LS. Kinetics and microbial ecology of batch sulfidogenic bioreactors for co-treatment of municipal wastewater and acid mine drainage. *J Hazard Mater* 2016;**305**:200−208.

DeNicola DM, Lellock AJ. Nutrient limitation of algal periphyton in streams along an acid mine drainage gradient. *J Phycol* 2015;**51**:739−749.

Dopson M, Johnson DB. Biodiversity, metabolism and applications of acidophilic sulfur-metabolizing microorganisms. *Environ Microbiol* 2012;**14**:2620−2631.

Drerup SA, Vis ML. Extracellular enzyme activity suggests phosphorus limitation of biofilm productivity in acid mine drainage remediated streams. *Hydrobiologia* 2016;**784**:225−236.

Drewniak L, Krawczyk PS, Mielnicki S *et al.* Physiological and metagenomic analyses of microbial mats involved in self-purification of mine waters contaminated with heavy metals. *Front Microbiol* 2016;**7**:1252. doi: 10.3389/fmicb.2016.01252.

Driver T, Trivedi DK, McIntosh OA, *et al.* Two Glycerol-3-Phosphate Dehydrogenases from *Chlamydomonas* have distinct roles in lipid metabolism. *Plant Physiol* 2017;**174**: 2083−2097.

Expósito N, Kumar V, Sierra, J *et al.* Performance of *Raphidocelis subcapitata* exposed to heavy metal mixtures. *Sci Total Environ* 2017;**601-602**:865−873.

Fox RJ, Donelson JM, Schunter C, Ravasi T, Gaitán-Espitia JD. Beyond buying time: the role of plasticity in phenotypic adaptation to rapid environmental change. *Philos Trans R Soc Lond B Biol Sci* 2019;**374**(1768):20180174.

Gao C, De Schamphelaere KAC, Smolders E. Zinc toxicity to the alga *Pseudokirchneriella subcapitata* decreases under phosphate limiting growth conditions. *Aquat Toxicol* 2016;**173**:74−82.

García-García JD, Peña-Sanabria KA, Sánchez-Thomas R, Moreno-Sánchez R. Nickel accumulation by the green algae-like *Euglena gracilis*. *J Hazard Mater* 2018;**343**:10−18.

García-Meza JV, Barrangue C, Admiraal W. Biofilm formation by algae as a mechanism for surviving on mine tailings. *Environ Toxicol Chem* 2005;**24**:573−581.

Gerhardt A, Janssens de Bisthoven L, Soares AMVM. Macroinvertebrate response to acid mine drainage: community metrics and on-line behavioural toxicity bioassay. *Environ Pollut* 2004;**130**:263−274.

Gerloff-Elias A, Spijkerman E, PrÖSchold T. Effect of external pH on the growth, photosynthesis and photosynthetic electron transport of *Chlamydomonas acidophila* Negoro, isolated from an extremely acidic lake (pH 2.6). *Plant Cell Environ* 2005;**28**: 1218−1229.

Gerson AR, Rolley PJ, Davis C, *et al.* Unexpected non-acid drainage from sulfidic rock waste. *Sci Rep* 2019;**9**:4357. doi: 10.1038/s41598-019-40357−4.

Gray NF. Acid mine drainage composition and the implications for its impact on lotic systems. *Water Res* 1998;**32**:2122−2134.

Ghalambor CK, McKay JK, Carroll SP, Reznick DN. Adaptive versus non-adaptive phenotypic plasticity and the potential for contemporary adaptation in new environments. *Functional Ecol* 2007;**21**(3):394-407.

Ghalambor CK, Hoke KL, Ruell EW *et al.* Non-adaptive plasticity potentiates rapid adaptive evolution of gene expression in nature. *Nature* 2015;**525**:372. doi: 10.1038/nature15256.

Grettenberger CL, Pearce AR, Bibby KJ *et al.* Efficient low-pH iron removal by a microbial iron oxide mound ecosystem at scalp level run. *Appl Environ Microbiol* 2017;**83**, e00015−17. doi: 10.1128/AEM.00015-17.

Halter D, Goulhen-Chollet F, Gallien S *et al.* In situ proteo-metabolomics reveals metabolite secretion by the acid mine drainage bio-indicator, *Euglena mutabilis*. *ISME J* 2012;**6**: 1391−1402.

Hedrich S, Johnson DB. Remediation and selective recovery of metals from acidic mine waters using novel modular bioreactors. *Environ Sci Technol* 2014;**48**:12206−12212.

Herbert Jr RB, Winbjörk H, Hellman M, Hallin S. Nitrogen removal and spatial distribution of denitrifier and anammox communities in a bioreactor for mine drainage treatment. *Water Res* 2014;**66**:350−360.

Hyka P, Lickova S, Přibyl P *et al.* Flow cytometry for the development of biotechnological processes with microalgae. *Biotechnol Adv* 2013;**31**:2−16.

Ji Y, Sherrell RM. Differential effects of phosphorus limitation on cellular metals in *Chlorella* and *Microcystis*. *Limnol Oceanogr* 2008;**53**:1790−1804.

Jiang Z, Wang X, Rastrick SPS *et al.* Metabolic responses to elevated pCO_2 in the gills of the Pacific oyster (*Crassostrea gigas*) using a GC-TOF-MS-based metabolomics approach. *Comp Biochem Physiol Genomics Proteomics* 2019;**29**:330−338.

Johnson D. Acidophilic algae isolated from mine-impacted environments and their roles in sustaining heterotrophic acidophiles. *Front Microbiol* 2012;**3**:325.

Jones RM, Johnson DB. Iron Kinetics and evolution of microbial populations in low-ph, ferrous iron-oxidizing bioreactors. *Environ Sci Technol* 2016;**50**:8239−8245.

Khan N, Bano A, Babar MDA. Metabolic and physiological changes induced by plant growth regulators and plant growth promoting rhizobacteria and their impact on drought tolerance in *Cicer arietinum* L. *PloS One* 2019;**14:**e0213040. doi: 10.1371/journal.pone.0213040.

Kim HK, Choi YH, Verpoorte R. NMR-based metabolomic analysis of plants. *Nature Prot* 2010;**5**:536. doi: 10.1038/nprot.2009.237.

Kügler S, Cooper RE, Wegner CE *et al.* Iron-organic matter complexes accelerate microbial iron cycling in an iron-rich fen. *Sci Total Environ* 2019;**646**:972−988.

Lande R. Adaptation to an extraordinary environment by evolution of phenotypic plasticity and genetic assimilation. *J Evolut Biol* 2009;**22**:1435−1446.

Li Y, Yuan Z, Mu J *et al.* Proteomic analysis of lipid accumulation in *Chlorella protothecoides* cells by heterotrophic n deprivation coupling cultivation. *Energy Fuels* 2013;**27**: 4031−4040.

Lombardi AT, Vieira AAH, Sartori LA. Mucilaginous capsule adsorption and intracellular uptake of copper by *Kirchneriella aperta* (Chlorococcales). *J Phycol* 2002;**38**:332−337.

Lv H, Cui X, Tan Z, Jia S. Analysis of metabolic responses of *Dunaliella salina* to phosphorus deprivation. *J Appl Phycol* 2017;**29**:1251−1260.

Ma NL, Aziz A, The KY *et al.* Metabolites re-programming and physiological changes induced in *Scenedesmus regularis* under nitrate treatment. *Sci Rep* 2018;**8**:9746. doi: 10.1038/s41598-018-27894-0.

Machado MD, Lopes AR, Soares EV. Responses of the alga *Pseudokirchneriella subcapitata* to long-term exposure to metal stress. *J Hazard Mater* 2015;**296**:82−92.

Martínez-Ruiz EB, Martínez-Jerónimo F. Nickel has biochemical, physiological, and structural effects on the green microalga *Ankistrodesmus falcatus*: an integrative study. *Aquat Toxicol* 2015;**169:**27−36.

McCauley CA, O'Sullivan AD, Milke MW *et al.* Sulfate and metal removal in bioreactors treating acid mine drainage dominated with iron and aluminum. *Water Res* 2009;**43**: 961−970.

Menon KR, Balan R, Suraishkumar GK. Stress induced lipid production in *Chlorella vulgaris*: relationship with specific intracellular reactive species levels. *Biotechnol Bioeng* 2013;**110**:1627−1636.

Merilä J, Hendry AP. Climate change, adaptation, and phenotypic plasticity: the problem and the evidence. *Evolut Appl* 2014;**7**:1−14.

Mori JF, Neu TR, Lu S *et al.* Iron encrustations on filamentous algae colonized by *Gallionella*-related bacteria in a metal-polluted freshwater stream. *Biogeosciences* 2015;**12**: 5277−5289.

Netto E, Madeira RA, Silveira FZ *et al*. Evaluation of the toxic and genotoxic potential of acid mine drainage using physicochemical parameters and bioassays. *Environ Toxicol Pharmacol* 2013;**35**:511−516.

Nordstrom DK, Alpers CN, Ptacek CJ *et al*. Negative pH and extremely acidic mine waters from Iron Mountain, California. *Environ Sci Technol* 2000;**34**:254−258.

Orandi S, Lewis DM, Moheimani NR. Biofilm establishment and heavy metal removal capacity of an indigenous mining algal-microbial consortium in a photo-rotating biological contactor. *J Ind Microbiol Biotechnol* 2012;**39**:1321−1331.

Orandi S, Lewis DM. Biosorption of heavy metals in a photo-rotating biological contactor-a batch process study. *Appl Microbiol Biotechnol* 2013;**97**:5113−5123.

Pérez-Martín M, Blaby-Haas CE, Pérez-Pérez ME *et al.* Activation of autophagy by metals in *Chlamydomonas reinhardtii*. *Eukaryot Cell* 2015;**14**:964−973.

Reichl C, Schatz M, Zsak G. World mining data. Volume 31, Minerals production. Vienna International Organizing Committee for the World Mining Congresses. 2016.

Sánchez-Thomas R, Moreno-Sánchez R, García-García JD. Accumulation of zinc protects against cadmium stress in photosynthetic *Euglena gracilis*. *Environ Exp Bot* 2016;**131**:19−31.

Scheuerl T, Stelzer CP. Patterns and dynamics of rapid local adaptation and sex in varying habitat types in rotifers. *Eco Evol* 2013;**3**:4253−4264.

Scheuerl T. Cairns J, Becks L, Hiltunen T. Predator coevolution and prey trait variability determine species coexistence. *Proc R Soc B* 2019;**286**:20190245.

Sivaram AK, Subashchandrabose SR, Logeshwaran P *et al.* Metabolomics reveals defensive mechanisms adapted by maize on exposure to high molecular weight polycyclic aromatic hydrocarbons. *Chemosphere* 2019;**214**:771−780.

Spijkerman E, Behrend H, Fach B, Gaedke U. Decreased phosphorus incorporation explains the negative effect of high iron concentrations in the green microalga *Chlamydomonas acidophila*. *Sci Total Environ* 2018;**626**:1342−1349.

Steffen MM, Dearth SP, Dill BD *et al.* Nutrients drive transcriptional changes that maintain metabolic homeostasis but alter genome architecture in *Microcystis*. ISME J 2014;**8**: 2080−2092.

Subashchandrabose SR, Megharaj M, Venkateswarlu K, Naidu R. Interaction effects of polycyclic aromatic hydrocarbons and heavy metals on a soil microalga, *Chlorococcum* sp. MM11. *Environ Sci Pollut Res* 2015;**22**:8876−8889.

Thavamani P, Samkumar RA, Satheesh V *et al.* Microbes from mined sites: harnessing their potential for reclamation of derelict mine sites. *Environ Pollut* 2017;**230**:495−505.

Tripathi BN, Gaur JP. Relationship between copper- and zinc-induced oxidative stress and proline accumulation in *Scenedesmus* sp. *Planta* 2004;**219**:397−404.

Venkateswarlu K, Nirola R, Kuppusamy S *et al.* Abandoned metalliferous mines: ecological impacts and potential approaches for reclamation. *Rev Environ Sci Bio/Technol* 2016;**15**: 327−354.

Wase N, Tu B, Allen JW *et al.* Identification and metabolite profiling of chemical activators of lipid accumulation in green algae. *Plant Physiol* 2017;**174**:2146−2165.

Webster RE, Dean AP, Pittman JK. Cadmium exposure and phosphorus limitation increases metal content in the freshwater alga *Chlamydomonas reinhardtii. Environ Sci Technol* 2011;**45**:7489−7496.

Yilancioglu K, Cokol M, Pastirmaci I *et al.* Oxidative stress is a mediator for increased lipid accumulation in a newly isolated *Dunaliella salina* strain. *PloS One* 2014;**9**:e91957. doi: 10.1371/journal.pone.0091957.

Zhang W, Tan NGJ, Li SFY. NMR-based metabolomics and LC-MS/MS quantification reveal metal-specific tolerance and redox homeostasis in *Chlorella vulgaris*. *Mol BioSyst* 2014; **10**:149−160.

Zhang W, Tan NGJ, Fu B, Li SFY. Metallomics and NMR-based metabolomics of *Chlorella* sp. reveal the synergistic role of copper and cadmium in multi-metal toxicity and oxidative stress. *Metallomics* 2015;**7**:426−438.

Zhu X, Wang J, Lu Y, Chen Q, Yang Z. Grazer-induced morphological defense in *Scenedesmus obliquus* is affected by competition against *Microcystis aeruginosa*. *Sci Rep* 2015;**5**:12743.

Zhu X, Wang J, Chen Q, Chen G, Huang Y, Yang Z. Costs and trade-offs of grazer-induced defenses in *Scenedesmus* under deficient resource. *Sci Rep* 2016;**6**:22594.

Chapter 7 Potential of immobilized acid-adapted microalgae, *Desmodesmus* sp. MAS1 and *Heterochlorella* sp. MAS3, in iron removal from acid mine drainage samples

7.1. Abstract

Acid mine drainage (AMD) resulting from mining activities is a serious threat to the environment affecting terrestrial and aquatic life. In this study, acid-adapted microalgae, *Desmodesmus* sp. MAS1 and *Heterochlorella* sp. MAS3, were assessed for their ability in iron (Fe) removal from acid mine drainage samples using varying cell densities in non-immobilized and immobilized systems. Use of free-cells and immobilized cells exhibited 46-48% and 65-79% Fe removal, respectively, after 48 h of incubation. Flow cytometry analysis revealed significant changes in morphology (FSC) and granularity (SSC) in non-immobilized cells than in cells immobilized in alginate beads exposed to AMD samples. Second derivative spectra from Fourier transform infrared (FTIR) spectroscopy revealed vibration stretching for polysaccharides (1094 cm^{-1}) of free-cells, and protein (1500-1700 cm^{-1}), hydroxyl (3000-3500 cm^{-1}) of immobilized cells as a protective mechanism against Fe present in AMD samples. Group clustering of variables of free-cells and immobilized cells of microalgal strains was very evident as revealed by principal component analysis. Artificial neural network modelling validated the experimental data obtained in column studies with R^2 >0.95. Fixed bed column was conducted using two different bed depths of 1 cm and 2 cm with immobilized microalgal strains of MAS1 and MAS3 achieved a greater breakthrough time for 2 cm bed height, indicating the requirement for an extended contact time of the adsorbate to the adsorbent. The present study demonstrates the application of microalgal cells entrapped in alginate beads in batch and column in a greener and economical approach to treat AMD for sustainable mining.

7.2. Introduction

Historic mining activities significantly contributed to the generation of acidic sulfate-rich wastewater or acid mine drainage (AMD) that potentially affects the ecosystem. There are more than one million abandoned mines distributed worldwide representing the potential hotspots of AMDs, of which 5% are located in Australia (Venkateswarlu et al., 2016). In fact, AMDs exhibit enormous negative potential towards the environment due to the extent of metal concentrations and their bioavailability at acidic pH. Nearly, 19,000 km of streams and 72,000 ha of lakes and reservoirs were affected by AMD, eventually polluting the oceans throughout the world (Johnson and Hallberg, 2005). Nieto et al. (2007) reported that Odiel and Tinto rivers

in Spain were contaminated with higher amounts of heavy metals, especially iron (7900 t yr^{-1}) and aluminium (5800 t yr^{-1}), through discharge from the AMDs. Bioavailable metals such as iron, copper, zinc and cadmium in AMD are greatly toxic to the phytoplankton community and eventually affect the food chain (Bortnikova et al., 2001). In view of the global warming, the United Nations recognized AMDs as the second major environmental issue (Tuffnell, 2017).

Generally, hydrolysis of Fe to hydroxides results in more acidity and further aggravates the buffering nature of AMDs with pH 2.5-3.5 (Sánchez España et al., 2005; Søndergaard et al., 2008). Treatment of AMD uses predominantly lime, wetland, bioreactors or limestone drains involving either active or passive process (Kefeni et al., 2017). Nevertheless, conventional application of chemicals like lime has severe limitations such as insolubility and lower dissolution rates (Hammarstrom et al., 2003). On the other hand, the use of passive bioreactors involving sulfate-reducing bacteria (SRB) is recommended as the most viable and attractive method for AMD treatment (Lens et al., 1998; Kefeni et al., 2017). However, requirement for rich carbon sources to support the growth of SRB is a significant limitation in the passive bioreactor system (Elliott et al., 1998; Liamleam and Annachhatre, 2007). Alternatively, treatment of AMDs involves selective metal precipitation, adsorption, electrochemical methods and membranes (Kefeni et al., 2015; Rodríguez-Galán et al., 2019; RoyChowdhury et al., 2019). However, higher concentrations of heavy metals in AMDs often limit the performance of such systems (Genty et al., 2020).

In most cases, Fe is the predominant metal in AMDs and its concentrations are higher compared to other metals such as Cu, Zn, Mn and Cd, irrespective of the geological conditions (Rodríguez-Galán et al., 2019). Due to several limitations in Fe removal, only marginal treatments of AMDs have been realized so far. For example, without the addition of any external substrates, constructed wetlands failed to buffer the acidity of an AMD containing Fe at concentrations of >75 mg L^{-1} (Wu et al., 2019). Similarly, Fe at >60 mg L^{-1} inhibited the population of SRB in an AMD, possibly due to competition with iron-reducing bacteria (Deng et al., 2016). In fact, the formation of metal hydroxide in a passive bioreactor system led to a significant decrease in SRB activity thereby limiting the treatment efficiency (Ayora et al., 2013). It has also been realized that AMD harbors several other microbial communities, notably 'microalgae' that are overwhelmingly known for their potential applications ranging from remediation to value-added product generation (Abinandan et al., 2018a, b). Microalgae occurring in AMD developed innate capability of tolerance to acidic conditions through the process of evolution (Gerloff-Elias et al., 2005; Spijkerman et al., 2014). Abinandan et al.

(2018b) described a mechanism of survival in acidophilic microalgae present in the form of biofilms in AMD. In some instances, even microalgal biomass serves as a substrate for growth of other microbes such as hyphomycetous fungi and bacteria to thrive in AMD (López-Archilla et al., 2001). During AMD remediation, acidophilic microalgae remove only 20-50% of metals when they are associated with other microbes in biofilms (Orandi and Lewis, 2013). Microalgae immobilized in alginate beads have been used for various applications such as nutrient and metal removal or pollutant degradation (Megharaj et al., 1993; Sreenivasulu et al., 2012; Subashchandrabose et al., 2017; Ahamed et al., 2018, 2019; Kube et al., 2019). Immobilization technology was also applied for remediation of synthetic AMD effluent using SRB sludge in the alginate beads (Min et al., 2008; Zhang et al., 2016; Zhang and Wang, 2016).

Very recently, we identified two acid-tolerant microalgae, *Desmodesmus* sp. MAS1 and *Heterochlorella* sp. MAS3, that can grow well at pH 3, tolerate and remove heavy metals such as Cu, Cd, Fe, Mn and Zn (Abinandan et al., 2019a, b, c). These strains, after growth for 100 generations at pH 3.5 (in order to negate the effect of pH, if any) even at a very minimal cell density exhibited several phenotypic (morphological, physiological and metabolomic) changes when exposed to AMD samples (Abinandan et al., 2020a). Also, the acid-adapted strains showed a great potential in iron recovery from synthetic mine drainage followed by biodiesel yield (Abinandan et al., 2020b). In the present study we used acid-adapted strains of microalgae in immobilization technology to assess their ability in iron removal from AMD samples collected from a local coal mine, NSW, Australia. In view of the higher concentartions of Fe available in AMD samples (200 mg L^{-1}), varying cell densities of microalgal strains were used for their entrapment in alginate beads. Changes in microalgal cells upon exposure to AMD samples, in terms of morphology, intracellular granularity (through forward and side scatter profiles) and FTIR derivative spectra, were monitored. In a feasibility study, the impact of bed height packed with beads of immobilized microalgae on iron removal from AMD sample was evaluated. Also, bed depth service time (BDST) in the fixed bed column was determined following artificial neural network (ANN) modelling. To our knowledge, this is the study that used immobilized acid-adapted microalgae to assess their potential in iron removal form AMD samples in batch and fixed bed columns

7.3. Material and Methods

7.3.1. Microalgal strains and immobilization in alginate beads

Two acid-tolerant microalgae, *Desmodesmus* sp. MAS1 and *Heterochlorella* sp. MAS3, were grown at pH 3.5 and constant temperature (23 ± 1 °C) with continuous cool illumination (60 µmol m^{-2} s^{-1}) in 500 mL Bold's basal medium (BBM) contained in 1 L Erlenmeyer flasks as described earlier (Abinandan et al., 2019b, c). Cells harvested at 8000 ×*g* for 10 min from aliquots of 10 mL of exponentially-growing cultures were washed twice with sterile distilled water, and the biomass concentration was determined gravimetrically (Abinandan et al., 2019a). Subsequently, culture suspensions were prepared from washed cells to provide a final biomass concentration, on dry weight basis, of 2, 3.5 and 5 g L^{-1}. The cell densities that correspond to the above biomass levels were 1, 1.75 and 2.6 ×10^6 cells mL^{-1} for strain MAS1 and 1.87, 3.5 and 5 ×10^6 cells mL^{-1} for strain MAS3.

Microalgal cells were immobilized in sodium alginate following the protocol described previously (Subashchandrabose et al., 2017). In brief, microalgal cell pellet, obtained by centrifugation at 8000 ×*g* for 10 min, was washed with NaCl (0.85%), mixed with 2% (w/v) sodium alginate solution, and the resultant cell suspension was dropped into calcium chloride solution (2%) using sterile syringe to stabilize the alginate beads. The beads with uniform size (4 mm dia) were stored in BBM for 12 h. Calcium alginate beads with no microalgal cells served as control beads. The cell density in beads was determined by dissolving 10 randomly selected beads in sodium citrate solution (200 mM) and counting the cells using haemocytometer (Abinandan et al., 2019a). The stocking densities of microalgal cells in a bead, on an average, were 2, 3.5 and 5 ×10^4 for strain MAS1, and 3.7, 7 and 10 ×10^4 for strain MAS3.

7.3.2. Batch and fixed bed column studies

In a batch study, the cell suspensions or the beads (50 nos) immobilized with cells of strain MAS1 and MAS3 were transferred into triplicates of 30 mL AMD samples placed in 100 mL Erlenmeyer flasks. Aliquots (30 mL) of AMD sample that received no microalgal cells or control beads served as controls. After 24 and 48 h of incubation at constant temperature (23 ± 1 °C) and continuous illumination of 60 µmol m^{-2} s^{-1}, triplicate samples from each treatment were withdrawn for different analyses.

Fixed bed column experiment was also carried out using mini columns made up of borosilicate glass (14 cm long and 2.3 cm outer dia) with perforated plate inside the column to hold the packing material (Fig. 7.1). The alginate beads entrapped with cells of strains MAS1

(1.75×10^4 cells $bead^{-1}$) and MAS3 (3.5×10^4 cells $bead^{-1}$) were packed at different bed depths of 1 cm (70 beads) and 2 cm (140 beads) in the columns. Samples of AMD were fed to the packed column in a downward flow at a constant rate of 0.25 mL min^{-1} by using a peristaltic pump (BT 100S, Golander, USA) connected with silicone tubing. Samples were collected at regular intervals up to 24 h for determining iron concentration remained in the AMD samples that came through the columns. The column experiments were repeated twice, and the average data values were expressed as means.

Fig 7.1. Column experimental setup

In order to validate the experimental data, computational modelling based on artificial neural network (ANN) was performed since this approach for bio-sorption experiments is useful because it tends to capture and verify complex nonlinear relationship between independent variable and response from the experiments performed (Witek-Krowiak et al., 2014). Finally, the nftool in Matlab (R2017a) with multilayer feedforward back propagation algorithm and training with Levenberg Marquardt function with means square error was used for the validation (Venkatakrishnan et al., 2018).

7.3.3. Iron and FTIR analysis

The residual Fe in AMD samples after incubation with free cells or cells immobilized in beads was determined using ICP-OES (Perkin Elmer, Germany), and expressed as per cent removal (Abinandan et al., 2019c). Relative physiological changes such as cell morphology and intracellular granularity were determined by forward scatter (FSC) and side scatter (SSC) signals collected through autofluorescence laser (695/40 nm band pass filter) in a BD FACS Canto flow cytometer (Becton Dickinson Instruments) at the end of 48 h (Abinandan et al., 2019a). FTIR analysis was performed in strains of MAS and MAS3 exposed to AMD samples using attenuated reflectance technique (ATR) (Abinandan et al., 2019a). In brief, at the end of 48 h, the non-immobilized cells were harvested and the biomass was washed twice with distilled water, while the immobilized cells were suspended in sodium citrate solution, and used for FTIR spectroscopy in Cary 660 FT-IR (Agilent Technologies, USA) working in mid IR range (4000-400 cm^{-1}). Resolutions Pro software (Agilent Technologies, USA) was used to process and export the data in CSV format for second derivative analysis following SIMCA V.15 (Umetrics) software.

7.3.4. Statistical analysis

The standard deviations for the experimental data means (n = 3) were calculated using Graphpad Prism V.8 software, and the statistical significance ($P \leq 0.05$) of the means was determined following one-way ANOVA and Duncan's multiple range (DMR) test using IBM SPSS statistical software (version 24, USA). A general linear model developed following Minitab software V.19 was used to determine the effects of cell density and treatment of acid-adapted microalgal strains in response to AMD sample.

7.4. Results and discussion

7.4.1. Potential of immobilized acid-adapted microalgal strains in Fe removal

The amount of Fe in AMD sample was three-fold higher than the concentration previously used while determing heavy metal tolerance in strains MAS1 and MAS3 (Abinandan et al., 2019b). Therefore, increased cell densities of MAS1 and MAS3 were used in the present study to assess their potential in Fe removal from AMD sample. Under non-immobilized condition, the data presented in Fig. 7.2a related to the use of free cells indicate that increased cell densities are directly proptional to the Fe removal from AMD sample. The strains MAS1 and MAS3 with cell densities of 1-1.75 and 1.87-3.5 $\times 10^6$ cells mL^{-1} signficantly removed Fe with incubation time until 48 h. The use of higher cell density of 2.6-5 $\times 10^6$ cells

mL^{-1} of the microalgal strains resulted in a maximum removal 44-46% Fe from AMD sample after 24 h incubation. Such an enhanced removal at higher cell density could be attributed to the increased sorption process as reported with *Dunaliella salina* in the removal of Fe (Anghel et al., 2018). However, there was no significant difference in Fe removal by both the strains with higher cell density even after 48 h incubation. Thus, the incubation time did not seem to influence Fe removal even with higher cell densities of both the strains. Similarly, Ahmad et al., (2018) observed that the sorption of Fe (II) was constant with higher densities of free cells of a microalga, *Chlorella vulgaris*.

The use of alginate beads with no stocking of microlagal cells (control beads) resulted in 46-48% of Fe removal after 48 h incubation (Fig. 7.2b). Interestingly, Fe removal was significantly higher (>1.2-1.5-fold) with alginate beads immobilized with the cells of acid-adapted strains used in the present study. Thus, entrapment of strain MAS1 in alginate beads with a density of 2×10^4 cells $bead^{-1}$ resulted in 80% removal of Fe from AMD sample while the per cent removal was 68 when the beads stocked with strain MAS3 at 10×10^4 cells $bead^{-1}$ after 24 h. Again, entrapment of both the strains in alginate beads at higher cell density did not increase Fe removal even after 48 h of incubation. However, the baseline data generated on bioaccumulation, bio-sorption or both from non-immobilized and immobilized systems are generally used in remediating environments contaminated with metals (Ahmad et al., 2018; Li et al., 2018). Subramaniyam et al., (2016) observed a better iron removal with free cells (non-immobilized) when compared with immobilized *Chlorella* sp. MM3, and was attributed to a passive surface adsorption and active intracellular accumulation. On the other hand, Mehta and Gaur (2001) observed that cells of *C. vulgaris* entrapped in beads exhibited a better uptake of nickel and copper with incubation time than free cells. Increased Fe removal by immobilized acid-adapted cells observed in the present study could be due to a protective environment available for microalgae exposed to mixed metals present in AMD sample (Covarrubias et al., 2012). Another plausible reason for such a better Fe removal by immobilized microalgal cells is the competition of metals towards binding sites of cells exposed to an environment having mixed contaminants (Ahmad et al., 2018).

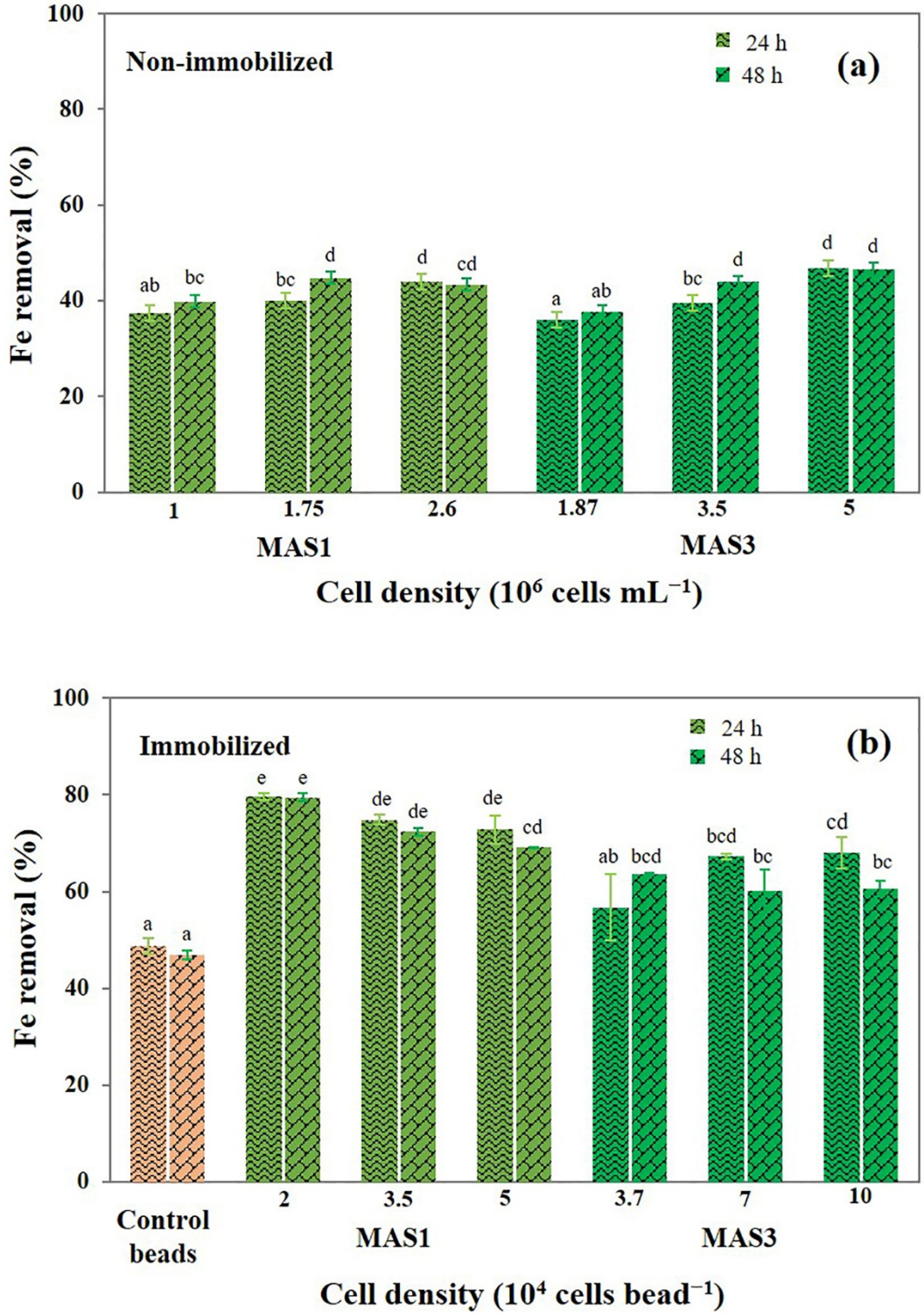

Fig. 7.2. Iron removal by (a) Non-immobilized and (b) Immobilized cells of acid-adapted microalgae, *Desmodesmus* sp. MAS1 and *Heterochlorella* sp. MAS3, at varying cell densities after 24 and 48 h of incubation in AMD samples

Biological systems are suitable alternatives to physico-chemical processes in remediation of contaminated sites because they are economical in terms of cost effectiveness. In particular, the application of microalgal immobilization technology in bioremediation has several advantages over the use of free-living cells. In fact, suspending cells in the effluents is inefficient in nutrient removal and may also lead to eutrophication. Compared to a wide array of immobilization techniques, cell entrapment in alginate matrix is more convenient and advantageous in bioremediation studies because alginate is nontoxic, highly permeable and transparent for light penetration (Moreno-Garrido, 2008). Moreover, immobilization offers repeated use of the microalgal cells for successive treatments (Suzuki et al., 1998). In the present algal immobilization technology, we did not observe any disruption and dissolution of the alginate beads probably because of the low concentration of phosphates in AMD samples used.

7.4.2. Changes in immobilized acid-adapted microalgae upon their exposure to AMD samples

FSC of microalgal cells analyzed following flow cytometry reveal changes in cell size, while SSC signal helps in understanding cell granularity, particularly in terms of intracellular changes occurred due to external perturbations such as metals (Hyka et al., 2013). Non-immobilized microalgal cells exhibited variations in FSC and SSC as a result of changes in size and granularity of cells exposed to AMD samples (Fig. 7.3). However, no significant differences in changes were observed with varying stocking cell densitites of both the microalgal strains. These observations are consistent with our earlier results on phenotypic changes (morphological, physiological and metabolomic) in acid-adapted microalgal strains exposed to AMD samples (Abinandan et al., 2020). This scenario directed us to compare one cell density of non-immobilized system with varying cell densities of immobilized system (Fig. 7.4). As with the non-immobilized cells, there were no significant differences in FSC and SSC of cells immobilized in alginate beads. However, FSC and SSC intensites in free cells were greater than those in immobilized cells implying that alginate acted as a barrier. Further, we analyzed the AMD effect on cell densities and strains using general linear model on FSC and SSC. ANOVA of FSC revealed that strains MAS1 and MAS3 exhibitied significant differences while SSC exhibited a *P* value of 0.063 indicating that the intracellular granularity is not greatly influenced by AMD (Table 7.1). Zhou et al., (2012) observed increased starch granules inside a microalga, *Chlorella pyrenoidosa*, due to the exposure to excess concentrations of zinc and copper. The increased cell size observed could be attributed to the large accumulation of

photosynthetic products due to exposure to metals (Debelius et al., 2009). Also, the higher intensities of FSC and SSC in non-immobilized cells may be ascribed to the bioaccumulation of metals in cytoplasm and other intracellular structures (Abinandan et al., 2019b). In all, our present results clearly indicate that cells of both the acid-adapted microalgal strains entrapped in alginate beads exhibited less changes compared to the non-immobilized cells.

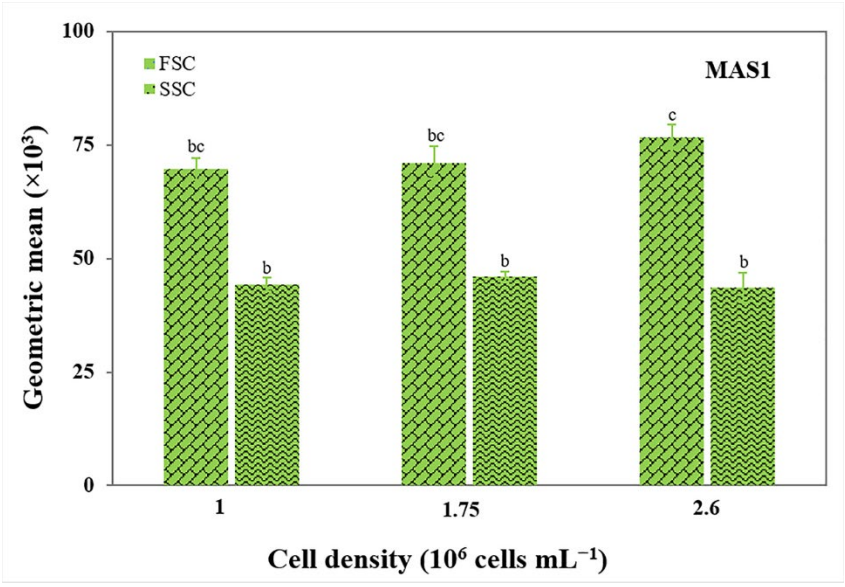

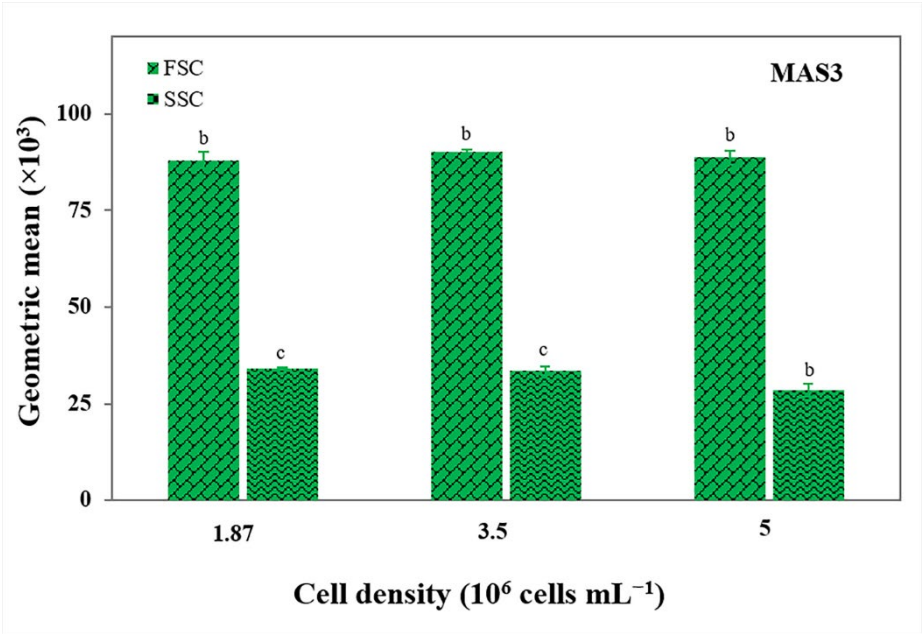

Fig 7.3. FSC and SSC changes in non-immobilized acid-adapted microalgae at various cell densities

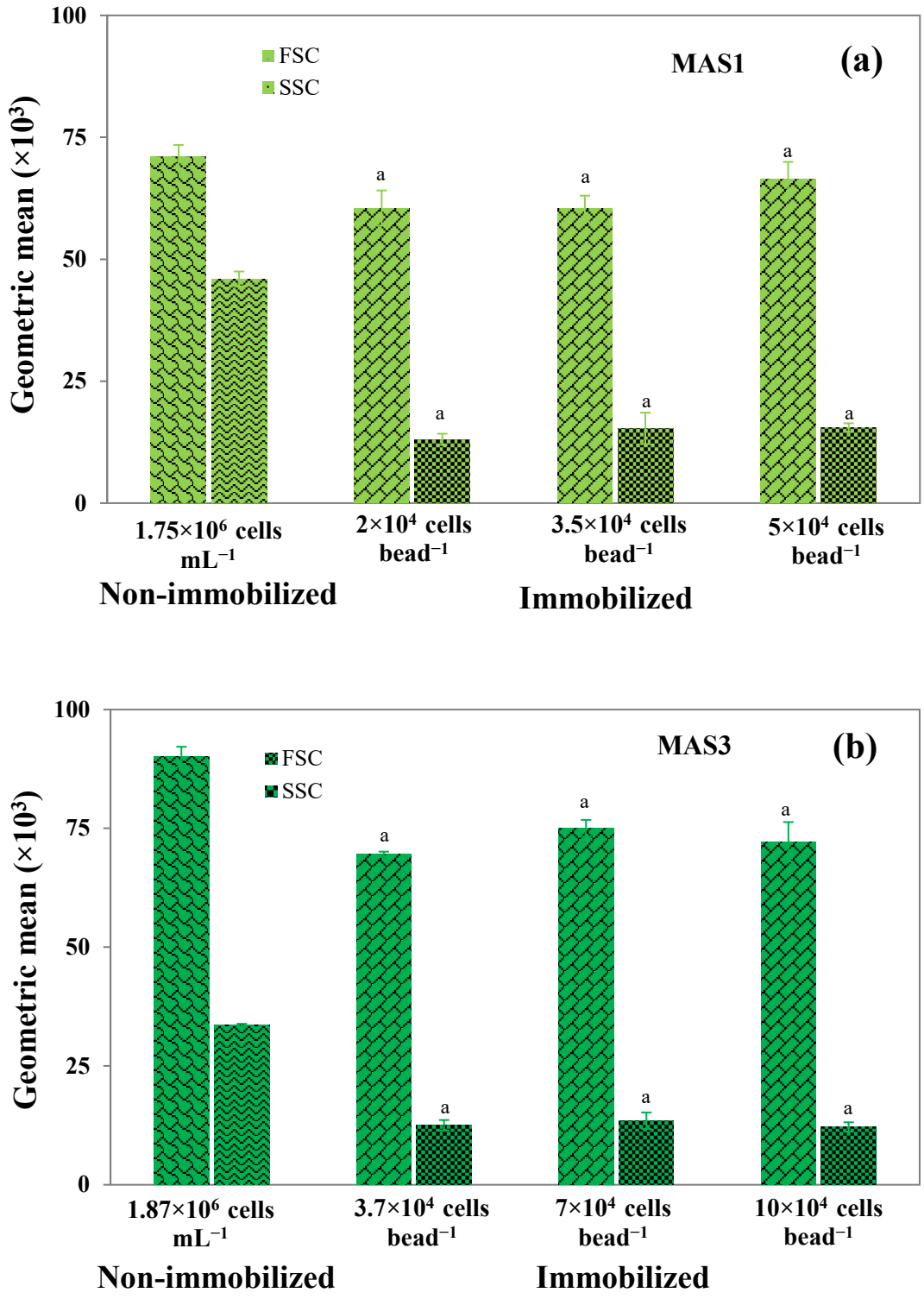

Fig. 7.4. Cell morphology (FSC) and granularity (SSC) in non-immobilized and immobilized acid-adapted (a) *Desmodesmus* sp. MAS1 and (b) *Heterochlorella* sp. MAS3 at varying cell densities after 48 h of incubation in AMD samples

Table 7.1. ANOVA following generalized linear model to determine the effects of cell density and strain of immobilized acid-adapted microalgae in AMD

Parameter	Source	DF	Adj SS	Adj MS	F-value	P-value
FSC	Cell density	2	37803049	18901524	1.55	0.286
	Strains	1	288826032	288826032	23.74	0.003*
	Cell density*Strains	2	41027258	20513629	1.69	0.262
	Error	6	73004262	12167377		
	Total	11	440660601			
SSC	Cell density	2	5278789	2639394	1.25	0.352
	Strains	1	10913761	10913761	5.17	0.063
	Cell density*Strains	2	3871101	1935550	0.92	0.449
	Error	6	12664753	2110792		
	Total	11	32728404			

*P <0.05

For better insights into the changes in microalgal cells entrapped in beads, FTIR analysis was carried out to obtain second derivative spectra (Fig. 7.5). This is in view of the fact that the secondary derivative spectral analysis replaces the maxima band from the raw spectrum to minimal to highlight or distinguish the responses (Dao et al., 2017). Free-cells of both the strains MAS1 and MAS3 showed a significant peak at 1094 cm^{-1} that was totally absent in immobilized cells. This observation could be due to the vibrational stretching frequencies in the region of carbohydrates, mostly belonging to exopolysaccharides, as a defence mechanism to metal stress imposed by AMD samples in free-cells. Mori et al. (2015) suggested that the accumulation of iron from AMD as a crust was due to the presence of polysaccharides in *Tribonema* sp. Moreover, immobilized cells of strains MAS1 and MAS3 exhibited changes in the region of 3000-3500 cm^{-1} which could be attributed to the vibrations of OH and NH groups present on the cell surface. Anghel et al. (2018) also observed strong absorption peaks at 3200, 3500, 1648, 1545 and 925-1150 cm^{-1} that correspond to OH, NH vibration stretching, primary and secondary amide in Fe-exposed cells of *Dunaliella salina*. In addition, the presence of strong absorption peaks at 1500-1700 cm^{-1} in immobilized cells of strains MAS1 and MAS3 may be ascribed to the protein peaks observed in response to exposure to AMD samples (Fig. 7.5). Ahmad et al. (2019) also observed changes in the carboxylic stretching in immobilized cells of *Chlorella vulgaris* exposed to Fe.

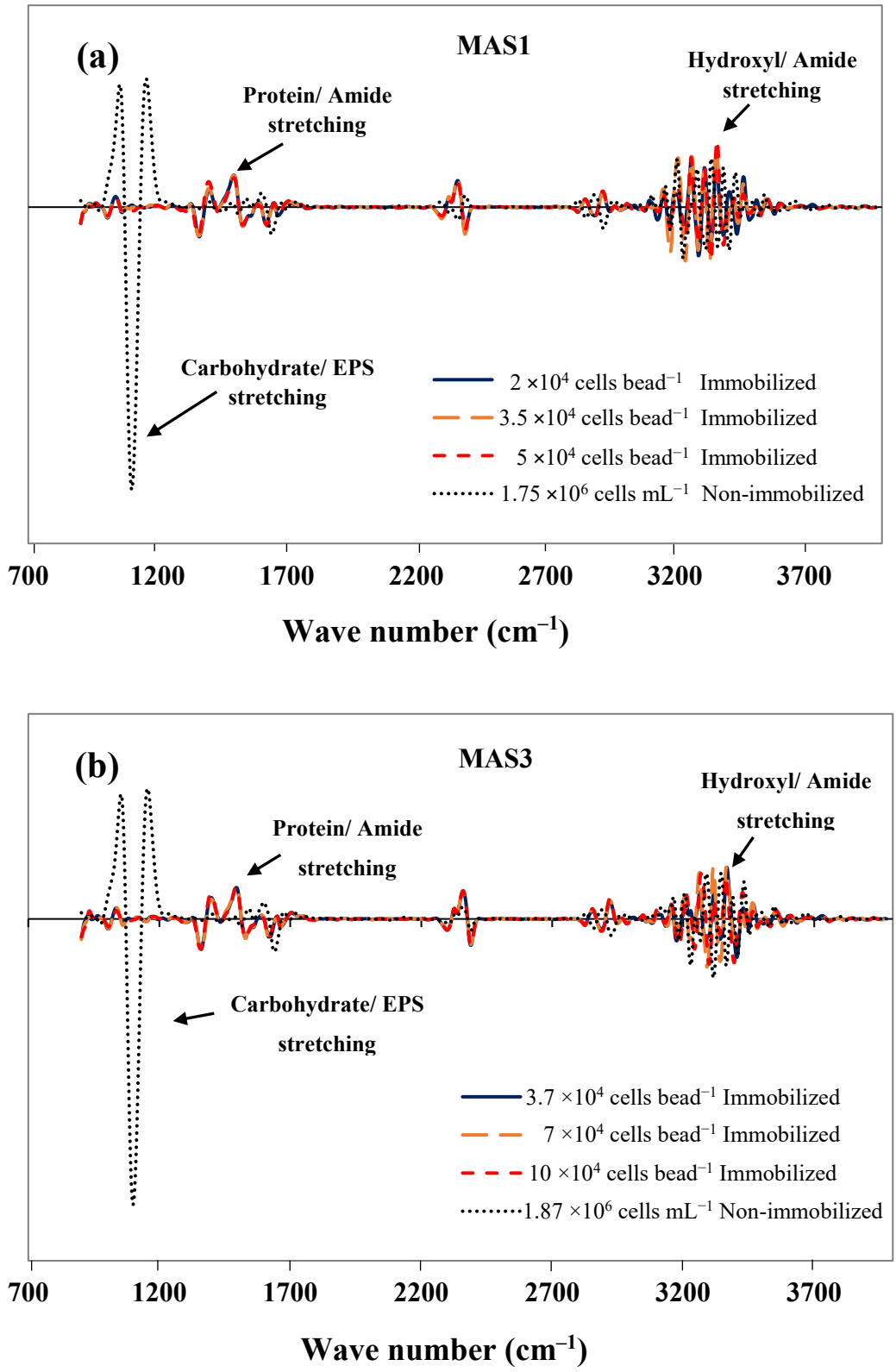

Fig 7.5. Second deriative spectra of non-immobilized and immobilized cells. (a) *Desmodesmus* sp. MAS1 and (b) *Heterochlorella* sp. MAS3 at varying cell densities after 48 h of incubation in AMD samples

7.4.3. Potential of fixed bed column in Fe removal by immobilized acid-adapted microalgae

The BDST model is widely used to physically measure the capacity of a bed to unravel the relationship between biosorption and iron removal from AMD (Abdolali et al., 2017). In a feasibility study, two different beds of 1 and 2 cm consisiting of 70 and 140 beads entrapped with a cell density of 1.75 $\times 10^4$ cells bead^{-1} of strain MAS1 or 3.5 $\times 10^4$ cells bead^{-1} of strain MAS3 were chosen to evaluate their Fe removal potential from AMD (Fig. 4). The break through times at 95% were 25.16, 29.9 and 29.4 min and R^2 values were 0.95, 0.96 and 0.91 in case of beads with no microalgae, cells of strain MAS1 and MAS3, respectively, at a bed height of 1 cm. A bed height of 2 cm realized significantly (95%) better break through times with 356.369, 352.05 and 353.18 min and R^2 values of 0.75,0.97 and 0.98 in columns packed with control beads, cells of strains MAS1 and MAS3, respectively (Fig. 7.6). Vilvanathan and Shanthakumar (2017) also observed that an increase in bed height greatly increased the breakthrough as well as exhaustion time while treating nickel and cobalt solution using biochar. Such an increased breakthrough time as a result of enhanced bed height indicates a better contact time available for the metal ions and immobilized algal beads (Wang and Chen, 2009). Wider mass transfer zone extending the curves to be steeper, better mass transfer (diffusion process) compared with the axial dispersion phenomenon, and availability of better binding sites are the other possible reasons for enhanced breakthrough time due to increased bed depth (Abdolali et al., 2017). A prediction of the ratio between metal inlet and outlet concentration in AMD samples indicates that the removal efficiency is a complex proposition especially in biosorption leding to the neural networking approach (Giri et al., 2011). ANN is divided into training, validation and testing to process the input variable through various neurons to achieve best mean square error (MSE) of the process (Venkatakrishnan et al., 2018). The MSE value of 7.16 $\times 10^{-5}$ with an R^2 value of 0.98. (Fig. 7.7) attained based on ANN approach validates the experimental data obtained from the fixed bed column study.

.

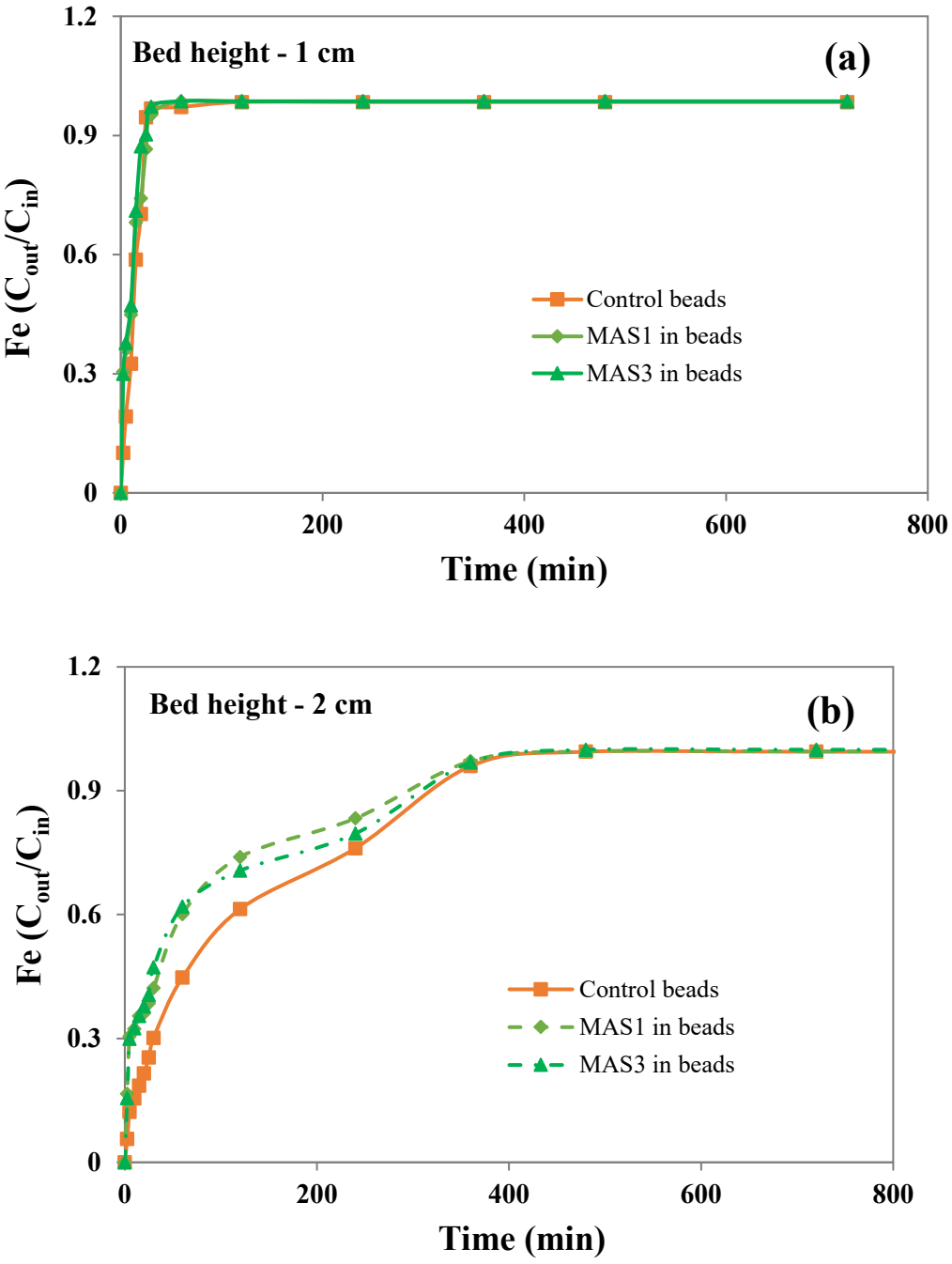

Fig 7.6. Fixed bed column experiments for iron removal from AMD using immobilized cells of MAS1 and MAS3

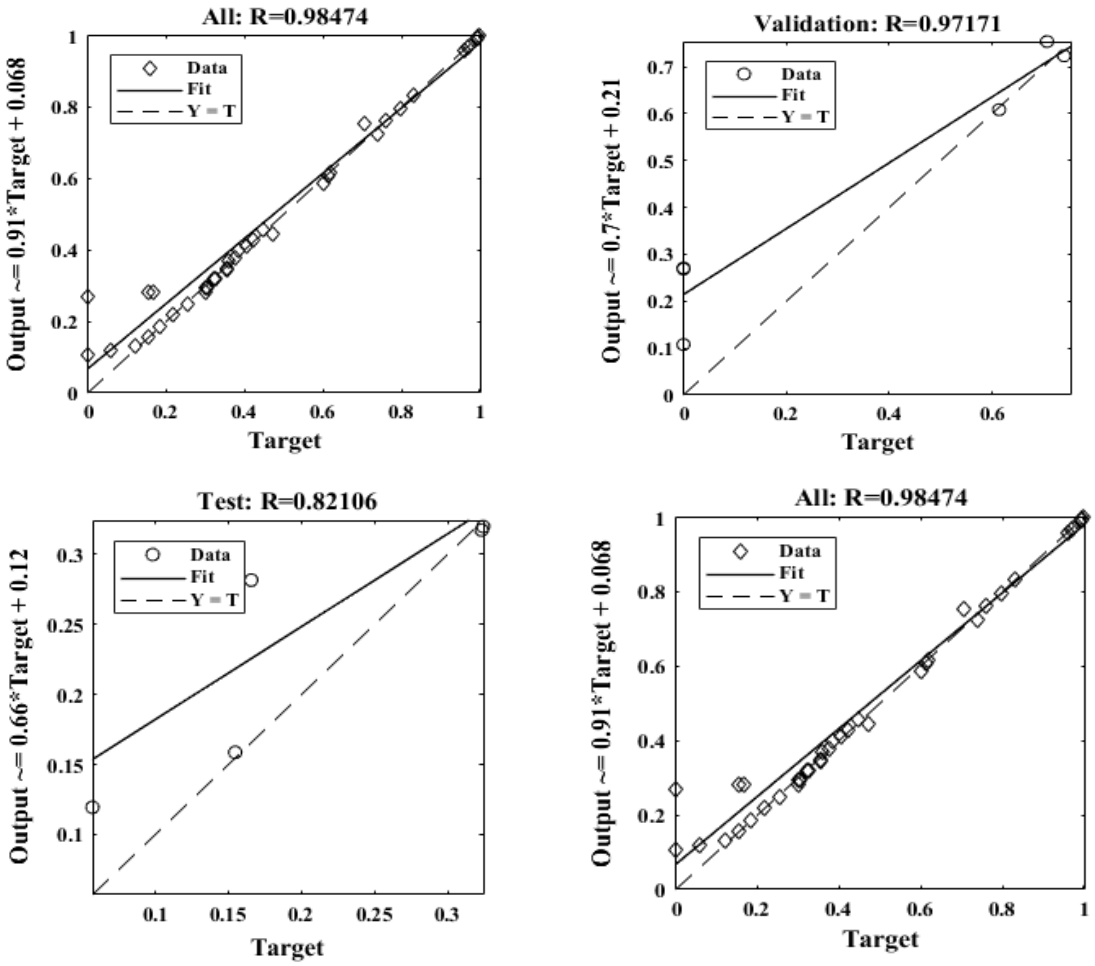

Fig 7.7. ANN modelling of the experimental data

7.5. Conclusion

The results of the present investigation indicate that acid-adapted microalgal strains have the potential in AMD remediation. Higher Fe removal (>40%) was achieved with free-cells at high cell desnities of the strains MAS1 and MAS3 after 24 h of incubation. Incubation time influenced the removal of Fe from AMD samples by microalgal cells entrapped in alginate beads. Both the cell morphology and granularity in non-immobilized cells of the strains MAS1 and MAS3 significantly changed upon direct exposure to AMD samples. Secondary derivative FTIR spectra revealed that microalgal cells immobilized in alginate beads had higher absorption frequencies at 1500-1650 and 3200-3500 cm−1 while non-immobilized cells exhibited changes at 1095 cm−1 when exposed to AMD samples. PCA analysis weighed the differences among non-immobilized and immobilized systems through clustering at different regions. Fixed bed column studies with a

bed height of 2 cm demonstrated the feasbilty of acid-adapted microalgal strains in removing Fe from AMD samples. Further optimization of bed height and flowrate provided a greater picture on the application of acid-adapted microalgal strains in AMD treatment at a pilot-scale. Thus, the present study demonstrated the use of greener and sustainable immobilization technology for Fe removal from extreme environments such as AMD using acid-adapted microalgae, *Desmodesmus* sp. MAS1 and *Heterochlorella* sp. MAS3

References

1. Abdolali, A., Ngo, H.H., Guo, W., Zhou, J.L., Zhang, J., Liang, S., Chang, S.W., Nguyen, D.D., Liu, Y., 2017. Application of a breakthrough biosorbent for removing heavy metals from synthetic and real wastewaters in a lab-scale continuous fixed-bed column. Bioresour. Technol. 229, 78–87. https://doi.org/10.1016/j.biortech.2017.01.016
2. Abinandan, S., Subashchandrabose, S.R., Venkateswarlu, K., Megharaj, M., 2018a. Nutrient removal and biomass production: advances in microalgal biotechnology for wastewater treatment. Crit. Rev. Biotechnol. 1–17. https://doi.org/10.1080/07388551.2018.1472066
3. Abinandan, S., Subashchandrabose, S.R., Venkateswarlu, K., Megharaj, M., 2018b. Microalgae–bacteria biofilms: a sustainable synergistic approach in remediation of acid mine drainage. Appl. Microbiol. Biotechnol. 102, 1131–1144. https://doi.org/10.1007/s00253-017-8693-7.
4. Abinandan, S., Subashchandrabose, S.R., Cole, N., Dharmarajan, R., Venkateswarlu, K., Megharaj, M., 2019a. Sustainable production of biomass and biodiesel by acclimation of non-acidophilic microalgae to acidic conditions. Bioresour. Technol. 271, 316–324. https://doi.org/10.1016/j.biortech.2018.09.140.
5. Abinandan, S., Subashchandrabose, S.R., Panneerselvan, L., Venkateswarlu, K., Megharaj, M., 2019b. Potential of acid-tolerant microalgae, *Desmodesmus* sp. MAS1 and *Heterochlorella* sp. MAS3, in heavy metal removal and biodiesel production at acidic pH. Bioresour. Technol. 278, 9–16. https://doi.org/10.1016/j.biortech.2019.01.053.
6. Abinandan, S., Subashchandrabose, S.R., Venkateswarlu, K., Perera, I.A., Megharaj, M., 2019c. Acid-tolerant microalgae can withstand higher concentrations of invasive cadmium and produce sustainable biomass and biodiesel at pH 3.5. Bioresour. Technol. 281, 469–473. https://doi.org/10.1016/j.biortech.2019.03.001.
7. Aguilera, A., Manrubia, S.C., Gómez, F., Rodríguez, N., Amils, R., 2006. Eukaryotic community distribution and its relationship to water physicochemical parameters in an extreme acidic environment, Río Tinto (Southwestern Spain). Appl. Environ. Microbiol. 72, 5325–5330. https://doi.org/10.1128/AEM.00513-06.
8. Ahmad, A., Bhat, A.H., Buang, A., 2018. Biosorption of transition metals by freely suspended and Ca-alginate immobilised with *Chlorella vulgaris*: Kinetic and equilibrium modeling. J. Clean. Prod. 171, 1361–1375. https://doi.org/10.1016/j.jclepro.2017.09.252.

9. Ahmad, A., Bhat, A.H., Buang, A., 2019. Enhanced biosorption of transition metals by living *Chlorella vulgaris* immobilized in Ca-alginate beads. Environ. Technol. 40, 1793–1809. https://doi.org/10.1080/09593330.2018.1430171.
10. Anghel, L., Duca, G., Cepoi, L., Iatco, I., Rudi, L., Erhan, R.V., 2018. The effects of operational parameters on the iron(III) uptake by micro-algae *Dunaliella salina*. Clean-Soil Air Water 46, 1800157. https://doi.org/10.1002/clen.201800157.
11. Ayora, C., Caraballo, M.A., Macias, F., Rötting, T.S., Carrera, J., Nieto, J.M., 2013. Acid mine drainage in the Iberian Pyrite Belt: 2. Lessons learned from recent passive remediation experiences. Environ. Sci. Pollut. Res. 20, 7837–7853. https://doi.org/10.1007/s11356-013-1479-2.
12. Bortnikova, S.B., Smolyakov, B.S., Sidenko, N.V., Kolonin, G.R., Bessonova, E.P., Androsova, N.V., 2001. Geochemical consequences of acid mine drainage into a natural reservoir: inorganic precipitation and effects on plankton activity. J. Geochem. Explor. 74, 127–139. https://doi.org/10.1016/S0375-6742(01)00179-0.
13. Covarrubias, S.A., de-Bashan, L.E., Moreno, M., Bashan, Y., 2012. Alginate beads provide a beneficial physical barrier against native microorganisms in wastewater treated with immobilized bacteria and microalgae. Appl. Microbiol. Biotechnol. 93, 2669–2680. https://doi.org/10.1007/s00253-011-3585-8.
14. Dao, L., Beardall, J., Heraud, P., 2017. Characterisation of Pb-induced changes and prediction of Pb exposure in microalgae using infrared spectroscopy. Aquat. Toxicol. 188, 33–42. https://doi.org/10.1016/j.aquatox.2017.04.006.
15. Debelius, B., Forja, J.M., DelValls, Á., Lubián, L.M., 2009. Toxicity and bioaccumulation of copper and lead in five marine microalgae. Ecotox. Environ. Safe. 72, 1503-1513. https://doi.org/10.1016/j.ecoenv.2009.04.006.
16. Deng, D., Weidhaas, J.L., Lin, L.S., 2016. Kinetics and microbial ecology of batch sulfidogenic bioreactors for co-treatment of municipal wastewater and acid mine drainage. J. Hazard. Mater. 305, 200−208. https://doi.org/10.1016/j.jhazmat.2015.11.041.
17. Elliott, P., Ragusa, S., Catcheside, D., 1998. Growth of sulfate-reducing bacteria under acidic conditions in an upflow anaerobic bioreactor as a treatment system for acid mine drainage. Water Res. 32, 3724−3730. https://doi.org/10.1016/S0043-1354(98)00144-4.
18. Gerloff-Elias, A., Spijkerman, E., Schubert, H., 2005. Light acclimation of Chlamydomonas acidophila accumulating in the hypolimnion of an acidic lake (pH 2.6). Freshw. Biol. 50, 1301−1314. https://doi.org/10.1111/j.1365-2427.2005.01400.x.
19. Giri, A.K., Patel, R.K., Mahapatra, S.S., 2011. Artificial neural network (ANN) approach for modelling of arsenic (III) biosorption from aqueous solution by living cells of *Bacillus cereus* biomass. Chem. Eng. J. 178, 15−25. https://doi.org/10.1016/j.cej.2011.09.111.
20. Genty, T., Bussière, B., Benzaazoua, M., Neculita, C.M., Zagury, G.J., 2020. Treatment efficiency of iron-rich acid mine drainage in a tri-unit pilot system. Environ. Sci. Pollut. Res. 27, 8418–8430. https://doi.org/10.1007/s11356-019-07431-w.
21. Hammarstrom, J.M., Sibrell, P.L., Belkin, H.E., 2003. Characterization of limestone reacted with acid-mine drainage in a pulsed limestone bed treatment system at the Friendship Hill National Historical Site, Pennsylvania, USA. Appl. Geochem. 18, 1705−1721. https://doi.org/10.1016/S0883-2927(03)00105-7.

22. Hyka, P., Lickova, S., Přibyl, P., Melzoch, K., Kovar, K., 2013. Flow cytometry for the development of biotechnological processes with microalgae. Biotechnol. Adv. 31, 2−16. https://doi.org/10.1016/j.biotechadv.2012.04.007.
23. Johnson, D.B., Hallberg, K.B. 2005. Acid mine drainage remediation options: A review. Sci. Tot. Environ. 338, 3−14. https://doi.org/10.1016/j.scitotenv.2004.09.002.
24. Kefeni, K.K., Msagati, T.M., Mamba, B.B., 2015. Synthesis and characterization of magnetic nanoparticles and study their removal capacity of metals from acid mine drainage. Chem. Eng. J. 276, 222−231. https://doi.org/10.1016/j.cej.2015.04.066.
25. Kefeni, K.K., Msagati, T.A. Mamba, B.B., 2017. Acid mine drainage: prevention, treatment options, and resource recovery: a review. J. Clean. Prod. 151, 475−493. https://doi.org/10.1016/j.jclepro.2017.03.082.
26. Lens, P.N.L., Visser, A., Janssen, A.J.H., Pol, L.W.H., Lettinga, G. 1998. Biotechnological treatment of sulfate-rich wastewaters. Crit. Rev. Environ. Sci. Tech. 28, 41−88. https://doi.org/10.1080/10643389891254160.
27. Li, Y., Yang, X., Geng, B. 2018. Preparation of immobilized sulfate-reducing bacteria-microalgae beads for effective bioremediation of copper-containing wastewater. Water. Air. Soil. Pollut. 229, 54. https://doi.org/10.1007/s11270-018-3709-1.
28. Liamleam, W., Annachhatre, A.P. 2007. Electron donors for biological sulfate reduction. Biotechnol. Adv. 25, 452−463. https://doi.org/10.1016/j.biotechadv.2007.05.002
29. López-Archilla, A.I., Marin, I., Amils, R. 2001. Microbial community composition and ecology of an acidic aquatic environment: the Tinto River, Spain. Microb. Ecol. 41, 20−35. https://doi.org/10.1007/s002480000044.
30. Mehta, S.K., Gaur, J.P. 2001. Removal of Ni and Cu from single and binary metalsolutions by free and immobilized *Chlorella vulgaris*. Eur. J. Protist. 37, 261−271. https://doi.org/10.1078/0932-4739-00813.
31. Min, X., Chai, L., Zhang, C., Takasaki, Y., Okura, T. 2008. Control of metal toxicity, effluent COD and regeneration of gel beads by immobilized sulfate-reducing bacteria. Chemosphere 72, 1086−1091. https://doi.org/10.1016/j.chemosphere.2008.04.001.
32. Moreno-Garrido, I., 2008. Microalgae immobilization: current techniques and uses. Bioresour. Technol. 99, 3949–3964. https://doi.org/10.1016/j.biortech.2007.05.040.
33. Mori, J.F., Neu, T.R., Lu, S., Händel, M., Totsche, K.U., Küsel, K. 2015. Iron encrustations on filamentous algae colonized by *Gallionella*-related bacteria in a metal-polluted freshwater stream. Biogeosciences 12, 5277−5289. https://doi.org/10.5194/bg-12-5277-2015.
34. Megharaj, M., Pearson, H.W., Venkateswarlu, K. 1992. Removal of nitrogen and phosphorus by immobilized cells of *Chlorella vulgaris* and *Scenedesmus bijugatus* isolated from soil. Enzyme. Microb. Technol. 14, 656−658. https://doi.org/10.1016/0141-0229(92)90042-M.
35. Nancucheo, I., Johnson, D.B. 2010. Production of glycolic acid by chemolithotrophic iron- and sulfur-oxidizing bacteria and its role in delineating and sustaining acidophilic sulfide mineral-oxidizing consortia. Appl Environ Microbiol 76, 461−7. https://doi.org/ 10.1128/AEM.01832-09.
36. Nieto, J.M., Sarmiento, A.M., Olías, M., Canovas, C.R., Riba, I., Kalman, J., Delvalls, T.A. 2007. Acid mine drainage pollution in the Tinto and Odiel rivers (Iberian Pyrite Belt, SW Spain)

and bioavailability of the transported metals to the Huelva Estuary. Environ. Int. 33, 445−455. https://doi.org/10.1016/j.envint.2006.11.010
37. Orandi, S., Lewis, D.M. 2013. Biosorption of heavy metals in a photo-rotating biological contactor − a batch process study. Appl. Microbiol. Biotechnol. 97, 5113−23. https://doi.org/10.1007/s00253-012-4316-5.
38. Rodríguez-Galán, M., Baena-Moreno, F.M., Vázquez, S., Arroyo-Torralvo, F., Vilches, L.F., Zhang, Z. 2019. Remediation of acid mine drainage. Environ Chem Lett 17, 1529–1538. https://doi.org/10.1007/s10311-019-00894-w.
39. RoyChowdhury, A., Sarkar, D., Datta, R. 2019. Removal of acidity and metals from acid mine drainage-impacted water using industrial byproducts. Environ. Manage. 63, 148−158. https://doi.org/10.1007/s00267-018-1112-8.
40. Samadani, M., Perreault, F., Oukarroum, A., Dewez, D. 2018. Effect of cadmium accumulation on green algae *Chlamydomonas reinhardtii* and acid-tolerant *Chlamydomonas* CPCC 121. Chemosphere 191, 174−182. https://doi.org/10.1016/j.chemosphere.2017.10.017.
41. Sánchez España, J., López Pamo, E., Santofimia, E., Aduvire, O., Reyes, J., Barettino, D., 2005. Acid mine drainage in the Iberian Pyrite Belt (Odiel river watershed, Huelva, SW Spain): geochemistry, mineralogy and environmental implications. Appl. Geochem. 20, 1320−1356. https://doi.org/10.1016/j.apgeochem.2005.01.011.
42. Søndergaard, J., Elberling, B., Asmund, G. 2008. Metal speciation and bioavailability in acid mine drainage from a high Arctic coal mine waste rock pile: temporal variations assessed through high-resolution water sampling, geochemical modelling and DGT. Cold Reg. Sci. Technol. 54, 89−96. https://doi.org/10.1016/j.coldregions.2008.01.003.
43. Spijkerman, E., Stojkovic, S., Beardall, J. 2014. CO_2 acquisition in *Chlamydomonas acidophila* is influenced mainly by CO_2, not phosphorus, availability. Photosynth. Res. 121, 213−221. https://doi.org/10.1007/s11120-014-0016-6.
44. Subashchandrabose, S.R., Logeshwaran, P., Venkateswarlu, K., Naidu, R., Megharaj, M. 2017. Pyrene degradation by *Chlorella* sp. MM3 in liquid medium and soil slurry: possible role of dihydrolipoamide acetyltransferase in pyrene biodegradation. Algal. Res. 23, 223−232. https://doi.org/10.1016/j.algal.2017.02.010.
45. Subramaniyam, V., Subashchandrabose, S.R., Thavamani, P., Chen, Z., Krishnamurti, G.S.R., Naidu, R., Megharaj, M. 2016. Toxicity and bioaccumulation of iron in soil microalgae. J. Appl. Phycol. 28, 2767−2776. https://doi.org/10.1007/s10811-016-0837-0
46. Suzuki, T., Yamaguchi, T. and Ishida, M., 1998. Immobilization of *Prototheca zopfii* in calciumalginate beads for the degradation of hydrocarbons. Process. Biochem. 33, 541–546. https://doi.org/10.1016/S0032-9592(98)00022-3.
47. Tuffnell, S. 2017. Acid drainage: The global environmental crisis you've never heard of. In The Conversation, Environment and Energy. The Conversation Media Group Melbourne, Australia. https://theconversation.com/acid-drainage-the-global-environmental-crisis-youve-never-heard-of-83515 (Accessed September 2019).
48. Venkatakrishnan, B., Sandhya, K., Abinandan, S., Vedaraman, N., Velappan, K. 2019. Fixation of carbon dioxide and optimization of liming process waste produced in tanneries using response surface methodology. J. Clean. Prod. 209, 855–861. https://doi.org/10.1016/j.jclepro.2018.10.275

49. Venkateswarlu, K., Nirola, R., Kuppusamy, S., Thavamani, P., Naidu, R., Megharaj, M., 2016. Abandoned metalliferous mines: ecological impacts and potential approaches for reclamation. Rev. Environ. Sci. BioTechnol. 15, 327−354. https://doi.org/10.1007/s11157-016-9398-6.
50. Vilvanathan, S., Shanthakumar, S. 2017. Column adsorption studies on nickel and cobalt removal from aqueous solution using native and biochar form of Tectona grandis. Environmental Progress & Sustainable Energy 36, 1030−1038. https://doi.org/10.1002/ep.12567.
51. Wang, J., Chen, C. 2009. Biosorbents for heavy metals removal and their future. Biotechnol. Ad. 27, 195−226. https://doi.org/10.1016/j.biotechadv.2008.11.002.
52. Witek-Krowiak, A., Chojnacka, K., Podstawczyk, D., Dawiec, A., Pokomeda, K. 2014. Application of response surface methodology and artificial neural network methods in modelling and optimization of biosorption process. Bioresour. Technol. 160, 150−160. https://doi.org/10.1016/j.biortech.2014.01.021.
53. Wu, S., Vymazal, J. and Brix, H. 2019. Critical review: biogeochemical networking of iron in constructed wetlands for wastewater treatment. Env. Sci. Technol. 53, 7930−7944. https://doi.org/10.1021/acs.est.9b00958.
54. Zhou, G.J., Peng, F.Q., Zhang, L.J., Ying, G.G. 2012. Biosorption of zinc and copper from aqueous solutions by two freshwater green microalgae *Chlorella pyrenoidosa* and *Scenedesmus obliquus*. Environ. Sci. Pollut. Res. 19, 2918−2929. https://doi.org/10.1007/s11356-012-0800-9
55. Zhang, M. and Wang, H., 2016. Preparation of immobilized sulfate reducing bacteria (SRB) granules for effective bioremediation of acid mine drainage and bacterial community analysis. Miner. Eng. 92, 63−71. https://doi.org/10.1016/j.mineng.2016.02.008.
56. Zhang, M., Wang, H. and Han, X. 2016. Preparation of metal-resistant immobilized sulfate reducing bacteria beads for acid mine drainage treatment. Chemosphere 154, 215−223. https://doi.org/10.1016/j.chemosphere.2016.03.103.

Chapter 8 Conclusion and Future Work

Acid mine drainage (AMD) is formed due to oxidation of pyrite rocks excavated during mining operations. The general characteristics of AMDs are acidic pH (2-4) with dissolved heavy metals that are readily bioavailable, posing a serious risk to the environment. Conventional treatment techniques of AMD involves intensive use of chemicals, filtration systems that require massive capital investment while sludge produced creates an additional burden to the environment. The use of bioreactors involving bacteria requires other substrates depending on the species involved, requiring additional capital investment. Microalgae are versatile organisms that have many advantages like adaptation to any habitats, consumption of CO_2 from the atmosphere for growth, remediation of contaminants (phycoremediaiton) and biomass produced can be used for value-added product generation. Besides, acidophilic algae found in AMDs have developed tolerance, but their role in remediation is very less clear. Hence, our research hypothesized acid-tolerant microalgae from other habitats could help to enhance AMD remediation, thus making the first approach to do so. Acid tolerant microalgae *Desmodesmus* sp. MAS1 and *Heterochlorella* sp. MAS3 isolated from non-acidophilic habitats were used in this study. These microalgae grew well in the medium containing metals such as Cu, Cd, Fe, Mn and Zn at concentrations up to 20 mg L^{-1} and 50 mg Fe L^{-1} and removed the metals from the medium predominantly through intracellular accumulation. The strains were able to adapt to an acid pH of 3.5 over 100 generations. MAS1 and MAS3 were able to grow in synthetic acid mine drainage (SAMD) with metals such as Mn, Cd, Zn, and Cu as found in real AMD samples. Acid adaptation modulated phenotypic plasticity of microalgae to survive in acid mine drainage samples. Increasing biomass concentrations influenced the metal (Fe) removal from real AMD in immobilized and non-immobilized techniques.

8.1. The major findings of the study

- Under acidic conditions, microalgae survived through passive diffusion of CO_2 with enhanced lipid secretion.
- The yield of microalgal biomass was significant with increased amounts of biochemicals, especially protein and lipids.
- FAME were rich in triglycerides and aliphatic fatty acid hydrocarbons in algal strains exposed to heavy metals.

- Increasing Fe concentration from 25 mg L^{-1} to 800 mg L^{-1} in SAMD revealed the tolerance of microalgae up to 200 mg Fe L^{-1} in SAMD.
- At high iron concentrations, both the strains exhibited extracellular polysaccharide accumulation in response to SAMD.
- FAME yield was 13-15% in MAS1 and MAS3 in SAMD containing 200 mg Fe L with metals partitioning into residual biomass rather than biodiesel.
- The strains MAS1and MAS3 exhibited good growth in real AMD treatment which was on par with control at 48 h incubation time.
- Phosphate limitation hindered the microalgae growth in real AMD through increasing metal uptake.
- Downregulation of amino acids alleviated the toxicity exerted by real AMD samples
- Bio-filter studies indicated the bed height of immobilized microalgae biomass played a crucial role in extending the breakthrough time for AMD remediation.

8.2. Propositions for future research

- Screening of potential acid-tolerant microalgae from oligotrophic environments.
- Extracellular polysaccharide could be a useful marker to identify other acid-tolerant strains that could be potentially explored for AMD remediation.
- Adaptation of acid-tolerant microalgae to a mixed environment with metals will help to understand remediation efficiency.
- Supplying low-cost phosphate as a nutrient in AMD treatment would help microalgae to sustain growth.
- exploring the potential of microalgae-bacteria consortia for AMD remediation.
- Microbial diversity changes in response to acid –tolerant microalgae survival in AMD environment should be investigated.
- Adapting microalgae through their growth on several generations in AMD and understanding molecular mechanism will provide a better insight into the adaption of microalgae and remediation.
- Optimization of various flow rates, bed heights will provide additional insights for biofilter scale-up potential in AMD remediation.